

AD-A173 808

## CARBON DIOXIDE LINE POSITIONS IN THE 20 AND 43 MICRON

1/4

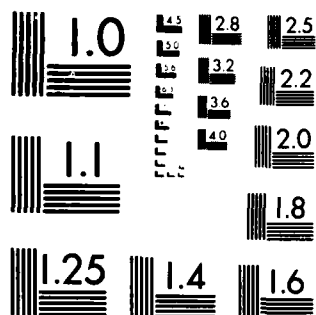
**UNCLASSIFIED**

SCIENTIFIC-16 AFGL-TR-86-0046

F/G 7/4

NL

[illegible]



MICROCOPY RESOLUTION TEST CHART  
NATIONAL BUREAU OF STANDARDS 1963-A

AD-A173 808

AFGL-TR-86-0046

Carbon Dioxide Line Positions in the  
2.8 and 4.3 Micron Regions at 800 Kelvin

Mark P. Esplin  
Hajime Sakai  
Laurence S. Rothman  
George A. Vanasse  
William M. Barowy  
Ronald J. Huppi

DTIC  
ELECTE  
NOV 03 1986  
S D

Stewart Radiance Laboratory  
Utah State University  
139 The Great Road  
Bedford, MA 01730

19 February 1986

Scientific Report No. 16

APPROVED FOR PUBLIC RELEASE; DISTRIBUTION UNLIMITED

DTIC FILE COPY

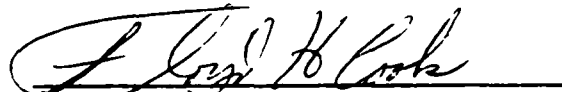
AIR FORCE GEOPHYSICS LABORATORY  
AIR FORCE SYSTEMS COMMAND  
UNITED STATES AIR FORCE  
HANSCOM AIR FORCE BASE, MASSACHUSETTS 01731

86 11 3 018

"This technical report has been reviewed and is approved for publication"

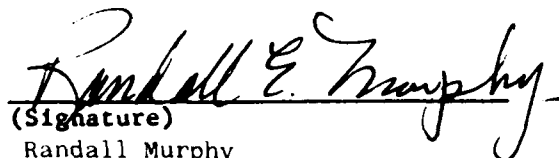
  
(Signature)

FRANK ROBERT  
Contract Manager

  
(Signature)

FLOYD COOK  
Branch Chief

FOR THE COMMANDER

  
(Signature)  
Randall Murphy  
Division Director

This report has been reviewed by the ESD Public Affairs Office (PA) and is releasable to the National Technical Information Service (NTIS).

Qualified requestors may obtain additional copies from the Defense Technical Information Center. All others should apply to the National Technical Information Service.

If your address has changed, or if you wish to be removed from the mailing list, or if the addressee is no longer employed by your organization, please notify AFGL/DAA, Hanscom AFB, MA 01731. This will assist us in maintaining a current mailing list.

Do not return copies of this report unless contractual obligations or notices on a specific document requires that it be returned.

Unclassified

SECURITY CLASSIFICATION OF THIS PAGE

AD-4123808

## REPORT DOCUMENTATION PAGE

1a. REPORT SECURITY CLASSIFICATION Unclassified		1b. RESTRICTIVE MARKINGS	
2a. SECURITY CLASSIFICATION AUTHORITY		3. DISTRIBUTION / AVAILABILITY OF REPORT Approved for public release; Distribution unlimited	
2b. DECLASSIFICATION / DOWNGRADING SCHEDULE			
4. PERFORMING ORGANIZATION REPORT NUMBER(S)		5. MONITORING ORGANIZATION REPORT NUMBER(S) AFGL-TR-86-0046	
6a. NAME OF PERFORMING ORGANIZATION Stewart Radiance Laboratory Utah State University	6b. OFFICE SYMBOL (If applicable)	7a. NAME OF MONITORING ORGANIZATION Air Force Geophysics Laboratory	
6c. ADDRESS (City, State, and ZIP Code) 139 The Great Road Bedford, MA 01730		7b. ADDRESS (City, State, and ZIP Code) Hanscom AFB Massachusetts 01731	
8a. NAME OF FUNDING / SPONSORING ORGANIZATION	8b. OFFICE SYMBOL (If applicable)	9. PROCUREMENT INSTRUMENT IDENTIFICATION NUMBER F19628-83-C-0056	
8c. ADDRESS (City, State, and ZIP Code)		10. SOURCE OF FUNDING NUMBERS	
		PROGRAM ELEMENT NO. 62101F	PROJECT NO. 7670
		TASK NO. 10	WORK UNIT ACCESSION NO. AK
11. TITLE (Include Security Classification) Carbon Dioxide Line Positions in the 2.8 and 4.3 Micron Regions at 800 Kelvin			
12. PERSONAL AUTHOR(S) Mark P. Esplin, Hajime Sakai, Laurence S. Rothman, George A. Vanasse, William M. Barowy, Ronald J. Huppi			
13a. TYPE OF REPORT Scientific Report #16	13b. TIME COVERED FROM TO	14. DATE OF REPORT (Year, Month, Day) 1986 February 19	15. PAGE COUNT 328
16. SUPPLEMENTARY NOTATION			
17. COSATI CODES		18. SUBJECT TERMS (Continue on reverse if necessary and identify by block number)	
FIELD	GROUP	SUB-GROUP	
		CO <sub>2</sub> line positions; High resolution interferometry; CO <sub>2</sub> molecular constants; Large FFT computer program; High temperature absorption cell	
19. ABSTRACT (Continue on reverse if necessary and identify by block number) <i>Micron. 4.3</i> A high resolution interferometer was used to measure the spectra of several different isotopically enriched carbon dioxide samples heated to 800 K in a high temperature absorption cell. An interactive line assignment computer program was developed and used to identify, in the two wavelength regions, a total of over 8000 lines belonging to 73 different rotation-vibration bands. In the 4.3 $\mu$ m region 19 bands were identified to $^{12}\text{C}^{16}\text{O}_2$ , 15 for $^{13}\text{C}^{16}\text{O}_2$ , 5 bands each for $^{12}\text{C}^{16}\text{O}^{18}\text{O}$ , $^{12}\text{C}^{18}\text{O}_2$ , and $^{13}\text{C}^{16}\text{O}^{18}\text{O}$ , and one band for $^{13}\text{C}^{16}\text{O}_2$ . In the 2.8 $\mu$ m region 11 bands were identified for $^{12}\text{C}^{16}\text{O}_2$ , 10 for $^{12}\text{C}^{16}\text{O}^{18}\text{O}$ , and 2 for $^{12}\text{C}^{18}\text{O}_2$ . New molecular constants were obtained for each band from a least-squares-fit to the observed line positions. The new molecular constants reproduce the position of spectral lines to within an accuracy of approximately 0.0004/cm <sup>-1</sup> .			
20. DISTRIBUTION / AVAILABILITY OF ABSTRACT <input type="checkbox"/> UNCLASSIFIED/UNLIMITED <input checked="" type="checkbox"/> SAME AS RPT <input type="checkbox"/> DTIC USERS		21. ABSTRACT SECURITY CLASSIFICATION Unclassified	
22a. NAME OF RESPONSIBLE INDIVIDUAL Frank Robert		22b. TELEPHONE (Include Area Code)	22c. OFFICE SYMBOL AFGL/LSP

### ACKNOWLEDGEMENTS

We would like to thank the many people who have played a part in this study, and in the preparation of this report. We would like to thank Fred Volz for measuring the transmission and reflection of the KBr beamsplitter. We thank Martin Reisfeld and Herbert Flicker of Los Alamos National Laboratory for providing the isotopic CO<sub>2</sub> samples. James H. Andrus provided engineering support. Vaughn Griffiths assisted in performing data processing and in the operation of the spectrometer. Gloria Foss helped in the preparation of the manuscript. Charles P. Dolan Jr. and Diane Plosia prepared the figures.

This research was sponsored by the Air Force Office of Scientific Research under the Atmospheric Sciences Project 2310.



Accession For	
NTIS CRA&I	<input checked="checked" type="checkbox"/>
DTIC TAB	<input type="checkbox"/>
Unannounced	<input type="checkbox"/>
Justification	
By	
Distribution /	
Availability Codes	
Dist	Avail and/or Special
A-1	

## TABLE OF CONTENTS

Acknowledgements . . . . .	3
Chapter	
I. INTRODUCTION . . . . .	9
II. HISTORY OF 4.3 $\mu\text{m}$ $\text{CO}_2$ MEASUREMENTS . . . . .	15
III. $\text{CO}_2$ THEORETICAL BACKGROUND . . . . .	21
Vibration . . . . .	23
Rotation . . . . .	35
Intensities . . . . .	38
IV. EXPERIMENTAL SETUP . . . . .	45
Overview of Experimental Setup . . . . .	46
High Temperature Absorption Cell . . . . .	48
Fourier Spectroscopy . . . . .	51
The AFGL Two-Meter Interferometer . . . . .	68
Modification of Interferometer . . . . .	87
V. DATA ANALYSIS . . . . .	107
Phase Correction . . . . .	110
Large FFT . . . . .	113
Spectral Line Positions . . . . .	116
Assignment of Spectral Lines . . . . .	121
Least-Squares-Fit . . . . .	143
VI. RESULTS AND DISCUSSION. . . . .	147
VII. CONCLUSION . . . . .	177
LIST OF REFERENCES . . . . .	181
APPENDIXES . . . . .	185
A. High Temperature $\text{CO}_2$ Spectrum . . . . .	187
B. Lines Used in Least-Squares-Fits . . . . .	199
C. Computer Program Listings . . . . .	279

# LIST OF FIGURES

1.	The three normal modes of vibration of the CO <sub>2</sub> molecule . . . . .	26
2.	Vibrational energy levels for CO <sub>2</sub> . . . . .	34
3.	Simplified schematic of the overall experimental setup . . . . .	47
4.	Schematic of the high temperature absorption cell	49
5.	Simplified schematic of a Michelson interferometer	53
6.	Two sampled cosine functions that appear identical	59
7.	Schematic of a Michelson interferometer showing finite beamsplitter thickness . . . . .	66
8.	Beamsplitter compensation using an additional compensator plate . . . . .	67
9.	Beamsplitter compensation using opposite faces of the same substrate plate . . . . .	69
10.	The optical layout of a cat's eye retro-reflector	71
11.	Photograph of the AFGL high resolution interferometer . . . . .	73
12.	Schematic of AFGL high resolution interferometer .	74
13.	Laser reference signal demonstrating the stepping and holding modes of the interferometer . . . .	78
14.	Data acquisition and stepping control electronics	80
15.	Flow chart of interferometer control and data acquisition program . . . . .	84
16.	The laser reference signal showing a stepping error and its correction . . . . .	86
17.	The pattern of germanium coatings on the beamsplitter . . . . .	90

18.	Transmission and reflection of the beamsplitter for a) the heavy coating used for the infrared b) the lighter coating used for the laser reference . . . . .	91
19.	The mount used for the KBr beamsplitter. . . . .	93
20.	Optical layout with KBr beamsplitter and copper doped germanium detectors . . . . .	96
21.	Detector preamplifier and filter design. . . . .	99
22.	Kadel liquid helium dewar. . . . .	100
23.	Spectrum of 100 torr of $\text{CO}_2$ broadened by 660 torr of $\text{N}_2$ in a 10 cm cell. . . . .	104
24.	HDO - $\text{H}_2\text{O}$ spectrum . . . . .	106
25.	Major steps in the data analysis process . . . . .	108
26.	Parameters that were determined for each absorption feature . . . . .	119
27.	The band head of the $\nu_3$ fundamental . . . . .	123
28.	The $\nu_3$ fundamental overlapped by the high frequency end of the R branch of the 01111 + 01101 band of $^{12}\text{C}^{16}\text{O}_2$ . . . . .	124
29.	Complex appearance of the $\text{CO}_2$ spectrum when several bands overlap . . . . .	125
30.	A large number of overlapping bands cause the spectrum to appear random . . . . .	126
31.	The range of J values and lower state energies for which spectral lines should be visible . . . . .	129
32.	The number of vibrational states with lower state energy less than or equal to a given energy . . .	130
33.	Loomis-Wood diagram for a hypothetical band of $\text{CO}_2$ . . . . .	134
34.	Part of the extended information Loomis-Wood diagram for the 00011 + 00001 band of $^{12}\text{C}^{16}\text{O}_2$ .	137

35.	Extended information Loomis-Wood diagram for the 02211e + 02201e band of $^{12}\text{C}^{16}\text{O}_2$ . . . . .	138
36.	Extended information Loomis-Wood diagram for the 13312 + 13302 band of $^{12}\text{C}^{16}\text{O}_2$ . . . . .	139
37.	Rotation-vibration bands for which molecular constants were obtained in the 4.3 $\mu\text{m}$ region . .	154
38.	Rotation-vibration bands for which molecular constants were obtained in the 2.8 $\mu\text{m}$ region . .	155
39.	Comparison of measured line positions with those computed using Guelachvili's and the AFGL (1978) constants for the 01111e + 01101e band of $^{12}\text{C}^{16}\text{O}_2$ . . . . .	164
40.	Comparison for the 01111f + 01101f band of $^{12}\text{C}^{16}\text{O}_2$ . . . . .	165
41.	Comparison for the 10012 + 10002 band of $^{12}\text{C}^{16}\text{O}_2$ .	166
42.	Comparison for the 10011 + 10001 band of $^{12}\text{C}^{16}\text{O}_2$ .	167
43.	Comparison for the 21111e + 11101e band of $^{12}\text{C}^{16}\text{O}_2$ . . . . .	168
44.	Comparison for the 11112e + 01101e band of $^{12}\text{C}^{16}\text{O}^{18}\text{O}$ . . . . .	169
45.	Comparison for the 10012 + 00001 band of $^{12}\text{C}^{18}\text{O}_2$ .	170
46.	Comparison for the 01121f + 01111f band of $^{13}\text{C}^{16}\text{O}_2$ . . . . .	171
47.	Comparison for the 10012 + 10002 band of $^{13}\text{C}^{16}\text{O}^{18}\text{O}$ . . . . .	172
48.	Comparison for the 00011 + 00001 band of $^{13}\text{C}^{16}\text{O}^{17}\text{O}$ . . . . .	173

# LIST OF TABLES

1. Amount of mixing of energy levels . . . . .	30
2. Comparison between Herzberg and AFGL notations . .	33
3. The CO <sub>2</sub> vibration partition sum . . . . .	42
4. Comparison between no apodization and triangular apodization . . . . .	57
5. Copper doped germanium detector performance and test specifications . . . . .	97
6. Identification codes used to identify rotation- vibration bands . . . . .	136
7. Table of experimental line properties for the 02211e + 02201e band of <sup>12</sup> C <sup>16</sup> O <sub>2</sub> . . . . .	140
8. Isotopic composition of CO <sub>2</sub> samples used in this study . . . . .	149
9. Summery of experimental conditions for measured spectra . . . . .	150
10. Observed CO lines used to check calibration of spectrometer . . . . .	151
11. Bands for which molecular constants were obtained in the 4.3 μm region . . . . .	156
12. Bands for which molecular constants were obtained in the 2.8 μm region . . . . .	157
13. Molecular constants resulting from the least- squares-fits in the 4.3 μm region . . . . .	158
14. Molecular constants resulting from the least- squares-fits in the 2.8 μm region . . . . .	160

## C H A P T E R I

### INTRODUCTION

The  $\text{CO}_2$  molecule is one of the most important atmospheric molecules because of the vital role it plays in the heat balance of our atmosphere. The  $\text{CO}_2$  concentration in the earth's atmosphere has dramatically increased over the last 100 years. The predicted global temperature increase as a result of this  $\text{CO}_2$  build-up in the atmosphere is a problem of international concern which will have to be faced in the near future. Aside from the atmospheric concerns, the  $\text{CO}_2$  molecule is a subject of interest from the molecular physics point of view.

One of the goals of molecular physics is to describe the energy states of a molecule from first principles, that is by solving the Schrödinger equation for the electrons and the nuclei making up the molecule. Although in principle such a calculation is possible on a digital computer, in practice, such a massive calculation involving so many degrees of freedom would be extremely difficult on any existing computer or any of the near future. At present, the computational problem is made manageable through the use of a number of approximations, the most important of which is the Born-Oppenheimer approximation.<sup>1</sup> In this approximation the rapid motions of the electrons are considered separable from the much slower

motions of the massive nuclei. The "cloud" of electrons, assumed to readjust rapidly to each new configuration of the nuclei, provides the molecular potential that "glues" the molecule together. The shape of this potential "well", or potential function, is generally determined by working backward from the measured spectrum of the molecule. This method provides far better accuracy than does calculating directly the effect of the electrons as a function of the nuclear configuration.

The energy due to the rotational and vibrational motions of a linear molecule can be specified in terms of the molecular constants  $G$ ,  $B$ ,  $D$ , and  $H$ . For diatomic molecules these molecular constants have been successfully related to the molecular potential function. However, for more complex polyatomic molecules such as  $\text{CO}_2$ , it is still somewhat uncertain how well the molecular constants  $G$ ,  $B$ ,  $D$ , and  $H$  can be related to the molecular potential. One of the reasons why this uncertainty still exists, in spite of previous experimental work, is the difficulty of obtaining experimental data on large numbers of rotation-vibration levels, particularly on the higher energy levels. For the present study, these experimental difficulties were overcome by heating the  $\text{CO}_2$  sample to excite large numbers of lines, using a high resolution Fourier spectrometer and making extensive use of the computer for data analysis. The present study consisted of determining for a number of

different isotopic species the molecular constants G, B, D, and H for as many vibrational states as possible. These molecular constants were then compared to molecular constants determined by other researchers. It is particularly interesting to compare these molecular constants with those calculated by Chedin,<sup>2</sup> since in his work he makes a single global determination of the CO<sub>2</sub> potential function, instead of fitting each band or groups of bands individually.

In order to extend the observable range of rotation-vibration energy levels, the CO<sub>2</sub> sample was heated to 800K. Although heating the CO<sub>2</sub> sample makes it possible to obtain information on many rotation-vibration levels, the resulting additional spectral lines greatly increase the difficulty of analyzing the spectrum. The spectrum of hot CO<sub>2</sub> stretches across hundreds of wavenumbers and consists of thousands of lines. As an example, see Appendix A, where the 4.3  $\mu\text{m}$  region of the spectrum of a sample of CO<sub>2</sub> with natural isotopic abundance is plotted. In order to obtain meaningful information from experimental spectra, individual rotation-vibration lines must be resolved.

The spectral measurements were made using the Air Force Geophysics Laboratory (AFGL) high resolution interferometer at resolutions of 0.007  $\text{cm}^{-1}$  for the 4.3  $\mu\text{m}$  region and 0.006  $\text{cm}^{-1}$  for the 2.8  $\mu\text{m}$  region. This study

was supported by the Air Force, since an increased understanding of the high temperature spectrum of  $\text{CO}_2$  relates to the problem of detecting the  $\text{CO}_2$  in the exhaust plumes of rocket and jet engines.

Huge quantities of data are associated with the high resolution broad band coverage of a complex spectrum. Handling these data was made practical through the extensive use of computers. Although some of the computer programs (software) had been developed previously, a substantial portion of the effort associated with the present study was spent in upgrading the existing software and developing and implementing new techniques. The major contributions made to the software development include:

1. Adding diagnostic and automatic error correction capabilities to the interferometer control software.
2. Working out the procedure to perform arbitrarily large Fourier transformations using a fixed memory size.
3. Developing an interactive semi-automatic rotation-vibration line assignment procedure.

This report on the study of high temperature  $\text{CO}_2$  is composed of three main sections. The first section, comprising the first three chapters, is introductory in nature. Chapter I is the introduction, Chapter II gives a brief history of previous studies of the  $\text{CO}_2$  spectrum in the  $4.3 \mu\text{m}$  region, and Chapter III is a review of the notation and theoretical concepts used to describe the  $\text{CO}_2$  molecule.

The second section, consisting of Chapters IV and V, gives detailed information on how the study was carried out. Chapter IV describes the experimental setup, and Chapter V, the data handling procedure. In the third section, Chapters VI and VII, the results and conclusions are presented. The results are discussed in Chapter VI. The conclusions and recommendations for future work are given in Chapter VII.

## CHAPTER II

### HISTORY

The spectral study of high temperature  $\text{CO}_2$  is not new. What is new with the present study is using a spectrometer with both high resolution and wide spectral coverage so that the complete high temperature rotation-vibration band structures at  $4.3\text{ }\mu\text{m}$  and  $2.8\text{ }\mu\text{m}$  could be observed with sufficient spectral resolution to resolve most of the individual rotation-vibration lines. These new data make accurate line position determination for thousands of lines possible, including many lines originating from highly excited rotational states.

In 1910, A. Trowbridge and R. W. Wood<sup>3</sup> used one of their recently developed blazed gratings to study a Bunsen burner flame. They observed peaks in the spectrum due to  $\text{CO}_2$  at  $4.2\text{ }\mu\text{m}$ ,  $4.4\text{ }\mu\text{m}$  and  $4.5\text{ }\mu\text{m}$ . Somewhat later (1922), E. F. Barker<sup>4</sup> realized by looking at both a room temperature  $\text{CO}_2$  sample and a Bunsen burner flame that the third peak observed by Trowbridge and Wood was an artifact of observing a hot Bunsen burner flame through the cold  $\text{CO}_2$  in the atmosphere. He observed that the band centered at  $4.3\text{ }\mu\text{m}$  was a doublet consisting of two distinct absorption features (the unresolved P and R branches). By the 1950's infrared spectrometers with sufficient spectral resolution had been developed to start observing the individual

rotation-vibration lines. E. K. Pyler et al.<sup>5</sup> used a grating to make measurements on the 4.3  $\mu\text{m}$  spectrum of  $\text{CO}_2$  both in emission and in absorption. The emission measurements were made by observing the flame from a glassblower's torch. They used a grating spectrometer with a spectral resolution of 0.2 to 0.3  $\text{cm}^{-1}$  to obtain a wavenumber accuracy of about 0.02  $\text{cm}^{-1}$ .

In 1968 a joint measurement was carried out on room temperature  $\text{CO}_2$  samples in the 4.3  $\mu\text{m}$  region by two groups, R. Oberly and K. N. Rao of Ohio State University and Y. H. Hahn and T. K. McCubbin Jr., of Pennsylvania State University,<sup>6</sup> using grating spectrometers with moderate spectral resolution. The spectral accuracy of their combined measurement was approximately 0.004  $\text{cm}^{-1}$ . In addition to observing transitions originating from the ground vibrational state, they also observed several hot bands with transitions originating from lower lying vibrational excited states.

During the 1970's the use of better infrared spectrometers and a variety of infrared sources made possible an increase in knowledge of the  $\text{CO}_2$  molecule, particularly of vibrationally excited states. In 1974, T. K. McCubbin et al.<sup>7</sup> used a grating spectrometer to observe the  $\text{CO}_2$  emission from an electrical discharge in a low pressure  $\text{CO}_2\text{-N}_2\text{-He}$  mixture. An electrical discharge can raise the vibrational temperature of a molecule to

extremely high values while leaving the rotational temperature at approximately room temperature. By varying the components of the mixture and the electrical current of the discharge, different vibrational series were observed. In 1978, D. Bailly et al.<sup>8</sup> used a SISAM spectrometer with a resolution of  $0.25 - 0.30 \text{ cm}^{-1}$  to observe additional hot bands in an electrical discharge. At about the same time, A. Baldacci et al.<sup>9</sup> used a grating spectrometer with a resolution of  $0.02 - 0.03 \text{ cm}^{-1}$  and a wavenumber accuracy of about  $0.003 \text{ cm}^{-1}$  to observe a low pressure  $\text{CO}_2$  sample in a 24 meter absorption cell. The long path length made possible the observation of lines originating from excited rotation-vibration states.

During the last several years, high resolution Michelson interferometers and tunable lasers have made possible very accurate measurements of the  $\text{CO}_2$  spectrum. In 1980, G. Guelachvili<sup>10</sup> used a high-resolution Michelson interferometer to observe in absorption the Doppler limited spectrum (approximately  $0.002 \text{ cm}^{-1}$  resolution) of a low pressure room temperature  $\text{CO}_2$  sample. He measured the position of rotation-vibration lines of the vibrational fundamental and several other hot bands with an accuracy of about  $0.0001 \text{ cm}^{-1}$ . Since this spectral measurement was made using a room temperature sample, lines originating from high rotational states were not observed.

In order to observe higher rotational lines, A. S. Pine<sup>11</sup> used a tunable laser difference-frequency spectrometer to observe a CO<sub>2</sub> sample heated to 985 K in a high temperature absorption cell. He made measurements on the R-branch head of the vibrational fundamental and combined his data with the room temperature measurements of Guelachvili. Pine showed that the molecular constants obtained from Guelachvili's very accurate room temperature measurements do not accurately predict the position of spectral lines at high temperatures.

The present study addresses the problem of obtaining information on highly excited rotational transitions for a large number of vibrational states of several different isotopically substituted species of CO<sub>2</sub>. A total of over 8000 lines belonging to 6 different isotopic species have been identified in the observed spectra. The positions of these lines were measured with an accuracy of up to 0.0004 cm<sup>-1</sup> for well isolated lines. Molecular constants for 73 rotation-vibration bands have been determined from these observed lines. The partial results of this continuing study have been published when they have become available. The <sup>12</sup>C<sup>16</sup>O<sub>2</sub> 4.3 μm results were presented at the 1980 Topical Meeting on Spectroscopy in Support of Atmospheric Measurements<sup>12</sup> and were used as the basis of the Ph.D. dissertation of M. P. Esplin.<sup>13</sup> These results were also incorporated into the AFGL 1980 compilation.<sup>14</sup>

The molecular constants and line positions for transitions in the 4.3  $\mu\text{m}$  region originating from the five lowest vibrational states of  $^{13}\text{C}^{16}\text{O}_2$ ,  $^{12}\text{C}^{18}\text{O}_2$ , and  $^{12}\text{C}^{16}\text{O}^{18}\text{O}$  and the  $\nu_3$  fundamental of  $^{13}\text{C}^{16}\text{O}^{17}\text{O}$  were published in the Journal of Molecular Spectroscopy.<sup>15</sup> These line positions were included in the AFGL 1982 compilation.<sup>16</sup> To be published<sup>17</sup> in the Journal of Molecular Spectroscopy are the molecular constants for additional transitions in the 4.5  $\mu\text{m}$  region originating from higher vibrational states of  $^{13}\text{C}^{16}\text{O}_2$  and  $^{13}\text{C}^{16}\text{O}^{18}\text{O}$  and from the  $\nu_3$  fundamental of  $^{13}\text{C}^{16}\text{O}^{17}\text{O}$ . This article also includes molecular constants for transitions in the 2.8  $\mu\text{m}$  region of  $^{12}\text{C}^{16}\text{O}_2$ ,  $^{12}\text{C}^{16}\text{O}^{18}\text{O}$  and  $^{12}\text{C}^{18}\text{O}_2$ .

In 1983, D. Bailly<sup>18</sup> completed her Ph.D. dissertation on the  $\text{CO}_2$  spectrum observed in an electrical discharge with an extremely high resolution Michelson interferometer. She was able to determine the position of spectral lines with an accuracy of approximately  $0.0001 \text{ cm}^{-1}$ . An electrical discharge is an effective technique for achieving excitation of very high vibrational levels, but not high rotational levels. Since Bailly's measurements included only a portion of the bands reported in the present work, and do not include high rotational lines, her measurements do not supersede those of the present study, except for spectral lines originating from low rotational

states of some of the vibrational bands.

Many other spectroscopic techniques have recently been employed to provide access to energy levels of carbon dioxide not observed before at high resolution. Among these approaches have been the heterodyne frequency measurements of laser-sequence band transitions<sup>19a</sup> (these have achieved very high accuracy, but not high rotational levels) and the long path room temperature absorption measurements conducted at the solar facility at Kitt Peak National Observatory<sup>19b</sup> (these measurements provide information on transitions that are weak even at elevated temperatures).

# CHAPTER III

## CO<sub>2</sub> THEORETICAL BACKGROUND

Carbon dioxide is a linear molecule with the two oxygen atoms located on either side of the central carbon atom. The oxygen and carbon atoms can be modeled as hard spheres and the forces between them as springs. This model helps in visualizing what will happen when energy is added to the molecule. The molecule will vibrate in a number of different ways as well as rotate as a whole. The same motions occur for the real CO<sub>2</sub> molecule, but unlike the case of the spheres and spring model where a continuum of vibrations and rotations are possible, quantum mechanics tells us that only certain discrete values of vibration and rotation are possible. The purpose of this chapter is to demonstrate how these discrete values of vibration and rotation (or energy levels) are calculated. The transition between the energy levels will also be examined.

In addition to the energy levels that arise from vibrational and rotational motions of the nuclei, there are also energy levels associated with the configuration of the electrons. However, at the temperatures used in the present study and using infrared radiation to probe the molecule, sufficient energy is not available to raise the molecule from the lowest electronic state. Even when excited electronic states are not involved, the electronic

configuration of the lowest state or ground electronic state may play an important role in determining the rotation-vibration energy levels of a molecule, since the orbital or spin angular momentum of the electrons can couple with the motion of the nuclei. The ground electronic state of the  $\text{CO}_2$  molecule is a  $^1\Sigma_g^+$  state so the net orbital and spin angular momentum of the electrons is zero. Hence, there is no net electronic angular momentum to couple with the angular momentum due to the vibration and rotation of the nuclei.

The motion of the electrons, the vibration of the nuclei, and the rotation of the molecule as a whole are usually considered separately. The total energy of the  $\text{CO}_2$  molecule is then given by

$$E = E_e + E_v + E_r , \quad (1)$$

where  $E_e$  is the electronic energy,  $E_v$  is the vibrational energy, and  $E_r$  is the rotational energy. This is usually a good approximation, but it is possible that it is starting to break down and is contributing to the discrepancies observed (see Chapter VI) between the experimental line positions and the line positions predicted using the molecular constants Chedin<sup>2</sup> calculated from an empirically determined potential function.

The spectroscopic technique can not be used to obtain information directly about the energy levels of a molecule,

instead information on the transitions between levels is obtained, from which information on the energy levels can be inferred. Lines in the absorption spectrum occur when a  $\text{CO}_2$  molecule in a lower energy state absorbs a quantum of energy and is raised to a higher energy state. Electronic transitions are usually found in the visible portion of the electromagnetic spectrum, while pure rotational transitions are found in the microwave region. These transitions were not observed as part of the present work and so will not be considered further. Only the infrared transitions involving changes in both vibration and rotational energies are considered in the present study.

### Vibration

The complex vibrational motions of a molecule can be reduced to a set of normal modes if the system is considered as being made up of small amplitude coupled oscillators. Small amplitude motion implies that the potential function is basically quadratic. The vibrational motion of each normal mode is then that of a one dimensional simple harmonic oscillator.

Simple Harmonic Oscillator. The present discussion of the harmonic oscillator follows that given by Herzberg.<sup>20</sup> The

potential energy of a one dimensional harmonic oscillator is

$$V = \frac{1}{2} k x^2 . \quad (2)$$

where  $k$  is the force constant, and  $x$  is the distance from the equilibrium position. The energy levels and the eigenfunctions of a mass,  $\mu$ , moving in a harmonic oscillator potential can be determined from the one dimensional Schrödinger equation

$$-\frac{\hbar^2}{2\mu} \frac{d^2 \psi}{dx^2} + \frac{1}{2} k x^2 \psi = E \psi . \quad (3)$$

The resulting energy eigenvalues are

$$E_v = \hbar \sqrt{\left(\frac{k}{\mu}\right)} \left(v + \frac{1}{2}\right) = h\nu \left(v + \frac{1}{2}\right) , \quad (4)$$

where  $v$  is the vibrational quantum number and  $\nu$  is the classical vibration frequency

$$\nu = \frac{1}{2\pi} \sqrt{\left(\frac{k}{\mu}\right)} . \quad (5)$$

In spectroscopy it is convenient to define the energy term value  $G_v$  as

$$G_v = \frac{E_v}{hc} = \frac{\nu}{c} \left(v + \frac{1}{2}\right) = \omega \left(v + \frac{1}{2}\right) . \quad (6)$$

The vibrational frequency  $\omega$  is measured in units of  $\text{cm}^{-1}$ .

The orthonormal eigenfunctions for the harmonic oscillator are

$$\psi_n(x) = N_n H_n(\alpha x) e^{-\frac{1}{2}\alpha^2 x^2} , \quad (7)$$

where  $H_n$  is the Hermite polynomial of order  $n$ . The

normalization constant for each eigenfunction is

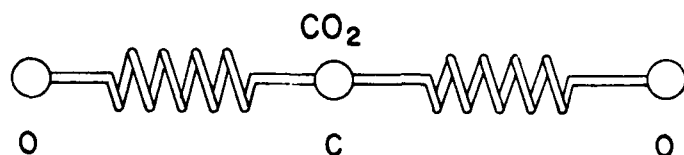
$$N_n = \left( \frac{\alpha}{\sqrt{\pi} 2^n n!} \right)^{\frac{1}{2}}, \quad (8)$$

where

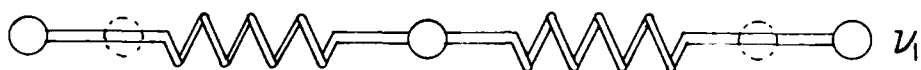
$$\alpha = 2\pi \sqrt{\left( \frac{\mu v}{h} \right)}. \quad (9)$$

The Normal Modes of CO<sub>2</sub>. The number of degrees of internal freedom or number of normal modes of vibration for a linear molecule is  $3N - 5$ .<sup>21</sup> Since CO<sub>2</sub> is composed of three atoms, the number of normal modes is 4. However, since the two bending modes are degenerate, there are only three modes with distinct energies. The normal vibrational modes of the CO<sub>2</sub> molecule are illustrated in Figure 1. The  $\nu_1$  mode is a symmetric stretch mode with an energy of  $\omega_1 = 1336 \text{ cm}^{-1}$ . The two orthogonal bending vibrations  $\nu_{2x}$  and  $\nu_{2y}$  have an energy of  $667 \text{ cm}^{-1}$ . The asymmetric stretch, mode  $\nu_3$ , has an energy of  $\omega_3 = 2362 \text{ cm}^{-1}$ . Instead of designating the state of the molecule using the degenerate  $\nu_{2x}$  and  $\nu_{2y}$  vibration quantum numbers, it is usually preferable to use the quantum numbers  $\nu_2$  and  $\ell$ , where  $\nu_2$  is the number of quanta of bending vibrational energy and  $\ell$  is the vibrational angular momentum about the internuclear axis. The allowed values of  $\ell$  are  $\nu_2, \nu_2-2, \dots, 2-\nu_2, -\nu_2$ .

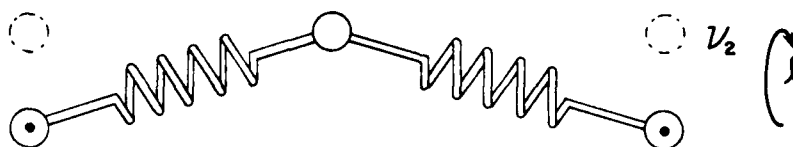
The energy of the CO<sub>2</sub> molecule is the sum of the energies in each normal mode. In the harmonic oscillator



SYMMETRIC STRETCH



BENDING MODE



ASYMMETRIC STRETCH

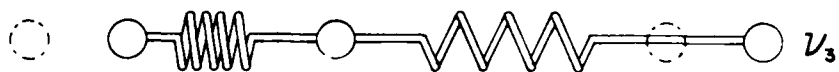


Figure 1. The three normal modes of vibration of the  $\text{CO}_2$  molecule.

approximation, the vibrational energy (neglecting the zero point energy) of the  $\text{CO}_2$  molecule in a given vibrational state characterized by  $v_1$ ,  $v_2$ ,  $v_3$  and  $\ell$ , is given by

$$G_v = \omega_1 v_1 + \omega_2 v_2 + \omega_3 v_3 . \quad (10)$$

Note, that in the harmonic oscillator approximation the energy of a molecule is independent of  $\ell$ .

So far this discussion has assumed a quadratic potential function with no cross terms, which is not the case for the real  $\text{CO}_2$  molecule. Since the effective potential includes nonquadratic terms and cross terms, the concept of normal modes breaks down somewhat, although it is still useful. However, correction terms must be added, and the effects of interactions between vibrational states must be considered.

If the interactions between states are not too strong, then by adding higher order powers of  $v_1$ ,  $v_2$ ,  $v_3$  and  $\ell^2$  to Equation (10) as correction terms, energy levels which agree with experiment can be obtained. This expansion including terms up to the third power of the quantum numbers is:

$$G_v = \sum_i \omega_i v_i + \sum_{i,j} x_{ij} v_i v_j + x_{\ell\ell} \ell^2 + \sum_{i,j,k} y_{ijk} v_i v_j v_k + \sum_i y_{i\ell\ell} v_i \ell^2 . \quad (11)$$

Interaction Between Levels. There are  $\text{CO}_2$  levels for which the interactions between levels are so strong that using an expansion like Equation (11) fails. In such cases a full Hamiltonian matrix is generated, Equation (11) can be used to generate the diagonal elements and then the strong interactions between levels are included as off diagonal elements of the matrix. Alternatively, the cross terms can be removed from Equation (11) before using it to create the diagonal elements, then all interactions, not just the strong interactions, would be included in the off diagonal elements of the matrix. The energy levels are obtained by diagonalizing the Hamiltonian matrix. For  $\text{CO}_2$  the main interactions are Fermi, Coriolis, and  $\ell$ -type doubling.

The amount that the energy levels will be effected by the presence of interactions between states depends not only on the strength of the interaction term but also on how close in energy the unperturbed levels would have been.

To illustrate this effect consider a two state system with energies  $E_1$  and  $E_2$  and an interaction between them of  $W$ . The new energy eigenvalues, taking into account the interaction between the two states, will be

$$\lambda = \frac{E_1 + E_2 \pm [(E_1 + E_2)^2 - 4(E_1 E_2 - W^2)]^{1/2}}{2} . \quad (12)$$

Let the new energy levels be represented by  $\lambda^+$  and  $\lambda^-$ , where  $\lambda^+$  is the energy levels using the (+) sign in Equation (12) and  $\lambda^-$  is the energy level when the (-) sign

is used. Each of the original energy levels will be shifted by an amount  $\Delta$ . The level  $E_2$  is assumed to have an energy greater than or equal to  $E_1$ , so that

$$\lambda^+ = E_2 + \Delta \quad (13)$$

and

$$\lambda^- = E_1 - \Delta .$$

The difference between the two new energy eigenvalues is

$$\lambda^+ - \lambda^- = E_2 - E_1 + 2\Delta . \quad (14)$$

From Equation (12) it can be seen that,

$$\lambda^+ - \lambda^- = [(E_1 + E_2)^2 - 4(E_1 E_2 - W^2)]^{\frac{1}{2}} . \quad (15)$$

Combining Equation (14) and (15) and solving for  $\Delta/W$  results in

$$\frac{\Delta}{W} = \frac{1}{2} ( \sqrt{(x^2 + 4)} - x ) \quad (16)$$

where  $x = (E_2 - E_1)/W$ . The value of  $\Delta/W$  is tabulated as a function of  $x$  in Table 1. Equation (16) or Table 1 provide a means by which energy shifts caused by a perturbing levels can quickly be determined.

In order to determine the mixing between states it is necessary to calculate the eigenvectors. The eigenvectors for a two level system are calculated by substituting the eigenvalues given in Equation (13) back into the Hamiltonian matrix of a two level system with interaction

Table 1. The amount the energy levels are perturbed and the amount of mixing of states as a function of  $x$ , where  $x = (E_2 - E_1)/W$ .

$x$	$\frac{\Delta}{W}$	$100b^2$ (% mixing from perturbing state)
0	1	50
0.01	0.995	49.8
0.02	0.990	49.5
0.04	0.980	49.0
0.08	0.961	48.0
0.1	0.951	47.5
0.2	0.905	45.0
0.4	0.820	40.2
0.8	0.677	31.4
1	0.618	27.6
2	0.414	14.6
4	0.236	5.3
8	0.123	1.5
10	0.099	1.0
20	0.050	0.2
40	0.025	0.1
80	0.012	0.0
100	0.010	0.0

term  $W$ . The resulting normalized eigenvectors are:

$$\begin{pmatrix} a \\ b \end{pmatrix} \text{ and } \begin{pmatrix} b \\ -a \end{pmatrix}, \quad (17)$$

where

$$a = \frac{1}{\left[ \left( \frac{\Delta}{W} \right)^2 + 1 \right]^{\frac{1}{2}}} \quad \text{and} \quad b = \frac{\frac{\Delta}{W}}{\left[ \left( \frac{\Delta}{W} \right)^2 + 1 \right]^{\frac{1}{2}}}. \quad (18)$$

Each new state consists of a contribution from the original state plus a contribution from the perturbing state. The

percent mixing from the perturbing state, given by  $100b^2$ , is also tabulated in Table 1. If the percent mixing is 50% then the original state is equally mixed with the perturbing state.

It can readily be seen from Equations (16) and (17) or Table 1 that for the same size of off-diagonal term  $W$ , the amount the energy levels will be perturbed, as well as the amount of mixing of states depends on the energy separation of the original energy levels.

The strongest interactions between  $\text{CO}_2$  states are caused by Fermi resonance. Cross terms in the potential function result in nonzero off-diagonal elements in the Hamiltonian matrix. Fermi resonance only occurs when there is a common  $\lambda$  (common symmetry type) for the interacting states. It arises due to the interaction between the symmetric stretch  $v_1$  and the bending mode  $v_2$ ; it occurs between states of the form  $(v_1, v_2+2, v_3)$  and  $(v_1+1, v_2, v_3)$ . The mixing between affected states is particularly strong since the energy of the symmetric stretch  $\omega_1 = 1336 \text{ cm}^{-1}$  is approximately equal to  $2\omega_2 = 1334 \text{ cm}^{-1}$ . For example the interaction term  $W$  between the state with  $v_1 = 1, v_2 = 0$ , and  $v_3 = 0$  and the state with  $v_1 = 0, v_2 = 2$ , and  $v_3 = 0$  is approximately  $50 \text{ cm}^{-1}$ , so  $x$  would be  $(1336 - 1334)/50 = 0.04$ . From Table 1 it can be seen that each state will be perturbed by  $0.98W$  and that the states are nearly uniformly mixed (49% mixing).

This large amount of mixing of states makes the identification of states by the quantum numbers  $v_1$ ,  $v_2$ ,  $v_3$ , and  $l$  ambiguous. To minimize this ambiguity instead of using the usual Herzberg notation for triatomic molecules, in which the vibrational states of a molecule are given as  $v_1 v_2^l v_3$ , a notation developed by W. S. Benedict,<sup>22</sup> known as the AFGL notation was used. In the AFGL notation the vibrational states are identified by  $v_1 v_2^l v_3 r$ , where "r" is the ranking index assigned to each member of a Fermi resonating group of levels. When a state is not involved in Fermi resonance,  $r = 1$  and the AFGL notation is essentially the same as the Herzberg notation. For example, the state  $01^1 0$  in Herzberg notation is 01101 in AFGL notation. When Fermi resonance is present the ranking index,  $r$ , is appended to the quantum numbers of the interacting state with the highest  $v_1$ . For example the AFGL notation for the two states  $10^0 0$  and  $02^0 0$ , which are highly mixed by Fermi resonance, is 10001 and 10002. The AFGL notation is compared to the Herzberg notation in Table 2. To illustrate the position of the different vibrational levels an energy level diagram for  $^{12}\text{C}^{16}\text{O}_2$  is given in Figure 2.

In classical mechanics the apparent tangential force on an object as it moves radially in a rotating coordinate system is called the Coriolis force. A similar effect is

Table 2. Comparison between Herzberg and AFGL notations

Herzberg ( $v_1 v_2^2 v_3$ )	AFGL ( $v_1 v_2^2 v_3^r$ )
00 <sup>0</sup> 0	00001
01 <sup>1</sup> 0	01101
10 <sup>0</sup> 0, 02 <sup>0</sup> 0	10002, 10001
02 <sup>2</sup> 0	02201
11 <sup>1</sup> 0, 03 <sup>1</sup> 0	11102, 11101
03 <sup>3</sup> 0	03301
00 <sup>0</sup> 1	00011
20 <sup>0</sup> 0, 12 <sup>0</sup> 0, 04 <sup>0</sup> 0	20003, 20002, 20001
12 <sup>2</sup> 0, 04 <sup>2</sup> 0	12202, 12201
04 <sup>4</sup> 0	04401
01 <sup>1</sup> 1	01111
21 <sup>1</sup> 0, 13 <sup>1</sup> 0, 05 <sup>1</sup> 0	21103, 21102, 21101
13 <sup>3</sup> 0, 05 <sup>3</sup> 0	13302, 13301
05 <sup>5</sup> 0	05501
10 <sup>0</sup> 1, 02 <sup>0</sup> 1	10012, 10011
02 <sup>2</sup> 1	02211

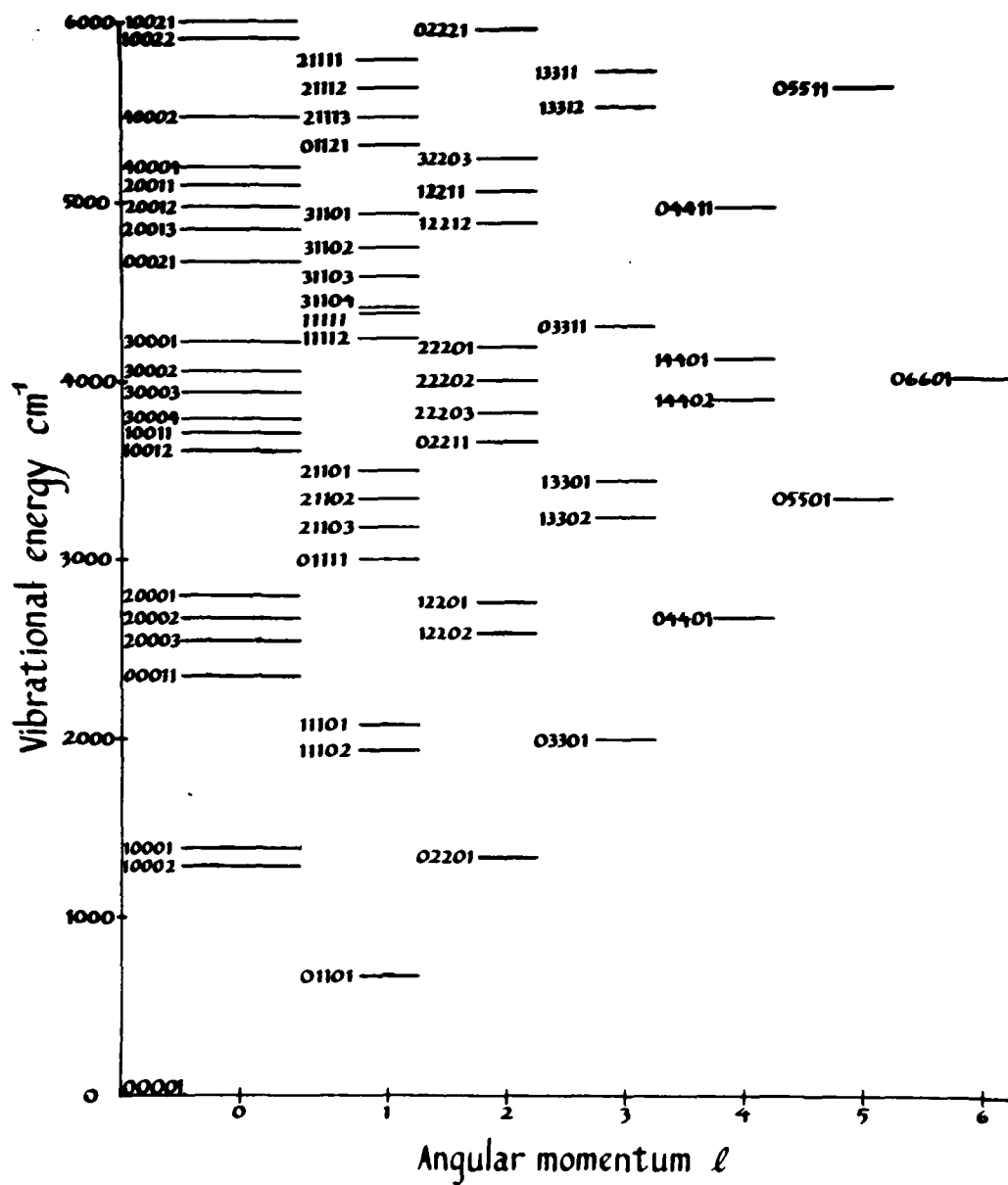


Figure 2. Vibrational energy levels for  $^{12}\text{C}^{16}\text{O}_2$ .

observed for the  $\text{CO}_2$  molecule. As the molecule rotates, the radial vibrations  $\nu_1$  and  $\nu_3$  become coupled with the bending mode  $\nu_2$ . This interaction, called Coriolis interaction, takes place between states of the form  $(\nu_1, \nu_2, \nu_3)$  and  $(\nu_1-1, \nu_2-1, \nu_3+1)$ .<sup>21</sup> As in all molecular interactions, if the effects are to be strong, the energies of the interacting states must be approximately equal.

The  $\ell$ -type doubling interaction occurs for non- $\Sigma$  type vibrational levels ( $\ell \neq 0$ ). Each vibration-rotation energy level splits into two levels under the influence of  $\ell$  - type doubling, an "e" level with a symmetric wave function, and a "f" level with an antisymmetric wave function. The degeneracy of the e and the f energy levels is removed by the rotation of the molecule. More information about  $\ell$ -type doubling will be given in the next section of this report.

### Rotation

In addition to internal vibration, the  $\text{CO}_2$  molecule rotates. The effects of rotation, assuming the molecule is completely rigid (rigid rotator), will first be considered. Then the assumption of rigid rotation will be relaxed and the effect on the energy levels will be investigated.

Rigid Rotator. If a molecule is only to rotate, the potential energy is a constant. The Schrödinger equation has solutions<sup>23</sup> which are single-valued, finite, and continuous when

$$E = \frac{\hbar^2 J(J+1)}{2I} , \quad (19)$$

where  $I$  is the moment of inertia of the molecule about an axis perpendicular to the internuclear axis. The moment of inertia of a linear polyatomic molecule is

$$I = \sum_i^N m_i r_i^2, \quad (20)$$

where  $m_i$  is the mass of the  $i^{\text{th}}$  nucleus and  $r_i$  is the distance from the center of mass. In spectroscopy it is convenient to give energy in terms of the rotational term value defined as  $F(J) = E/hc$ , given by

$$F(J) = \frac{h}{8\pi^2 c I} J(J+1) = B J(J+1) , \quad (21)$$

where the rotational constant  $B$  is defined as

$$B = \frac{h}{8\pi^2 c I} . \quad (22)$$

The average moment of inertia of a molecule is a function of the vibrational quantum numbers. Hence, the rigid rotator  $B$  in Equations (21) and (22) must be replaced by  $B_v$ , which is a function of vibration.

Nonrigid Rotator. The  $\text{CO}_2$  molecule is not totally rigid, as it rotates it also deforms. The largest of these deformations is a centrifugal stretch. This stretch increases the moment of inertia or decreases  $B_v$ . The effects of the molecular stretch as well as other distortions are taken into account by adding higher order terms with coefficients  $D_v$  and  $H_v$  to the expression for the rotational energy (Equation (21)). The rotational term value becomes

$$F(v,J) = B_v J(J + 1) - D_v \{J(J + 1)\}^2 + H_v \{J(J + 1)\}^3. \quad (23)$$

When these distortion terms are included, the rotational energy of the molecule can be expressed with the same accuracy that is observed experimentally.

For non- $\Sigma$  type levels ( $l^2 > 0$ ), each energy level is split into two levels under the influence of rotation. The effects of this  $l$ -type doubling can be taken into account by using two sets of rotational constants, one for the  $e$  levels and the other for the  $f$  levels. The interdependence<sup>24</sup> between these two sets of rotational constants is a function of  $l$ . When  $l = 1$ , the vibrational term values  $G_e$  and  $G_f$  are equal. When  $l = 2$ , in addition to having  $G_e$  equal to  $G_f$ , the rotational constants  $B_e$  and  $B_f$  are equal. When  $l = 3$ , then  $G_e = G_f$ ,  $B_e = B_f$ , and  $D_e = D_f$ . When  $l \geq 4$ ,  $H_e$  and  $H_f$  are also equal.

### Intensities

The absorption,  $A_\nu$ , of a gas at frequency  $\nu$  is defined as

$$A_\nu = 1 - \frac{I_\nu}{I_\nu^0} , \quad (24)$$

where  $I_\nu^0$  is the intensity of the light at frequency  $\nu$  before it enters the gas sample and  $I_\nu$  is the intensity after exiting the sample. If we assume a gas sample of uniform density and in thermal equilibrium along the optical path, the absorption is given by

$$A_\nu = 1 - e^{-k_\nu l} , \quad (25)$$

where  $k_\nu$  is the absorption coefficient for a given spectral line and  $l$  is the optical path through the gas sample. When  $N$  spectral lines are present the absorption at frequency  $\nu$  is given by

$$A_\nu = 1 - e^{-\sum_{i=1}^N k_\nu^i l} , \quad (26)$$

where  $k_\nu^i$  is the absorption coefficient for the  $i^{\text{th}}$  spectral feature at frequency  $\nu$ . The integrated intensity,  $S$ , is given by

$$S = \int_0^\infty k_\nu d\nu , \quad (27)$$

and is related to the molecular parameters as follows:

$$S = N_m B_{mn} h\nu_{mn} \left\{ 1 - e^{-\frac{\nu_{mn} hc}{kT}} \right\}, \quad (28)$$

where  $N_m$  is the number of molecules in the lower state  $m$ ,  $B_{mn}$  is the Einstein transition probability of a molecule going from state  $m$  to state  $n$ , and  $h\nu_{mn}$  is the energy of the absorbed photon. The first two factors of Equation (28),  $N_m$  and  $B_{mn}$ , will be discussed in more detail in the next two sections of this report. The factor in brackets is due to stimulated emission. Stimulated emission has the effect of reducing  $S$ . However, in the  $4.3 \mu\text{m}$  region at temperatures less than or equal to  $800 \text{ K}$ , the stimulated emission term differs from 1 by not more than 0.015.

Number of Molecules in a Given State. The first factor in Equation (28), the number of molecules in states of energy  $E$ , will now be considered in more detail. It is this term in the expression of the intensity that explains why heating a gas sample makes possible the observation of thousands of additional spectral lines.

The probability that a molecule in thermal equilibrium will have a given energy  $E$  is proportional to the degeneracy of that level and to the Boltzmann factor  $e^{-E/kT}$ . If the energy of a state is large compared to the available thermal energy,  $kT$ , the probability of finding the molecule in that state is small. As the temperature is

increased the number of molecules in higher energy states will increase. The fraction of molecules with a given energy  $E$  is obtained by dividing by the partition sum, which is approximately equal to the product of the vibration and rotation partition sums. The number of molecules in a state  $m$  is then given by

$$N_m = \frac{N g(v,J)}{Q_r Q_v} e^{-\frac{E(v,J)}{kT}}, \quad (29)$$

where:  $N$  = total number of molecules  
 $g$  = degeneracy of states  
 $E$  = energy of the given level  
 $Q_r$  = rotation partition sum  
 $Q_v$  = vibration partition sum.

The rotation partition sum is obtained by summing over all rotational energy states of the molecule. Each term in this sum is weighted by the degeneracy of the given energy level. The degeneracy of a rotational state with  $J$  quanta of angular momentum is  $2J+1$ . When the energy is approximated by  $BJ(J+1)hc$ , (the first term in Equation (23) times  $hc$ ) the expression for the rotation partition sum becomes

$$Q_r = \sum_{J=0}^{\infty} (2J+1) e^{-\frac{hc}{kT} BJ(J+1)}. \quad (30)$$

This sum can be approximated by an integral to yield an approximate value for the rotation partition sum,

$$Q_r = \frac{kT}{hcB}. \quad (31)$$

Replacing the sum by an integral is a very good approximation, particularly for the higher temperatures.

A good approximation to the vibration partition sum,  $Q_v$ , is obtained by summing over the energy levels which result from the harmonic oscillator approximation. Each term in the sum must be weighted by its degeneracy. The degeneracy of the  $v_1$  and  $v_3$  vibrational levels is unity. In the harmonic oscillator approximation all states with a common  $v_2$  but different  $\ell$  have the same energy, therefore the degeneracy of the  $v_2$  levels is  $v_2+1$ . For example if  $v_2 = 5$ , possible values of  $\ell$  are 5, 3, 1, -1, -3, -5 making 6 states in all. Remembering that the energy in  $\text{cm}^{-1}$  of each of the three normal modes are respectively  $\omega_1$ ,  $\omega_2$ , and  $\omega_3$ , the vibrational partition sum is given by

$$Q_v = \sum_{v_1=0}^{\infty} \sum_{v_2=0}^{\infty} \sum_{v_3=0}^{\infty} (v_2+1) e^{-\frac{hc\omega_1 v_1}{kT}} e^{-\frac{hc\omega_2 v_2}{kT}} e^{-\frac{hc\omega_3 v_3}{kT}}. \quad (32)$$

The sums on  $v_1$  and  $v_3$  are simply geometric series and can be readily summed. The sum on  $v_2$  is slightly more complicated but can also be summed. After combining the sums from the three fundamental modes, the vibration partition sum becomes:

$$Q_v = \left( \frac{1}{1 - e^{-\frac{\omega_1 hc}{kt}}} \right) \left( \frac{1}{1 - e^{-\frac{\omega_2 hc}{kt}}} \right)^2 \left( \frac{1}{1 - e^{-\frac{\omega_3 hc}{kt}}} \right). \quad (33)$$

Numerical values of Equation (33) are tabulated in Table 3. If instead of using the harmonic oscillator energy levels to calculate the vibration partition sum, experimental energy levels were used, the resulting value of the vibration partition sum would probably be more accurate. Gray and Young have done such a calculation,<sup>25</sup> but their values for the vibration partition sum do not differ by more than 0.01 from those given in Table 3.

Table 3. The  $\text{CO}_2$  vibration partition sum,  $Q_v$ , as a function of T using the harmonic oscillator approximation.

Temperature	$Q_v$
100	1.00
200	1.02
300	1.09
400	1.22
500	1.40
600	1.64
700	1.93
800	2.28
900	2.70
1000	3.18

Einstein Absorption Coefficients. The Einstein absorption coefficient,  $B_{mn}$ , which is the second factor in Equation (28), measures the rate at which molecules make the transition from the lower state m to the higher state n by

absorbing a photon of energy  $h\nu_{mn}$ . The coefficient  $B_{mn}$  is equal to a constant times the square of the matrix element of the electric dipole moment  $R^{mn}$ ,

$$B_{mn} = \frac{8\pi^3}{3h^2c} |R^{mn}|^2 . \quad (34)$$

It is instructive to calculate  $R^{mn}$  for the case of a simple harmonic oscillator potential. Let the lower vibrational state be designated by  $v''$  and the higher by  $v'$ , then

$$R^{v''v'} = \int \Psi_{v''}^*(x) M(x) \Psi_{v'}(x) dx , \quad (35)$$

where  $M(x)$  is the electric dipole moment of the molecule. Expanding the electric dipole moment about the equilibrium position and dropping higher order terms, yields

$$\begin{aligned} R^{v''v'} &= M(0) \int \Psi_{v''}^*(x) \Psi_{v'}(x) dx \\ &+ \frac{dM}{dx}(0) \int \Psi_{v''}^*(x) x \Psi_{v'}(x) dx . \end{aligned} \quad (36)$$

The first integral vanishes since the harmonic oscillator eigenfunctions are orthogonal. The second also vanishes except when  $v' = v'' + 1$ . The transition moment then becomes

$$R^{v''v'} = \frac{dM}{dx}(0) \frac{1}{2\alpha} \left( \frac{N_{v''}}{N_{v''+1}} \right) = \frac{1}{\alpha} \frac{dM}{dx}(0) \sqrt{\left( \frac{v''+1}{2} \right)} . \quad (37)$$

Since the intensity of the electric dipole transition is

proportional to the square of the transition matrix element  $R^{v''v'}$ , the intensity is proportional to the consecutive integers 1, 2, 3, . . . for the vibrational transitions  $0 \rightarrow 1$ ,  $1 \rightarrow 2$ ,  $2 \rightarrow 3$ , and so forth.

The potential function for each normal mode of the real  $\text{CO}_2$  molecule is of course not that of a simple harmonic oscillator, but the general harmonic oscillator behavior is still present.

## C H A P T E R   I V

### EXPERIMENTAL SETUP

The CO<sub>2</sub> sample used in this study was heated to make possible the observation of spectral lines originating from high rotation-vibration states. The sample was placed in a stainless steel absorption cell which was heated using an electric furnace to temperatures up to 800 K. Heating the CO<sub>2</sub> sample excited so many rotation-vibration lines in the CO<sub>2</sub> spectrum that the use of a high resolution spectrometer was essential to resolve individual lines. Furthermore, since entire rotation-vibration bands were to be observed, broad spectral coverage was also necessary.

Although there were a number of spectroscopic techniques that could have been used, a Michelson interferometer was the most suitable candidate for providing the required high resolution broad band coverage. Some of the other commonly used spectroscopic techniques are: tunable laser, fixed frequency laser heterodyne, and scanning grating. Tunable lasers and fixed frequency laser heterodyne techniques provide more than sufficient resolution, but do not provide the required broad spectral coverage. A scanning spectrometer using an extremely large grating could conceivably have been used to make the measurement, but since a grating is much less efficient than an interferometer in making use of the energy supplied

by the source, a scanning grating spectrometer was not considered a viable alternative. It can be argued that making effective use of the energy supplied by the source is not necessary for absorption spectroscopy, since the source can be made arbitrarily bright. However, a practical limit for source brightness is soon reached, making the efficient use of the source's energy important. A further advantage of using a Michelson interferometer in making line position measurements is the ease of accurately calibrating the wavenumber scale.

#### Overview of Experimental Setup

A simplified schematic of the overall experimental setup is given in Figure 3. A Nernst glower was used as the source of the infrared radiation. A Nernst glower<sup>26</sup> is a small cylinder made of rare-earth oxides, which when heated by passing an electrical current through it, has a color temperature of roughly 1600 K. The energy from the Nernst glower is first focused down so as to enter the high temperature absorption cell. This absorption cell will be discussed briefly in the next section. After exiting the absorption cell the energy is again focused to an image, where it is chopped using a Bulova vibrating reed chopper. The chopped beam then passes through an infrared filter which limits the energy in the beam to a spectral region of interest. After passing through the infrared filter, the

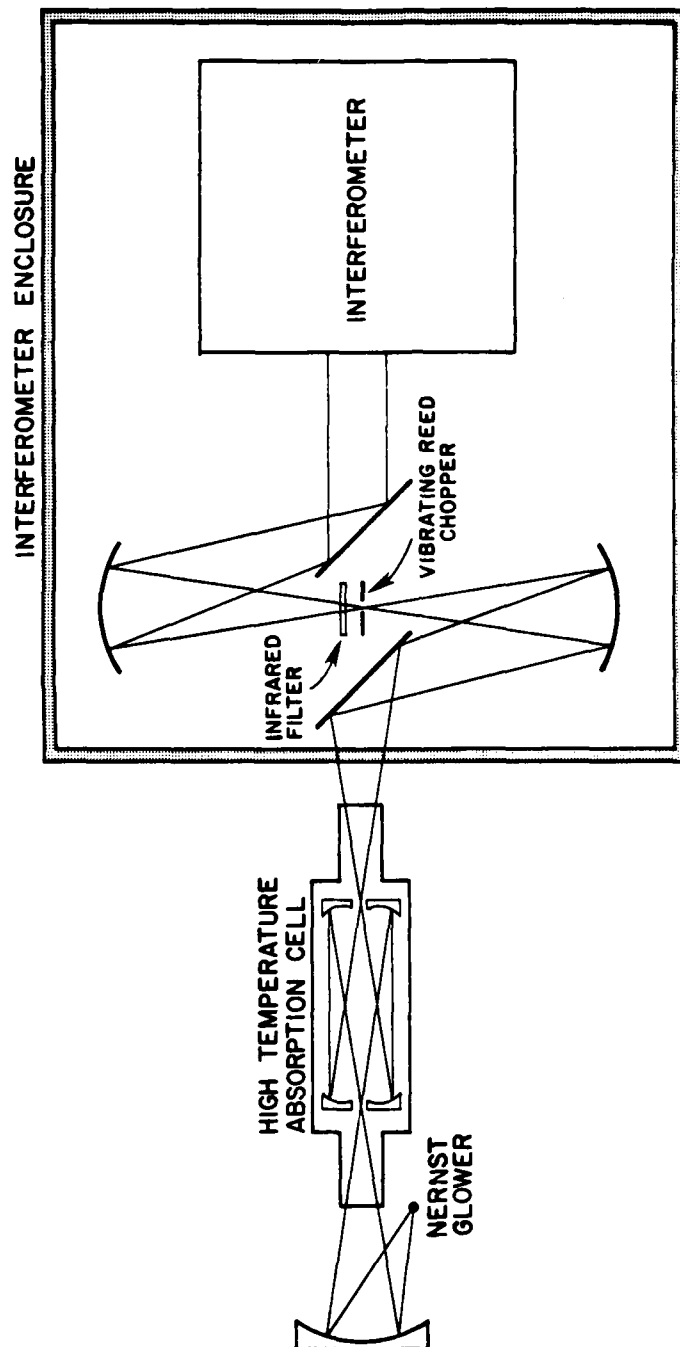


Figure 3. Simplified schematic of the overall experimental setup.

energy is collimated in preparation for entering into the Michelson interferometer. The interferometer will be described in detail in a subsequent section of this report. The entire optical path is maintained under a vacuum, except for a small (5 cm) section between the high temperature absorption cell and the interferometer enclosure, which is purged with dry nitrogen.

#### High Temperature Absorption Cell

The design and fabrication of high temperature optical systems are beset with many technical difficulties. A major problem is finding optical materials for windows and mirrors that maintain their mechanical and optical properties at high temperatures. In addition, the large thermal expansion the optical components experience when being heated from room temperature to 800 K makes it difficult to maintain optical alignment while avoiding stressing the optical components. Since the high temperature absorption cell used in this work has been described in other publications<sup>27</sup> only a brief description of the cell will be given here.

The absorption cell was constructed using rhodium coated fused silica mirrors in the Pfund configuration (Figure 4). J. H. Taylor has demonstrated that a Pfund cell can be used affectively to study high temperature gases.<sup>28</sup> The absorption cell mirrors could be aligned at

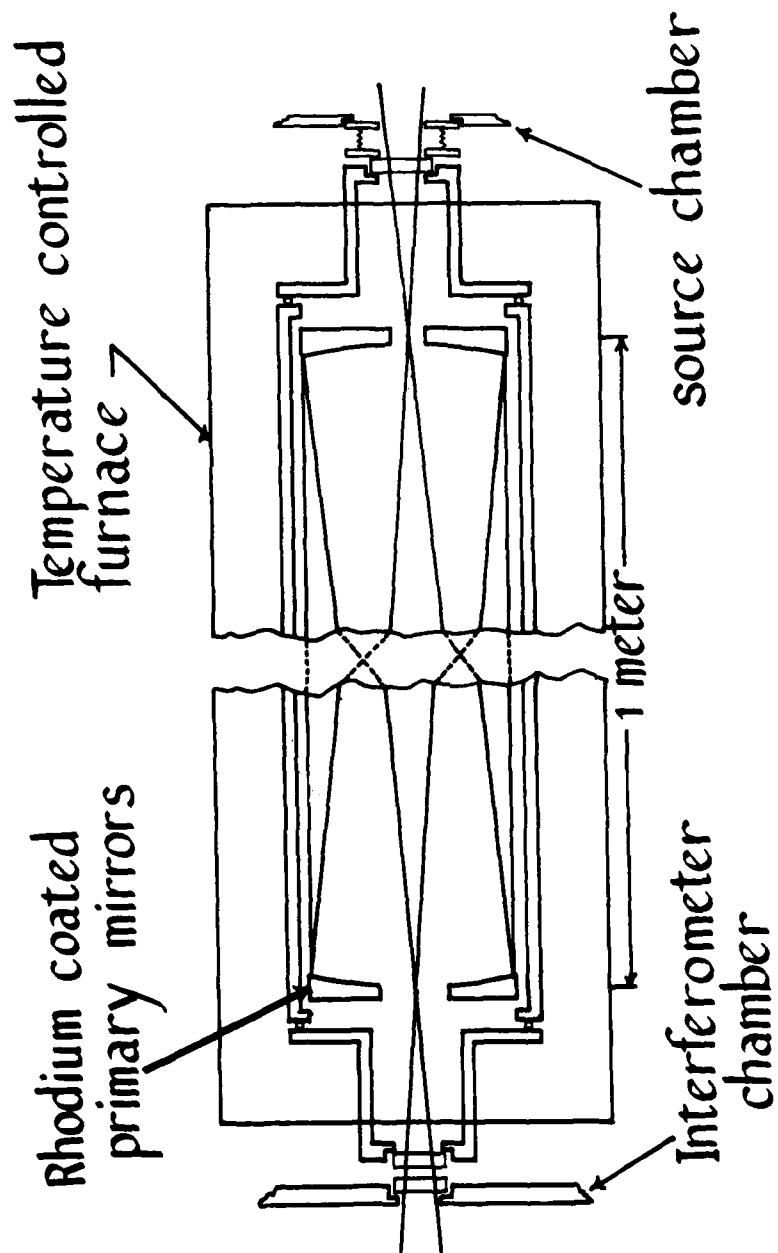


Figure 4. Schematic of the high temperature absorption cell.

room temperature and then the cell heated to 800 K without realigning the cell, due to the Pfund configuration's high tolerance to mirror motion. An additional reason for using a triple pass Pfund configuration cell instead of a multi-traversal cell such as a White<sup>29</sup> cell was the low reflectivity of the rhodium mirrors. After the rhodium coated mirrors had been operated for any length of time at temperatures above 600 K, their reflectivity was substantially reduced.

One disadvantage of the absorption cell used was the nonuniform temperature of the gas sample. Due to the difficulty of maintaining vacuum seals at high temperatures, the  $\text{CaF}_2$  windows were maintained near room temperature, while the temperature of the central one-meter region of the cell was maintained within  $\pm 2$  K of 800 K. The absorption path therefore consisted of three meters of uniform 800 K temperature and two sections of 1/4 meter each in which the temperature rapidly drops from 800 K to near room temperature. Since the objective of the present study was to measure the position of spectral lines, and the position of spectral lines is unaffected by temperature, using an absorption cell with a nonuniform gas temperature was not a problem. However, if the scope of the study had been broadened to include making intensity measurements of spectral lines, the present absorption cell would have caused serious problems. Although it is

possible to determine the intensities of spectral lines in an absorption cell with a nonuniform temperature profile, it is a complicated process for which the temperature profile of the gas sample must be known. Determining the temperature profile of a low pressure gas sample is not simple, particularly since the temperature profile of the gas is not necessarily the same as that of the cell walls due to the likelihood of convective gas currents within the cell.

#### Fourier Spectroscopy

A Fourier spectrometer, unlike a conventional dispersive spectrometer which records the spectrum directly, encodes the spectrum making necessary the use of a Fourier transformation to recover the spectrum. A Fourier spectrometer uses the energy supplied by the source very efficiently. The two main light gathering advantages of a Fourier spectrometer over a conventional dispersive spectrometer are, a multiplex, or Fellgett<sup>30</sup> advantage, and a throughput, or Jacquinot<sup>31</sup> advantage. Unlike a grating spectrometer, which scans each spectral element in sequence, an interferometer is continually gathering information on all spectral elements. This is the multiplex advantage. The throughput advantage will be discussed in a later section.

Principle of Operation of  
a Michelson Interferometer.

A schematic that illustrates the principle of operation of a Michelson interferometer is given in Figure 5. A collimated beam of light from the source falls on the beamsplitter (B. S.) and is divided into two parts. One is reflected off the beamsplitter and is sent to mirror  $M_1$ , the other goes through the beamsplitter and is reflected off the moveable mirror  $M_2$ . Both beams of light recombine at the beamsplitter where they interfere; part of the light is sent to the detector, while the remainder is reflected back to the source. The amount of light reaching the detector is a function of the position of the moveable mirror  $M_2$ .

Let an incoming plane wave of amplitude  $A$  be represented by  $A e^{i(2\pi\sigma x - \omega t)}$  where  $\omega$  is the angular frequency, and  $\sigma$  is the wavenumber of the light. If the amplitude of the wave transmitted through the beamsplitter is  $t$  and the amplitude of the reflected wave is  $r$ , the intensity at the detector is

$$Int = |rt A e^{i(2\pi\sigma x_1 - \omega t)} + tr A e^{i(2\pi\sigma x_2 - \omega t)}|^2, \quad (38)$$

where  $x_1$  is the round trip distance the light travels in going from the beamsplitter to mirror  $M_1$  and back again. The corresponding distance for  $M_2$  is  $x_2$ . By rearranging Equation (38) and letting  $x = x_1 - x_2$ , we find that the

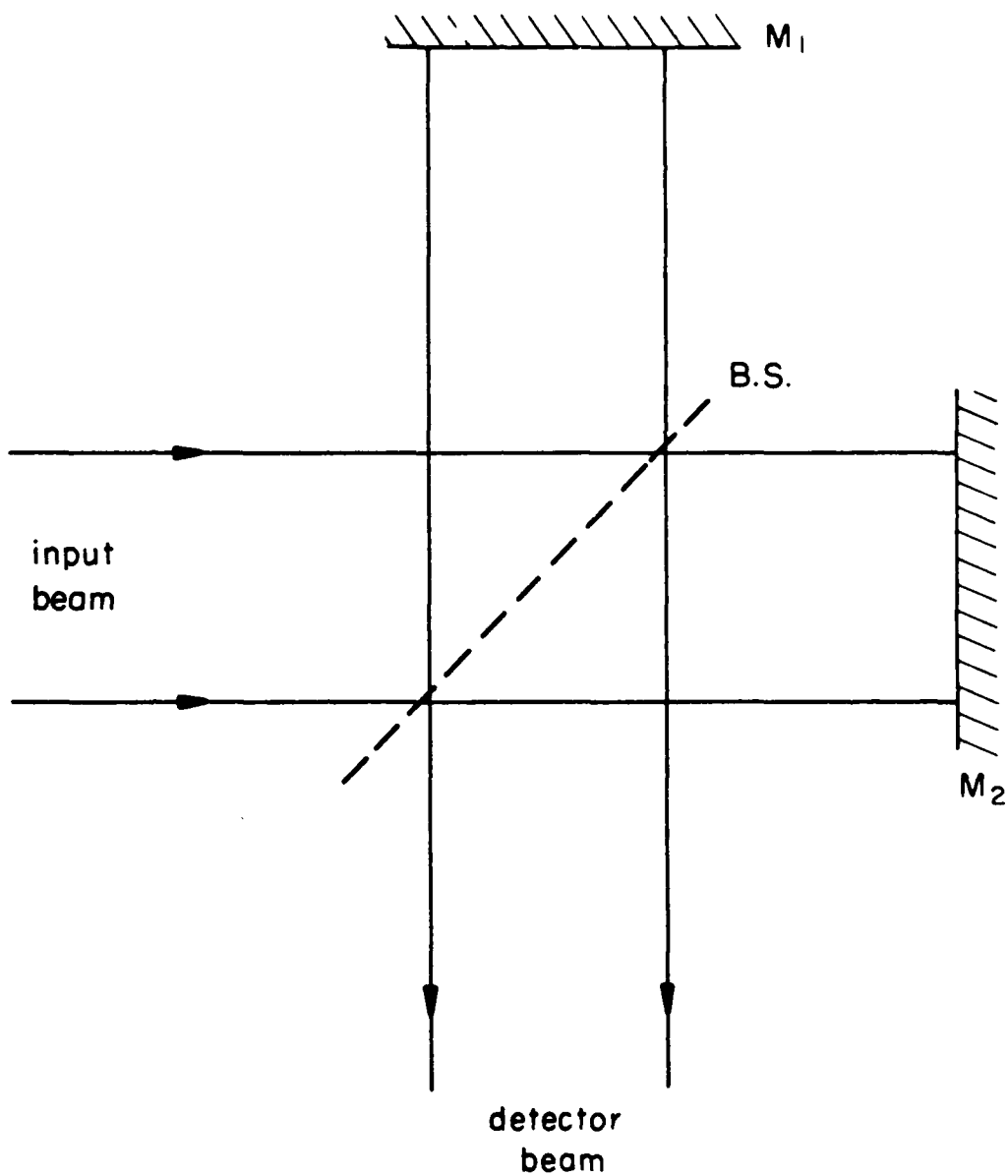


Figure 5. Simplified schematic of a Michelson interferometer.

intensity is given by

$$\text{Int} = 2 A^2 |tr|^2 (1 + \cos(2\pi\sigma x)) . \quad (39)$$

The beamsplitter efficiency is  $|tr|^2$ . For a polychromatic source of intensity  $B(\sigma) = A^2$ , the intensity at the detector is

$$\text{Int} = \int_0^\infty 2 B(\sigma) |tr|^2 (1 + \cos(2\pi\sigma x)) d\sigma . \quad (40)$$

The part of Equation (40) that varies with optical path difference,  $x$ , is defined as the interferogram,  $I(x)$ .

$$I(x) = 2 |tr|^2 \int_0^\infty B(\sigma) \cos(2\pi\sigma x) d\sigma . \quad (41)$$

The spectrum,  $B(\sigma)$ , is obtained by taking the Fourier transformation of the interferogram.

The Fourier transformation can be defined as

$$B(\sigma) = \int_{-\infty}^{\infty} I(x) e^{2\pi i \sigma x} dx , \quad (42a)$$

and the inverse transformation as

$$I(x) = \int_{-\infty}^{\infty} B(\sigma) e^{-2\pi i \sigma x} d\sigma . \quad (42b)$$

When the input function is real and even, its Fourier transformation reduces to the cosine transform.

$$B(\sigma) = 2 \int_0^\infty I(x) \cos(2\pi\sigma x) dx \quad (43)$$

Apodization. The interferogram produced by a real Michelson interferometer can not cover the entire range of  $x$ , from  $-\infty$  to  $+\infty$ , as was implied in Equations (41 and 42), but is limited to the finite range  $-L$  to  $+L$ . Limiting the range of  $x$  to a finite range broadens the instrument function of the interferometer. Any spectrometer provides a spectral signal given by the true spectrum convolved with the instrument function. A spectrometer with infinite resolution generates no spectral distortion, so its instrument function is a Dirac delta function. Real spectrometers, however, provide a finite spectral resolution.

If the input signal to a Michelson interferometer is a monochromatic beam of light, the resulting interferogram is a cosine function truncated at the maximum optical path difference  $L$ . The resulting spectrum, i. e., the Fourier transform of the interferogram, is

$$\text{sinc}(2L\sigma) = \frac{\sin(2\pi L\sigma)}{2\pi L\sigma} . \quad (44)$$

Hence the instrument function for an interferometer, if no other distortion is present in the measured interferogram, is a sinc function with its first zero at  $1/(2L)$ . Hence, the resolution,  $\Delta\sigma$ , of a Michelson interferometer is

$$\Delta\sigma = \frac{1}{2L} . \quad (45)$$

The sinc instrument function has a serious disadvantage, in that it converges to zero very slowly. An instrument function which exhibits faster convergence to zero than the sinc function is created by removing the sharp edges at the end of the interferogram by multiplying the interferogram by various functions. This process is called apodization.

The function used to apodize the interferograms for this work was the triangular function  $T$  given by

$$\begin{aligned} T(x) &= 1 - \frac{|x|}{L} & \text{for } |x| \leq L \\ T(x) &= 0 & |x| > L \end{aligned} \quad (46)$$

Application of the triangular function  $T$  for apodization results in the following instrument function:

$$\text{sinc}^2(L\sigma) = \left\{ \frac{\sin(\pi L\sigma)}{\pi L\sigma} \right\}^2. \quad (47)$$

The instrument function with no apodization and using a triangular function for apodization are compared in Table 4. Note that with no apodization the central feature of the instrument function is sharper, while with apodization the side lobes converge to zero much faster. The disadvantage of all functions used for apodization is their degradation of spectral resolution caused by the broadening of the instrument function.

Table 4. Comparison between no apodization (sinc) and triangular apodization ( $\text{sinc}^2$ ).

x	$\text{sinc}(x)$	$\text{sinc}^2\left(\frac{x}{2}\right)$
0.0	1.0000	1.0000
0.5	0.6366	0.8106
1.0	0	0.4053
1.5	-0.2122	0.0901
2.0	0	0
2.5	0.1273	0.0324
3.0	0	0.0450
3.5	-0.0909	0.0165
4.0	0	0
4.5	0.0707	0.0100
5.0	0	0.0162
5.5	-0.0579	0.0067
6.0	0	0
6.5	0.0490	0.0048
7.0	0	0.0083
7.5	-0.0424	0.0036
8.0	0	0
8.5	0.0374	0.0028
9.0	0	0.0050
9.5	-0.0335	0.0022
10.0	0	0

Sampling the Interferogram. In practice the interferogram produced by a Michelson interferometer is not a continuous function of  $x$ , but is a function which is sampled at equidistant intervals separated by  $\Delta x$ . These sampling locations are determined from the interferogram of a single frequency HeNe laser, which is coaligned with the infrared

beam. The movable mirror  $M_2$  can either be stepped or scanned continuously. In the stepping mode, the interferometer is maintained at a fixed optical path difference,  $x_1$ , while the energy falling on the detector,  $I(x_1)$ , is measured. Mirror  $M_2$  is then stepped to its next position, and the next interferogram data point  $I(x_{1+1})$  is collected.

The spectrum is recovered from the sampled interferogram by means of a discrete Fourier transformation. The discrete Fourier transformation is obtained from the continuous Fourier transformation (Equation (42)) by replacing  $x$  by  $j\Delta x$ ,  $\sigma$  by  $k\Delta\sigma$ , and the integral with a summation over the total number of data points  $N$ . Since the range of the interferogram is from  $-L$  to  $+L$  the interval  $\Delta x$  is given by

$$\Delta x = \frac{2L}{N} . \quad (48)$$

Similarly the spectral interval  $\Delta\sigma$  is

$$\Delta\sigma = \frac{2(\sigma_{\max} - \sigma_{\min})}{N} , \quad (49)$$

where  $\sigma_{\min}$  is the lowest wavenumber in the signal bandpass and  $\sigma_{\max}$  is the highest. It can clearly be seen from Figure 6, where two sampled cosine waves with different periods appear identical, there must be a restriction on the value that  $\Delta x$  can assume. This proper sampling

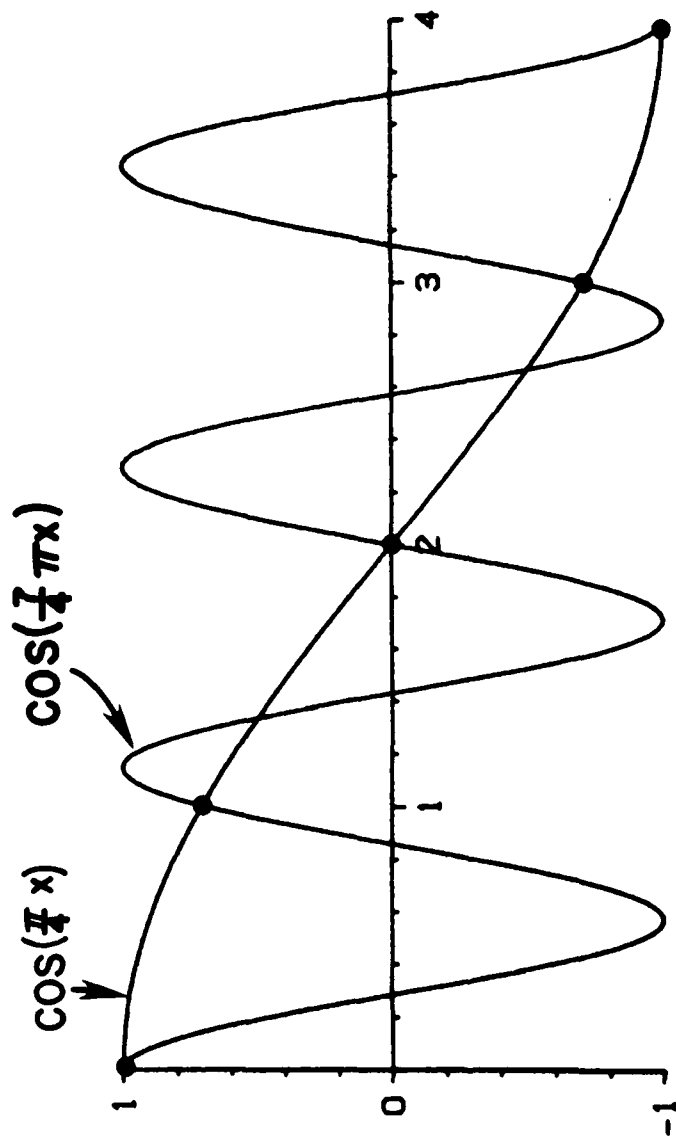


Figure 6. Two sampled cosine functions that appear identical for a sampling interval of  $\Delta x = 1$ .

interval,  $\Delta x$ , for a given spectral bandpass, is given by,<sup>32,33</sup>

$$\Delta x = \frac{1}{2(\sigma_{\max} - \sigma_{\min})} \quad (50)$$

Combining Equations (49) and (50) gives the following important relation

$$\Delta x \Delta \sigma = \frac{1}{N} \quad (51)$$

This relation is then used to write down the discrete Fourier transformation

$$B(k) = \sum_{j=0}^{N-1} I(j) e^{\frac{2\pi i k j}{N}}, \quad (52a)$$

and its inverse

$$I(j) = \frac{1}{N} \sum_{k=0}^{N-1} B(k) e^{-\frac{2\pi i k j}{N}}. \quad (52b)$$

There is a certain amount of arbitrariness in the definition of the discrete Fourier transformation. An alternative definition which is more consistent with the continuous Fourier transformation defined in Equation (42) is

$$B(k) = \Delta x \sum_{j=0}^{N-1} I(j) e^{\frac{2\pi i k j}{N}}, \quad (53a)$$

and the inverse

$$I(j) = \Delta \sigma \sum_{k=0}^{N-1} B(k) e^{-\frac{2\pi i k j}{N}}. \quad (53b)$$

However, Equation (52) is the definition of more standard usage<sup>34,35</sup> and so will be used for the remainder of the present work.

Finite Field of View. A complication that arises with Fourier spectrometers is that both the source and the detector are finite in size. Therefore the light going through the interferometer is comprised of rays with a range of finite angular extent. The optical path differs by a factor of  $\cos\alpha$  for off-axis rays compared to on-axis rays, where  $\alpha$  is the off-axis angle. When a detector of finite size is used, the interferogram, Equation (41), has to be modified by integrating over the solid angle,  $\Omega$ , subtended by the detector,

$$I(x, \Omega) = 2 |tr|^2 \int_{-\infty}^{\infty} B(\sigma) \int_{\Omega} \cos(2\pi\sigma x \cos\alpha) d\sigma d\Omega'. \quad (54)$$

When the small angle approximation is used, and a circular detector assumed,  $\Omega$  is equal to  $\pi\alpha^2$ . After integrating over  $\Omega'$ , Equation (54) becomes

$$I(x, \Omega) = 2 |tr|^2 \int_{-\infty}^{\infty} B(\sigma) \Omega \operatorname{sinc}\left(\frac{\sigma x \Omega}{2\pi}\right) \cos\left(2\pi\sigma x \left(1 - \frac{\Omega}{4\pi}\right)\right) d\sigma. \quad (55)$$

It can be seen that a finite detector introduces two effects; the amplitude of the interferogram is modulated by a sinc function, and the positions of spectral features are

shifted from their true position by

$$\frac{\delta \sigma}{\sigma} = - \frac{\Omega}{4\pi} . \quad (56)$$

The decrease in amplitude of the interferogram caused by the multiplying sinc function can be reduced to an acceptable level by limiting the solid angle  $\Omega$ . The solid angle is conventionally limited so that the argument of the sinc is always less than or equal to 1/2,

$$\Omega \leq \frac{\pi}{\sigma_{\max} L} , \quad (57)$$

where  $\sigma_{\max}$  is the highest optical frequency and  $L$  is the maximum optical path difference in the interferogram. Alternatively the off-axis angle  $\alpha$  for the detector must be specified by

$$\alpha \leq \left( \frac{1}{\sigma_{\max} L} \right)^{\frac{1}{2}} . \quad (58)$$

When this criterion is used, the amplitude of the interferogram is attenuated by less than a factor of 0.64, even at the highest optical frequency.

Throughput Advantage. The throughput,  $E$ , or étendue, of an optical system is defined as

$$E = A\Omega , \quad (59)$$

where  $A$  is the area of the collecting optics, and  $\Omega$  is the solid angle accepted by the system.

The throughput advantage of a Michelson interferometer over a grating spectrometer is demonstrated by comparing the throughput of the two systems. The throughput of a Michelson interferometer,  $E_m$ , is the area of the interferometer optics,  $A$ , times the solid angle accepted by the interferometer (Equation (57)),

$$E_m = \frac{A\pi}{\sigma L} . \quad (60)$$

The resolving power of a spectrometer is defined as

$$R = \frac{\sigma}{\Delta\sigma} . \quad (61)$$

Combining Equations (60), (61) and (45) gives the throughput of a Michelson interferometer in terms of the resolving power  $R$  as

$$E_m = \frac{2\pi A}{R} . \quad (62)$$

The throughput of a grating spectrometer,<sup>36</sup>  $E_g$ , is

$$E_g = \frac{lA}{fR} , \quad (63)$$

where  $l$  is the length of the grating spectrometer slit, and  $f$  is the collimator focal length. The throughput advantage of a Michelson interferometer is then

$$\frac{E_m}{E_g} = \frac{2\pi}{l/f} . \quad (64)$$

It is very difficult to construct a grating spectrometer for which the slit length,  $l$ , is not considerably shorter than the collimator focal length,  $f$ . Even when compared to a very fast grating spectrometer, the ratio,  $E_m/E_g$ , is on the order of 200.<sup>36</sup>

Wavenumber Calibration. Aligning the infrared beam to be parallel with the laser reference beam does not insure accurate wavenumber calibration unless the solid angle subtended by the two beams is identical. In practice, the solid angle of the laser reference beam is generally much smaller than that of the infrared beam. The wavenumber shift factor, Equation (56), depends on the solid angle subtended by the detector,  $\Omega$ , so it is necessary to introduce a small correction to the wavenumber scale of the recovered spectrum. It is possible to measure the field of view of the infrared beam and the reference laser beam very accurately, and then calculate this wavenumber correction. However, in practice, it is usually easier to calibrate the wavenumber scale of the recovered spectrum using the position of a few very accurately measured lines. Since Fourier spectrometers intrinsically provide broad spectral coverage, it is not difficult to find a few lines of CO, CO<sub>2</sub>, or lines of some other molecule that have been as accurately measured to serve as an internal wavenumber standard.

Beamsplitter Compensation. Beamsplitters used in the infrared region of the spectrum are usually constructed using a thin dielectric film deposited on a substrate material which is transparent in the infrared. A schematic of a Michelson interferometer showing the finite thickness of the beamsplitter substrate is given in Figure 7. The part of the beam that is reflected to mirror  $M_1$  and back to the beamsplitter does not pass through the beamsplitter substrate while the part of the beam which is transmitted through the beamsplitter and subsequently reflected from mirror  $M_2$  must traverse the beamsplitter substrate twice. Since the optical thickness of the beamsplitter substrate is a function of wavenumber, the position of zero path difference for optical signals of each wavenumber is shifted by an amount  $\delta(\sigma)$ . The interferogram,  $I'(x)$ , which including the effects of dispersion in the beamsplitter substrate is

$$I'(x) = \int_{-\infty}^{\infty} B(\sigma) e^{-2\pi i \sigma [x - \delta(\sigma)]} d\sigma . \quad (65)$$

There is now no clear position of zero path difference, since the phase of each cosine wave comprising the interferogram is different. To minimize this phase difference, a compensator plate made of the same substrate material as the beamsplitter is usually placed in front of the beamsplitter to equalize the dispersion between the two paths of the interferometer (Figure 8). In the case

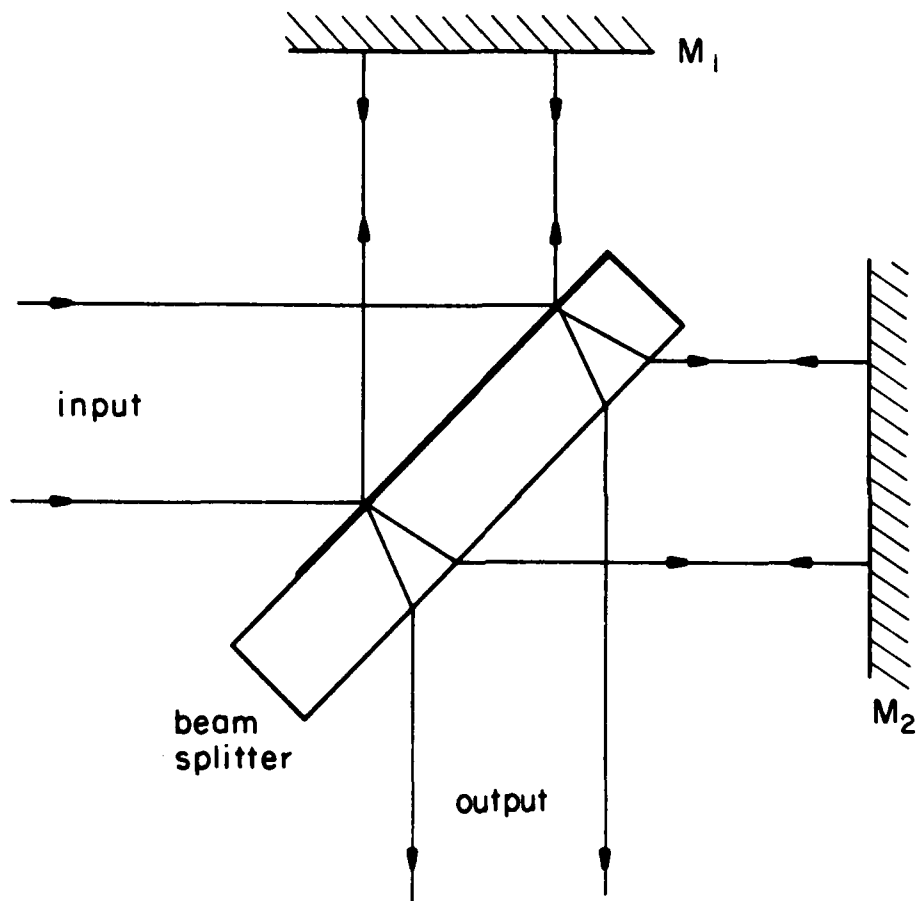


Figure 7. Schematic of a Michelson interferometer showing finite beamsplitter thickness.

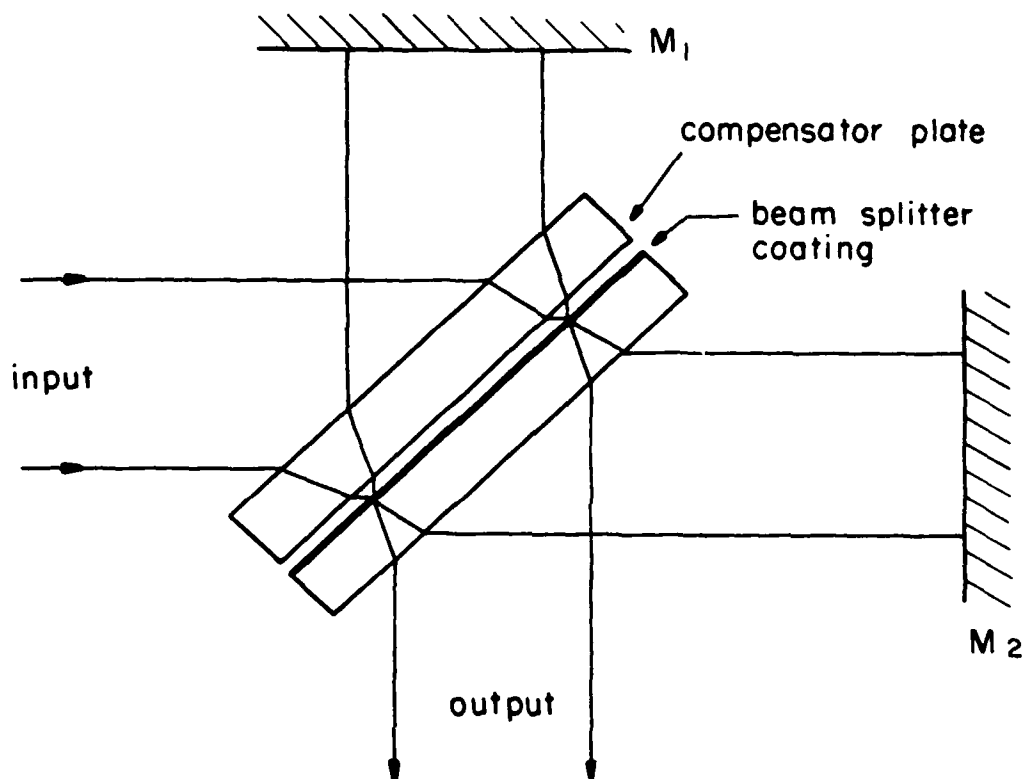


Figure 8. Beamsplitter compensation using an additional compensator plate.

of a cat's eye interferometer, such as the AFGL Two-meter Interferometer, the input and output beams are physically displaced. This physical displacement makes possible beam-splitter compensation by depositing the beamsplitter coatings on opposite faces of the same substrate plate (Figure 9).

#### The AFGL Two-Meter Interferometer

The interferometer that was used for the present study was built by Idealab for the Air Force. It is located at the Air Force Geophysics Lab (AFGL) on the Hanscom Air Force Base in Bedford, Massachusetts. Although the interferometer was designed to achieve a maximum optical path difference of two meters, for the present study a maximum optical path of only 83 cm was used. The interferometer is of the step and hold type, where the interferogram is sampled at a fixed optical path difference, the interferometer is then stepped to the next holding location and the next data point of the interferogram sampled. A Digital Equipment PDP-8/E minicomputer is used to provide the commands which control the interferometer stepping. The PDP-8/E is also used to record the interferogram data. The interferometer has been used previously by Hajime Sakai to record the spectra of several atmospheric molecules<sup>37,38</sup> and has been described in previous publications.<sup>39,40</sup> During the course of the

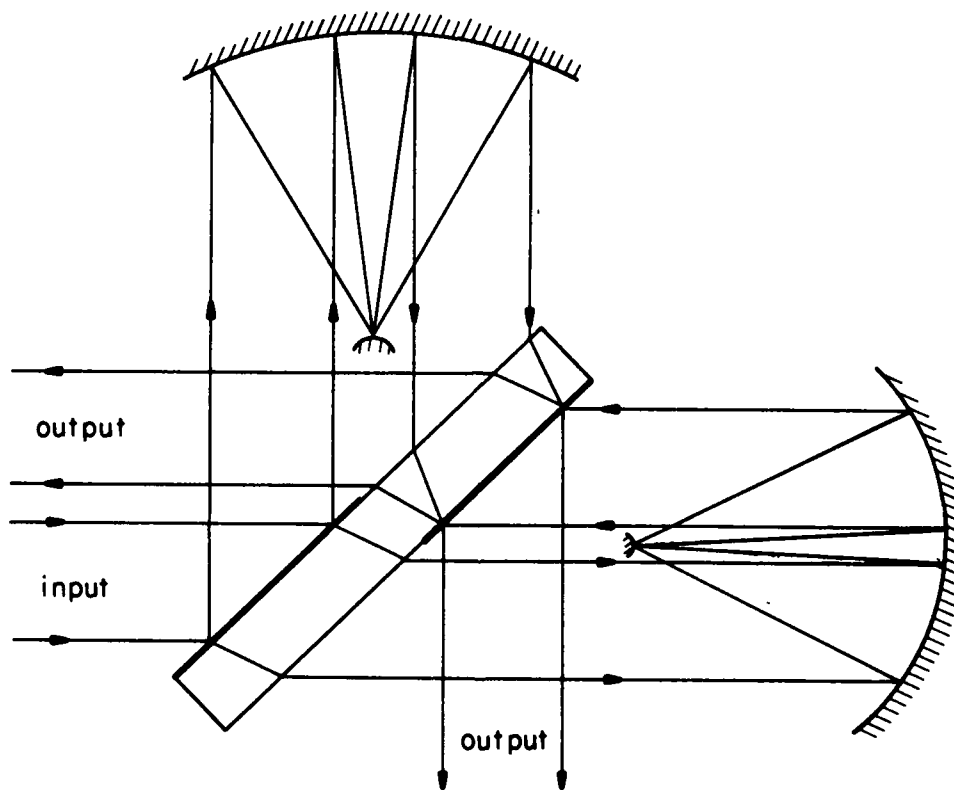


Figure 9. Beamsplitter compensation using opposite faces of the same substrate plate.

present study the reliability of the interferometer stepping has been markedly improved by upgrading the PDP-8/E stepping control software. This enhanced stepping software provides detailed diagnostic information on all stepping peculiarities and provides automatic self correction for the more commonly occurring stepping errors.

Overview of Interferometer. The AFGL interferometer uses cat's eye retroreflectors instead of flat mirrors. A cat's eye retroreflector consists of a small convex mirror mounted at the focal point of a large concave mirror as illustrated in Figure 10. The outgoing beam from a cat's eye retroreflector stays parallel to the incident beam, even when the incident beam is tilted with respect to the optical axis of the cat's eye. There are two main advantages that a cat's eye interferometer has over a conventional flat mirror interferometer. First, due to the property that the outgoing beam is parallel to the incoming beam, the use of a cat's eye retroreflector relaxes the required parallelism of the interferometer drive mechanism and makes the interferometer alignment very stable. The AFGL two-meter interferometer will stay in alignment for over a year at a time. The second advantage of a cat's eye system is that the incident and the reflected beams are laterally displaced allowing the use of two complementary detectors. The resulting interferogram is the difference

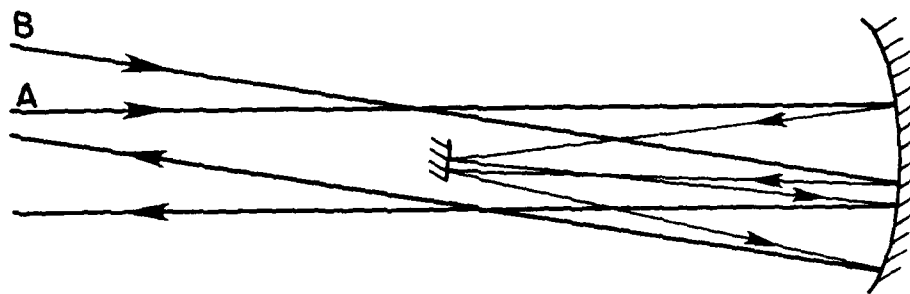


Figure 10. The optical layout of a cat's eye retro-reflector. Note that for either an on-axis ray (a) or an off-axis ray (b) the outgoing ray is parallel to the incident ray.

between these two complementary channels. Use of two detectors helps minimize the effects of source fluctuations and instrumental drifts. The two detectors and their preamplifiers are matched, making the measured interferogram insensitive to any perturbing effect which influences both channels equally.

A photograph of the AFGL interferometer is given in Figure 11 and a detailed schematic in Figure 12. The infrared energy enters the interferometer from the bottom in the photograph and from the left in the schematic. The infrared beam first passes above mirror  $M_4$  and strikes the upper half of the beamsplitter, BS, where it is divided into two beams. One beam is sent to the stationary cat's eye,  $CE_1$ , and the other to the moveable cat's eye,  $CE_2$ . Since the cat's eyes introduce a shear, the returning beams strike the lower half of the beamsplitter. One output beam goes to detector  $D_1$  by means of folding mirrors  $M_1$  and  $M_2$  and collecting mirror  $M_3$ . The second output beam goes to detector  $D_2$  by means of folding mirrors  $M_4$  and  $M_5$  and collecting mirror  $M_6$ . The beam from the HeNe reference laser follows a path similar to that of the infrared energy. Mirror  $M_7$  directs the laser beam to the beamsplitter where the laser beam is split into two beams. After recombining again at the beamsplitter, one output beam is directed to the laser detector  $D_3$  by means of folding mirror  $M_8$  and the other goes directly to detector  $D_4$ .

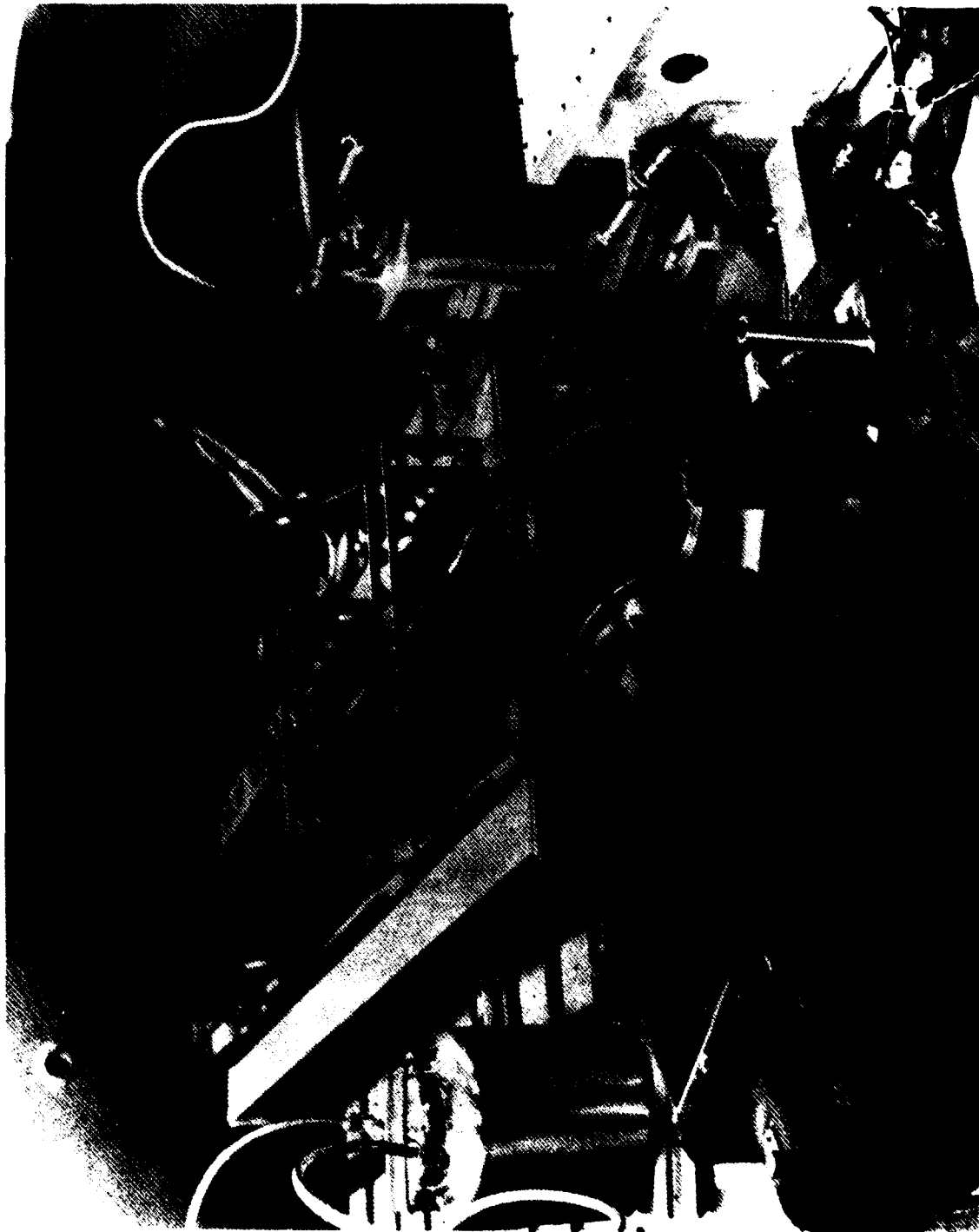


Figure 11. Photograph of the AFGL high resolution interferometer

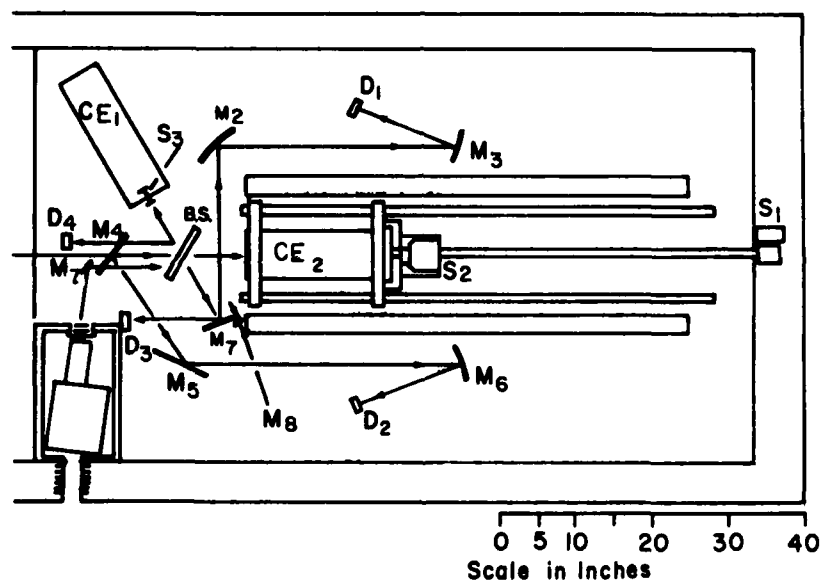


Figure 12. Schematic of AFGL high resolution interferometer. See text for further explanation.

The interferometer is housed in a vacuum enclosure. There are three main advantages of operating an interferometer in a vacuum. First, evacuating the interferometer avoids the problem of atmospheric lines in the spectrum arising in the instrument instead of from the source to be observed. This is particularly important when the observed source contains  $\text{CO}_2$ . Second, no wavenumber correction for the index of air need be made to the spectrum. The index of refraction of air is not constant for the laser reference frequency and the different infrared frequencies. Therefore, when an interferometer is operated in air, a non-linear correction term must be applied to the measured spectrum. Finally, operating in a vacuum, eliminates acoustic vibrations transmitted through the air which can disrupt the interferometer stepping. To further reduce vibrations, the interferometer enclosure is mounted on a set of air filled vibration isolators.

The Interferometer Drive. The interferometer drive mechanism provides a path length stability of approximately  $0.01 \mu\text{m}$  at each holding position, yet can be stepped to provide more than a meter of optical path difference. This represents a range of motion covering 8 orders of magnitude. Three sources of change in optical path difference are used, each with its own range of motion. These are shown in the schematic of Figure 12, they are: 1)

a dc motor which drives a lead screw,  $S_1$ ; 2) a linear magnetic motor,  $S_2$ ; and 3) a piezoelectric transducer,  $S_3$ . Large, but not very accurate, changes in optical path difference are provided by the dc motor turning the lead screw. The lead screw is coupled to the movable cat's eye by a linear electric motor with a range of motion of about 1 cm. Very delicate adjustments in path length are provided by mounting the small mirror of the fixed cat's eye on a stack of piezoelectric barium titanate crystals. The piezoelectric stack is driven with up to 100 volts to produce small (about  $0.2 \mu\text{m}$ ) but fast changes in path length.

Considerable care must be taken in the design of an interferometer to ensure that the moveable cat's eye will translate smoothly, while minimizing vibration and mechanical stresses. Thus, the movable cat's eye is mounted on a cart that rides on a set of precision bearings. These bearings ride on two very accurately aligned parallel stainless steel rails called ways. Also attached to the cart are two oil-filled dashpots to help damp out oscillations. In order to avoid vibration and possible mechanical stress, the cart is coupled to the lead screw only through the magnetic induction of the linear electric motor.

The three sources of motion are coupled together into a single servo system to provide large, yet very accurate,

changes in optical path difference. An inductive type position sensor is used for the source of feedback for the lead screw motor. The feedback signal for both the linear motor and the piezoelectric stack is supplied by the laser reference signal. For a cat's eye interferometer, the laser reference signal is the difference in signal between the two complementary detectors. An example of the laser reference signal is given in Figure 13. When the signal is maximum, constructive interference is occurring at one detector and destructive interference at the other. When the signal is minimum, the role of the two detectors has been reversed. During the holding mode the interferometer is maintained at a position where the signals from the two complementary detectors are equal. At this position the reference signal is the most sensitive to changes in path length.

In the holding mode both the linear electric motor and the piezoelectric stack are used to maintain a fixed value of the optical path length. To carry out a one laser wavelength step, the hold servos are turned off and the linear motor drives the mirror to the next holding position, where the hold servos are again turned on. When the linear motor moves a short distance from the center of its working range, the dc motor drives the lead screw to recenter it.

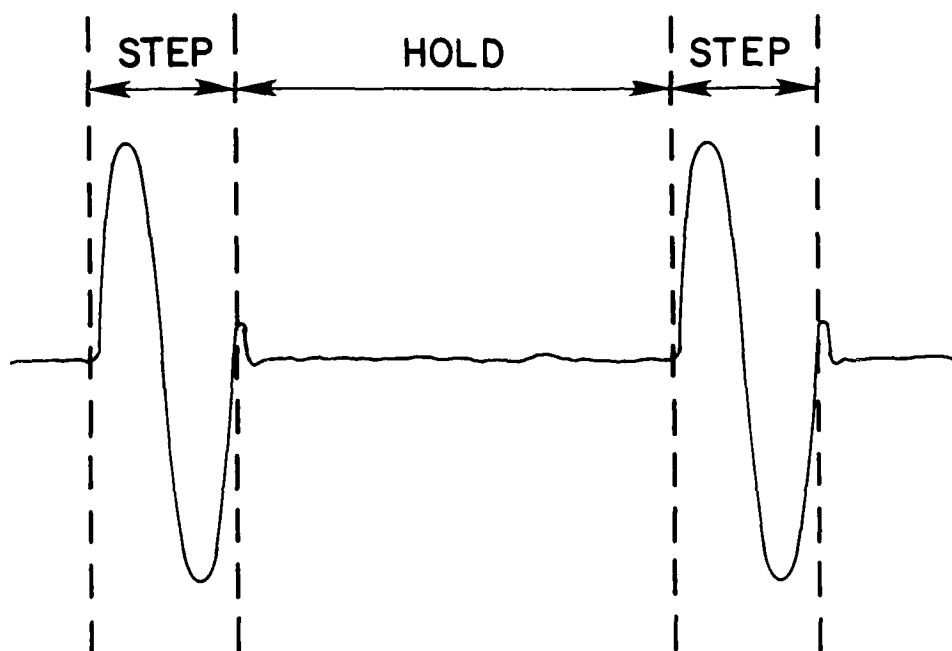


Figure 13. Laser reference signal demonstrating the stepping and holding modes of the interferometer.

Data Acquisition. The data acquisition system is a hybrid system in which part of the processing is done with dedicated electronics and part with a PDP-8/E minicomputer. In addition to data acquisition, the PDP-8/E minicomputer also controls interferometer stepping. Analog electronics are used to difference the signals from the two complementary infrared detectors, while synchronous demodulation and signal averaging is performed with the minicomputer.

A block diagram of the data acquisition and stepping control electronics is given in Figure 14. The signals from the two infrared detectors are slightly rounded 400 Hz square waves, since the infrared beam is chopped at 400 Hz by a vibrating-reed chopper before entering the interferometer. The signals from the two complementary detectors are first amplified using separate preamplifiers. Next, since the signals from the two infrared detectors are not precisely matched, one of the signals is sent through a variable gain amplifier in order to match the two signals. The two signals are then differenced. Since the signals from the infrared detectors are complementary, this process doubles the interferogram signal while canceling the signal from the background. The interferogram signal is next matched to the range of the ADC ( $\pm 1$  volt) with a variable gain amplifier. The interferogram signal then enters the analog multiplexer of the PDP-8/E data acquisition system.

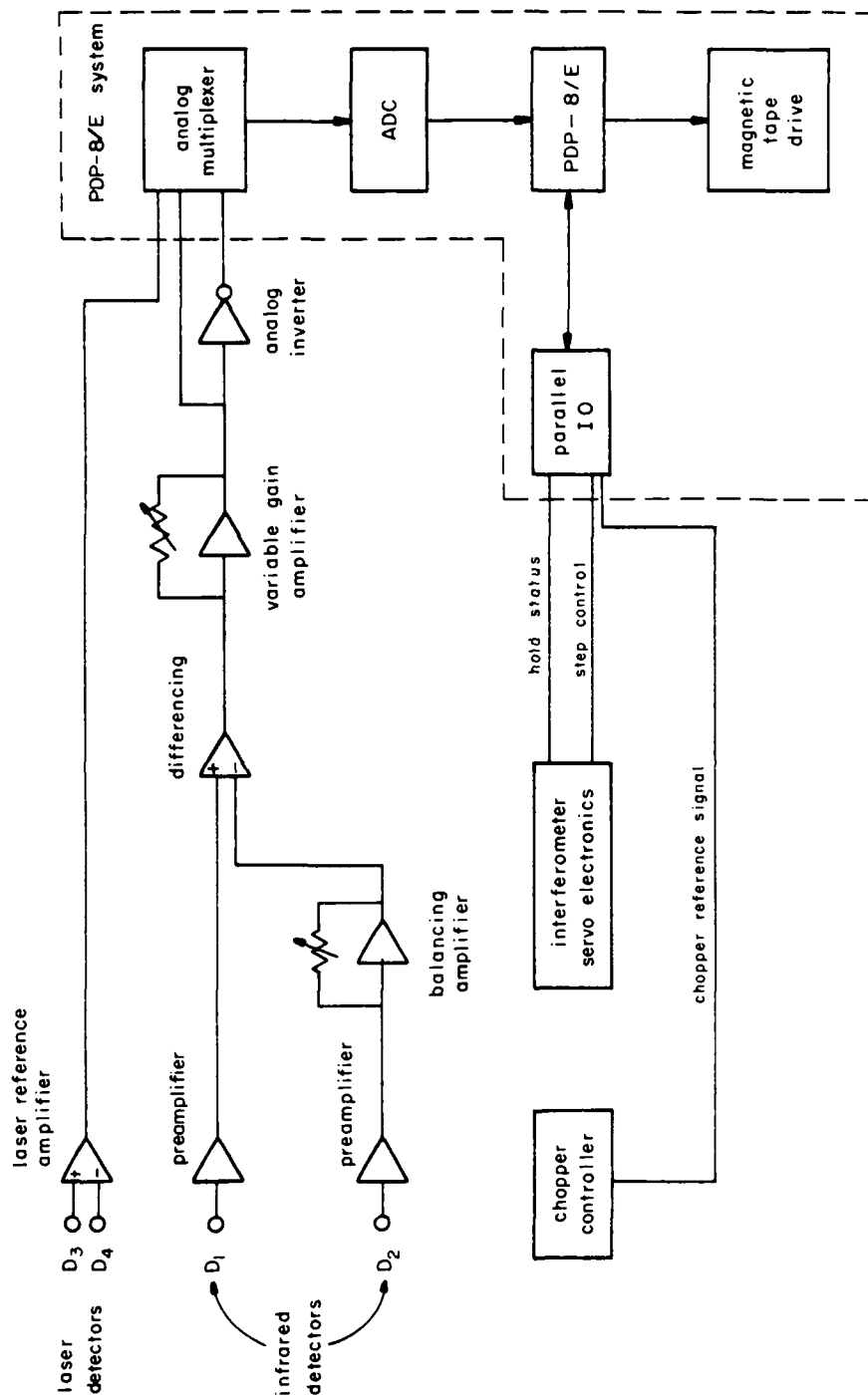


Figure 14. Data acquisition and stepping control electronics.

To assist in the demodulation of the chopped signal, the inverse interferogram signal is also fed into a channel of the analog multiplexer.

Synchronous demodulation is accomplished digitally. The computer is programmed to monitor the chopper reference signal to determine the state of the chopper. As soon as the chopper opens the Digital Equipment 10 bit ADC converter samples the signal repeatedly and sums the samples into a double precision PDP-8/E 24-bit word. When the chopper closes, the resulting background signal is subtracted by switching the analog multiplexer to the inverse interferogram signal and again sampling repeatedly and summing to the same double precision 24-bit word. The interferometer is typically maintained in the same holding position for 12 chopper cycles, and the interferogram sampled 24 times each chopper cycle, making a total of 288 samples per holding position. Summing 288 10-bit samples together improves the precision of the signal by a factor of the square root of 288 or about 17, making the precision of the data slightly more than 14 bits. After 640 points of the interferogram have been sampled, averaged, and stored in a buffer, they are then written on magnetic tape. The buffer is filled repeatedly until the entire interferogram has been recorded. The typical recording time for a  $10^6$  point interferogram is 15 hours.

Computer Control of the Interferometer. The PDP-8/E computer stepping and holding control software was upgraded during the course of the present study. In this upgraded software system, in addition to generating the commands causing the interferometer to step, the computer monitors the quality of each stepping and holding period. The quality of each stepping or holding motion is determined from the characteristic of the laser reference signal. The computer records detailed information about any stepping or holding peculiarities that arise. The computer has also been programmed to take, if necessary, corrective action for the most commonly occurring errors. Making the system partially self-correcting has increased the reliability of the interferometer, but the most significant benefit has been the improved diagnostic capability. Before the computerized diagnostic feature was implemented, it was almost impossible to determine the nature of infrequently occurring errors. When errors occur at rates as low as one in 10,000 steps, or lower, it is almost impossible to "catch" the interferometer in the "act" of a misstep without implementing some sort of automatic error detection method. When the nature of stepping errors are known, the servo parameters can usually be adjusted to eliminate the errors.

A flow chart illustrating the main features of the

interferometer control and data acquisition computer program is given in Figure 15. A listing of the assembly language program CONTST (CONTRol and stepping TeST) is given in Appendix C. The program was written with the goal of multiplexing efficiently several tasks at once. For example while the ADC converter is in the process of performing a conversion, the computer is processing the results from the previous conversion. The analog multiplexer on the Digital Equipment data acquisition system makes it possible to sample the infrared interferogram signals as well as to monitor the laser reference signal with one ADC. The laser reference signal is monitored only while the signal from the infrared detectors would not be valid interferogram data. These times occur when the interferometer is stepping, when the interferometer is settling down after a step, and when the chopper is in transition from open to closed, or from closed to open. Since the natural frequencies of the interferometer drive are lower than the chopper frequency, the interferometer motion can be adequately monitored at chopper cycle intervals.

The most common type of stepping error occurs in the transition period between the turning off of the holding servos and the turning on of the step drive. If a vibration of sufficient amplitude and the right phase is present during this transition period, the movable mirror

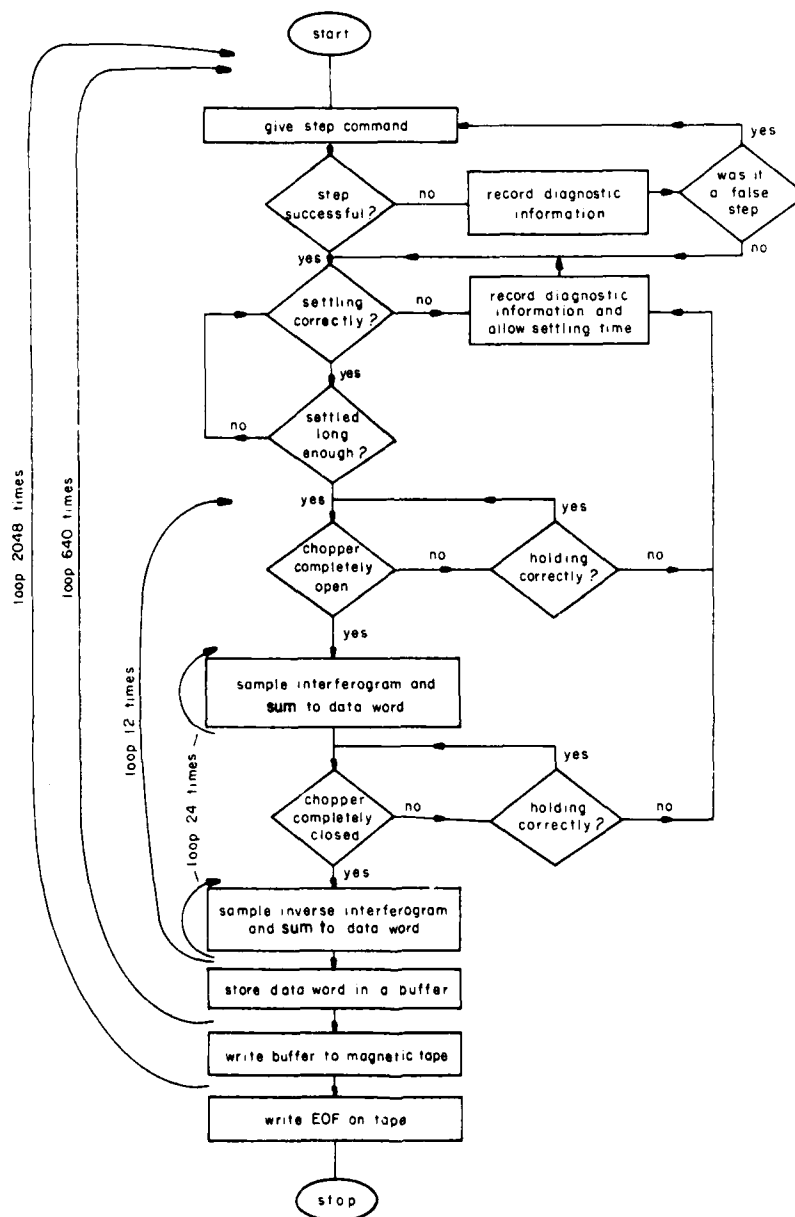


Figure 15. Flow chart of interferometer control and data acquisition program.

can be pushed backward a considerable distance. After being forced backward, the interferometer starts driving forward again. The laser reference signal soon matches the preset level where the interferometer servo controller interprets the step as having been completed. The holding servos are again turned on, but instead of completing a step, the interferometer has returned to its original position. The laser reference signal that results when this type of false step occurs is represented in Figure 16. The computer, monitoring the laser reference signal, detects the lack of a positive peak as a stepping error. The stepping software corrects this type of error by causing the interferometer to step again.

The laser reference signal is monitored during the holding mode as well as during the stepping mode. The control software detects when the interferometer is not holding properly (within about  $0.05\text{ }\mu\text{m}$ ). When this happens the computer stops taking data until the interferometer has settled down, then retakes the affected interferogram data point.

If a mechanical vibration of the interferometer mirrors cause the optical path length to change by more than half a laser wavelength ( $0.3\text{ }\mu\text{m}$ ), the hold servos will no longer provide negative feedback and so will not be able to bring the interferometer back to the proper holding position. This condition is monitored by the control

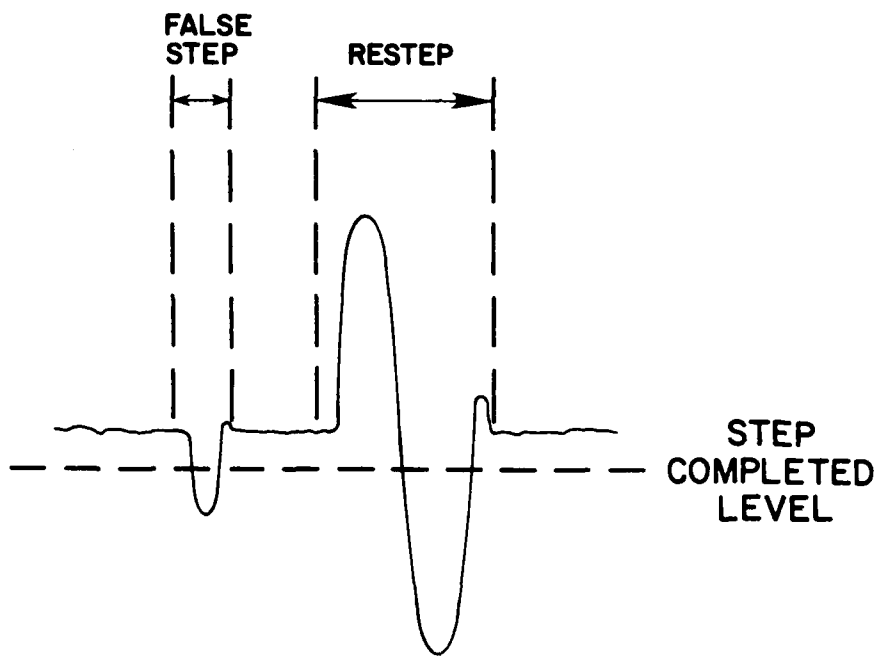


Figure 16. The laser reference signal showing a stepping error and its correction.

software and diagnostic information is recorded, but corrective action is not taken. Using the air-filled vibration isolators and operating in a vacuum make these irrecoverable errors uncommon. However, the acoustic vibrations from a thunder shower will sometimes couple through the interferometer enclosure sufficiently to cause irrecoverable errors.

#### Modification of Interferometer

In addition to the CO<sub>2</sub> bands in the 4.3 and 2.8  $\mu\text{m}$  regions which were analyzed in the present study, there are important CO<sub>2</sub> bands in the 15  $\mu\text{m}$  region which could not be observed without modification of the interferometer. To meet this need, and to make the interferometer more flexible for future observations, the spectral coverage of the interferometer was extended to over 20  $\mu\text{m}$  by replacing the CaF<sub>2</sub> beamsplitter and gold doped germanium detectors with a KBr beamsplitter and copper doped germanium detectors. The upgraded interferometer was then used to take preliminary CO<sub>2</sub> data in the 15  $\mu\text{m}$  region and HDO data in the 7.3  $\mu\text{m}$  region. It would have been possible to take some HDO measurement without upgrading the interferometer, but it would have been difficult, since the response of the interferometer before the upgrade was so low at the longer wavelengths.

KBr Beamsplitter. The optical properties of KBr make it a good material to use for infrared beamsplitters. It has a low index of refraction and transmits from the visible to beyond 25  $\mu\text{m}$ . However, since KBr is soft and hygroscopic, it is difficult to work with. We had on hand a KBr beamsplitter with a germanium coating that had been in storage for a number of years. Since KBr has a tendency to cold flow, there was considerable risk that the beamsplitter would not be sufficiently flat to be still usable. In addition, even though the beamsplitter had been stored with a desiccant in an airtight container, there could have been subtle damage to the beamsplitter or the coating. To insure that the beamsplitter had not been damaged by this long storage, several tests were performed on it before it was mounted. Special care was taken in the design and fabrication of the mount for the KBr beamsplitter, since even a small amount of stress on the beamsplitter would have distorted it. As the mount was being tightened on the beamsplitter, the flatness of the beamsplitter was monitored to insure that it was not being stressed.

Since the input and output beams for the AFGL High Resolution Interferometer are physically displaced it is not necessary to use two KBr plates, one for the beamsplitter and the other for the compensator. Instead a

single KBr plate with coatings covering part of each face of the plate is used (Figure 9). The energy coming into the interferometer is split into the two components using the coating on the front of the KBr plate and then recombined at the coating on the back surface of the KBr plate. The germanium coatings on each face of the KBr plate consist of two separate regions of coating, a heavier germanium coating for the infrared signal and a lighter germanium coating for the visible reference laser. The pattern of coatings for the beamsplitter is given in Figure 17.

The flatness of the beamsplitter was tested by placing an optical flat in contact with the beamsplitter and then observing the fringes produced from a helium lamp. The beamsplitter was flat to within two fringes ( $1/10$  fringe at  $10\mu\text{m}$ ), except for three areas near the edge where the nonflatness was greater than 10 waves. These areas appear to have been damaged by a previous mounting of the beamsplitter, possibly when the beamsplitter was being fabricated. It was possible to orient the beamsplitter in the mount so that these damaged areas of the beamsplitter would not be used.

The optical properties of the beamsplitter were verified by measuring the transmission and reflectance of the beamsplitter. Spectral traces (Figure 18) were obtained from regions of the beamsplitter with both types of coating, the light coating used for the reference laser

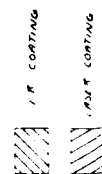
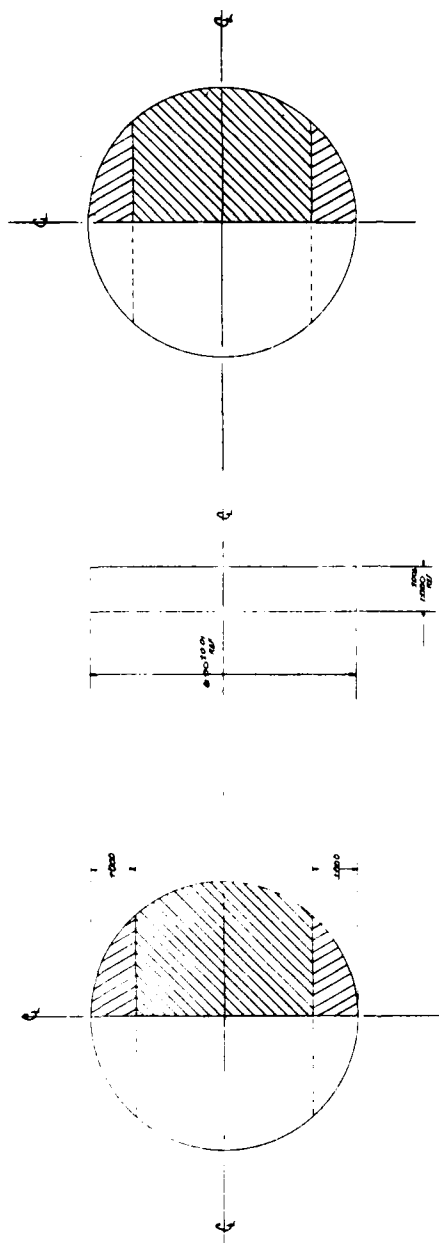


Figure 17. The pattern of germanium coatings on the beamsplitter.

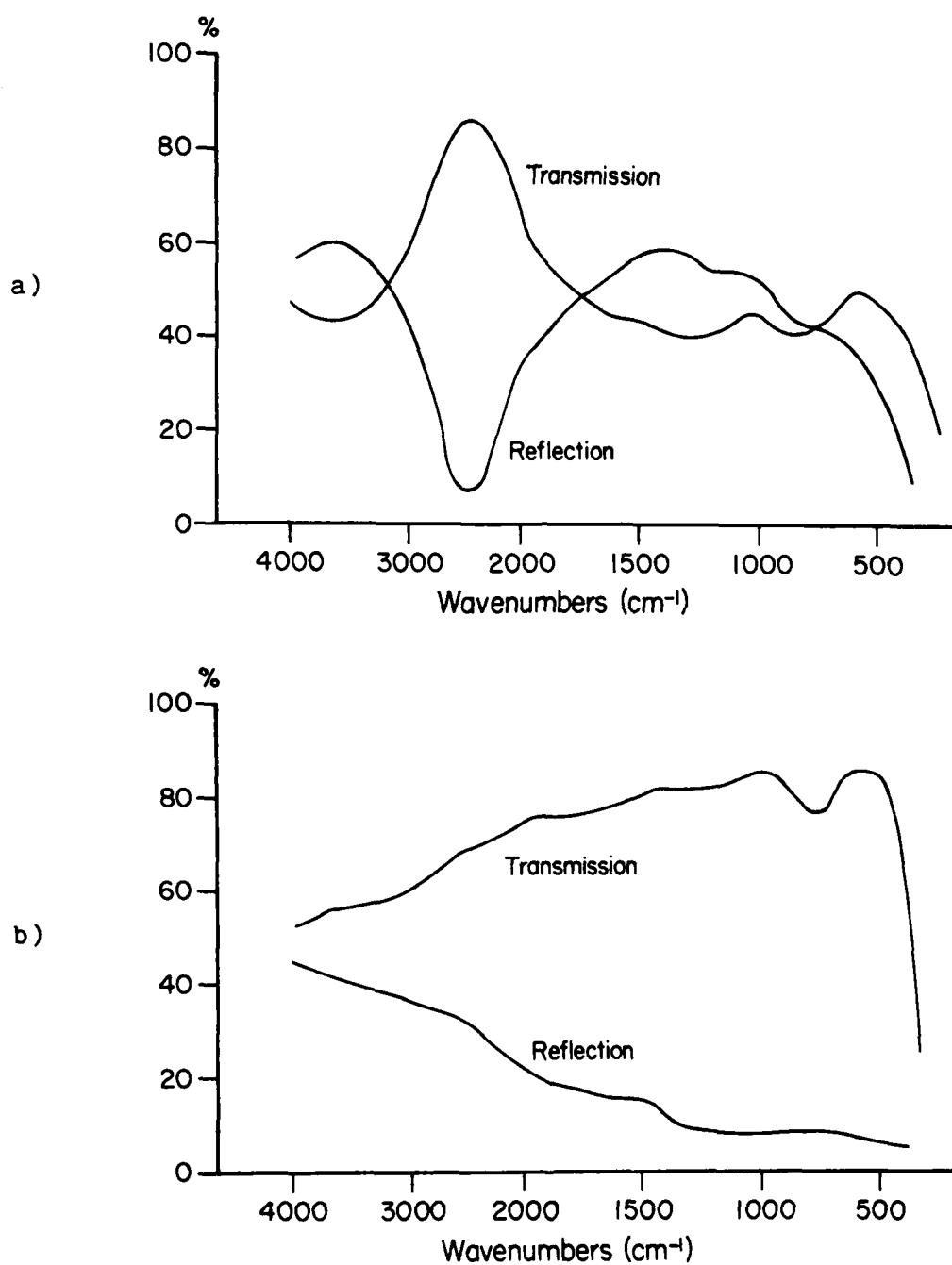


Figure 18. Transmission and reflection of the beamsplitter for a) the heavy coating used for the infrared, and b) the lighter coating used for the laser reference.

and the heavy coating used for the infrared signal. The spectral traces were measured by Fred Volz on a Perkin-Elmer 180 spectrometer. Due to the configuration of his optical setup, the transmission measurement was performed at normal incidence and the reflection measurement at  $10^{\circ}$  incidence. Since the beamsplitter was to be used at an angle of  $30^{\circ}$ , these measurements could not be used directly to determine the expected efficiency of the interferometer, but they did show there were no major problems with the beamsplitter.

A diagram of the mount that was used for the KBr beamsplitter is given in Figure 19. The beamsplitter is held by spring pressure against three pads. The tension in the springs was adjusted such that the pressure from the pads on the beamsplitter was 20 psi (well below KBr's elastic limit of approximately 160 psi). Additional radial support for the beamsplitter was provided at three locations by using a nylon screw to hold a support against the edge of the beamsplitter at each of the three locations. If no precautions were taken, even the small excursions of temperature expected in a laboratory environment would cause sufficient differential expansion between the aluminum mount and the KBr substrate to stress the KBr. To minimize this problem, instead of mounting the KBr beamsplitter directly against the three mounting pads, two plastic shims were placed between each pad and the

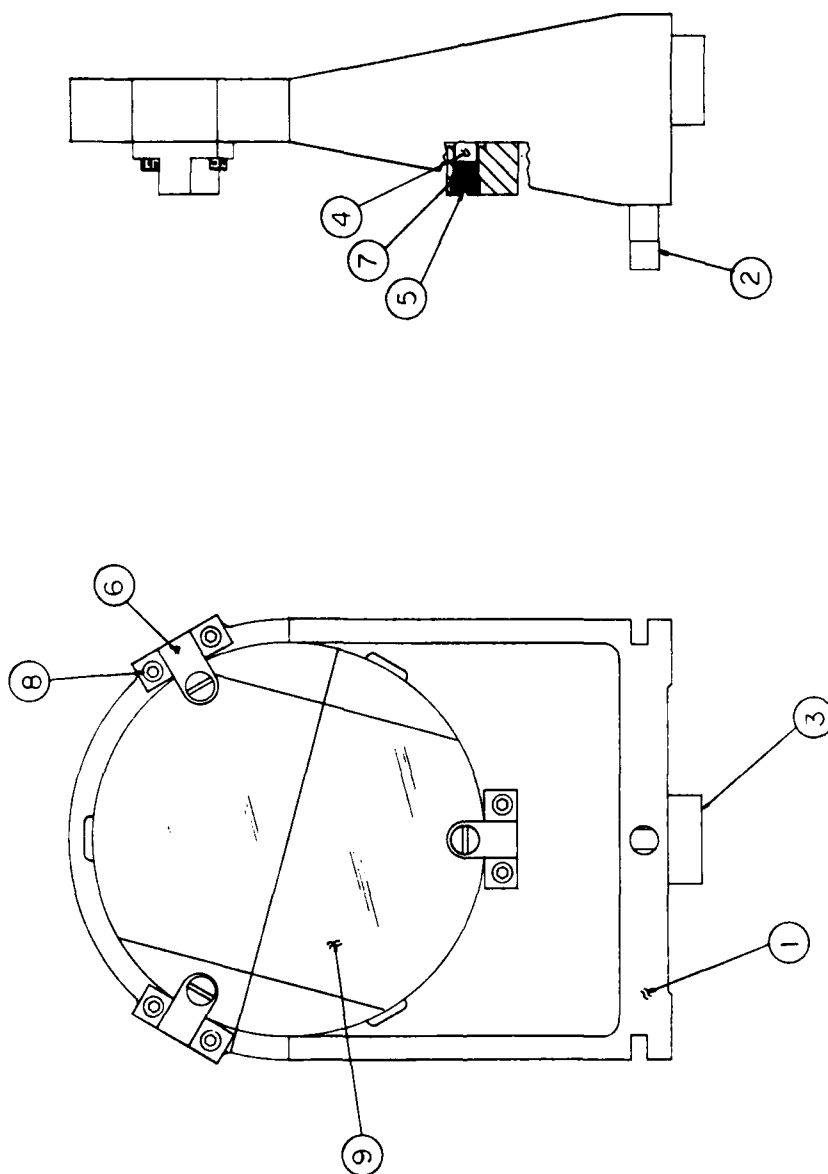


Figure 19. The mount used for the KBr beamsplitter: 1) KBr beamsplitter mount, 2) Rotating pin, 3) Location pin, 4) Pressure pin, 5) Pressure pin locking screw, 6) Pressure pin pedestal, 7) Compression spring, 8) Socket head cap screw, 9) KBr beamsplitter.

beamsplitter. The differential expansion between the beamsplitter and the mount is compensated by these plastic shims slipping past each other.

To insure that the mounting process was not distorting the beamsplitter as the mounts were being tightened, an optical flat was placed in contact with the beamsplitter and the fringes observed as the loading on the beamsplitter was slowly applied.

The Detectors. Copper doped germanium detectors were used, because of their high detectivity over a broad spectral range, to extend the wavelength coverage of the interferometer. A disadvantage of Cu:Ge detectors is that they will not operate at liquid nitrogen temperatures, but must instead be operated at liquid helium temperatures. Not only is liquid helium much more expensive than liquid nitrogen, it is also much more difficult to work with, partly due to the colder temperatures involved, and partly due to the low heat of vaporization of liquid helium. The AFGL High Resolution Interferometer uses two detectors instead of the more conventional single detector. In the upgraded interferometer both detectors were placed in a single liquid helium dewar. By placing both detectors in a single liquid helium dewar the complexity of filling and maintaining two dewars was avoided. Having a single dewar also reduces the quantity of liquid helium consumed. In

addition, having both detectors in the same dewar helps keep the environmental conditions for the two detectors matched, so that proper common mode rejection can take place. It was however necessary to reroute the optical beams of the interferometer. The new optical configuration is shown in Figure 20.

The size of the detectors and the way they were mounted simplifies future modifications to the interferometer. The 0.5 mm diameter detectors are mounted behind interchangeable cold stops. Provisions were also made for cold filters in front of the detectors. The cold stops and cold filters are used to minimize photon noise. At present, the cold stops are set at  $7.2^\circ$  full angle and no cold filters are being used. The cold stop angle was set at  $7.2^\circ$  since the interferometer is currently operating with f/8 collection optics. The 0.5 mm diameter detectors are smaller than needed for f/8 collection optics, but will be well suited for future reductions in the f-number of the interferometer collection optics.

The Cu:Ge detectors were obtained from SBRC (The Santa Barbara Research Center). The detectors were tested at SBRC by illuminating them with a calibrated blackbody source. The results and conditions of the test are summarized in Table 5.

The preamplifiers that were used to amplify the signal from the detectors incorporated low noise FET-input op-amps

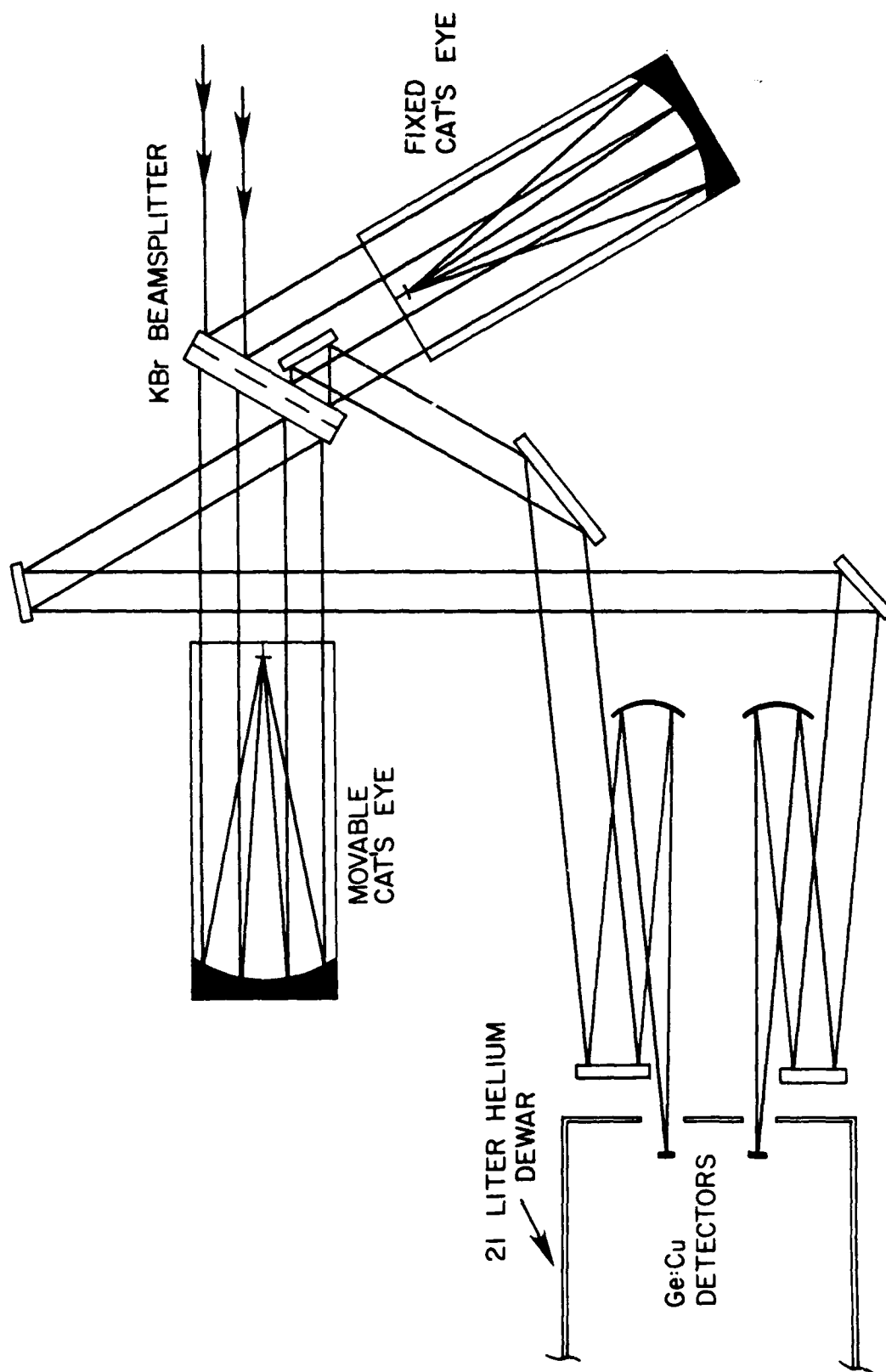


Figure 20. Optical layout with KBr beamsplitter and copper doped germanium detectors.

AD-A173 808

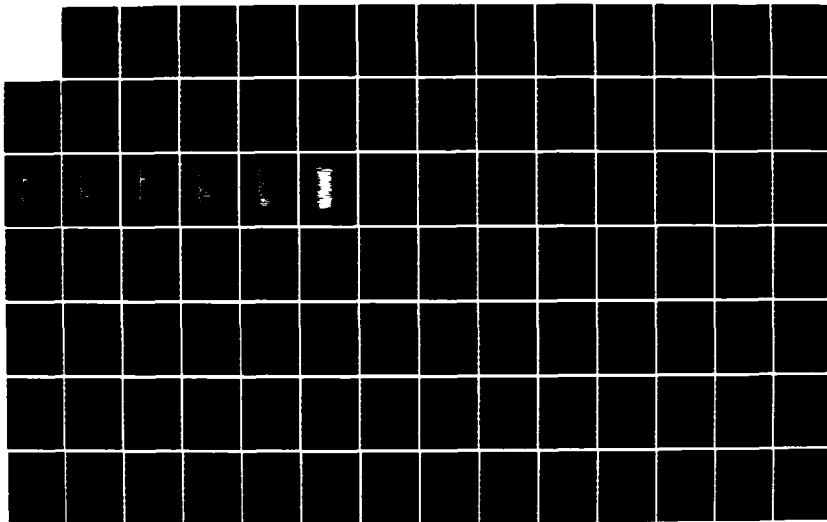
CARBON DIOXIDE LINE POSITIONS IN THE 28 AND 43 MICRON  
REGIONS AT 800 KELV. (U) UTAH STATE UNIV BEDFORD MA  
STEMART RADIANCE LAB M P ESPLIN ET AL. 19 FEB 86  
SCIENTIFIC-16 AFGL-TR-86-0046

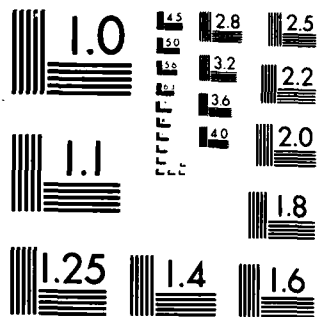
2/4

UNCLASSIFIED

F/G 7/4

ML





MICROCOPY RESOLUTION TEST CHART  
NATIONAL BUREAU OF STANDARDS-1963-A

Table 5. Copper doped germanium detector test specifications and detector performance.

<u>TEST SPECIFICATIONS</u>			
Filtering:	KRS-5 window	Irradiance:	$1.26 \mu\text{w-cm}^{-2}$
Blackbody Temperature:	500°K	Bandwidth:	10Hz
Chopping Frequency:	400Hz	Load Resistance:	2.5 megohms
Operating Temperature:	10°K	Amplifier:	G=100
Background:	$8 \times 10^{15} \text{ ph cm}^{-2} \text{ s}^{-1}$		

DETECTOR INFORMATION	Detector Number		<u>units</u>
	E278-1	E278-2	
Detector Diameter:	0.5	0.5	mm
Spectral Response:	2-27	2-27	$\mu\text{m}$
Detector Resistance:	18	15	megohms
Signal:	59	63	$10^{-3}$ volts
Noise:	0.9	1.0	$10^{-4}$ volts
Signal-to-Noise Ratio:	656	630	
NEP ( $\lambda$ ):	6.2	6.21	$10^{-13} \text{ WHz}^{-1/2}$
$D^*$ ( $\lambda$ pk):	7.42	7.13	$10^{10} \text{ cm Hz}^{1/2} \text{ W}^{-1}$
Responsivity $_{\lambda}$ (in circuit):	2.4	2.4	A/W
$\lambda_{\text{pk}}$ :	25	25	$\mu\text{m}$
Applied Voltage:	45	60	volts

used in the transimpedance mode. After the detector signals have been amplified the signals are filtered. A schematic of the design used for the preamplifiers and filters is given in Figure 21. The bandwidth of the signal was left at a relatively high 10 khz, since further filtering is done digitally. The rest of the signal processing is identical to that used with the Au:Ge detectors and was described previously (see Figure 14).

The requirements on the liquid helium dewar were that it have at least a 24 hour hold time, and that it could be filled without opening the interferometer enclosure. A print of the dewar, which was custom manufactured by Kadel Engineering Corp., is given in Figure 22. The 21 liter liquid helium dewar has a hold time of approximately 30 hours. A liquid helium dewar must be much larger than a nitrogen dewar to obtain the same hold time, even though the thermal resistance of helium dewars is typically higher than liquid nitrogen dewars. When the Kadel dewar is filled with liquid nitrogen, it has a hold time of about 30 days. To make it possible to fill the liquid helium dewar without opening up the interferometer, transfer lines leading from the dewar to the outside of the interferometer enclosure were necessary. These transfer lines are six feet long. The heat loss through these long transfer lines is not excessive, since during normal operation of the

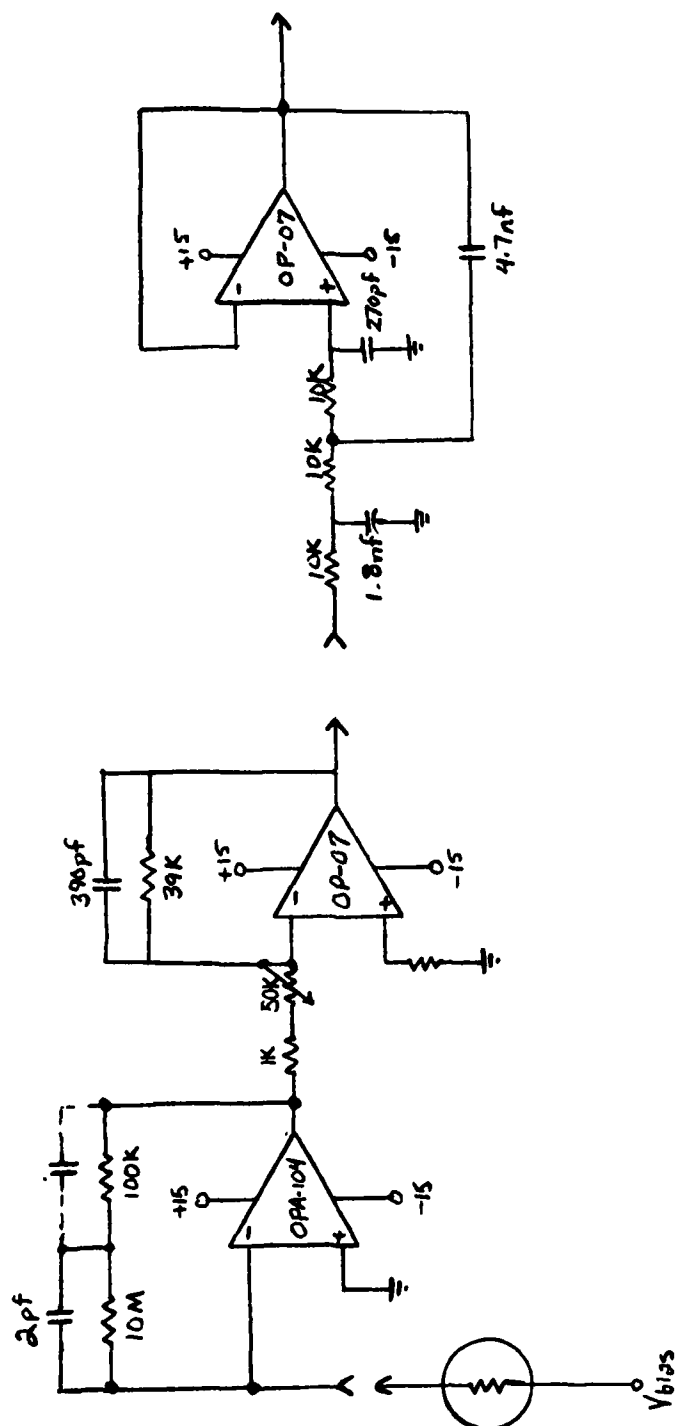


Figure 21. Detector preamplifier and filter design.

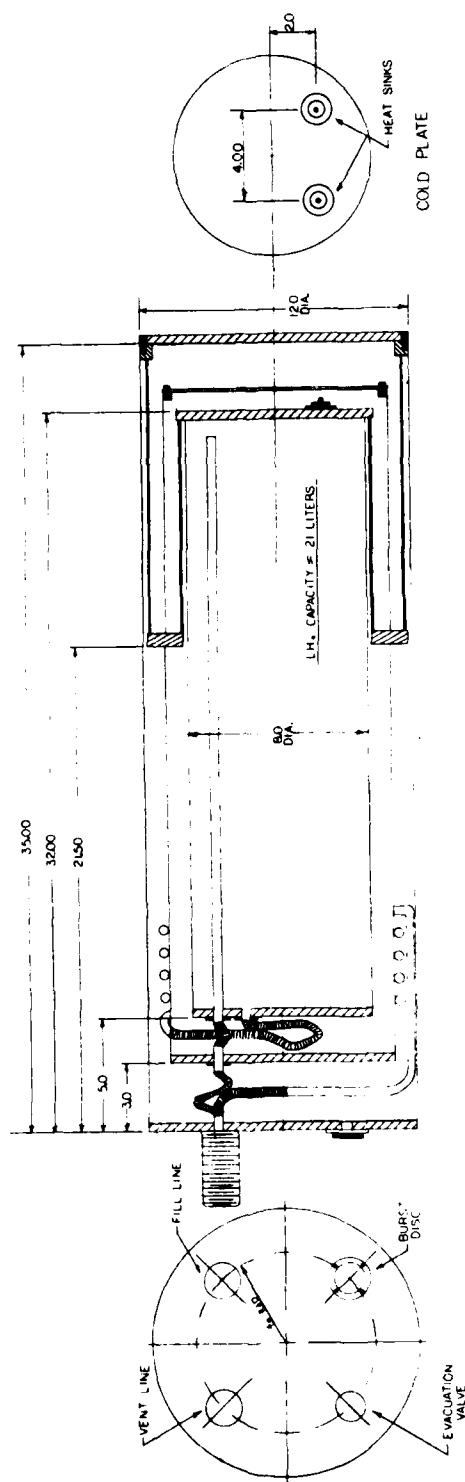


Figure 22. Kadel liquid helium dewar.

interferometer a vacuum is maintained in the interferometer enclosure.

The most troubling problem that we have experienced in connection with the liquid helium dewar was acoustic oscillations in the transfer lines. These vibrations were a problem both during the filling process and during the entire time that the dewar contained liquid helium. Acoustic oscillations in tubes connected with a liquid helium dewar are called Taconis vibrations.<sup>41</sup> These oscillations are standing waves in the tubes driven by large temperature gradients. Since they transfer heat from the warm outside into the cold dewar, they decrease the hold time of the liquid helium dewar. These vibrations are most intense when a tube that is closed on the room temperature end opens into a liquid helium dewar and there is a large temperature gradient at the midpoint of the tube.<sup>42</sup> It should be possible to minimize these oscillations by making the transfer tube a less effective resonator or decreasing the temperature gradient of the tube. During the filling process it was found helpful not to vent the helium directly to the atmosphere, but instead vent the helium through a length of tubing packed with steel wool. During the time when the dewar was holding helium it was found that placing low pressure check valves on both the fill and vent lines was effective in dampening out vibrations.

Testing the Modified Interferometer. After overcoming a few problems, the interferometer was used to take preliminary data. The most troubling problem was with the germanium coating on the portion of the beamsplitter used for the laser reference beam. A workable solution to this problem was arrived at by modifying the laser detector electronics. There was also a problem due to channel spectrum caused by the ZnSe windows on the dewar. The channel spectrum was removed by replacing the flat windows with wedged windows.

The problem with the portion of the beamsplitter used for the laser reference beam arose because of the high absorption of visible light by germanium. The problem was not with insufficient energy transmitted through the beamsplitter, since the coating is very thin, but with the phase of the transmitted and reflected beams. Since the AFGL High Resolution Interferometer uses cat's eye retroreflectors, both output beams of the interferometer are accessible. For a dielectric beamsplitter, the phase of these two output beams is complementary and the interferogram is taken as the difference of the signals from the two detectors. In this subtraction process, all perturbing influences which affect both channels equally are subtracted out. However, when a metallic beamsplitter is used, the signals from the two detectors are in phase<sup>43</sup>

and so cannot be subtracted. Since germanium absorbs so strongly in the visible, the germanium coating acts almost like a metallic coating resulting in the two outputs from the laser reference beam being nearly in phase. To get around the problem, the electronics for the laser reference signal was modified to use only one detector. A new beamsplitter that will not use germanium for the laser reference beam has been ordered, but for the present, modifying the electronics to use only one detector has proved quite satisfactory.

The first spectra to be taken with the interferometer after the modification were  $\text{CO}_2$  broadened with  $\text{N}_2$ . These spectra were taken at moderate resolution (maximum optical path difference of 8 cm). An example of one of these experimental spectra is given in Figure 23 for 100 torr of  $\text{CO}_2$  broadened with 660 torr of  $\text{N}_2$ . It was while doing these  $\text{CO}_2$  measurements that the severity of the channel spectrum due to the ZnSe detector windows was discovered. Most of the small structure in Figure 23 around 620 wavenumbers is due to channel spectrum. The flat ZnSe windows have since been replaced with windows that are wedged 12 arc minutes. Future plans include remeasuring the  $\text{CO}_2$  spectrum using the wedged window.

Measurements of HDO have also been performed using the modified interferometer. These measurements were made at

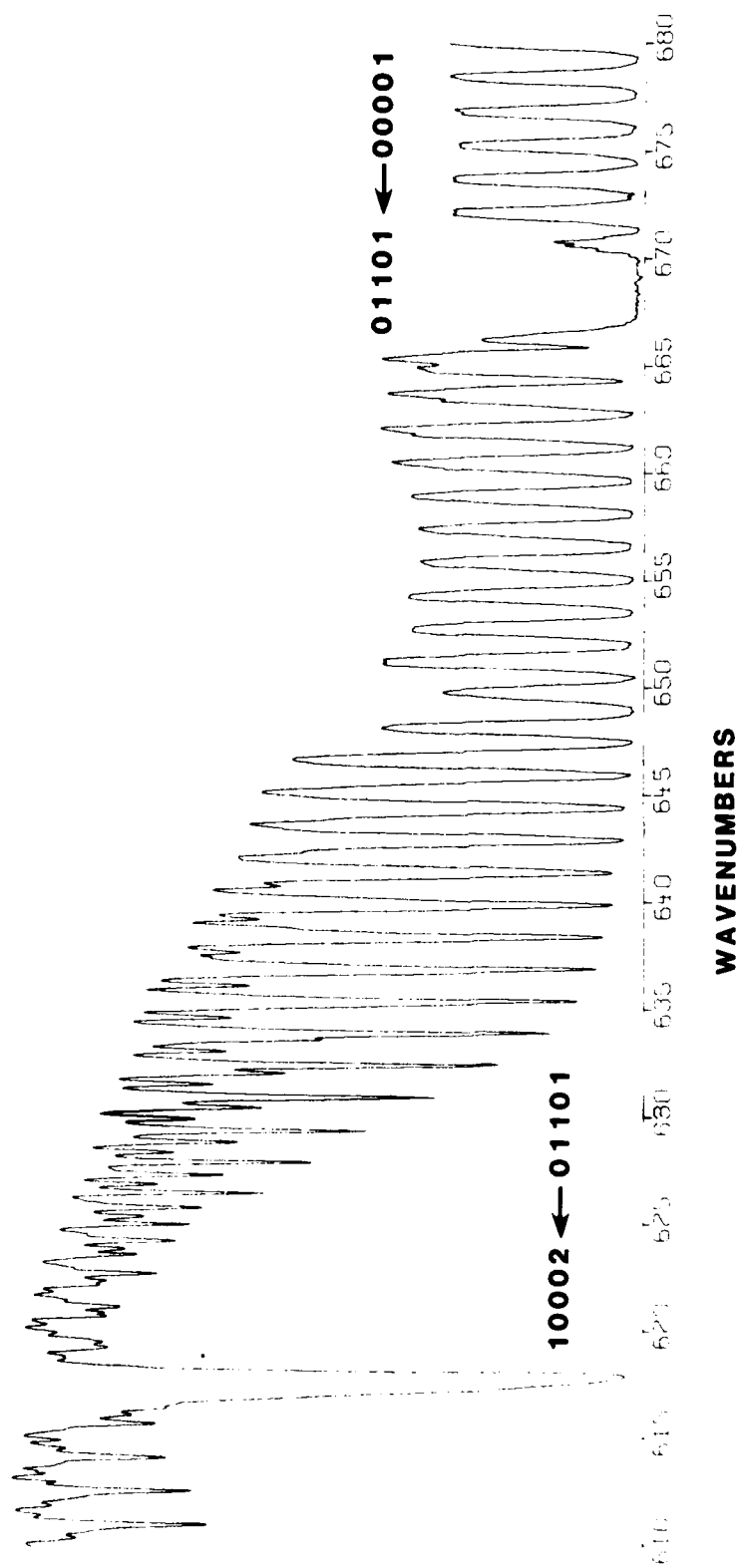


Figure 23. Spectrum of 100 torr of  $\text{CO}_2$  broadened by 660 torr of  $\text{N}_2$  in a 10 cm cell.

high resolution (maximum optical path of 83 cm) using the wedged ZnSe windows. The HDO is formed by mixing  $\text{H}_2\text{O}$  and  $\text{D}_2\text{O}$  and letting the hydrogen and deuterium exchange to form a mixture of  $\text{H}_2\text{O}$ , HDO, and  $\text{D}_2\text{O}$ . The experimental spectrum in Figure 24 is of a room temperature sample of a mixture of  $\text{H}_2\text{O}$ , HDO, and  $\text{D}_2\text{O}$  in a 10 cm long cell. In the future, additional measurements will be made at elevated temperatures.

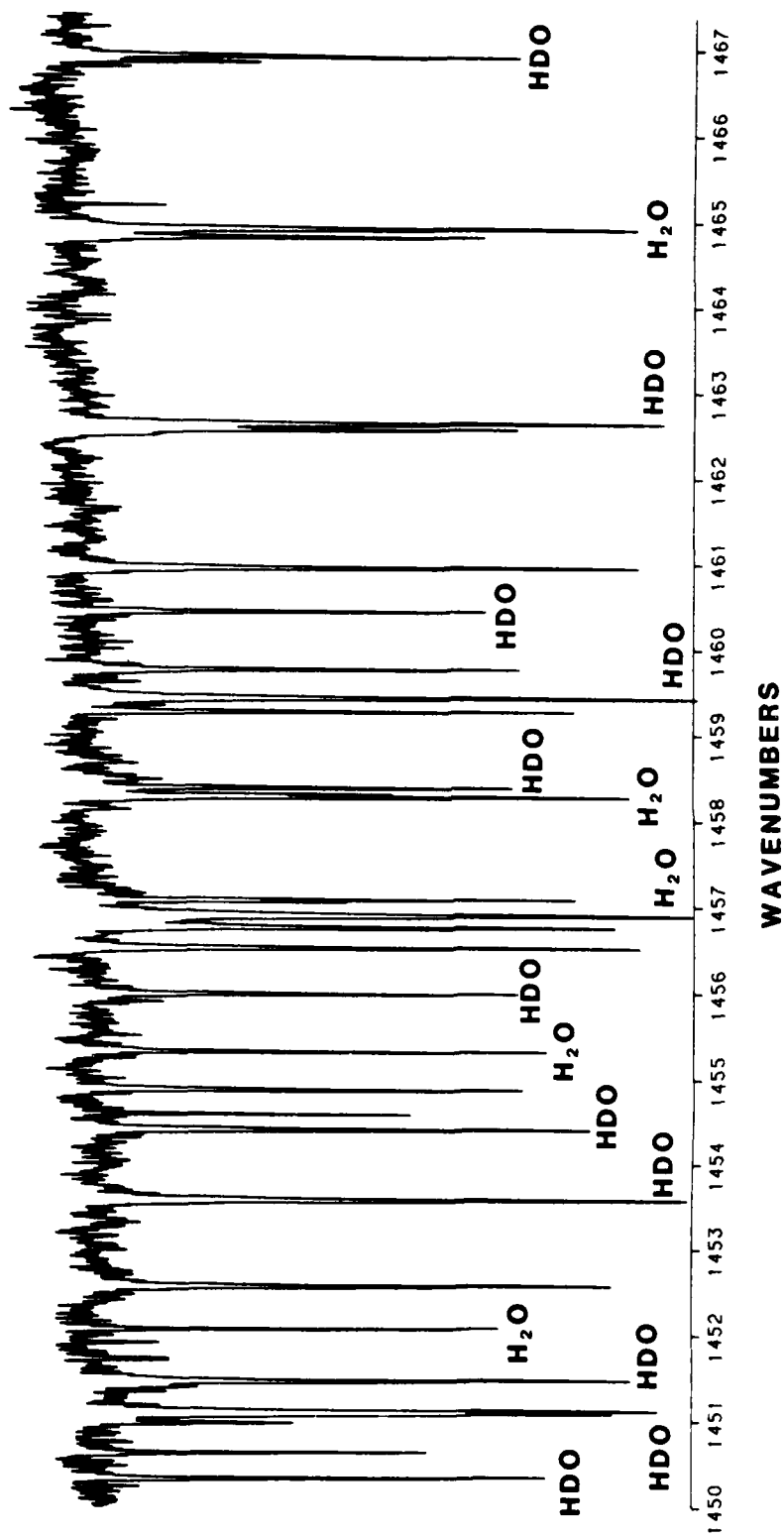


Figure 24. HDO - H<sub>2</sub>O spectrum.

## CHAPTER V

### DATA ANALYSIS

A considerable amount of effort was required to obtain molecular parameters from the raw interferogram data. Performing spectroscopy using high resolution broadband spectral coverage inherently means a large amount of data. The interferograms for the present work consisted of over a million data points and the resulting spectra contained thousands of lines. The only reasonable way to make use of these large quantities of data was through the extensive use of computers. The raw interferogram data were recorded using a PDP-8/E computer and all subsequent processing of the data was performed using a Control Data mainframe computer.

The block diagram of Figure 25 shows the steps that were necessary in obtaining molecular parameters from the raw interferogram. The first step in the data analysis was to perform the appropriate masking and shifting operation to map the 24 bit double precision PDP-8/E words into 60 bit CDC words. Next, a phase correction was performed on the interferograms to correct incomplete beamsplitter compensation and nonsymmetric sampling of the interferograms. A numerical filtering technique was included as part of the phase correction process to eliminate all frequencies from the interferograms with the

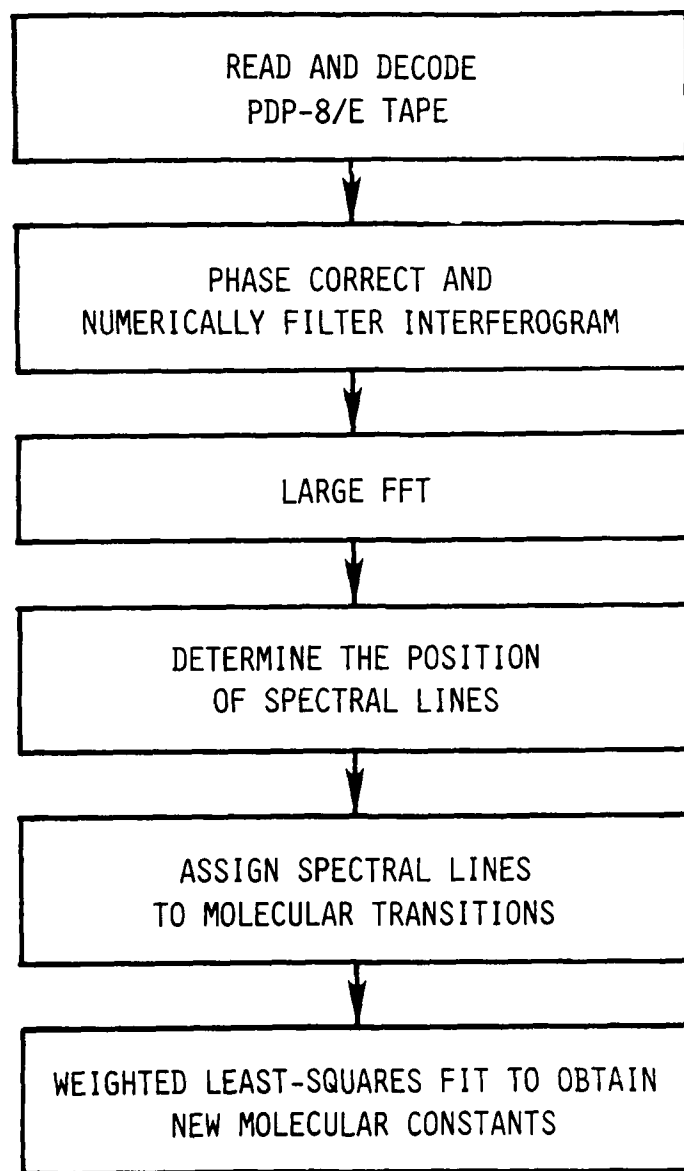


Figure 25. Major steps in the data analysis process.

exception of a region of interest. This process typically reduced the size of the required Fourier transformation by a factor of 10. The filtered interferograms, consisting of 131072 data points, were then transformed using the FFT algorithm. Even though a large scale computer was used, insufficient memory was available to routinely process the interferograms without the use of a special "large FFT" algorithm. After the spectral recovery was completed by applying the Fourier transformation to the data, the position of each spectral line was determined and recorded on a disk file for subsequent use. In addition to line position, other parameters, such as intensities and width of spectral lines, were also determined. The next step in the data analysis was assigning the absorption features to the proper molecular transitions. This step proved to be the most difficult and most time consuming of the data analysis process. The computer program that assisted in performing this step was written to display graphically the data relevant to a given rotation-vibration band. The pattern recognition capability of a human operator was then utilized to make a tentative assignment of the observed spectral lines. A least-squares-error fitting procedure was then applied to the tentatively assigned spectral lines resulting in new molecular constants. This procedure was iterated until a good fit was obtained for most of the

observed lines of each rotation-vibration band. The final step was a weighted least-squares fit resulting in new molecular constants. The major steps: phase correction, large FFT, spectral lines location, identification of spectral lines, and weighted least-squares fitting will be considered in the following sections of this chapter.

### Phase Correction

There are two major causes of phase errors in interferograms produced by a Michelson interferometer, 1) nonsymmetrical sampling of the interferogram, and 2) incomplete beamsplitter compensation (see Chapter IV). Nonsymmetrical sampling of the interferogram gives rise to a linear phase error and incomplete beamsplitter compensation results in a nonlinear phase error. Both linear and nonlinear phase error can be corrected by convolving a correction function with the interferogram. A numerical filter can also be incorporated into the same function used for phase correction to reduce the spectral coverage of the interferogram to a region of interest. The spectrum is then recovered from the symmetrized and filtered interferogram by applying a cosine transformation.

The interferogram,  $I'(x)$ , when phase error is present was given in Chapter IV as Equation (65). This equation

can be rewritten as

$$I'(x) = \int_{-\infty}^{\infty} B(\sigma) e^{2\pi i \sigma \delta(\sigma)} e^{-2\pi i \sigma x} d\sigma, \quad (66)$$

where  $B(\sigma)$  is the optical input to the interferometer, and  $\delta(\sigma)$  is the phase error. In the case of linear phase error,  $\delta(\sigma)$  is simply a constant. Taking the Fourier transformation of both sides of Equation (66) yields

$$B'(\sigma) = e^{2\pi i \sigma \delta(\sigma)} B(\sigma). \quad (67)$$

The Fourier transform of the uncorrected interferogram,  $B'(\sigma)$ , is then the desired spectrum  $B(\sigma)$  multiplied by a phase factor. This phase factor can be isolated from  $B'(\sigma)$  by dividing by the magnitude of  $B'(\sigma)$ , that is:

$$e^{2\pi i \sigma \delta(\sigma)} = \frac{B'(\sigma)}{|B'(\sigma)|}. \quad (68)$$

The desired spectrum,  $B(\sigma)$ , can be recovered by multiplying the transform of the uncorrected interferogram,  $B'(\sigma)$ , by the complex conjugate of the phase factor. Multiplying two functions together in the spectral domain is equivalent to convolving their transforms in the interferogram domain. The function  $\phi(x)$  with which the original interferogram is convolved is then

$$\phi(x) = \int_{-\infty}^{\infty} e^{-2\pi i \sigma \delta(\sigma)} e^{2\pi i \sigma x} d\sigma. \quad (69)$$

Numerical convolution is extremely computationally intensive and is not usually very practical except when one of the functions to be convolved has small nonzero extent. The phase error  $\delta(\sigma)$  is a slowly varying function of  $\sigma$ , making  $\phi(x)$  essentially equal to zero except for a small region around zero spatial frequency. For a typical  $10^6$  point interferogram, 128 nonzero points were sufficient to adequately express  $\phi(x)$ .

Numerical Filtering. When the interferogram is sampled every 6328 Å (the wavelength of the HeNe reference laser), the free spectral range of the resulting spectrum is  $7899 \text{ cm}^{-1}$ . It is often advantageous to limit the wavenumber coverage to a much narrower region of interest. By limiting the spectral bandwidth of the measured interferogram it is possible to decrease the number of data points required to express the interferogram and consequently the size of the Fourier transformation needed for a given resolution. Either an optical filter or a numerical filter can be used to reduce the spectral bandwidth. Both have their advantages, an optical filter also reduces photon noise, while a numerical filter is much more flexible. For this work, an optical filter was used to limit the spectral coverage to a rough area of interest which was then refined with a numerical filter. The function used for numerical filtering,  $f(\sigma)$ , can be

incorporated into the phase correction function  $\phi(x)$  as

$$\phi'(x) = \int_{-\infty}^{\infty} f(\sigma) e^{-2\pi i \delta(\sigma)} e^{2\pi i \sigma x} d\sigma . \quad (70)$$

Both phase correction and filtering are now accomplished by convolving  $\phi'(x)$  with the original interferogram. A significant reduction in the size of the Fourier transformation is obtained by this technique.

A typical raw interferogram for this work consisted of 1,150,000 points. The phase-corrected and filtered interferogram consisted of 131,072 points with a spectral coverage of  $1755 \text{ cm}^{-1}$  to  $2633 \text{ cm}^{-1}$ . Since the numerical filter did not provide an infinitely sharp cutoff, the usable portion of the spectrum was roughly  $1800 \text{ cm}^{-1}$  to  $2600 \text{ cm}^{-1}$ .

#### Large FFT

The development of the Fast Fourier Transform (FFT) algorithm by Cooley-Tukey<sup>44</sup>, in 1965, was crucial to the development of the technique of Fourier spectroscopy. Without the dramatic increase in computation speed provided by the FFT algorithm, recovering the spectrum from an interferogram would have remained impractical. Even though there exists an extensive amount of published information about the FFT algorithm, including computer programs, there are very few programs available to perform Fourier

transformations on data sizes larger than those fitting into the central memory of a computer. The large FFT programs that do exist are very machine-dependent and require features which are not supported by FORTRAN. If an in-memory algorithm is used with a virtual memory system, the number of calls to mass storage can be extremely large, since data processed in the FFT algorithm can come from widely scattered locations. The need existed for a general program that would run on a small computer or run under the limited memory allowed under the time-share environment of a large computer. The program written to fill this need is nearly machine independent. It is an extension of a program developed by Hajime Sakai.<sup>40</sup> The only nonstandard FORTRAN feature needed to execute the program is the ability to access blocks of data randomly on a mass storage device under FORTRAN control. This is no problem on most systems because of the uniform block size used in this program. The program is capable of performing Fourier transformations of arbitrary size, limited only by the size of mass storage available. The flexibility of the program, which was developed using the CDC Cyber 175 computer at the University of Massachusetts, was verified by its successful implementation on a PDP-11 minicomputer with only minor modifications.

In the large FFT, the set of interferogram data points

is divided into blocks. Only two of these blocks of data reside in the central memory of the computer at a given time. The rest of the blocks of data reside on a random access mass storage device. The input data must first be sorted into a particular order, an in-memory FFT is then applied to each block of data, and finally the data from the various blocks are combined to form the Fourier transformation of the entire data set. The manner in which the data are sorted into the appropriate blocks and the way the data from the blocks are combined into the Fourier transformation of the entire data set is analogous to the standard FFT.

In the standard FFT, the input data may be considered as a linear array of data points. The output array is also an array of the same number of elements. The output array is obtained from the input array by successive passes through the data. For each iteration two elements which are separated by a fixed offset are combined to give two elements of the next iteration. The offset between the two processed elements is doubled each pass. The entire transformation is completed after  $N \log_2 N$  passes through the data, where  $N$  is the number of data points.

In the large FFT the sorting and combining operations mentioned above are performed in an analogous way to the standard FFT. In this analogy, blocks of data correspond to the individual elements of the standard FFT and an array

of data blocks on the mass storage device corresponds to the linear array.

Both the FFT algorithm and its extension, the large FFT, are applied to arbitrary complex data sets. It is inefficient to use a general complex Fourier transformation on a phase-corrected interferogram which is real and even. A real even function can be uniquely expressed using  $1/4$  of the storage required for an arbitrary complex function, since the imaginary part is zero and the negative part is identical to the positive part. In order to make the Fourier transformation of the phase corrected interferogram more efficient, a technique for transforming real even functions was used.<sup>35</sup> The technique preprocesses the interferogram into a new complex function containing the same number of unique elements as the original function. A Fourier transformation was performed on this complex function, and finally a postprocessing step completes the Fourier transformation of the phase-corrected (even and real) interferogram.

#### Spectral Line Positions

For this work only the position of spectral lines has been reported, but a complete set of parameters was determined for each absorption feature. These additional parameters were very useful in making the line assignments and in determining the quantity of line merging present.

Line merging occurs when spectral lines fall so close together that they are not resolved. In order to determine the line positions, as well as the other parameters, it was necessary to interpolate between the discrete points which resulted from the large FFT.

Interpolating the Discrete Spectrum. A sinc interpolating function was used for this interpolation. The interpolation process consisted of convolving the set of discrete spectral points with a sinc function that was sampled with a spacing 16 times finer than the spectrum. Computationally this was most easily done by transforming to the spatial domain, adding zeroes to the interferogram, then transforming back to the spectral domain. Strictly speaking the entire spectrum should be retransformed, or the zeroes should have been added to the interferogram before the interferogram was originally transformed. However, in order to facilitate the computation, the spectrum was broken up into sections. A section of the spectrum was transformed into the spatial domain, zeroes added, and then transformed back into the spectral domain. This method makes the size of the transform required much more manageable, while giving good results except near the edges of each section of spectrum so transformed. To minimize edge effects, each section of the spectrum was overlapped with the next section so that no spectral data

was used within 50 points of the end of a section. Using this method, errors in the interpolating function do not occur before the interpolating sinc function has dropped to approximately one fiftieth of its central value.

Determined Line Parameters. In addition to line positions, several other line parameters were also determined. The other parameters were: width, asymmetry, intensity, transmission at the line center position, and height of each absorption feature. Since the only purpose of these additional parameters was to assist in making line assignments and to determine the expected uncertainties of line positions, nonstandard definitions of parameters could be used. The definitions that were used are described in the remainder of this section and illustrated in Figure 26.

The line positions were determined by simply taking the local minimum of the interpolated spectrum as the line position. A more precise method of determining line positions would have been used if the random variations in the positions of experimental lines had been less. The primary cause of these random variation was line merging. Nearly all of the spectral lines showed some symptoms of line merging. Line merging would have been only slightly reduced if the resolution of the interferometer was infinite, since the resolution of the spectrometer is approaching the Doppler limited resolution.

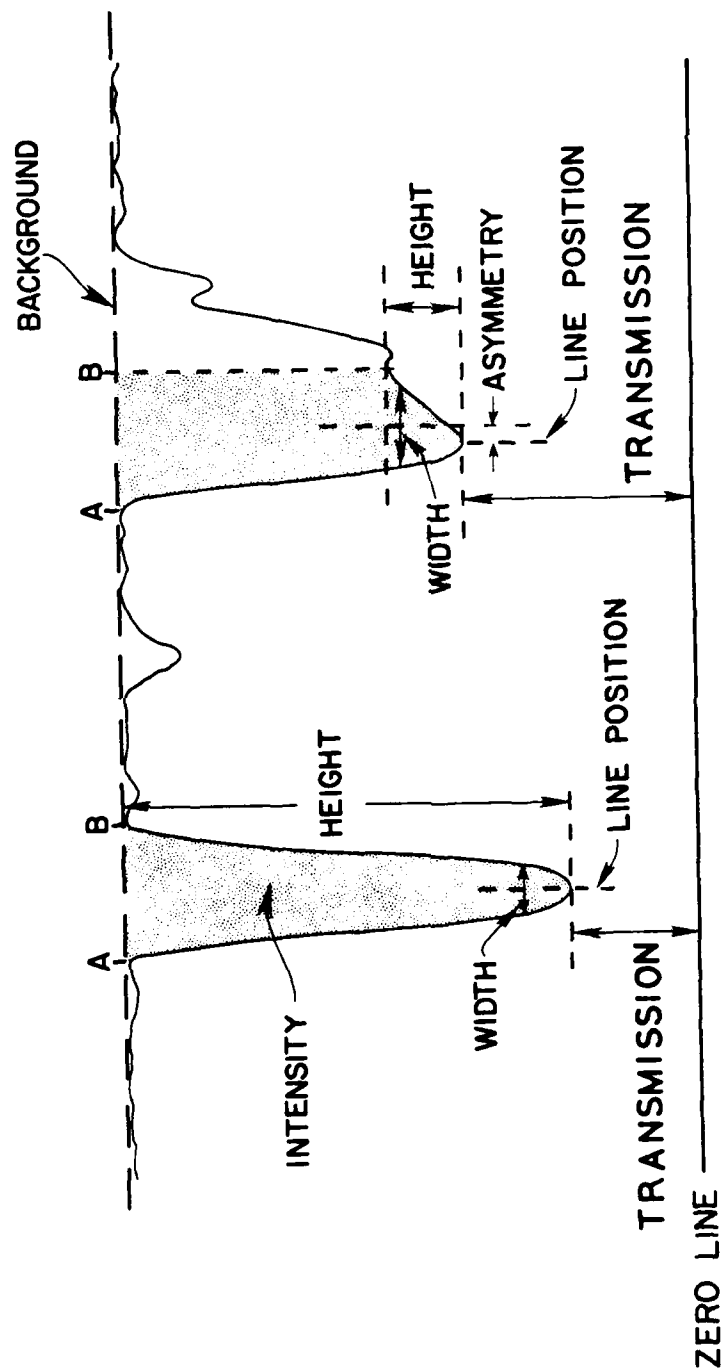


Figure 26. Parameters that were determined for each absorption feature: the line position, a line width, asymmetry, intensity, transmission and line height.

The line asymmetry was determined by using an alternative method for finding the line position and comparing the results to the local minimum method. This second method of finding the line position used the center of a chord drawn across the absorption line a small distance up from the minimum as the line center. For symmetric lines, the center of this chord coincides with the line position found from the local minimum method. This chord drawn across the absorption line was also used to determine the line width, since the line width is proportional to the length of the chord.

Due to the existence of thermal gradients in the absorption cell, no attempt to make a careful measurement of line intensities was made. However, approximate line intensities were found to be very helpful in the band identification process. In order for the line intensities to be obtained, an estimate of the background was necessary. A simple linearly sloping background obtained from a visual inspection of the spectrum was used for the  $4.3 \mu\text{m } ^{12}\text{C}^{16}\text{O}_2$  data. For the other experimental spectra the background was determined by measuring the spectrum of the high temperature absorption cell with no gas in the cell. This empty cell spectrum was smoothed using a 13 point running average before it was used as the background. The line intensity was considered to be the area between

the spectral trace and the background (the shaded area of Figure 26). The area was obtained using Simpson's rule to integrate from the point (a) on the left side of the spectral line where the slope was zero to the corresponding point (b) on the right-hand side. Any line that had an intensity below a predetermined minimum value was considered to be noise and was dropped. The height of the absorption feature was taken to be the difference between the absorptance at the line center and the absorptance at point (a) or point (b), whichever was the minimum.

After parameters for each line had been determined, they were stored on a random access disk file. Since the identification and fitting programs required a number of iterations, reading the spectral line data from a random access disk file resulted in considerable saving in computer time and increased convenience over what would have been possible, if the identification and fitting programs would have read and interpolated the spectrum directly.

#### Assignment of Spectral Lines

Probably the most difficult aspect of the work on high temperature CO<sub>2</sub> was assigning the correct rotation-vibration transitions to each absorption feature in the experimental spectrum, but through the use of computer-aided identification techniques, over 10000 lines belonging

to 73 different rotation-vibration bands were identified. The degree of difficulty involved in identification of lines belonging to a particular rotation-vibration band depended on the amount of overlapping of bands and on how well the molecular constant for each band could be estimated from previous work. It was very easy to make the identification when the line density was low, since the lines of a band of a linear molecule such as  $\text{CO}_2$  form a set of lines of nearly equal spacing. As the  $\text{CO}_2$  temperature increased, the appearance of the spectrum became very complicated. High temperature greatly increased the problems due to line merging and fragmentary hot bands.

The appearance of the experimental spectrum is demonstrated in Figures 27 through 30. These figures show portions of the spectrum where overlapping of bands is not a problem, as well as regions of the spectrum where overlapping of bands is very serious. The band head at the high frequency end of the R branch of the  $\nu_3$  fundamental of  $^{12}\text{C}^{16}\text{O}_2$  is clearly visible in Figure 27. The high frequency end of the R branch of the transition  $01111 \leftarrow 01101$  originating from the next excited state of  $^{12}\text{C}^{16}\text{O}_2$  is also quite easily seen (Figure 28), since it is only overlapped by one band, the  $\nu_3$  fundamental. However, lines belonging to transitions originating from higher vibrational bands are so overlapped that they are difficult to identify (Figure 29). Figure 30 illustrates how complex

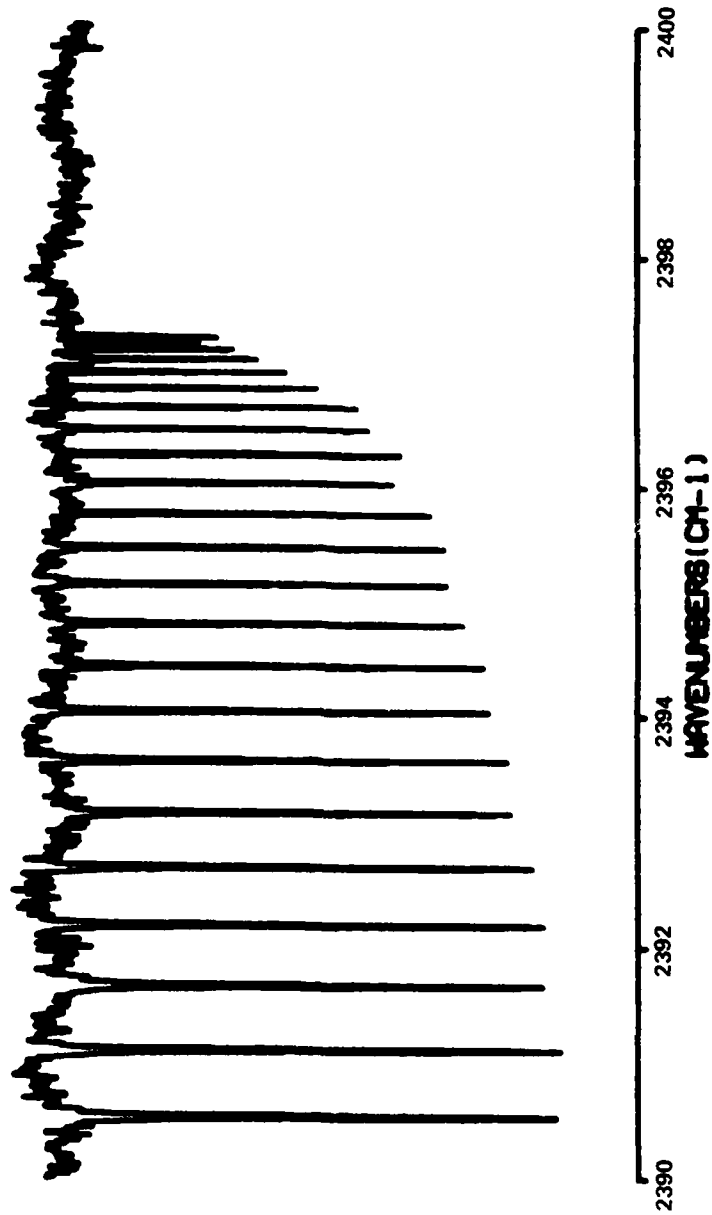


Figure 27. The band head of the  $\nu_3$  fundamental of  $^{12}\text{C}^{16}\text{O}_2$ .

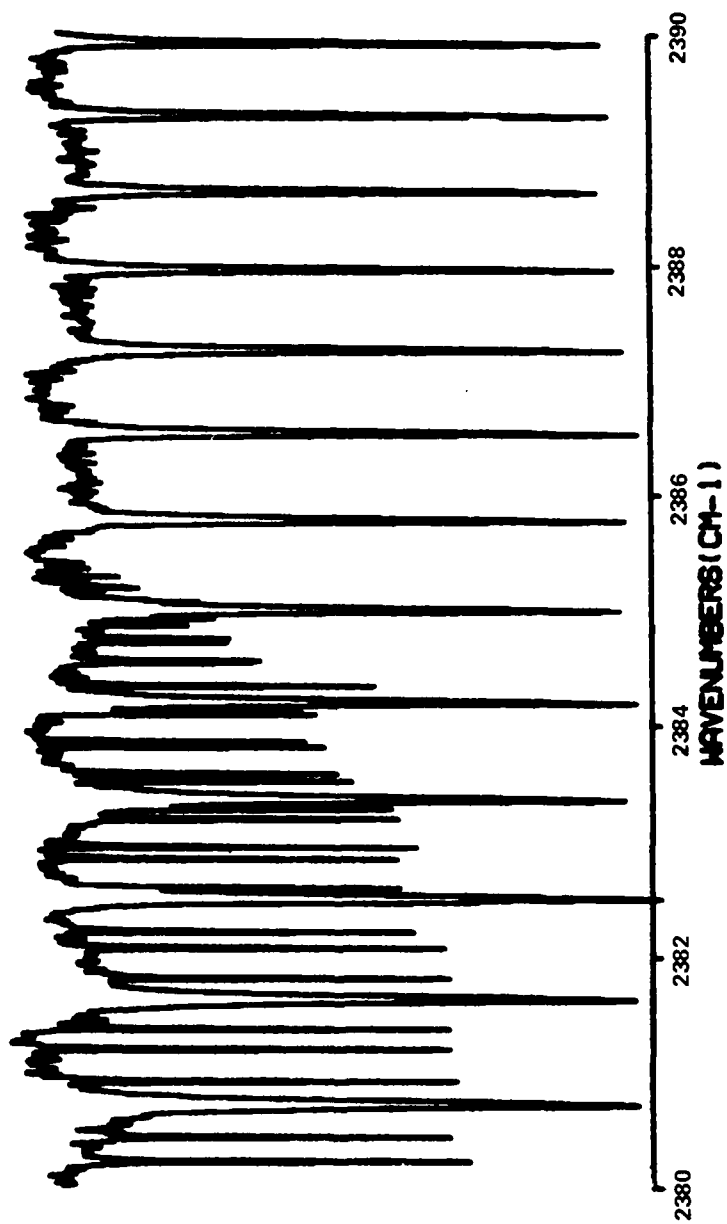


Figure 28. The  $\nu_3$  fundamental overlapped by the high frequency end of the R branch of the  $01111 \leftarrow 01101$  band of  $^{12}\text{C}^{16}\text{O}_2$ .

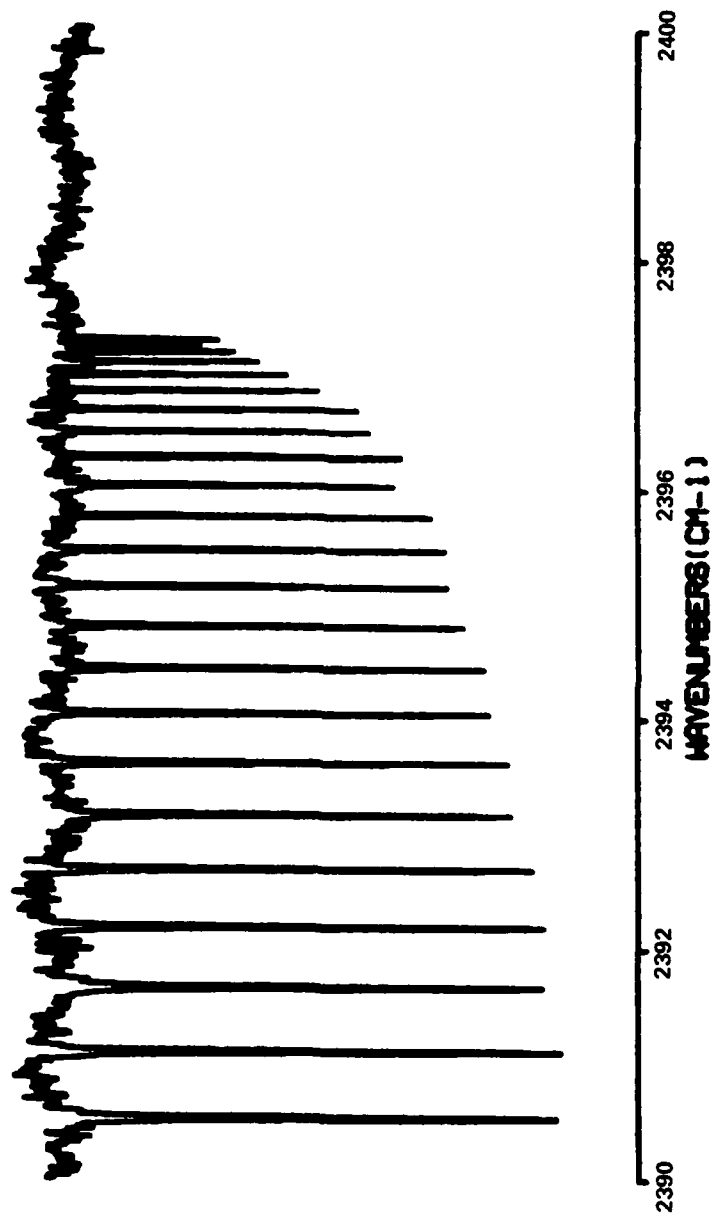


Figure 27. The band head of the  $\nu_3$  fundamental of  $^{12}\text{C}^{16}\text{O}_2$ .

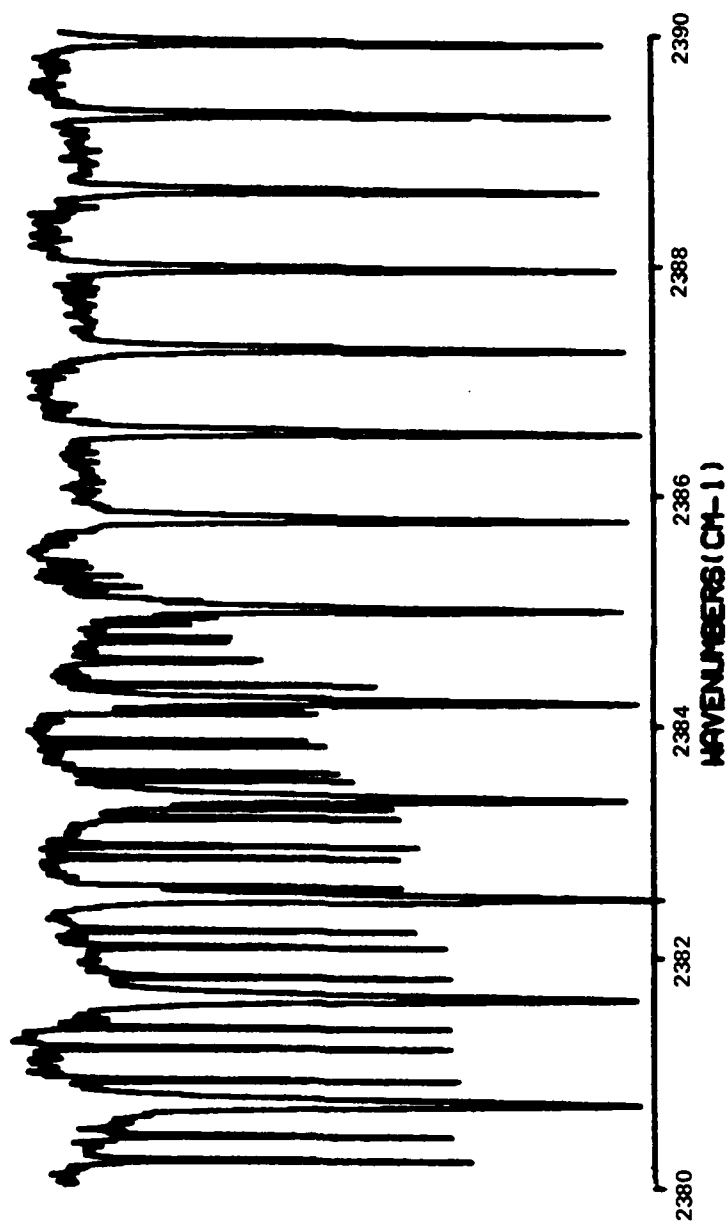


Figure 28. The  $\nu_3$  fundamental overlapped by the high frequency end of the R branch of the 01111 + 01101 band of  $^{12}\text{C}^{16}\text{O}_2$ .

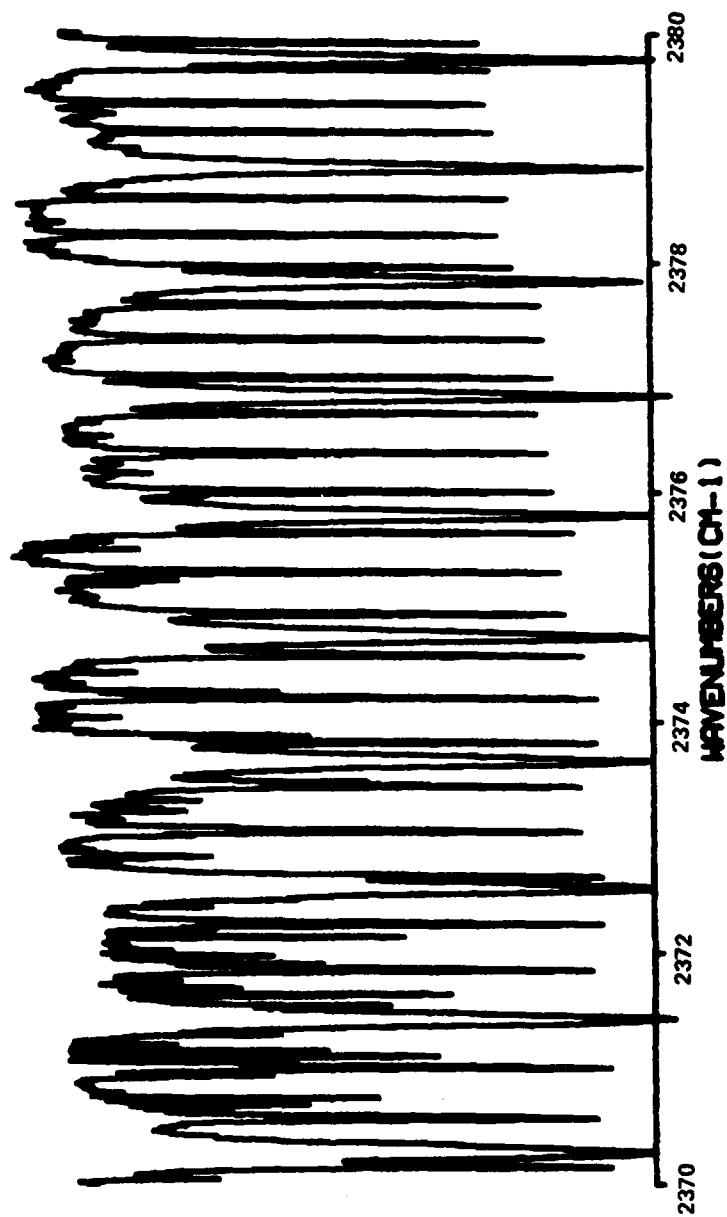


Figure 29. Complex appearance of the  $\text{CO}_2$  spectrum when several bands overlap.

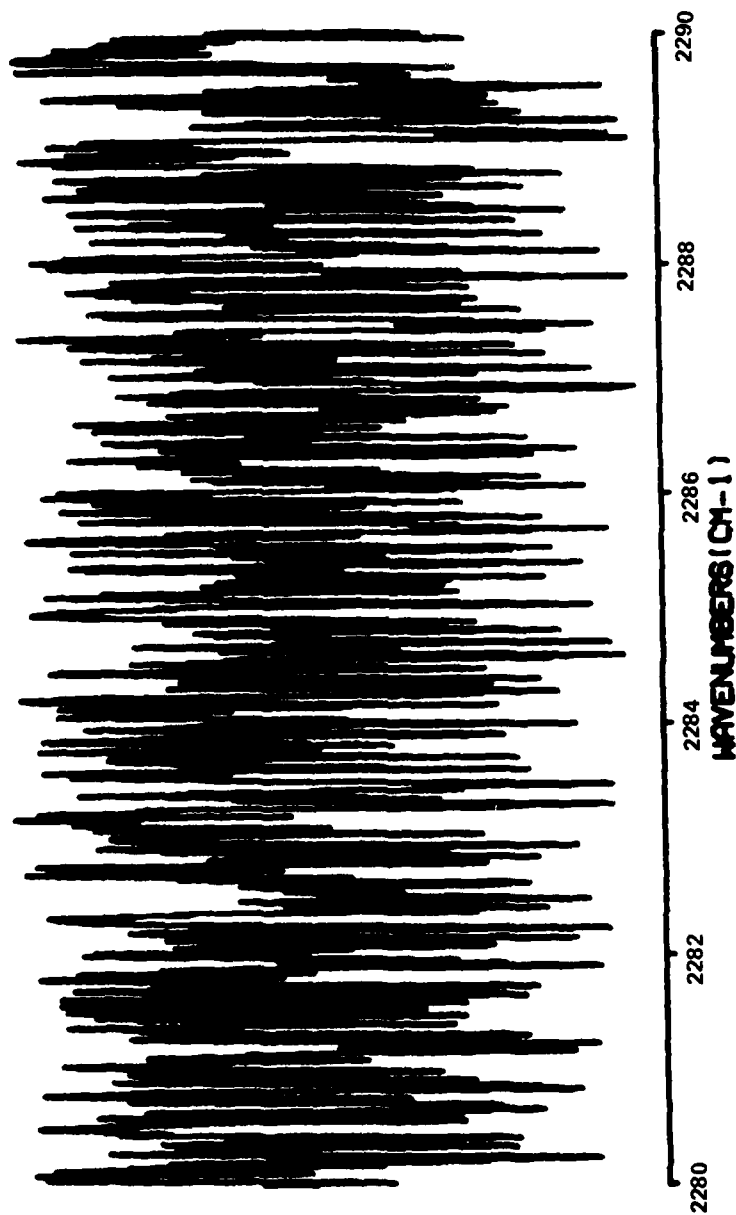


Figure 30. A large number of overlapping bands mask the regular structure of each of the CO<sub>2</sub> rotation-vibration bands and cause the spectrum to appear random.

the high temperature  $\text{CO}_2$  spectrum can appear even though each band is still composed of a set of lines with nearly equal spacing.

Lines Visible in High Temperature Spectrum. Due to the many problems associated with identifying fragmentary bands, little effort was expended in attempting to identify lines belonging to extremely highly excited vibrational states. As the temperature of  $\text{CO}_2$  is increased, there is an ever increasing density of excited vibrational energy levels. Bands originating from very high vibrational energy levels yield a low number of lines that are intense enough to be visible. The result is a large number of bands with so few lines visible that identification is extremely difficult and subject to misidentification. An additional problem in identifying these bands is that the intensity is not sufficiently strong to see the distinctive pattern of lines formed at the band center. However, lines from these unidentified bands complicated the identification of the other bands.

Insight into how the number of lines visible in an experimental spectra change with temperature is gained by considering the  $4.3 \mu\text{m}$  bands of  $^{12}\text{C}^{16}\text{O}_2$ . Assume that the transition probabilities for all these  $\Delta v_3 = 1$  bands are equal except for the Boltzmann factor. This approximation is reasonably good since the changes in intensity due to

changes in the Boltzmann factors are large compared to changes in intensity due to other factors for this class of similar  $\Delta v_3 = 1$  bands. Figure 31 illustrates, for different temperatures, the approximate range of J values for which experimental lines should just be visible. The curve marked 800 K is for 6 Torr of  $\text{CO}_2$  at 800 K in a 3.5 meter path hot cell. Other curves correspond to the same quantity of gas at different temperatures. The region enclosed between the curve and the axis corresponds to the range of lower vibrational state energies and J values for which spectral lines should be visible. For example, for a lower state energy of  $2000 \text{ cm}^{-1}$  the range of J values for which lines should be visible is  $J = 2$  to  $J = 32$  for a temperature of 300 K and  $J = 0$  to  $J = 106$  for a temperature of 800 K.

The reason for the large number of fragmentary bands is illustrated by using the harmonic oscillator approximation to estimate the number of vibrational states with a given lower state energy. A plot of the number of vibrational states with energy lower than or equal to a given lower state energy is given in Figure 32. The total number of states available to a molecule is the product of the number of rotational states times the number of vibrational states. From Figures 31 and 32 it can be seen that a large proportion of the lines visible in the spectrum belong to bands with high lower state energies

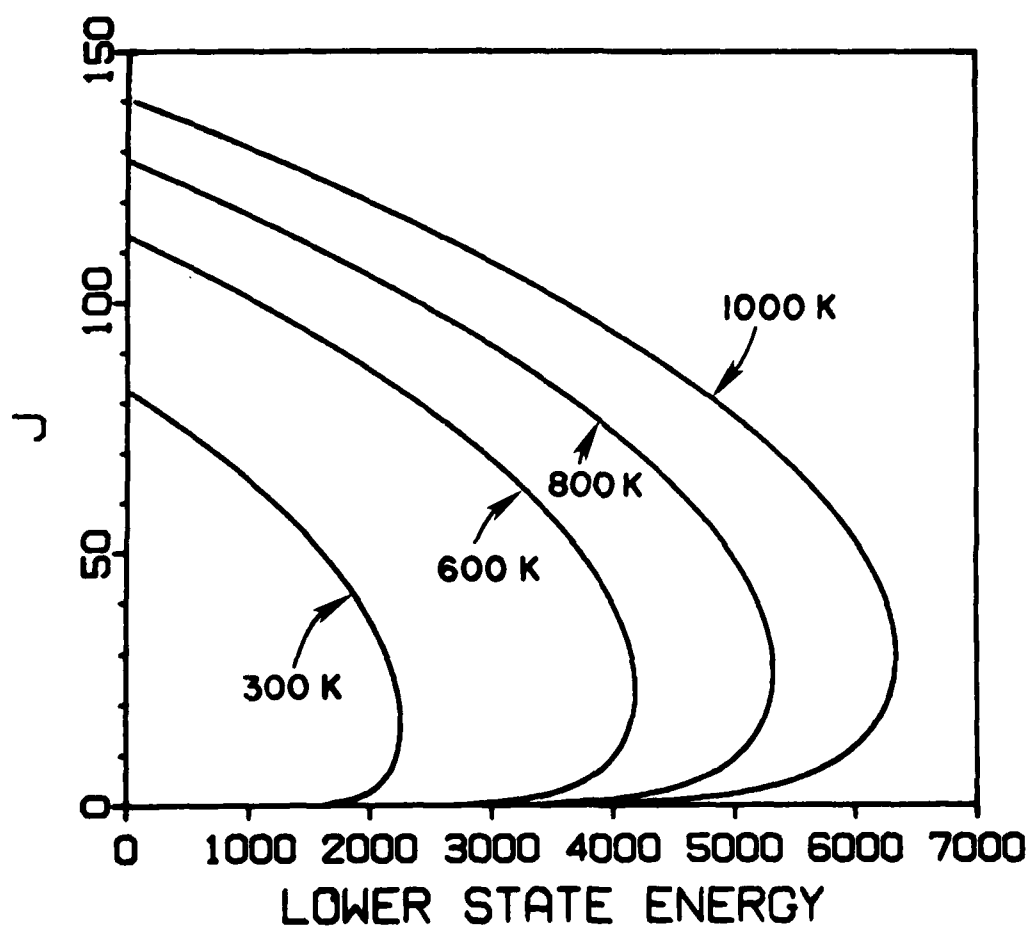


Figure 31. The range of  $J$  values and lower state energies for which spectral lines should be visible.

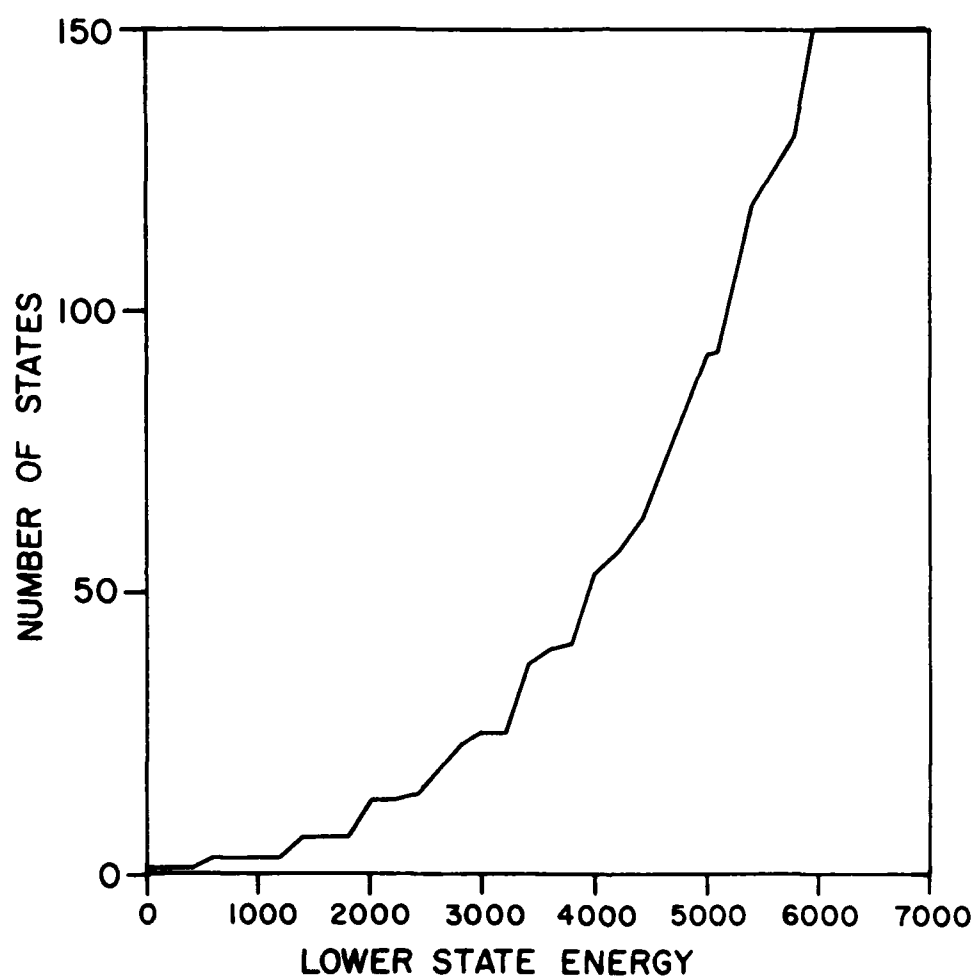


Figure 32. The number of vibrational states with lower state energy less than or equal to a given energy.

where the range of J values is low.

A high temperature absorption cell is very effective for making measurements on high rotational states of a molecule, but for studying high vibrational bands an electrical discharge gas cell or some other non-thermal equilibrium technique is probably better. In an electric discharge, the effective vibrational temperature is very high, while the rotational temperature remains at approximately room temperature. In an electric discharge the range of J values in the spectrum of a "hot" band is approximately the same as for the fundamental. Referring to Figure 31, the range of lines visible for the fundamental at room temperature is about  $J = 0$  to  $J = 82$ . Roughly the same range of lines will be visible in a hot cell heated to 800 K if the lower state vibrational energy is about  $3500 \text{ cm}^{-1}$ . Since a 800 K hot cell loses its advantage for lower state energies above about  $3500 \text{ cm}^{-1}$ , it was not considered worth putting much effort into identifying bands with a lower state energy above  $3500 \text{ cm}^{-1}$ . For this work, the highest vibrational state identified had a lower state energy of  $3659 \text{ cm}^{-1}$ .

Philosophy of Identification Programs. The programs that accomplished line identification and fitting were made interactive in an attempt to minimize the total overall effort involved with the identification process. Doing the

identification totally by hand seems nearly impossible when one realizes the amount of data involved. The  $\Delta v_3 = 1$   $^{12}\text{C}^{16}\text{O}_2$  spectral region stretches from about  $2100\text{ cm}^{-1}$  to  $2400\text{ cm}^{-1}$ . If this region was plotted with sufficient resolution that line positions could be obtained from the plot, to the accuracy of the experimental data (about  $0.0004\text{ cm}^{-1}$ ), the plot would be 310 feet long and consist of over 5000 distinct absorption features. This is assuming a plotting accuracy of 0.005 inches; if the accuracy of the plotter was less, the plot would have to be even longer. On the other hand, to make a program that could handle the intricacies of the total identification process would also be extremely difficult. The challenge was to use the computer to gather and store information on thousands of lines and present small amounts of that data in such a way that it could be meaningfully considered by the operator. The programs written to meet this challenge consisted of several steps with a large amount of operator interaction throughout. An attempt was made to make use of the inherent ability of a human operator to do pattern recognition and make subjective judgments, while minimizing operator confusion by having the computer sort through large amounts of data and present only that data which might be directly relevant.

Loomis-Wood Diagram. A Loomis-Wood diagram proved extremely helpful in picking out the lines that belong to one band in the presence of lines belonging to other bands and lines belonging to other isotopes of  $\text{CO}_2$ . The original Loomis-Wood procedure<sup>45</sup> relies on the assumption that lines comprising a band are nearly equally spaced. If no prior knowledge is known about the band the line spacing can usually be obtained from observing a series of a few lines that appear to form the band. This uniform line spacing assumption is used to calculate the position of all lines in the band. For each line in the band, the difference between the calculated position and the close-by experimental lines is plotted. If the spacing between the experimental lines exactly matches the spacing used to calculate line positions, the resulting pattern will be a vertical line in the center of the diagram. Deviation from equal spacing results in curvature of the displayed pattern. Lines belonging to other bands cross the diagram at such a high angle they do not usually form a recognizable pattern. An example of a Loomis-Wood diagram with a line spacing of  $1.56 \text{ cm}^{-1}$  for a hypothetical band of  $\text{CO}_2$  is given in Figure 33. Listed at the left of the diagram are the position and the identity of each calculated line.

The Loomis-Wood procedure used in this work contained several extensions to the usual Loomis-Wood procedure.

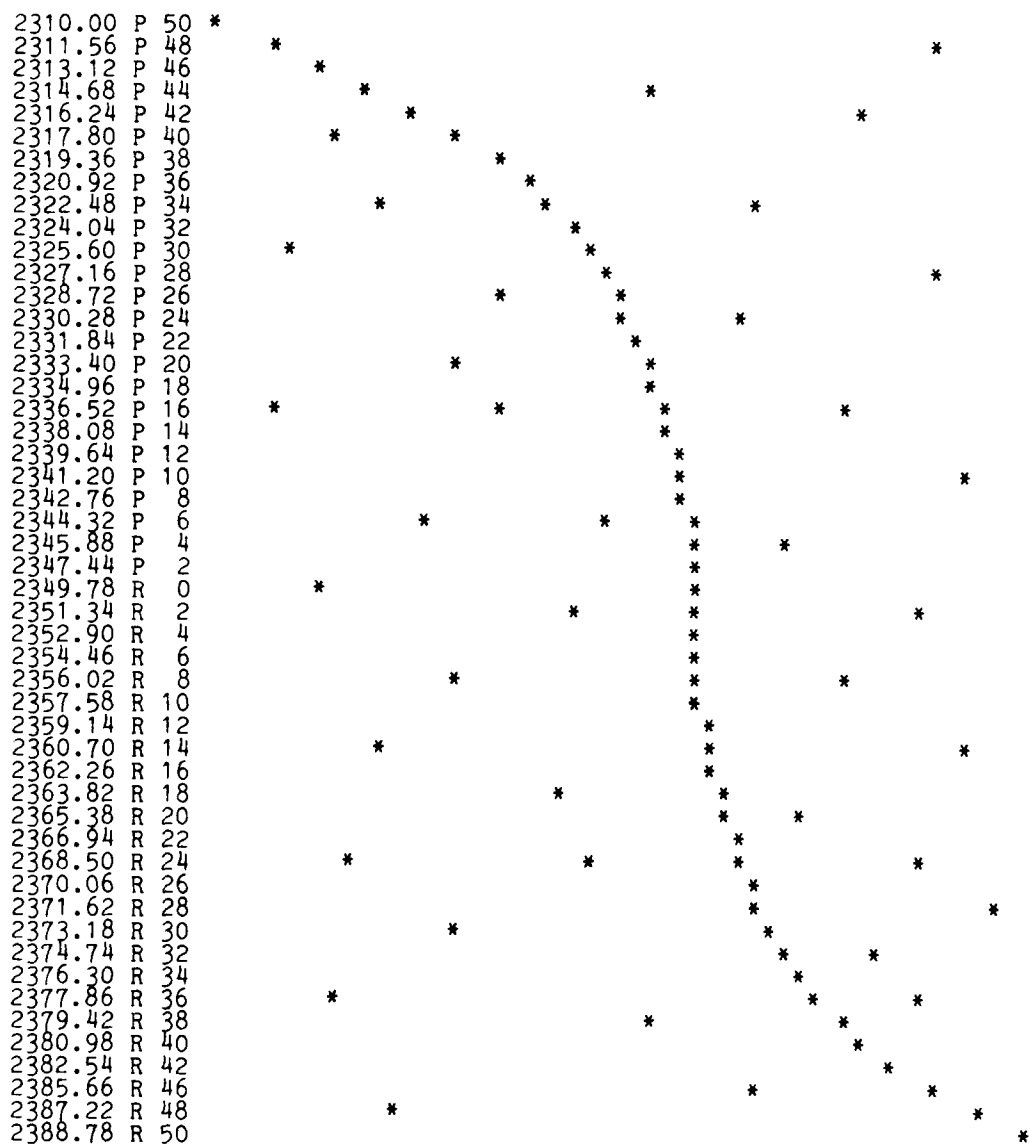


Figure 33. Loomis-Wood diagram for a hypothetical band of  $\text{CO}_2$

Since some prior knowledge about the spectroscopic constants for each band of  $\text{CO}_2$  was known either from theory or from other experimental measurements, it was not necessary to assume equally spaced lines. This knowledge of the approximate spectroscopic constants could be used to narrow the search to a small region around each calculated line position. Using a computer to implement the procedure made readily possible inclusion of a great deal of information on each line. For example, lines that had already been identified were indicated by a one-character identifier code (Table 6). If more than one line had already been associated with a single absorption feature, the line was indicated as being merged by a "M". An asterisk "\*" signified that the line had not yet been identified. In the diagrams, the width of each line is indicated by the number of adjacent symbols. For example "MMMM" indicates a merged line of twice the width of an unknown line "\*\*\*". The width of each line gives an estimate of the quality of the position measurement for that line. Wide lines are either saturated, making the peak position determination sensitive to noise, or merged with some other line.

Figures 34-36 give the extended information Loomis-Wood diagrams for several bands of  $^{12}\text{C}^{16}\text{O}_2$ . In each case the total wavenumber spread across the diagram is  $0.2 \text{ cm}^{-1}$ . If an experimental line is  $0.1 \text{ cm}^{-1}$  lower in frequency than

Table 6. One character identification codes used to identify rotation-vibration bands of  $^{12}\text{C}^{16}\text{O}_2$ .

Band	Identification code
00011 + 00001	A
01111 + 01101	B
10012 + 10002	C
02211 + 02201	D
10011 + 10001	E
11112 + 11102	F
03311 + 03301	G
11111 + 11101	H
20013 + 20003	J
04411 + 04401	L
20012 + 20002	N
00021 + 00011	P
20011 + 20001	Q
12211 + 12201	O
01121 + 01111	Y
10022 + 10012	3
02221 + 02211	4
05511 + 05501	5
13311 + 13301	6
13312 + 13302	7

the calculated wavenumber value, it will fall at the far left of the diagram; if the line is  $0.1\text{ cm}^{-1}$  higher than the calculated value, it will fall on the far right.

Data Table. Another useful tool in making line assignments was a table giving detailed information on the closest experimental line to each calculated line position. Table 7 is an example of a data tables for the 02211e + 02201e band of  $^{12}\text{C}^{16}\text{O}_2$ . The first column gives the observed line

Figure 34. Part of the extended information Loomis-Wood diagram for the 00011 + 00001 band of  $^{12}\text{C}^{16}\text{O}_2$ .

```

2242.6061 P 80 ** ***** ** ** ***** ** DD **
2245.1027 P 78** *** LLL* ***** DD 666
2247.5762 P 767 ** ** 44 MM *****
2250.0266 P 74 *** YY ***** ** D *****
2252.4539 P 72 ** MM ***** DD *** **
2254.8580 P 70 *****JJJ LL DD BB
2257.2389 P 68 *** ** MMMM **
2259.5966 P 66 *** 33 DD HH GG
2261.9310 P 64EE MMMM *** DD
2264.2421 P 62 ** MM DD
2266.5298 P 60 *** QQQQ MMM MM DDD
2268.7941 P 58 *** NN MM 66
2271.0351 P 56 *** BB MM EEE
2273.2526 P 54 ** ***** DD 44 BBB M
2275.4466 P 52 ** ** JJ DD ** EE
2277.6171 P 50 *** ***** DD MM
2279.7641 P 48MM HH ** DD MM
2281.8875 P 46 ** DD DDD *** MM
2283.9872 P 44MMMM *** DD ***
2286.0634 P 42 ** OO MM **
2288.1159 P 40 ** *** DDD NNN *****
2290.1446 P 38 BB MM FFF ***** MM
2292.1497 P 36 FF MM DD
2294.1309 P 34 ** ** MM
2296.0884 P 32*****7777 AAA MMM *****
2298.0221 P 30 ** DD 66666666 *****
2299.9319 P 28 ** DD ***** 33
2301.8178 P 26 777 DD GG ***** 444
2303.6798 P 24G ** MMMMMMMMMMMMMMMM MMMM FF
2305.5179 P 22 *** DDD **
2307.3320 P 20** ** ***** MM 44
2309.1220 P 18MMMM ** JJJ DD 666
2310.8881 P 16* 44 MM 66 666 LLL
2312.6301 P 14** ***** MM 66 77 *****
2314.3480 P 12 *** BBB MM 77
2316.0418 P 10 MM *** DD MMMM 77 777
2317.7114 P 8 MM MM GGG 77 LLL *****
2319.3569 P 6GGG OOO ***** MM
2320.9782 P 4 MM ** *** MM CC
2326.4617 R 2 44 DD 77 **
2327.9737 R 4 MM OOO DD *** GG
2329.4614 R 6 MMMM DD 000 33333333 ***
2330.9247 R 8 777 LLL MM *** OOO
2332.3637 R 10JJ MMMMMMMMMMMDDDDDDAAAAAAGGGGGGGGGG OOO
2333.7782 R 12 LL *** MM YYYMMMM
2335.1682 R 14 ** ** DD 0000000000000000
2336.5338 R 16 GG *** OOO MM *** MM
2337.8749 R 18** HHH MM MM *****
2339.1915 R 20 *** MM GGG MM MM OO MMMM
2340.4835 R 22 LLL BBB MM FFF JJJJ ***
2341.7509 R 24 *** YYYGGGG DDD HH
2342.9938 R 26** *** 33 DDD

```

Figure 35. Extended information Loomis-Wood diagram for the 02211e + 02201e band of  $^{12}\text{C}^{16}\text{O}_2$ .

```

2226.3188 P 66**      **      PP      EE      ****      77
2227.4828 P 65*      ***      *****      MM
2228.6411 P 64      ***      ***      MMM      **      MM
2229.7937 P 63      **      ***      **      **      MM
2230.9405 P 62      **      ****      ****      **      66      77      **
2232.0815 P 61      **      **      **      ***      666      77      **
2233.2169 P 60      **      **      ***      ***      666      77      **
2234.3464 P 59      YY      **      MM      ***      HH      77      **
2235.4702 P 58      QQ      OO      66      66      *****      77      ****
2236.5882 P 57      FFF      DD      GG      666      66      **      ***      MM      777      OO      JJ      **
2237.7005 P 56      **      ***      66      **      **      ***      MM      **
2238.8070 P 55      **      66      66      **      **      DDD      MMM      77      **
2239.9078 P 54      66      66      **      **      HH      ***      MM      ***      **
2241.0028 P 53      66      ***      ***      ***      HH      ***      MM      ***      **
2242.0920 P 52MM      *****      MM      ***      MM      **
2243.1754 P 51      ***      44      MM      77      **
2244.2531 P 50      **      ***      HH      44      77      ***      MM
2245.3250 P 49**      YY      ***      DD      **      77      44      ****
2246.3911 P 48      YY      ***      DD      **      MM      44
2247.4514 P 47      **      **      **      77      **
2248.5060 P 46**      **      *****      **      77      FF      **
2249.5548 P 45      LLL      HH      GG      77      ***      **
2250.5977 P 44      HHH      LL      77      GG      ****
2251.6349 P 43      **      NN      ***      PP      **
2252.6663 P 42      JJJ      77      LL      ****
2253.6919 P 41      *****      HH      DD      77      QQ      ***      MM
2254.7117 P 40      EE      *****      AA      77      **      *****      JJ      **
2255.7257 P 39      OO      ***      77      **
2256.7339 P 38      **      **      **      ***      ***      ***
2257.7363 P 37      **      **      **      7777      MM      FFF      **
2258.7328 P 36      **      **      **      77      ***      ***      **
2259.7236 P 35      DD      HHH      GGG      77      ***      DD      GGCGGG
2260.7085 P 34      **      **      ***      7777      ***      **
2261.6877 P 33      ***      ***      333      77      ***      **
2262.6610 P 32      ****      ***      ***      77      ***      HH
2263.6285 P 31PP      FF      77      ***      **      33
2264.5901 P 30MM      44      77      ***      NN      CC      ***
2265.5459 P 29***      **      QQQQ      MM      MM      DDDD
2266.4959 P 28      **      **      77      JJ      44
2267.4401 P 27      **      **      MM      HH      4444
2268.3784 P 26      **      **      77      ***      ***      G
2269.3109 P 25      MM      **      HH      77      **      ***      ***      PP
2270.2375 P 24      ***      ***      ***      ***      ***      ***
2271.1583 P 23      ***      ***      ***      ***      ***      ***
2272.0732 P 22      BBB      MM      ***      LL      ***      MM
2272.9823 P 21      **      **      777      **      OO      LLLLLLLLLLFFF
2273.8855 P 20      **      **      77      **      **      ***      ***      OO
2274.7829 P 19*      **      MM      **      **      ***      ***      Y
2275.6744 P 18EEEEEEEEMMMMMM      GGGG      MM      ***      ***      MM
2276.5600 P 17      ****      MM      ***      ***      ***
2277.4398 P 16      JJ      MM      33      FFF
2278.3137 P 15**      *****      777      QQQ      *****

```

Figure 36. Extended information Loomis-Wood diagram for the 13312 + 13302 band of  $^{12}\text{C}^{16}\text{O}_2$ .

Table 7. Table of experimental line properties for the 02211e ← 02201e band of  $^{12}\text{C}^{16}\text{O}_2$ .

Position	Line	Band	O-C	Intensity	Absorptance	Height	Width	Asymmetry
2213.7984	P102	*	.0004	3.9231	500.0769	100.7481	.0028	.0000
2216.5363	P100	D	.0030	6.3461	426.1855	197.7147	.0023	.0001
2219.2469	P 98	D	.0002	4.1225	449.6789	151.4639	.0022	.0001
2221.9400	P 96	D	.0018	4.9284	420.5376	238.4745	.0023	.0000
2224.6076	P 94	D	-.0001	4.2231	398.9627	242.3757	.0018	.0002
2227.2546	P 92	D	-.0004	6.0019	367.3233	326.5663	.0019	.0002
2229.8782	P 90	D67	-.0020	11.7228	296.1569	345.8769	.0023	.0001
2232.4834	P 88	D	.0002	7.4386	306.4332	285.7575	.0019	.0001
2235.0639	P 86	D	.0001	11.2586	273.0984	313.4593	.0019	.0001
2237.6222	P 84	D	.0001	6.9261	267.0354	331.1934	.0017	.0001
2240.1579	P 82	D	.0001	7.1051	277.7280	325.8813	.0017	.0001
2242.6710	P 80	D	-.0001	8.1875	253.4914	288.4843	.0018	.0000
2245.1632	P 78	D	.0014	8.8383	221.1760	341.4668	.0030	.0004
2247.6328	P 76	DY	.0030	15.2285	133.3870	405.8237	.0025	.0002
2250.0748	P 74	D	-.0004	9.1756	222.0989	425.0533	.0017	.0002
2252.4975	P 72	D	-.0002	10.6828	206.8045	378.0204	.0019	.0000
2254.8976	P 70	D	.0002	12.4589	184.9643	387.0764	.0022	.0001
2257.2848	P 68	AD4	.0104	18.3125	147.7952	414.4888	.0060	.0028
2259.6280	P 66	D	-.0003	14.6463	141.2526	385.8036	.0019	.0001
2261.9616	P 64	DO	.0024	13.4066	126.8862	333.0091	.0028	.0002
2264.2667	P 62	D	-.0004	12.4550	193.3011	457.9705	.0023	.0002
2266.5534	P 60	D	.0015	18.8331	132.1454	474.0271	.0040	.0007
2268.8154	P 58	DEF	.0019	21.5686	99.5474	227.1322	.0034	.0001
2271.0527	P 56	DO	.0008	18.2016	121.8781	250.6197	.0029	.0001
2273.2666	P 54	D	-.0005	15.8411	129.0623	524.9565	.0021	.0000
2275.4592	P 52	D	.0001	15.8116	111.8235	430.2756	.0024	.0001
2277.6274	P 50	D	-.0002	16.0144	98.7902	392.2572	.0024	.0000
2279.7735	P 48	D	.0007	17.8491	106.4010	475.5019	.0024	.0002
2281.8945	P 46	D	-.0001	20.4983	66.7109	447.2740	.0026	.0003
2283.9929	P 44	D	.0000	18.7736	89.6698	415.5681	.0024	.0001
2286.0682	P 42	D4	.0006	19.9789	77.9043	376.3704	.0029	.0001
2288.1193	P 40	D	.0005	18.9269	62.0000	349.3159	.0026	.0002
2290.1461	P 38	D3	-.0003	24.1051	42.4599	409.5401	.0025	.0001
2292.1504	P 36	D	-.0001	18.0617	84.0000	371.6608	.0025	.0000
2294.1299	P 34	DY	-.0009	25.0937	60.6544	461.1917	.0028	.0000

position. Each line is then identified by its branch (P or R), and J quantum number. If an asterisk appears by the J quantum number, the line will be used in the least-squares fit. In the next column, indicated by one character identifier codes (see Table 6) are all previously identified bands that could be contributing to the observed absorption feature. Next comes the difference between the observed and the calculated line position ( $O - C$ ), approximate strength, maximum absorptance at the line center position, height of the absorption feature, line width, and finally the line asymmetry. The definitions of these parameters were illustrated in the previous section of this report. The line positions, width, and asymmetry are given in units of  $\text{cm}^{-1}$ . The absorptance and line height are given in units where 1000 represents an absorptance of 1. The intensity is given in these units times  $\text{cm}^{-1}$ .

The Identification Procedure. The first step in the identification was to make a Loomis-Wood diagram and a table of data for each rotation-vibration band. Which procedure was applied next depended on the individual rotation-vibration band. For well known bands, such as the  $00011 + 00001$  band of  $^{12}\text{C}^{16}\text{O}_2$  (Figure 34), it was possible to make the identification of the experimental lines as simply the line closest to the position calculated

using existing spectroscopic constants. The lines belonging to the better known bands were identified first; hence, as the identification worked toward the more difficult bands, many of the lines would already have been identified. For other bands, such as the 02211 + 02201 band of  $^{12}\text{C}^{16}\text{O}_2$  (Figure 35), the positions of lines for low J have been well measured, but not for high J. In these cases, the line positions were again calculated and the experimental lines identified, starting at low J and moving to higher J, until there were no lines close (within about  $0.01\text{ cm}^{-1}$ ) to the calculated values. The band was then refit and new constants obtained. This process was iterated until no further extension to higher J was possible. Existing molecular constants for some bands such as the 13312 + 13302 band of  $^{12}\text{C}^{16}\text{O}_2$  (Figure 36), were so inaccurate that identifications could not be made by taking the experimental line closest to the calculated line position even for low J. For these bands a different iterative procedure was used. A Loomis-Wood diagram and a table of data were produced for each attempted fit. From this information, the operator determined possible alternative lines to be used in the next iteration of the fit. The significance of the various displayed information such as randomness of residuals, patterns of the intensity, width, asymmetry, and so forth were considered subjectively by the operator. Although it was sometimes difficult to decide

which lines belonged in the fit of a given band, it was generally possible to determine when the proper lines had finally been found, since the quality of the fit increased quite dramatically. That is, the resulting residuals were small and randomly orientated and such parameters as line intensity and width followed a smooth pattern over the entire range of J for which the particular band should have been observable.

It would have been possible to increase the automation of the identification process, but it would have been very doubtful if it could have been done without first identifying most of the bands by hand, due to the difficulty of determining a priori the significance of the various parameters such as randomness of residuals, and the patterns of intensity and width for each type of band.

#### Least-Squares Fit

After the spectral lines belonging to each band were identified in the experimental spectrum, a weighted least-squares fit was used to obtain new molecular constants. Although over 10000 lines were identified in the experimental spectrum, only about 8000 were used in the least-squares fits, due to line merging problems. Many of the remaining lines were slightly affected by the presence of close-by spectral lines. These slightly merged lines were included in the least-squares fit, but with reduced

weighting. Each band was fit independently without making any attempt to combine the information from the various bands into a single global self consistent set of energy levels for the  $\text{CO}_2$  molecule.

There were several constraints placed on the spectroscopic constants. These constraints depended on the statistical significance of the various constants, and on the value of the vibrational angular momentum  $\ell$ . Each band was fit twice, once using H's, and once without. The spectroscopic constants  $H'$  and  $H''$  were included in the final least-squares fit only when their inclusion markedly improved the quality of the fit (a reduction in the rms error of more than 20%) and the uncertainties in H were smaller than the value of H for both the upper and the lower states. Occasionally, an exception was made for bands where  $\ell$ -type doubling was present (bands where  $\ell > 0$ ). For example, if the e levels indicated the need of an H and the f levels did not, for consistency H's were sometimes used for both sets of levels. The two sets of spectroscopic constants that occur for bands where  $\ell$ -type doubling occurs are not independent, as was discussed in Chapter III. For these bands, several of the spectroscopic constants for the e and the f set of levels were constrained to be equal.

In order that this weighted least-squares fitting

procedure could be used, it was necessary that an estimate of the uncertainty of each experimental line be made. The weight assigned each spectral line was the reciprocal of the expected uncertainty squared.<sup>46</sup> The factors that went into calculating the expected uncertainty of each line were: the random experimental noise in the spectrum, line asymmetry, abnormal width of spectral lines, and inconsistencies of line positions compared to other lines in the same band. The total uncertainty for each line was defined as the square root of the sum of squares of the individual uncertainties.

The individual uncertainties were determined from the experimental spectra. An estimate of  $0.0003 \text{ cm}^{-1}$  for the uncertainty due to random experimental noise was determined by examining the residuals to the fit of the lines at the high frequency end of the  $\nu_3$  fundamental R branch. These lines are known to not be merged with lines of any other band. In order to estimate the uncertainty due to asymmetry and abnormal line width, a chord was drawn across each absorption feature a small distance up from the bottom. This procedure was described in a previous section of this chapter. The uncertainty due to asymmetry was defined as being proportional to the total amount of asymmetry. The uncertainty due to abnormal width was defined as being proportional to the magnitude of the measured width minus a standard width. By looking at the

distribution of the residuals to the fit in Appendix B, it can be seen that the weights that were chosen are quite good.

If it would have seemed necessary, a more rigorous determination of the weighting of spectral lines could have been incorporated into the same basic framework. The various proportionality constants can be thought of as the leading terms in a Taylor series expansion of the true weighting function. One method for obtaining more precise values of these proportionality constants would be to synthesize a large number of line profiles with random spacings and intensities, and then use a least-squares fit to obtain the best values for the various constants. Higher order terms in the Taylor series expansion of the weighting function could have been obtained in the same manner.

The most noticeable effect of using a weight for each spectral line was to substantially reduce the uncertainty in the spectroscopic constants as predicted by the least-squares fitting program. However, the spectral line positions calculated using the resulting constants were found to be quite insensitive to the values of the weights chosen. This indicates that the effects of line merging on the position of spectral lines were essentially random for the high temperature CO<sub>2</sub> spectra considered in this study.

## CHAPTER VI

### RESULTS AND DISCUSSION

The more than 8000 lines which were not seriously merged with other spectral lines, were used to obtain new molecular constants for 50 bands of  $\text{CO}_2$  in the  $4.3 \mu\text{m}$  region and 23 bands in the  $2.8 \mu\text{m}$  region. The results of the present study, in addition to being a useful source of information on line positions of transitions originating from highly excited rotational states, demonstrate other interesting principles. Extrapolating the position of high temperature lines from room temperature measurements is not very effective, even when the positions of the room temperature lines are known with a great deal of precision. The molecular constants obtained from a more theoretical approach such as Chedin<sup>2</sup> has done, while giving a good qualitative fit to the experimental data, do not predict the position of spectral lines to within the experimental accuracy. However, Chedin's molecular constants are a big help in the identification of the experimental lines, since they serve as an excellent starting point from which to begin the search for the lines of each band in the experimental spectra. His molecular constants are particularly helpful for those bands that have not been observed previously.

Several checks were made on the data to insure its

high quality. The wavenumber calibration of the interferometer and the correct functioning of the computer program that determined line positions were verified by measuring the position of some very well know lines and comparing the positions obtained to those reported by other workers. As a check that the identification procedure was working correctly, the new molecular constants determined for the  $4.3\text{ }\mu\text{m}$   $^{12}\text{C}^{16}\text{O}_2$  bands were used to synthesize an artificial spectrum which was then compared point by point to the experimental spectrum.

For the present study, the spectra of three  $\text{CO}_2$  samples having different isotopic composition were measured using a variety of different temperatures and pressures. Taking data under different experimental conditions assists in the identification process and maximizes the number of spectral lines measured under optimal conditions. The isotopic composition of the three different  $\text{CO}_2$  samples is given in Table 8. A summary of the experimental condition for the different spectra is given in Table 9. Typical measurement times for each spectrum were 15 hours. The spectra in the  $4.3\text{ }\mu\text{m}$  region were taken at a resolution of  $0.007\text{ cm}^{-1}$  and the spectra in the  $2.8\text{ }\mu\text{m}$  region at a resolution of  $0.006\text{ cm}^{-1}$ . When several spectra were taken under identical experimental conditions the spectra were coadded to improve the signal to noise. The line positions and expected uncertainties for each line were then

Table 8. Isotopic composition of different CO<sub>2</sub> samples used in this study.

---

---

Natural sample:

$^{12}\text{C}^{16}\text{O}_2$	= 0.984	$^{12}\text{C}^{16}\text{O}^{18}\text{O}$	= 0.004
$^{13}\text{C}^{16}\text{O}_2$	= 0.011	$^{12}\text{C}^{16}\text{O}^{17}\text{O}$	= 0.001

C-13 sample:

$^{13}\text{C}^{16}\text{O}_2$	= 0.880	$^{12}\text{C}^{16}\text{O}_2$	= 0.005
$^{13}\text{C}^{16}\text{O}^{18}\text{O}$	= 0.106	$^{13}\text{C}^{16}\text{O}^{17}\text{O}$	= 0.004

O-18 sample:

$^{12}\text{C}^{16}\text{O}^{18}\text{O}$	= 0.465
$^{12}\text{C}^{16}\text{O}_2$	= 0.355
$^{12}\text{C}^{18}\text{O}_2$	= 0.167

---

determined as explained in Chapter V. The line positions and expected uncertainties determined from the spectra measured at different temperatures and pressures were combined into a single data set. Least-squares fits to obtain new molecular constants were then performed.

The calibration of the interferometer in the 4.3  $\mu\text{m}$  region was checked but no wavenumber correction was made since the indicated correction would have been less than 0.0001  $\text{cm}^{-1}$ . The check was performed by observing lines of the 1 + 0 band of  $^{12}\text{C}^{16}\text{O}$  and the  $\nu_3$  fundamental of  $^{12}\text{C}^{16}\text{O}_2$

Table 9. Summary of experimental conditions for measured spectra.

Region ( $\mu\text{m}$ )	Isotopic Sample	Temperature ( $^{\circ}\text{K}$ )	Pressure (Torr)	Number of Spectra
4.3	Natural	800	6	2
4.3	C-13	600	6	2
4.3	C-13	800	3	2
4.3	C-13	800	6	2
4.3	O-18	300	3	1
4.3	O-18	300	6	2
4.3	O-18	500	3	2
4.3	O-18	800	3	2
4.3	O-18	800	6	3
2.8	O-18	300	2	3
2.8	O-18	600	3	3
2.8	O-18	800	4	3
2.8	O-18	800	15	1
Total =				28

and comparing the measured line positions to those reported by other workers. The small amount of CO that was present in the high temperature CO<sub>2</sub> gas sample, possibly arose from a catalytic decomposition of the CO<sub>2</sub> on the walls of the absorption cell. These CO lines have been measured by G. Guelachvili<sup>47</sup> with a claimed error of less than 0.0001 cm<sup>-1</sup>. Table 10 compares the CO lines observed in the present experimental spectra with those measured by Guelachvili. The measured CO lines are 0.00014 cm<sup>-1</sup> higher

Table 10. Observed CO lines used to check calibration of spectrometer.

J	P	OBS	O-C	UNC	R	OBS	O-C	UNC
0					2147.0818	2	3	
1	2139.4269	3	4		2150.8567	2	3	
2	2135.5470	3	4		2154.5964	3	5	
3	2131.6323	2	3		2158.3002	0	4	
4	2127.6833	4	5		2161.9680	-7	9	
5	2123.6987	-6	9		2165.6014	-1	6	
6	2119.6815	0	5		2169.1985	1	6	
7	2115.6299	4	5		2172.7595	2	7	
8	2111.5437	2	4		2176.2837	-3	7	
9	2107.4243	6	7		2179.7724	0	4	
10	2103.2707	5	4		2183.2242	-1	8	
11	2099.0835	3	3		2186.6396	1	5	
12	2094.8629	1	4		2190.0182	2	5	
13	2090.6092	0	4		2193.3604	8	10	
14	2086.3225	1	3		2196.6636	-6	7	
15	2082.0023	-4	7		2199.9317	2	7	
16	2077.6507	5	4		2203.1613	-2	4	
17	2073.2652	1	4		2206.3537	-3	5	
18	2068.8479	5	4		2209.5088	0	5	
19	2064.3979	5	5		2212.6258	0	5	
20	2059.9153	2	3		2215.7056	6	10	
21	2055.4013	5	5		2218.7447	-13	13	
22	2050.8551	5	4		2221.7471	-17	18	
23	2046.2767	2	4		2224.7130	-2	4	
24	2041.6673	4	4		2227.6384	-7	8	
25	2037.0261	4	4		2230.5256	-8	6	
26	2032.3535	2	4		2233.3744	-4	5	
27	2027.6495	-1	5		2236.1846	3	7	
28	2022.9150	1	4		2238.9551	4	9	
29	2018.1494	2	4		2241.6842	-16	15	
30	2013.3534	6	5		2244.3785	10	29	
31	2008.5259	1	4		2247.0293	-4	4	
32	2003.6684	0	5		2249.6421	-2	5	
33	1998.7811	5	4					
34	1993.8628	2	5		2254.7478	1	9	
35	1988.9148	2	5		2257.2383	-20	13	

Observed minus calculated values (O-C) and the expected uncertainties (UNC) are in units of  $10^{-4} \text{ cm}^{-1}$ .

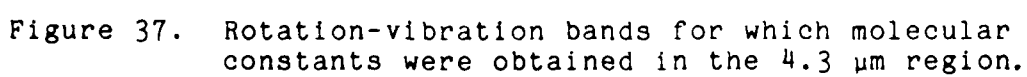
on the average than the positions reported by Guelachvili. The only  $\text{CO}_2$  band that has been observed previously at both high resolution and high temperature is the  $\nu_3$  fundamental of  $^{12}\text{C}^{16}\text{O}_2$ . A. Pine and G. Guelachvili<sup>11</sup> have made a joint measurement in which Pine used a tunable laser difference-frequency spectrometer to observe a  $\text{CO}_2$  sample heated to 985 K and combined his data with a room temperature  $\text{CO}_2$  spectrum measured by Guelachvili. The wavenumber calibration of this joint measurement was determined from Guelachvili's data. The line positions determined in the present work for this band were  $0.00017 \text{ cm}^{-1}$  lower on the average than Pine and Guelachvili's reported values. The rms line position scatter was  $0.0003 \text{ cm}^{-1}$  for the CO lines and  $0.0005 \text{ cm}^{-1}$  for the  $^{12}\text{C}^{16}\text{O}_2$  lines. The scatter in the positions of the CO lines was less than that of the  $\text{CO}_2$  lines since the CO lines were in a region of the spectra where line merging was minimal.

In the  $2.8 \text{ }\mu\text{m}$  region, the experimental spectra were calibrated by adjusting the wavenumber scale of the experimental spectra to match, on the average, the positions of the low J lines of the  $10011 + 00001$  and  $10012 + 00001$  bands of  $^{12}\text{C}^{16}\text{O}_2$  as reported in the 1982 line compilation.<sup>16</sup> These  $\text{CO}_2$  line positions are also indirectly tied to Guelachvili's line positions.

Recent work by other researchers<sup>49,50</sup> has shown that there are systematic errors in the line positions reported

by Guelachvili. His values are  $0.0002 \text{ cm}^{-1}$  to  $0.0004 \text{ cm}^{-1}$  too high. This implies that the line positions presented in this report are also too high by the same amount. No wavenumber correction was made, because the exact correction was still somewhat unclear, and a correction on the order of  $0.0003 \text{ cm}^{-1}$  would have been of questionable value, since the line positions of the present work are not accurate to more than  $0.0004 \text{ cm}^{-1}$  due to random noise in the experimental spectrum.

The 19  $^{12}\text{C}^{16}\text{O}_2$  bands that were identified in the  $4.3 \text{ }\mu\text{m}$  region are indicated on the energy level diagram of figure 37 and the 11  $^{12}\text{C}^{16}\text{O}_2$  bands in the  $2.8 \text{ }\mu\text{m}$  region on figure 38. There were fewer bands identified of the other isotopic variants of  $\text{CO}_2$ , primarily due to the increased difficulty in identifying these bands. A complete listing of the experimental lines used to obtain new molecular constants is given in Appendix B along with the expected uncertainties and the difference between the observed line positions and the positions calculated using the new molecular constants. Information on the least-squares fit for each band is given in Table 11 for the  $4.3 \text{ }\mu\text{m}$  bands and in Table 12 for the  $2.8 \text{ }\mu\text{m}$  bands. This information includes the range of J values, total number of lines, and the standard deviation. The new molecular constants are given in Table 13 and Table 14 for the  $4.3$  and  $2.8 \text{ }\mu\text{m}$  bands, respectively.



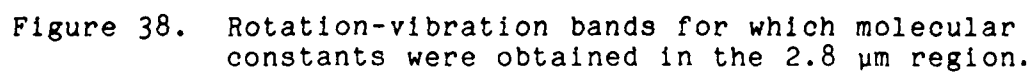


Table 11. Bands for which molecular constants were obtained in the 4.3  $\mu\text{m}$  region.

Transition	Isotope	Band Center ( $\text{cm}^{-1}$ )	Range of Measurement	Number of Lines	RMS Error ( $10^{-4}\text{cm}^{-1}$ )
*13311	13301	2288.3903	P(68)-R(63)	70	6
*13312	13302	2290.6806	P(80)-R(71)	86	5
*04411	04401	2299.2141	P(89)-R(75)	102	6
02221e	02211e	2299.2395	P(79)-R(71)	38	6
02221f	02211f	2299.2395	P(78)-R(76)	40	6
12211e	12201e	2301.0539	P(88)-R(60)	48	8
12211f	12201f	2301.0539	P(89)-R(81)	48	6
10022	10012	2302.3735	P(77)-R(73)	36	7
20011	20001	2302.5227	P(80)-R(78)	52	5
20013	20003	2305.2568	P(86)-R(74)	45	5
20012	20002	2306.6920	P(62)-R(56)	36	6
*03311	03301	2311.6681	P(90)-R(85)	116	5
01121e	01111e	2311.7008	P(86)-R(60)	45	9
01121f	01111f	2311.7008	P(89)-R(91)	57	5
11111e	11101e	2313.7726	P(95)-R(89)	59	5
11111f	11101f	2313.7726	P(92)-R(88)	61	6
11112e	11102e	2315.2350	P(61)-R(61)	48	6
11112f	11102f	2315.2350	P(98)-R(88)	65	6
02211e	02201e	2324.1410	P(102)-R(104)	82	4
02211f	02201f	2324.1410	P(107)-R(103)	83	4
00021	00011	2324.1820	P(99)-R(79)	69	6
10011	10001	2326.5980	P(108)-R(106)	88	5
10012	10002	2327.4327	P(106)-R(102)	86	4
01111e	01101e	2336.6330	P(113)-R(115)	105	4
01111f	01101f	2336.6330	P(114)-R(110)	96	3
00011	00001	2349.1446	P(126)-R(118)	76	3
*04411	04401	2236.6789	P(90)-R(95)	106	5
02221e	02211e	2236.6790	P(61)-R(55)	27	13
02221f	02211f	2236.6790	P(72)-R(60)	35	12
12211e	12201e	2238.5706	P(88)-R(40)	41	9
12211f	12201f	2238.5706	P(89)-R(77)	48	9
20013	20003	2240.5362	P(88)-R(90)	53	7
20012	20002	2242.3238	P(82)-R(62)	41	7
03311e	03301e	2248.3567	P(95)-R(93)	71	4
03311f	03301f	2248.3567	P(98)-R(96)	72	6
01121e	01111e	2248.3618	P(100)-R(92)	60	6
01121f	01111f	2248.3618	P(87)-R(71)	46	6
11111e	11101e	2250.6054	P(97)-R(83)	69	7
11111f	11101f	2250.6054	P(100)-R(84)	66	5
11112f	11102f	2250.6931	P(98)-R(78)	64	4
02211e	02201e	2260.0500	P(106)-R(104)	89	4
02211f	02201f	2260.0500	P(103)-R(101)	83	3
00021	00011	2260.0617	P(105)-R(103)	82	5
10012	10002	2261.9102	P(104)-R(104)	96	4
10011	10001	2262.8486	P(102)-R(102)	90	4
01111e	01101e	2271.7604	P(113)-R(107)	103	3
01111f	01101f	2271.7604	P(116)-R(112)	108	3
00011	00001	2283.4874	P(122)-R(122)	118	3
02211e	02201e	2242.8075	P(86)-R(75)	101	7
02211f	02201f	2242.8075	P(77)-R(74)	90	5
10011	10001	2245.2726	P(83)-R(81)	95	6
10012	10002	2245.4960	P(84)-R(80)	94	6
01111e	01101e	2254.3803	P(94)-R(94)	128	7
01111f	01101f	2254.3803	P(99)-R(101)	128	6
00011	00001	2265.9719	P(106)-R(100)	181	4

\* Separate e and f constants were not determined.

Transition	Isotope	Band Center ( $\text{cm}^{-1}$ )	Range of Measurement	Number of Lines	RMS Error ( $10^{-4} \text{cm}^{-1}$ )
02211e 02201e	$^{12}\text{C}^{18}\text{O}_2$	2289.5689	P( 94)-R( 72)	60	4
02211f 02201f		2289.5689	P(101)-R( 69)	70	6
10011 10001		2290.9720	P( 98)-R( 54)	65	5
10012 10002		2294.8795	P( 98)-R( 88)	64	7
01111e 01101e		2301.7996	P(111)-R(101)	88	5
01111f 01101f		2301.7996	P(122)-R(102)	92	4
00011 00001		2314.0489	P(128)-R(106)	102	4
02211e 02201e	$^{12}\text{C}^{16}\text{O}^{18}\text{O}$	2307.3830	P(100)-R( 92)	136	9
02211f 02201f		2307.3830	P( 96)-R( 98)	135	7
10011 10001		2309.2898	P(100)-R( 98)	125	5
10012 10002		2311.7151	P(103)-R( 92)	144	4
01111e 01101e		2319.7380	P(113)-R(113)	157	5
01111f 01101f		2319.7380	P(111)-R(105)	159	4
00011 00001		2332.1127	P(119)-R(117)	213	3
00011 00001	$^{13}\text{C}^{16}\text{O}^{17}\text{O}$	2274.0884	P( 73)-R( 80)	100	6

Table 12. Bands for which molecular constants were obtained in the 2.8  $\mu\text{m}$  region.

Transition	Isotope	Band Center ( $\text{cm}^{-1}$ )	Range of Measurement	Number of Lines	RMS Error ( $10^{-4} \text{cm}^{-1}$ )
12212e 02201e	$^{12}\text{C}^{16}\text{O}_2$	3552.8568	P( 46)-R( 50)	40	5
12212f 02201f		3552.8568	P( 41)-R( 43)	29	8
20013 10002		3568.2165	P( 56)-R( 60)	46	4
11112e 01101e		3580.3265	P( 57)-R( 65)	58	3
11112f 01101f		3580.3265	P( 70)-R( 74)	65	3
20012 10001		3589.6520	P( 56)-R( 52)	43	5
10012 00001		3612.8416	P( 82)-R( 86)	84	3
20012 10002		3692.4278	P( 62)-R( 64)	51	4
20011 10001		3711.4776	P( 56)-R( 58)	49	3
21111e 11101e		3713.7218	P( 39)-R( 35)	29	8
21111f 11101f		3713.7218	P( 40)-R( 40)	29	5
10011 00001		3714.7825	P( 84)-R( 86)	81	3
11111e 01101e		3723.2501	P( 77)-R( 75)	72	3
11111f 01101f		3723.2501	P( 70)-R( 70)	66	3
12211e 02201e		3726.6475	P( 52)-R( 56)	43	5
12211f 02201f		3726.6475	P( 53)-R( 57)	45	5
*12212 02201	$^{12}\text{C}^{16}\text{O}^{18}\text{O}$	3511.4117	P( 33)-R( 28)	50	5
20013 10002		3531.8352	P( 56)-R( 59)	95	5
11112e 01101e		3538.7785	P( 64)-R( 68)	120	4
11112f 01101f		3538.7785	P( 67)-R( 66)	120	3
20012 10001		3539.0176	P( 53)-R( 53)	74	7
10012 00001		3571.1409	P( 82)-R( 82)	155	3
20012 10002		3645.4356	P( 53)-R( 53)	82	4
10011 00001		3675.1337	P( 77)-R( 77)	148	3
20011 10001		3676.7399	P( 48)-R( 50)	63	6
11111e 01101e		3683.8136	P( 66)-R( 66)	106	4
11111f 01101f		3683.8136	P( 65)-R( 66)	113	4
12211e 02201e		3687.4754	P( 51)-R( 52)	76	8
12211f 02201f		3687.4754	P( 50)-R( 53)	70	9
10012 00001	$^{12}\text{C}^{18}\text{O}_2$	3525.2048	P( 62)-R( 74)	66	3
10011 00001		3638.0657	P( 78)-R( 74)	70	3

\* Separate e and f constants were not determined.

Table 13. Molecular constants resulting from the least-squares-fits in the 4.3  $\mu\text{m}$  region. ( $\text{cm}^{-1}$ )

Transition	Isotope	G' - G''	B'	D' $10^{-7}$	H' $10^{-13}$	B''	D'' $10^{-7}$	H'' $10^{-13}$
13311	$^{12}\text{C}^{16}\text{O}_2$	2288.3903	38924017	1.31589		39220925	1.36625	
13312		2290.6806	38971897	1.50200		39266187	1.51314	
04401		2299.2141	39010795	1.40537		39307699	1.42636	
0221e		2299.2395	38558866	1.27861		38861780	1.29631	
0221f		2299.2395	38558866	1.34986		38861780	1.35551	
1221e		2301.0539	38852763	1.32999	-15.193	39155212	1.38493	-14.793
1221f		2301.0539	38852763	1.28742	3.377	39155212	1.31005	3.542
10022		2302.3735	38450713	1.53830		38748352	1.53907	
20011		2302.5227	38748094	1.91378		39058527	1.91759	
20013		2305.2568	38819166	1.81070	6.146	39110450	1.81179	6.131
20012		2306.5920	38652911	1.32884		38956006	1.33253	
03311		2311.6681	38937881	1.40062		39238135	1.41430	
01121e		2311.7008	38456180	1.37531		38760588	1.37732	
01121f		2311.7008	38512919	1.35410		38819107	1.35747	
1111e		2313.7726	38736222	1.23187		39040693	1.24892	
1111f		2313.7726	38823967	1.20770		39133818	1.21662	
1112e		2315.2350	38777790	1.46037	1.733	39074013	1.46449	-2.554
1112f		2315.2350	38870231	1.56444	1.558	39168661	1.56032	1.026
0221e		2324.1410	38863731	1.37189	-2.592	39166800	1.38599	-2.802
0221f		2324.1410	38863731	1.37866	.376	39166800	1.38480	.345
00021		2324.1820	38406877	1.32429		38714344	1.33495	
10011		2326.5980	38706262	1.14622	2.196	39018838	1.15310	2.182
10012		2327.4327	38750450	1.57535	2.022	39048336	1.57037	2.047
0111e		2336.6330	38758765	1.34261		39063453	1.34870	
0111f		2336.6330	38818583	1.35253		39125043	1.35620	
00011		2349.1446	38713910	1.32721		39021715	1.33114	
04411	$^{13}\text{C}^{16}\text{O}_2$	2236.6789	39011145	1.39479		39295597	1.41303	
0221e		2236.6790	38578409	1.31278	-6.628	38869363	1.28826	-12.271
0221f		2236.6790	38578409	1.51164	31.110	38869363	1.48371	25.389
1221e		2238.5706	38825785	1.95409		39115785	1.01674	
1221f		2238.5706	38825785	1.23797		39115785	1.26190	
20013		2240.5362	38882367	1.78174		39164610	1.79071	
20012		2242.3238	38684311	1.31706		38969564	1.33098	
0331e		2248.3567	38939505	1.35075	-2.270	39227992	1.36339	-2.435
0331f		2248.3567	38939505	1.35075	-1.569	39227992	1.36339	-1.720
01121e		2248.3618	38476222	1.39545	5.530	38769142	1.39623	5.086
01121f		2248.3618	38535419	1.36520	.124	38830264	1.36794	.213

Transition	Isotope	G' - G"	B'	D' 10 <sup>-7</sup> H' 10 <sup>-13</sup>	B"	D" 10 <sup>-7</sup> H" 10 <sup>-13</sup>
1111e 11101e	$^{13}\text{C}^{16}\text{O}_2$	2250.6054	3871.4001	1.26668	.39006111	1.28338
1111f 11101f		2250.6054	.38793200	1.20791	.39090676	1.21462
1111f 11102f		2250.6931	.38915404	1.59241	.39203041	1.59351
0221e 02201e		2260.0500	.38869071	1.29387	.39160580	1.30508
0221f 02201f		2260.0500	.38869071	1.36606	.39160580	1.37267
00021 00011		2260.0617	.38430981	1.32330	.38727161	1.32676
10012 10002		2261.9102	.38802984	1.55770	.39090927	1.56325
10011 10001		2262.8486	.38672065	1.19580	.38971446	1.19900
0111e 01101e		2271.7604	.38767658	1.34200	.39060797	1.34879
0111f 01101f		2271.7604	.38828874	1.35162	.39123987	1.35557
00011 00001		2283.4874	.38727011	1.32484	.39023412	1.32895
0221e 02201e	$^{13}\text{C}^{16}\text{O}^{18}\text{O}$	2242.8075	.36674474	1.21848	.36949255	1.22527
0221f 02201f		2242.8075	.36674474	1.24022	.36949255	1.24208
10011 10001		2245.2726	.36517122	.98794	.36800331	.99252
10012 10002		2245.4960	.36582733	1.38100	.36853039	1.37904
0111e 01101e		2254.3803	.36579333	1.19559	.36855481	1.19941
0111f 01101f		2254.3803	.36533667	1.20041	.36911468	1.20309
00011 00001		2265.9719	.36538959	1.18088	.36817957	1.18402
0221e 02201e	$^{12}\text{C}^{18}\text{O}_2$	2289.5689	.34543473	1.14020	.34812574	1.15254
0221f 02201f		2289.5689	.34543473	1.08978	.34812574	1.09345
10011 10001		2290.9720	.34464928	.93151	.34740102	.93700
10012 10002		2294.8795	.34385155	1.16556	.34651747	1.15742
0111e 01101e		2301.7996	.34453039	1.06695	.34723371	1.07024
0111f 01101f		2301.7996	.34500966	1.07486	.34772525	1.07696
00011 00001		2314.0489	.34408575	1.04460	.34681253	1.04727
0221e 02201e	$^{12}\text{C}^{16}\text{O}^{18}\text{O}$	2307.3830	.36670706	1.25735	.36956360	1.26859
0221f 02201f		2307.3830	.36670706	1.21978	.36956360	1.22449
10011 10001		2309.2898	.36556626	1.00057	.36850491	1.00917
10012 10002		2311.7151	.36530654	1.37934	.36812023	1.36902
0111e 01101e		2319.7380	.36574752	1.21711	.36861755	1.21930
0111f 01101f		2319.7380	.36625229	1.19384	.36913822	1.19722
00011 00001		2332.1127	.36528386	1.18182	.36818157	1.18479
00011 00001	$^{13}\text{C}^{16}\text{O}^{17}\text{O}$	2274.0884	.37574439	1.23942	.37861696	1.24224

Table 14. Molecular constants resulting from the least-squares-fits in the 2.8  $\mu\text{m}$  region. ( $\text{cm}^{-1}$ )

Transition	Isotope	$G' - G''$	$B'$	$D' \cdot 10^{-7} \text{H}' \cdot 10^{-13}$	$B''$	$D'' \cdot 10^{-7} \text{H}'' \cdot 10^{-13}$
*12212e 02201e	$^{12}\text{C}^{16}\text{O}_2$	3552.8568	388933665	1.44515	39167791	1.71666
*12212f 02201f		3552.8568	388933665	1.46575	39167791	1.55276
20013 10002		3568.2165	38818871	1.78000	39047458	1.54753
11112e 01101e		3580.3265	38778526	1.53072	39064187	1.39594
11112f 01101f		3580.3265	38770363	1.55643	39125370	1.35735
20012 10001		3589.6520	38654114	1.37074	39019787	1.17843
10012 00001		3612.8416	38750060	1.56715	39021640	1.32620
20012 10002		3692.4278	38653583	1.36970	39048356	1.56655
20011 10001		3711.4776	38748714	1.91235	39017719	1.10370
21111e 11101e		3713.7218	38742070	1.26521	39042557	1.39047
21111f 11101f		3713.7218	38860453	1.06619	39131737	1.19361
10011 00001		3714.7825	38706422	1.15452	39021991	1.34579
11111e 01101e		3723.2501	38736241	1.23235	39063731	1.34909
11111f 01101f		3723.2501	38823641	1.20492	39125635	1.36665
12211e 02201e		3726.6475	38852444	1.37511	39166615	1.37440
12211f 02201f		3726.6475	38852444	1.26191	39166615	1.38057
*12212 02201	$^{12}\text{C}^{16}\text{O}_2$	3511.4117	36693536	3.24024	36960119	2.32384
20013 10002		3531.8352	36575119	1.53088	36811249	1.30773
11112e 01101e		3538.7785	36571234	1.29734	36859887	1.19350
11112f 01101f		3538.7785	36649752	1.37081	36915432	1.21008
20012 10001		3539.0176	36484630	1.07248	36851693	1.01874
10012 00001		3571.1409	36530310	1.36043	36818002	1.17114
20012 10002		3645.4356	36483923	1.07619	36811764	1.36006
10011 00001		3675.1337	36557074	1.00300	36818290	1.18437
20011 10001		3676.7399	36612834	1.86682	36850891	1.02763
11111e 01101e		3683.8136	36575806	1.11703	36860280	1.21795
11111f 01101f		3683.8136	36558981	1.06446	36915117	1.20170
12211e 02201e		3687.4754	36682218	1.23351	36957038	1.26451
12211f 02201f		3687.4754	36682218	1.10124	36957038	1.19336
10012 00001		3525.2048	34385368	1.16084	34681349	1.04159
10011 00001		3638.0657	34464872	1.90536	34681474	1.04790

\* Coriolis perturbed level.

The constants reported in Tables 13 and 14 are effective molecular constants and so should not be expected to accurately represent the internal structure of the  $\text{CO}_2$  molecule. The purpose of these effective constants is to provide a means of reproducing within the experimental accuracy the position of spectral lines over the range of J values covered by the measurements. For the  $\text{CO}_2$  molecule there are a great many interactions between different vibrational states. The effects of these interactions are accounted for by allowing the different effective molecular constants to float freely in the least-squares fit of each band. Molecular constants obtained in this manner are not self-consistent. For example, the molecular constants obtained (see Table 13) for the vibrational state 00011 of  $^{12}\text{C}^{16}\text{O}_2$  from the 00011 + 00001 band are not consistent with those obtained from the 00021 + 00011 band. Molecular constants which are self-consistent and predict the position of spectral lines with nearly the accuracy of the experimental lines have also been determined,<sup>48</sup> but not as part of the present study.

The  $^{12}\text{C}^{16}\text{O}_2$  pressure in the high temperature absorption cell was too high for making accurate measurements of low J lines of the  $\nu_3$  fundamental, as the purpose of the present study was to observe lines originating from high rotation-vibration states. Hence only lines originating from states with  $J > 40$  were used in

the least-squares fit for this band. Notice that since low  $J$  lines were not used in the least-squares fit for the  $\nu_3$  fundamental of  $^{12}\text{C}^{16}\text{O}_2$  the resulting band center was too high by  $0.0013\text{ cm}^{-1}$ . If the  $\nu_3$  fundamental had not already been well measured<sup>10,11</sup> it would have been beneficial to make an additional measurement with less  $^{12}\text{C}^{16}\text{O}_2$  in the high temperature absorption cell.

There was one band, the 05511 + 05501 of  $^{12}\text{C}^{16}\text{O}_2$ , where the P branch was readily visible, but the R branch was not located. For  $\text{CO}_2$  there are some bands such as the 11101 + 00001 band where one branch has a much stronger intensity than the other branch. This nonsymmetric intensity pattern would not however be expected for a parallel band such as the 05511 + 05501 band, unless some unusual perturbation was occurring. Since there is a possibility that the lines attributed to the P branch of this band are misidentified, the 05511 + 05501 band is not included in Tables 11 as one of the bands successfully identified. However, lines from the P branch are included with the other observed lines in Appendix B.

There were a considerable number of lines in the experimental spectrum that were not identified. As was explained in Chapter V, little effort was expended in attempting to identify bands having a lower state vibrational energy greater than  $3500\text{ cm}^{-1}$ , since the resulting bands would have been so fragmentary.

The observed line positions for a number of the bands of the present study are compared to the line positions calculated using the molecular constants obtained by other workers on the residual plots of Figures 39 to 48. When comparing different plots, note that the scale on the residuals plots vary by more than a factor of ten. The range of the residuals vary from  $\pm 0.03 \text{ cm}^{-1}$  to  $\pm 0.5 \text{ cm}^{-1}$ .

Guelachvili<sup>10</sup> has previously measured several of these bands using a room temperature gas sample with more precision than the present work for low J lines. It is interesting to note how poorly these constants predict the position of high J lines (Figures 39 to 42). Notice the large discrepancies (Figures 39 and 40) between the line positions predicted using Guelachvili's molecular constants and the experimental line positions when  $J > 80$  for the  $01111 + 01101$  band of  $^{12}\text{C}^{16}\text{O}_2$ . Guelachvili's measurements extended from about P(64) to R(64). Also note the  $10011 + 10001$  band of  $^{12}\text{C}^{16}\text{O}_2$  (Figure 42) where the range of J's was P(40) to R(44). These large discrepancies could not have resulted from the wavenumber calibration problems present in Guelachvili's data that was mentioned earlier, since his calibration errors resulted in only a simple offset to the data. It appears to be a general principle that the molecular constants  $G_v$ ,  $B_v$ ,  $D_v$ , and  $H_v$  obtained using low J lines do not successfully predict the position of high J lines.

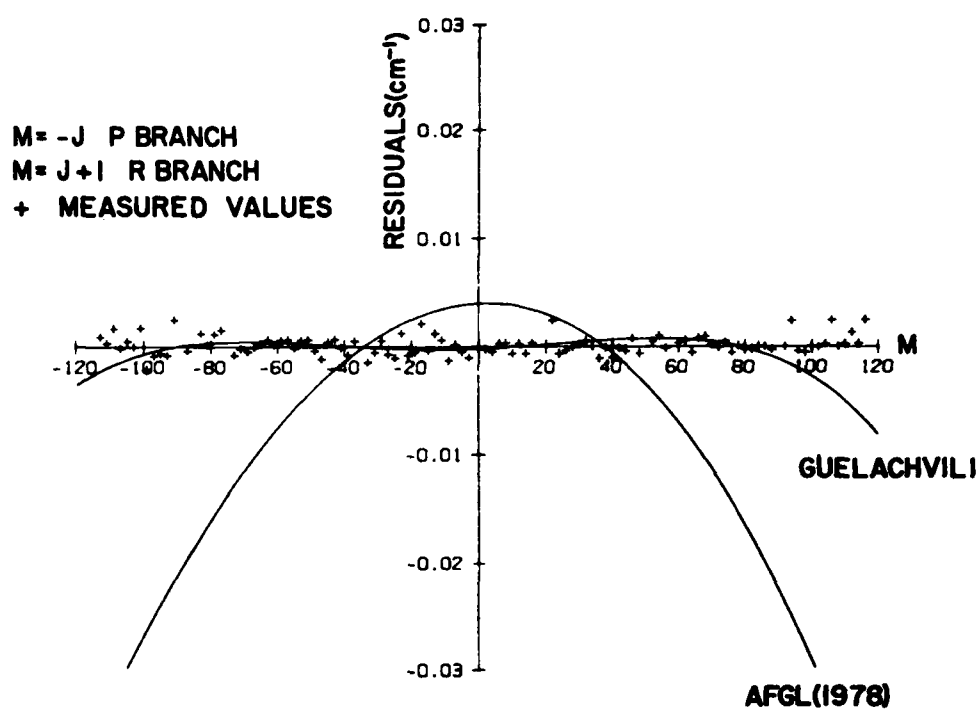


Figure 39. Comparison of measured line positions with those computed using Guelachvili's and the AFGL (1978) constants for the 01111e + 01101e band of  $^{12}\text{C}^{16}\text{O}_2$

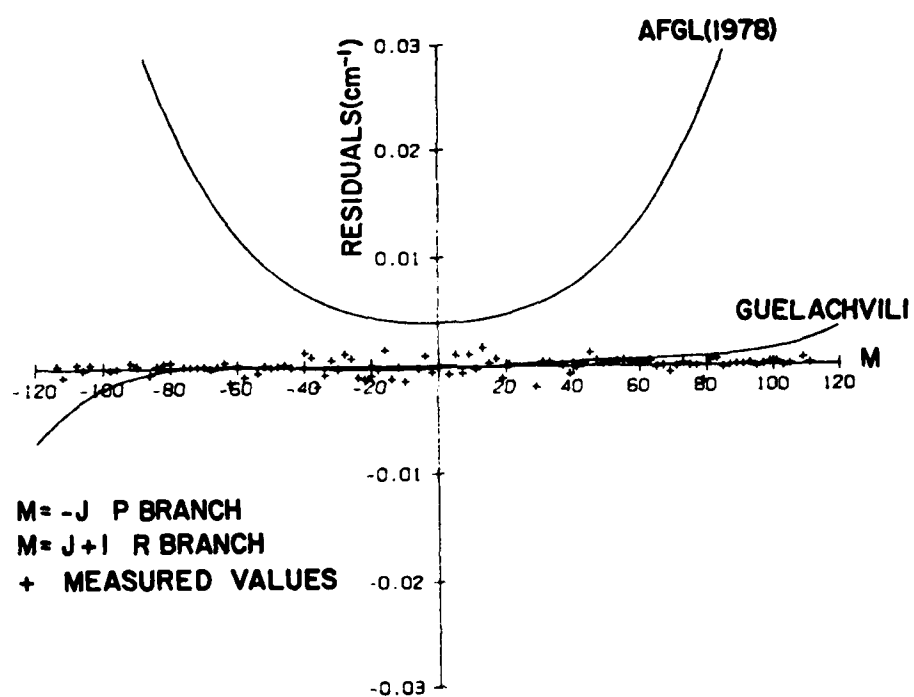


Figure 40. Comparison for the 01111f + 01101f band of  $^{12}\text{C}^{16}\text{O}_2$

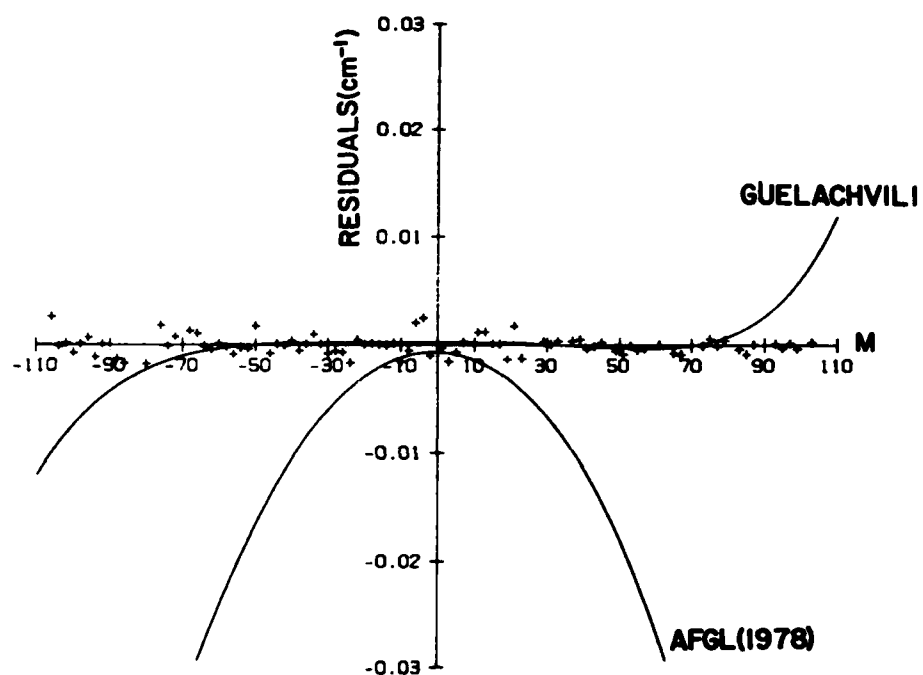


Figure 41. Comparison for the 10012 + 10002 band of  $^{12}\text{C}^{16}\text{O}_2$

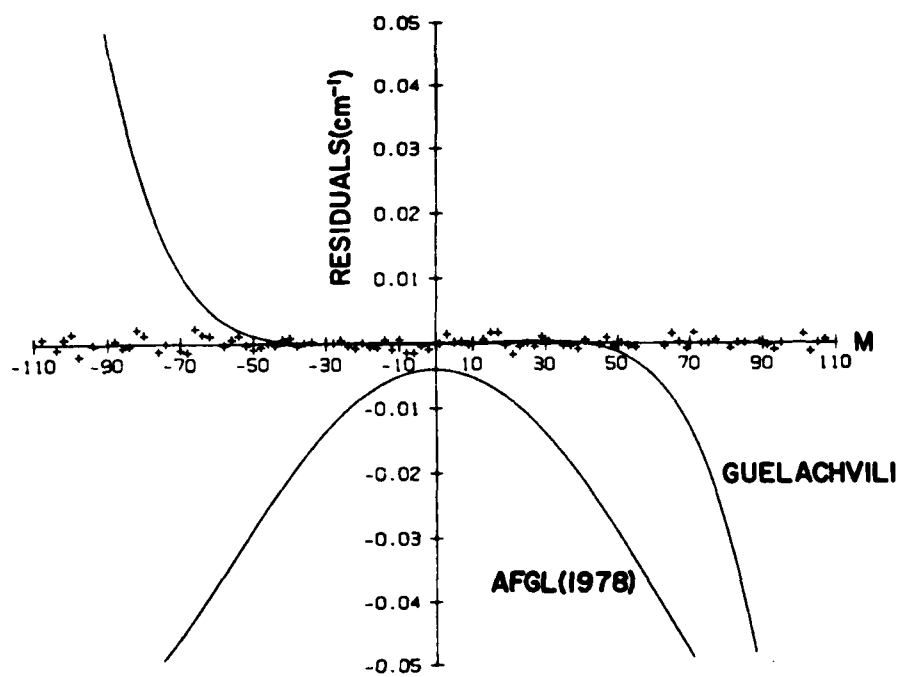


Figure 42. Comparison for the 10011 + 10001 band of  $^{12}\text{C}^{16}\text{O}_2$

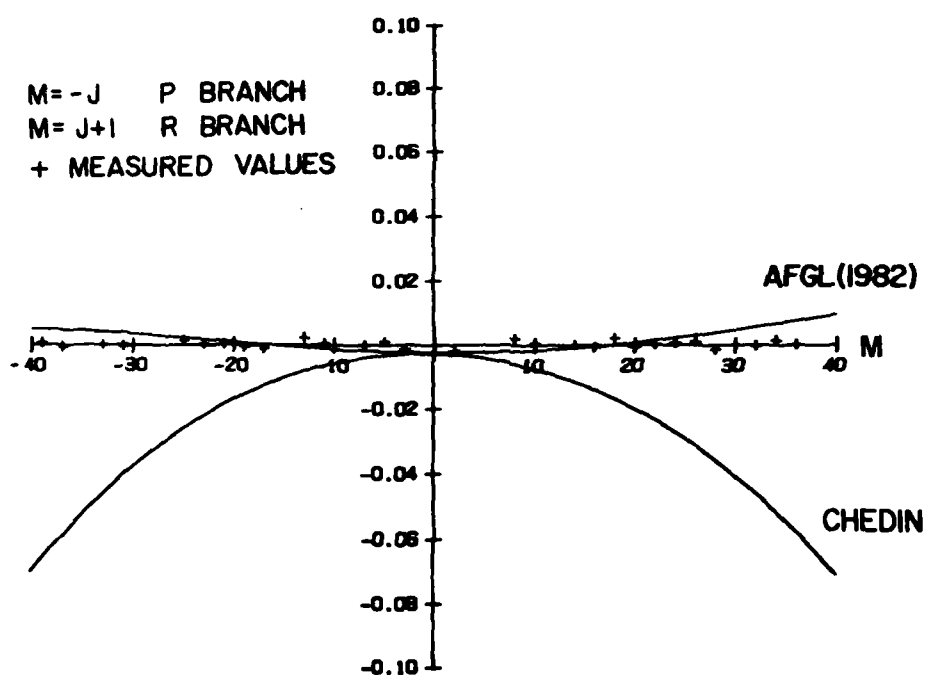


Figure 43. Comparison for the 21111e + 11101e band of  $^{12}\text{C}^{16}\text{O}_2$

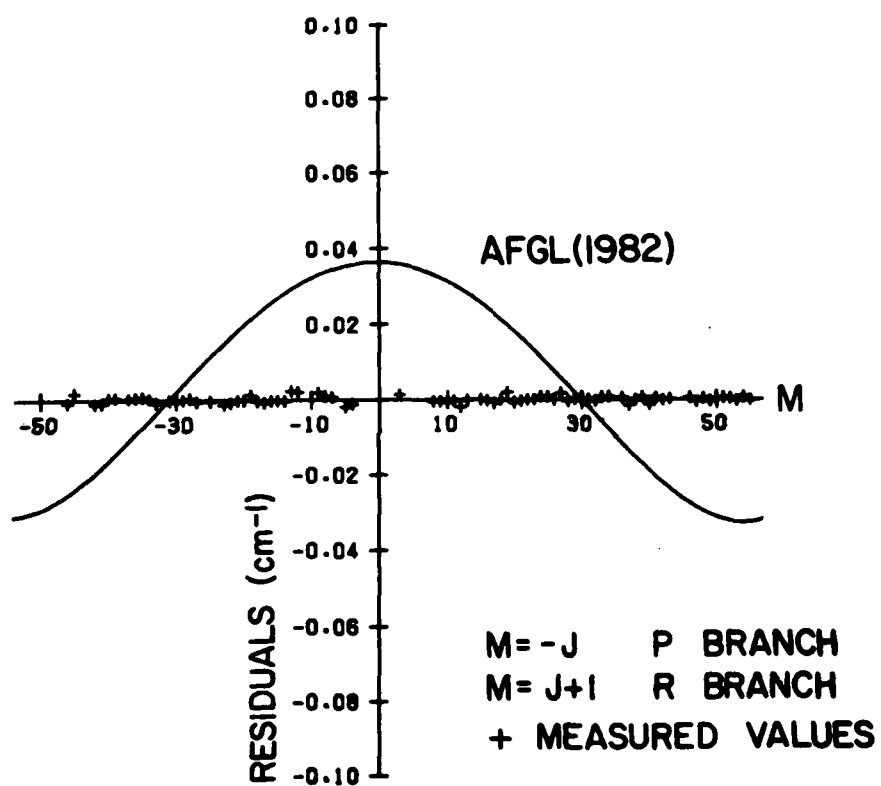


Figure 44. Comparison for the 11112e + 01101e band  
of  $^{12}\text{C}^{16}\text{O}^{18}\text{O}$

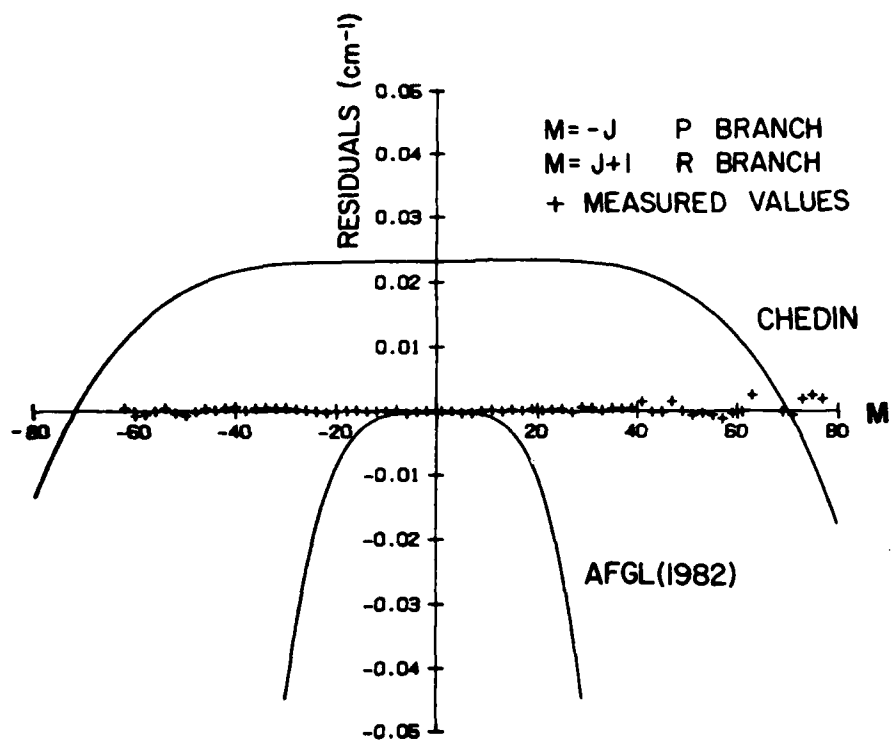


Figure 45. Comparison for the 10012 + 00001 band of  $^{12}\text{C}^{18}\text{O}_2$

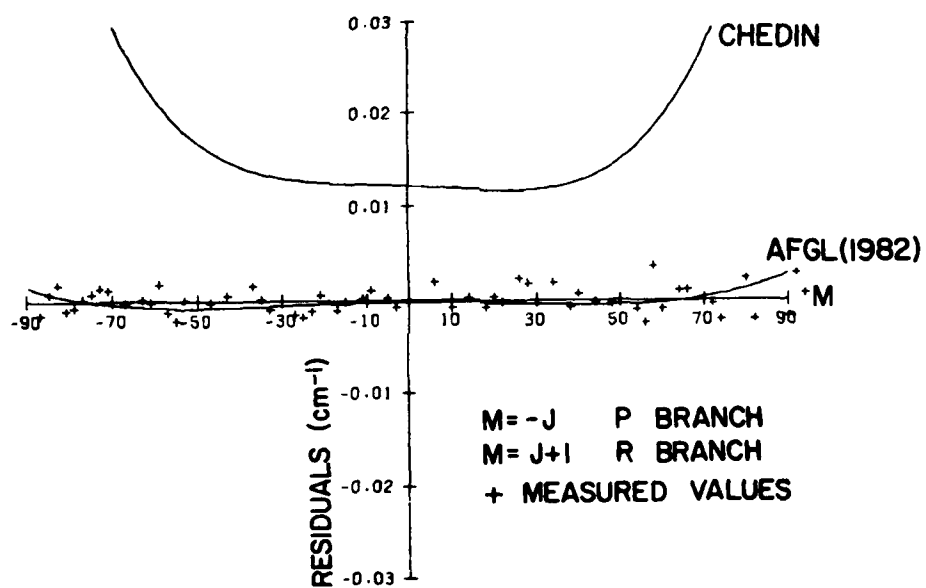


Figure 46. Comparison for the 01121f + 01111f band of  $^{13}\text{C}^{16}\text{O}_2$

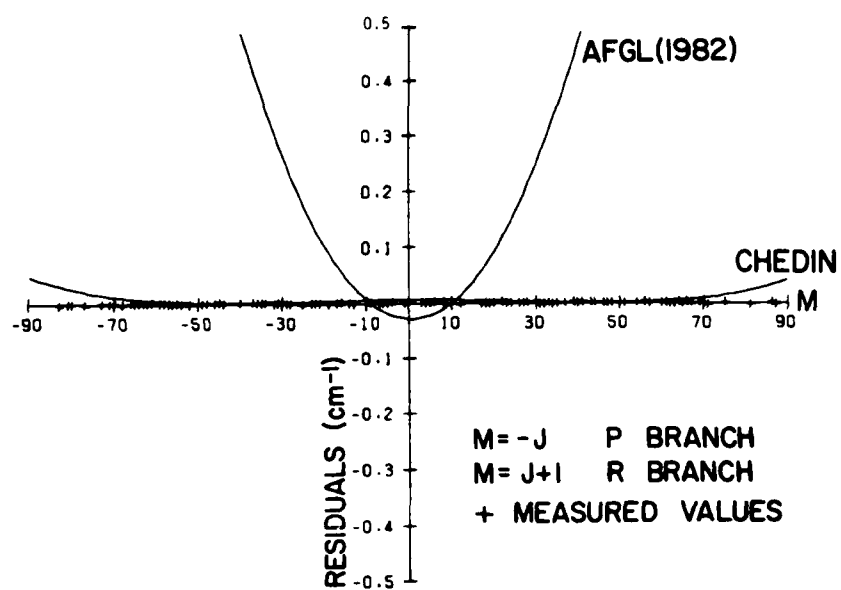


Figure 47. Comparison for the 10012 + 10002 band of  $^{13}\text{C}^{16}\text{O}^{18}\text{O}$

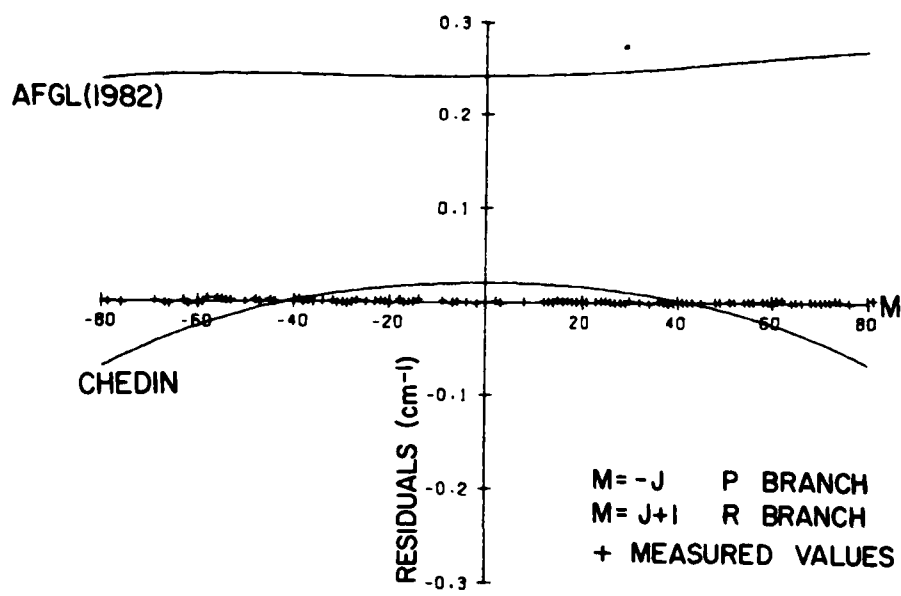


Figure 48. Comparison for the 00011 + 00001 band of  $^{13}\text{C}^{16}\text{O}^{17}\text{O}$

For the asymmetric CO<sub>2</sub> molecules  $^{12}\text{C}^{16}\text{O}^{18}\text{O}$ ,  $^{13}\text{C}^{16}\text{O}^{18}\text{O}$ , etc., each P and R branch is split into two branches by  $\ell$ -type doubling when  $\ell > 0$ . The e and f lines are so closely spaced for some values of J they were not resolved experimentally. The J dependence of this splitting result in the e and f lines always being very closely spaced near the band origin. For some bands, the difference between the e and f lines becomes very small at locations in the P and R branches other than at low J as well. In the 01111 + 01101 band of  $^{12}\text{C}^{16}\text{O}^{18}\text{O}$ , the e and f series cross at about R(65). Since  $B_e = B_f$  for the 02211 + 02201 band of  $^{12}\text{C}^{16}\text{O}^{18}\text{O}$ , the e and f lines were not resolved until about J = 60 of the P branch and J = 70 of the R branch. Having merged lines adversely effects the quality of the least-squares fits since the effects of line merging were not modeled. Unresolved lines were particularly a problem when the spacing between component lines of the spectral feature was just slightly less than the experimental resolution.

The range of rotational levels measured for the 12212 + 02201 band of  $^{12}\text{C}^{16}\text{O}^{18}\text{O}$  did not cover the wings of the band where the e and f sublevels had sufficient separation to determine unique constants. In addition the strong Coriolis resonance of the upper state with the level 23301 caused the unusually large higher order distortion constants for this band at  $3511\text{ cm}^{-1}$  as given in Table 14.

The constants for this band are only given to reproduce the lines observed in the present experiment. Similar caution should be exercised with the 12212 + 02201 band of  $^{12}\text{C}^{16}\text{O}_2$  for which a similar resonance exists.

Chedin's<sup>2</sup> model using an empirically determined potential function predicts the position of spectral lines within an accuracy of about  $0.01 \text{ cm}^{-1}$  for low J lines for most bands. This is about 25 times worse than the experimental determined line positions. How much of this inaccuracy is due to improper modeling of the  $\text{CO}_2$  molecule and how much is due to inconsistencies in the data used to obtain the empirically determined potential function is still unclear. However, Chedin has recently rerun his model using improved experimental data,<sup>51</sup> including a preliminary version of the  $^{12}\text{C}^{16}\text{O}_2$  data presented in this report.<sup>12</sup> The improvement for the bands considered in this report was minimal, implying that his model in its present form is approaching its limits. However, Chedin's model predicts the positions of spectral lines more accurately than previous models, such as the model used to calculate (for lines that have not been measured experimentally) the position of spectral lines for the AFGL line compilation.<sup>22</sup>

The AFGL 1978 line compilation<sup>52</sup> was based on lower temperature or lower resolution data, or both, than the

present work. The AFGL 1980 and 1982 line compilations were not compared with the  $4.3 \mu\text{m } ^{12}\text{C}^{16}\text{O}_2$  data of the present work, since they incorporated the data here presented.

## CHAPTER VII

### CONCLUSION

By heating the CO<sub>2</sub> gas sample and using a high resolution Fourier transform spectrometer it has been possible to observe 73 bands of CO<sub>2</sub> and measure the position of spectral lines with a wavenumber accuracy of 0.0004 cm<sup>-1</sup>, including lines originating from high rotational energy levels. This represents an improvement in the knowledge of the position of spectral lines, at least for the high J lines, for all the observed bands except the  $\nu_3$  fundamental of <sup>12</sup>C<sup>16</sup>O<sub>2</sub>. The spectrum of high temperature CO<sub>2</sub> is so rich in lines that the high resolution of the AFGL two meter path difference interferometer was needed to separate individual spectral lines from the many other overlapping bands. The large number of overlapping bands made the identification of the various bands very difficult. To overcome this problem a system of interactive computer programs was written incorporating, among other features, an automated Loomis-Wood diagram and an iterated least-squares fit to the data.

This improved knowledge of the position of CO<sub>2</sub> spectral lines can be used to further several different areas of research. Since the CO<sub>2</sub> molecule is one of the most important infrared absorbing molecules in the atmosphere and plays a fundamental role in the heat balance

of our atmosphere, this knowledge of the energy levels will be important to atmospheric studies. These improved spectroscopic constants will be particularly useful for problems that deal with high temperature  $\text{CO}_2$ . Data obtained on spectral lines originating from high energy levels and from different isotopic species provide information that is helpful in determining the shape of the  $\text{CO}_2$  potential function. Studies of the  $\text{CO}_2$  molecule of a more fundamental nature and studies of the general formulation of triatomic theory will also be benefited by these very accurate high temperature measurements of different isotopic species of  $\text{CO}_2$ .

In addition to the detailed information on the positions of spectral lines, this study demonstrated several more general principles. When the molecular constants  $G_v$ ,  $B_v$ ,  $D_v$ , and  $H_v$  are determined band by band, as they were in the present work, there is a great deal of interdependence among the different constants, particularly between the  $D_v$  and  $H_v$  constants. Extrapolating the position of high  $J$  lines from low  $J$  lines can quickly lead to large errors. The errors in the predicted line positions typically increased by an order of magnitude for every 10  $J$ 's of extrapolation. Existing global models of the  $\text{CO}_2$  molecule do not predict the position of spectral lines as accurately as they can be measured experimentally, even for low  $J$  lines. Chedin's<sup>2</sup> model predicted the

position of spectral lines with an accuracy of about  $0.01 \text{ cm}^{-1}$  where the experimental accuracy was closer to  $0.0004 \text{ cm}^{-1}$ .

Recommendations for Future Work. There remains a great deal of work to be done on the  $\text{CO}_2$  molecule, both theoretical and experimental. Experimental measurements need to be made on additional rotation-vibration bands in different regions of the spectrum, particularly in the  $15 \text{ }\mu\text{m}$  region where much additional information is available. It would also be useful to obtain information on still higher rotational and vibrational energy levels. This data could then be incorporated into a global model of the  $\text{CO}_2$  molecule. If a model of  $\text{CO}_2$  that could predict the position of spectral lines within the accuracy of the experimental spectrum could be developed, it would not be necessary to measure as many rotation-vibration bands, but at present the only way to determine line positions accurately is to measure them experimentally.



# LIST OF REFERENCES

1. M. Born and R. Oppenheimer, Ann. Physik. 84, 457 (1927).
2. A. Chedin, J. Mol. Spectrosc. 76, 430 (1979).
3. A. Trowbridge and R. W. Wood, Philosophical Magazine, Series 6, 20, 898 (1910).
4. E. F. Barker, Astrophys. Journ. 55, 391 (1922).
5. E. K. Pyler, L. R. Blaine, and E. D. Tidwell, J. Research Natl. Bur. Standards 55, 183 (1955).
6. R. Oberly, K. N. Rao, Y. H. Hahn, and T. K. McCubbin Jr., J. Mol. Spectrosc. 25, 138 (1968).
7. T. K. McCubbin Jr., J. Pliva, R. Pulfrey, W. Telfair, and T. Todd, J. Mol. Spectrosc. 49, 136 (1974).
8. D. Bailly, R. Farrenq, and C. Rossetti, J. Mol. Spectrosc. 70, 124 (1978).
9. A. Baldacci, V. M. Devi, D. Chen, and K. N. Rao, J. Mol. Spectrosc. 70, 143 (1978).
10. G. Guelachvili, J. Mol. Spectrosc. 79, 72 (1980).
11. A. S. Pine and G. Guelachvili, J. Mol. Spectrosc. 79, 84 (1980).
12. M. P. Esplin and H. Sakai, "High Temperature Absorption Spectrum of 4.3 Micron CO<sub>2</sub>," Proceedings of "Spectroscopy in Support of Atmospheric Measurements," WP11 (1980).
13. M. P. Esplin PhD Thesis, University of Massachusetts, May 1985.
14. L. S. Rothman and L. D. G. Young, J. Quant. Spectrosc. Radiat. Transfer 25, 505 (1981).
15. M. P. Esplin and L. S. Rothman, J. Mol. Spectrosc. 100, 193 (1983).
16. L. S. Rothman, R. R. Gamache, A. Barbe, A. Goldman, J. R. Gillis, L. R. Brown, R. A. Toth, J.-M. Flaud, and C. Camy-Peyret, Appl. Opt. 22, 2247 (1983).

17. M. P. Esplin and L. S. Rothman, J. Mol. Spectrosc., in press (1986).
18. D. Bailly, PhD Thesis, Universite de Paris-Sud, (1983); also see D. Bailly, R. Farrenq, G. Guelachvili, and C. Rossetti, J. Mol Spectrosc 90, 74 (1981); D. Bailly and C. Rossetti, J. Mol Spectrosc 102, 392 (1983).
- 19a. K. J. Siemsen and B. G. Whitford, Opt. Commun. 22, 11 (1977); K. J. Siemsen Opt. Commun. 34, 447 (1980).
- 19b. V. M. Devi, C. P. Rinsland, and D. C. Benner, Appl. Opt. 23, 4067 (1984); R. A. Toth, Appl. Opt. 24, 261 (1985); C. P. Rinsland, D. C. Benner, and V. M. Devi, Appl. Opt. 24, 1644 (1985).
20. G. Herzberg, Molecular Spectra and Molecular Structure, Vol. I, "Spectra of Diatomic Molecules," Van Nostrand Reinhold Company (1950).
21. G. Herzberg, Molecular Spectra and Molecular Structure, Vol. II, "Infrared and Raman Spectra of Polyatomic Molecules," Van Nostrand Reinhold Company (1950).
22. R. A. McClatchey, W. S. Benedict, S. A. Clough, D. E. Burch, R. F. Calfee, K. Fox, L. S. Rothman and J. S. Garing, "AFCRL Atmospheric Absorption Line Parameters Compilation," AFCRL-TR-73-0096 (1973). AD762904
23. M. W. Hanna, Quantum Mechanics in Chemistry, W. A. Benjamin, Inc. (1969).
24. M. P. Esplin, R. J. Huppi, H. Sakai, G. A. Vanasse, L. S. Rothman, "Absorption Measurements of CO<sub>2</sub> and H<sub>2</sub>O at High Resolution and Elevated Temperatures," AFGL-TR-82-0057 (1982). ADA113824
25. L. D. Gray and A. T. Young, J. Quant. Spectrosc. Radiat. Transfer 9, 569 (1969).
26. The Infrared Handbook, prepared by: The Infrared Information and Analysis Center (IRIA), Environmental Research Institute of Michigan for the Office of Naval Research, Department of the Navy (1978).
27. W. S. Dalton and H. Sakai, Appl. Opt. 19, 2413 (1980).
28. J. H. Taylor, PhD Thesis, The Johns Hopkins University, Baltimore Maryland (1952).

29. J. U. White, J. Opt. Soc. Am. 32, 285 (1942).
30. P. Fellgett, PhD Thesis, University of Cambridge (1951).
31. P. Jacquinot and C. Dufour, J. Rech. du C.N.R.S. 6, 91 (1948).
32. J. Connes, Rev. Opt. 40, 45 (1961).
33. G. A. Vanasse and H. Sakai, "Fourier Spectroscopy," in Progress in Optics Vol. 16, Ed. E. Wolf, North-Holland Publishing Company (1967).
34. R. N. Bracewell, The Fourier Transform and Its Application, McGraw-Hill (1965).
35. J. Connes, "Computing Problems in Fourier Spectroscopy," proceeding of "Aspen international Conference on Fourier Spectroscopy," AFCRL-TR-71-0019 (1971). AD724100
36. E. V. Loewenstein, "Fourier Spectroscopy: An Introduction," proceeding of "Aspen international Conference on Fourier Spectroscopy," AFCRL-TR-71-0019 (1971). AD724100
37. H. Sakai and G. A. Vanasse, "High Resolution Spectra of CO<sub>2</sub> in the 3500 to 3770 cm<sup>-1</sup> Region at 625 K," AFGL-TR-77-0039 (1977). ADA040746
38. H. Sakai, "High-Resolution Spectra of CH<sub>4</sub> in the 2700 to 3200 cm<sup>-1</sup> Region," AFGL-TR-76-0280 (1976). ADA036331
39. H. Sakai, "High-Resolution Fourier Spectroscopy," AFCRL-TR-74-0571 (1974). ADA006688
40. H. Sakai, "High Resolving Power Fourier Spectroscopy," in Spectrometric Techniques, Vol. 1, Ed. G. A. Vanasse, Academic Press (1977).
41. K. W. Taconis, J. J. M. Beenakker, A. O. C. Nier and L. t. Aldrich, Physica 15, 733 (1949).
42. T. Yazaki, A. Tominaga, and Y. Narahara, J. Low Temperature Physics, 41, 45 (1980).
43. L. Mertz, Transformations in Optics, John Wiley, New York (1965).

44. J. W. Cooley and J. W. Tukey, Math. Comput. 19, 296 (1965).
45. F. W. Loomis and R. W. Wood, Phys. Rev. 32, 223 (1928).
46. Philip R. Bevington, Data Reduction and Error Analysis for the Physical Sciences, McGraw-Hill, Inc. (1969).
47. G. Guelachvili, J. Mol. Spectrosc. 75, 251 (1979).
48. L. S. Rothman and M. P. Esplin, "Self-Consistent Analysis for Line Positions of Carbon Dioxide," Symposium on Molecular Spectroscopy, The Ohio State University, Columbus, Ohio (1982).
49. C. R. Pollock, F. R. Petersen, D. E. Jennings, and J. S. Wells, and A. G. Maki, J. Mol. Spectrosc. 99, 357 (1983).
50. L. R. Brown and R. A. Toth, J. Opt. Soc. Am. B. 2, 842 (1985).
51. A. Chedin and J.-L. Teffo, J. Mol. Spectrosc. 107, 333 (1984).
52. L. S. Rothman, Appl. Opt. 17, 3517 (1978).

APPENDIXES

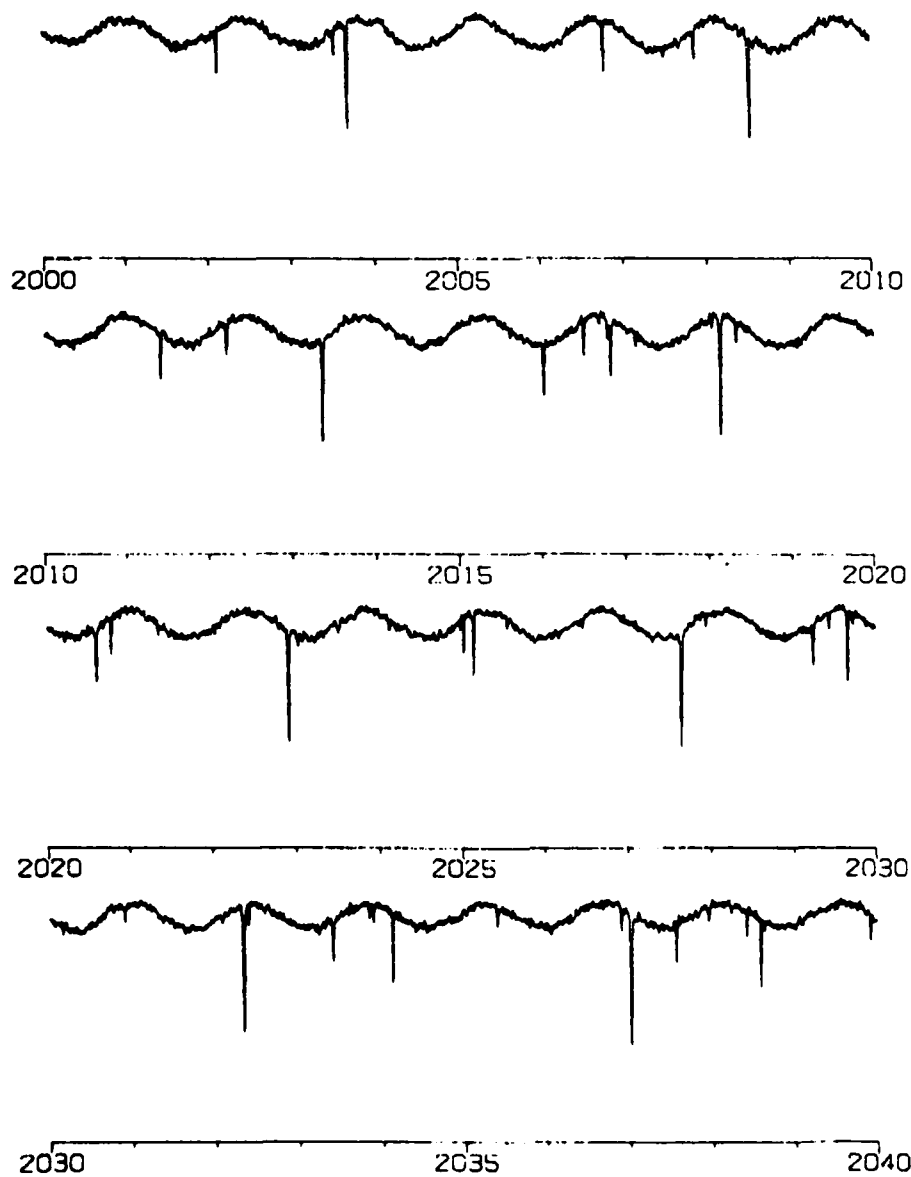


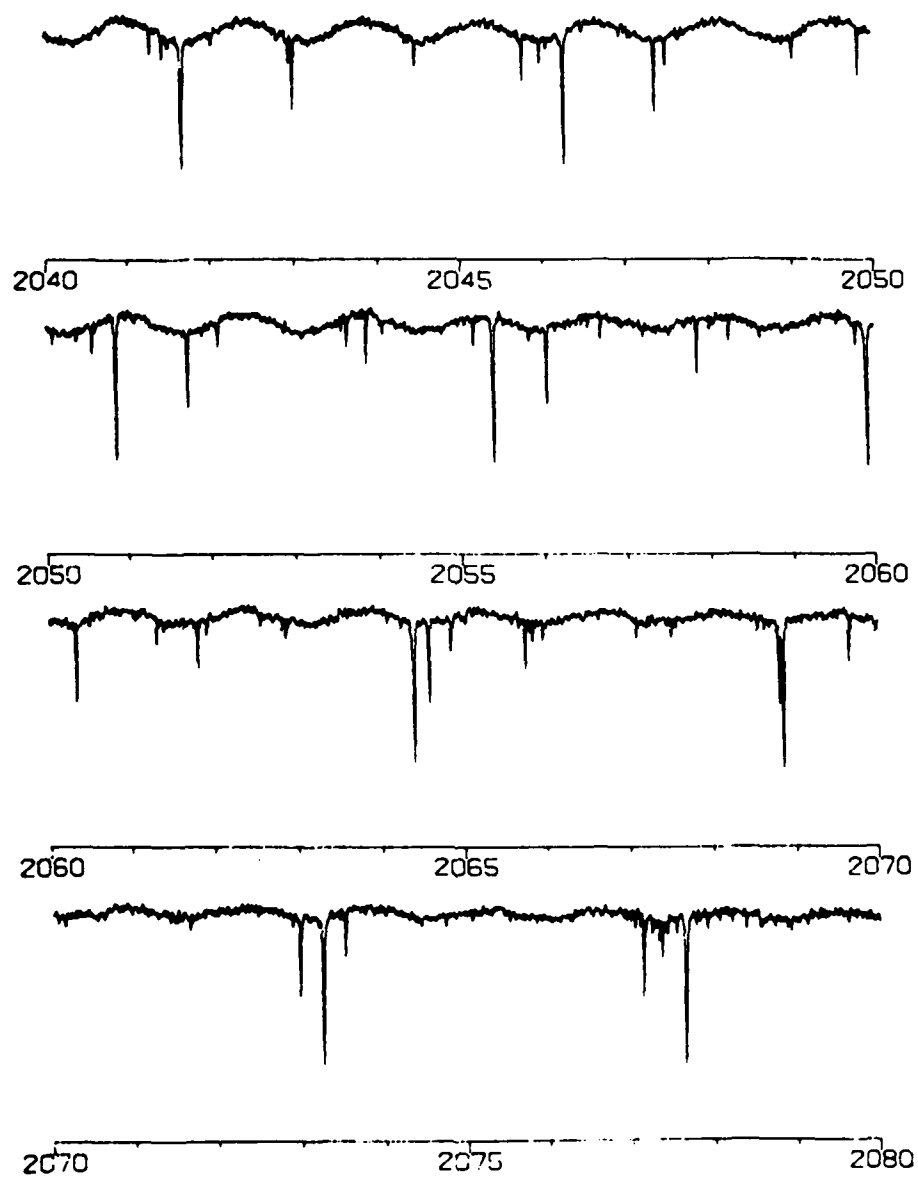
APPENDIX A

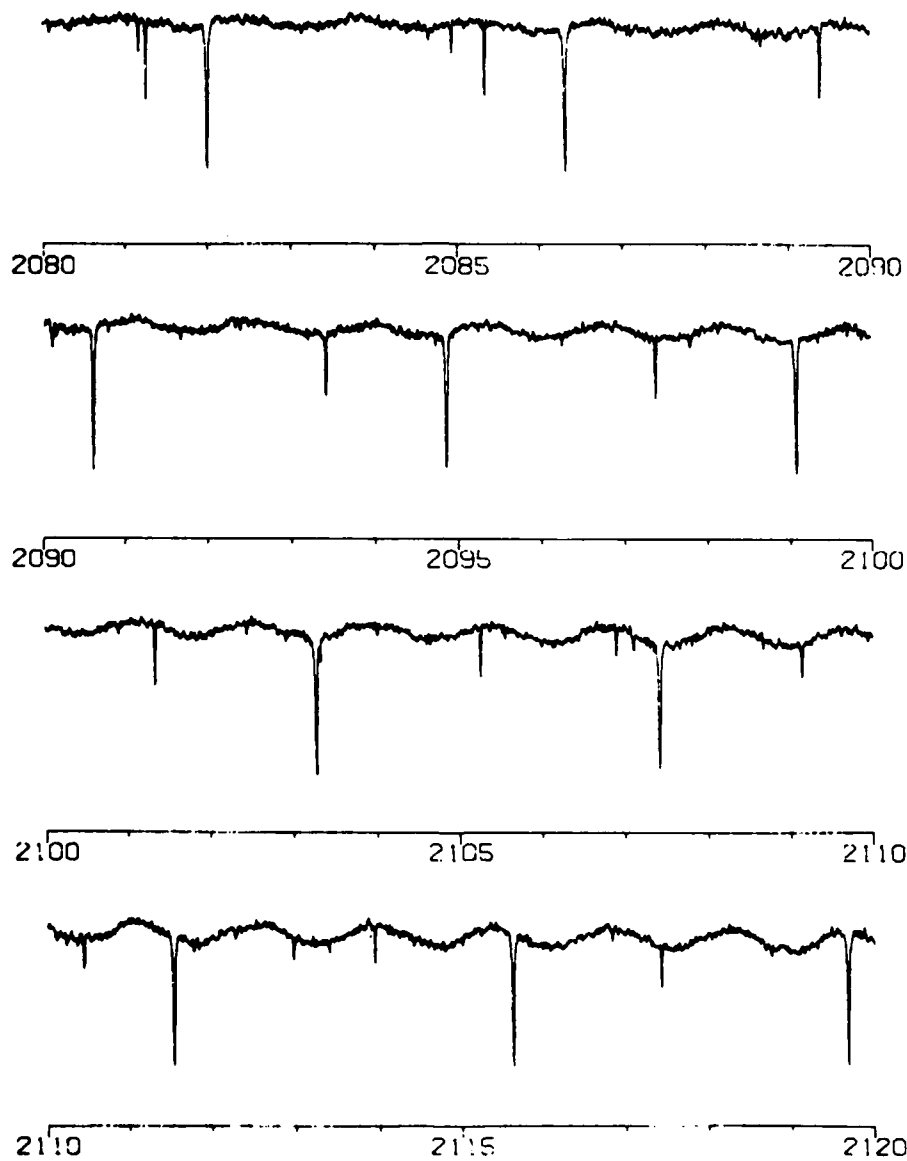
High Temperature CO<sub>2</sub> Spectrum

EXPERIMENTAL CONDITIONS:

Temperature:	800 K
Absorption Path Length:	3.5 m
Pressure:	6 Torr
Isotopic Composition:	Natural Abundance







AD-A173 808

CARBON DIOXIDE LINE POSITIONS IN THE 20 AND 43 MICRON  
REGIONS AT 800 KELV. (U) UTAH STATE UNIV BEDFORD MA  
STEWART RADIANCE LAB M P ESPLIN ET AL. 19 FEB 86  
SCIENTIFIC-16 AFGL-TR-86-0046 F/G 7/4

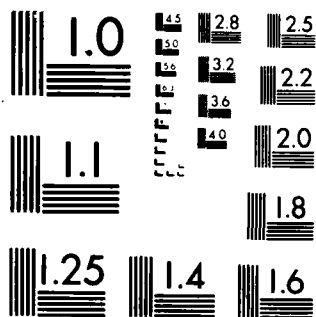
3/4

UNCLASSIFIED

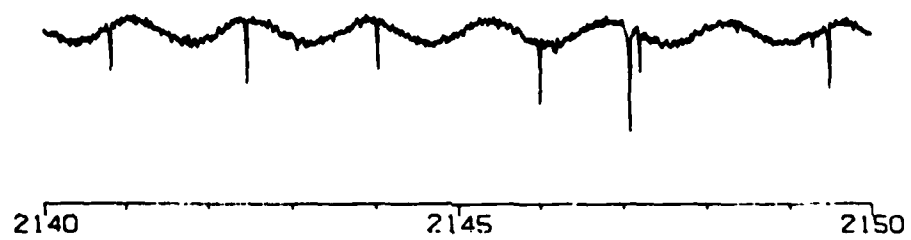
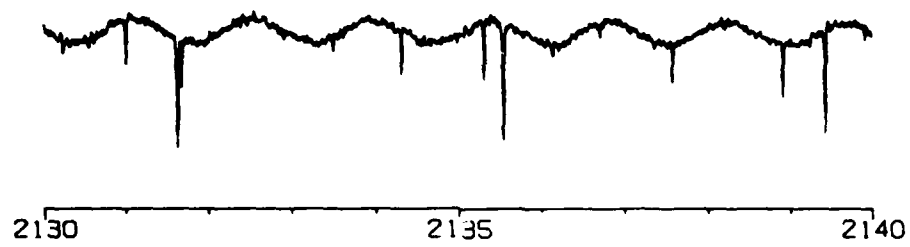
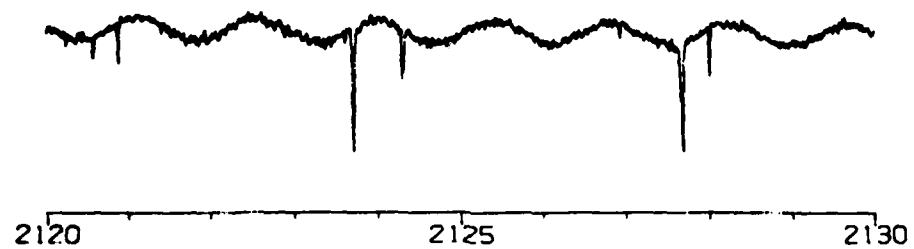
F/G 7/4

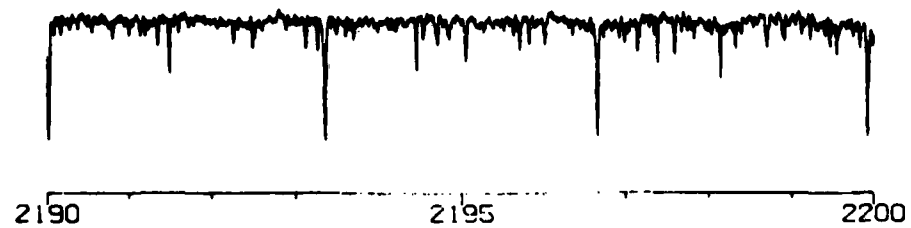
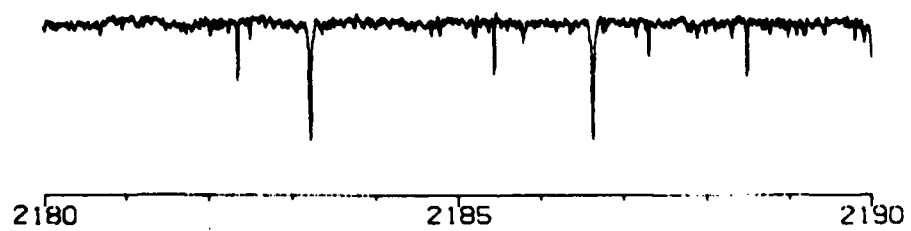
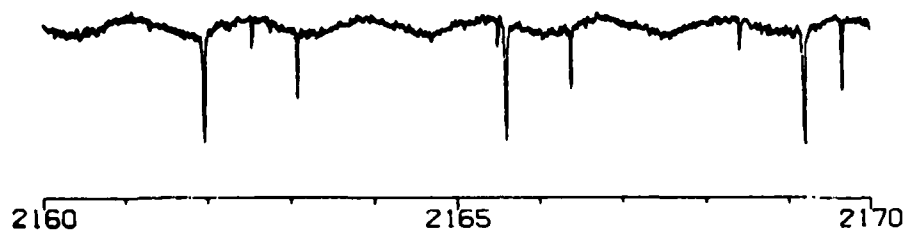
NL

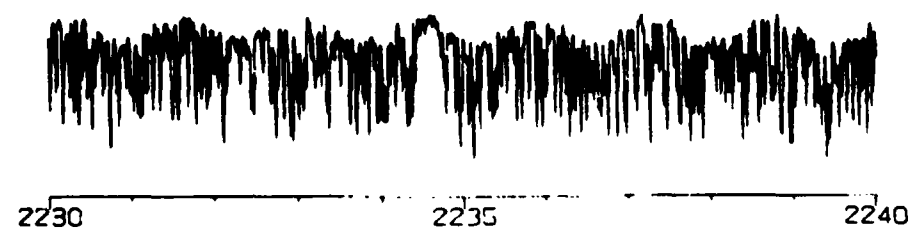
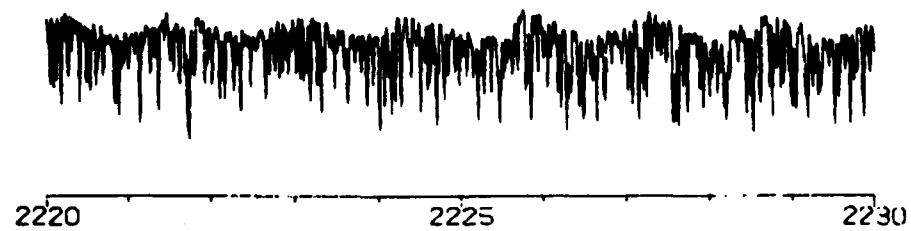
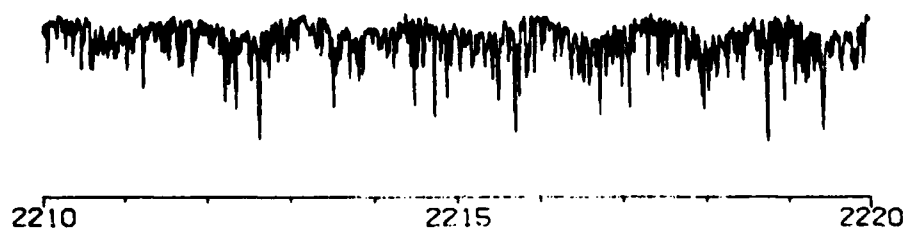
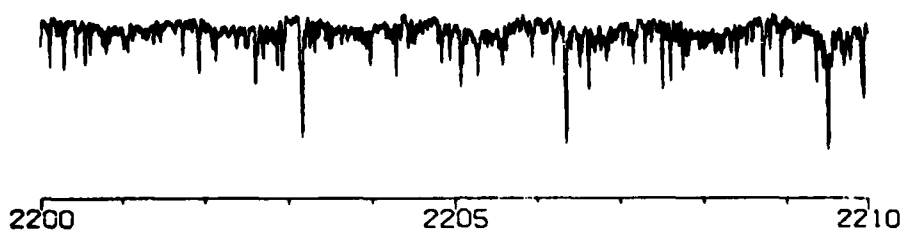
[illegible]

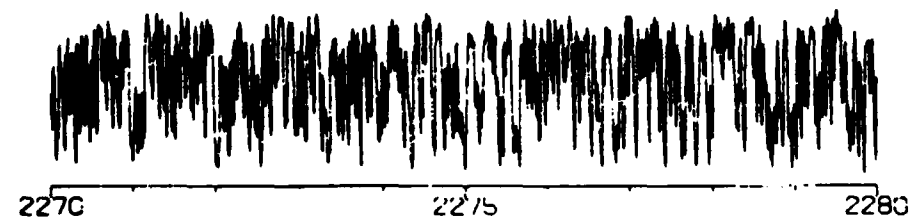
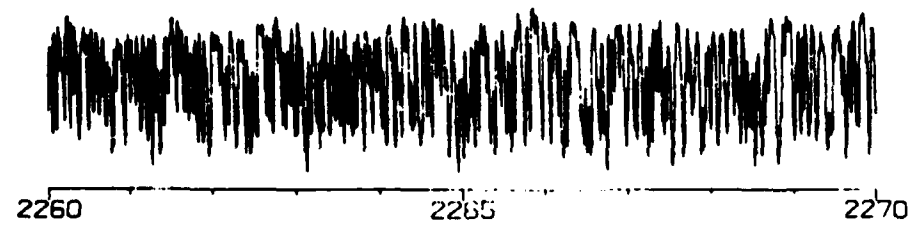
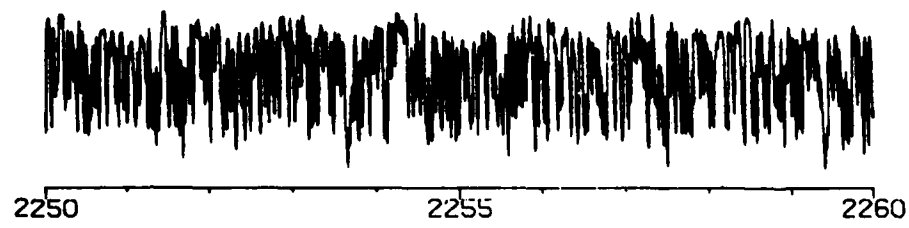
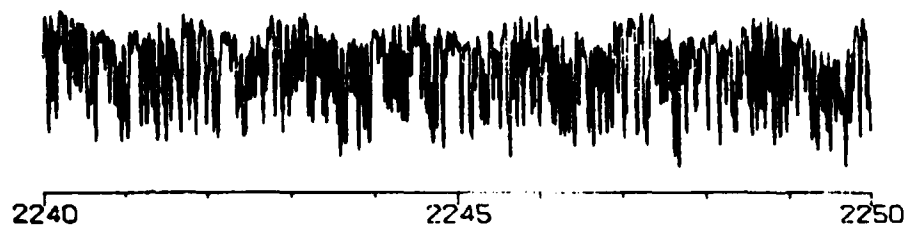


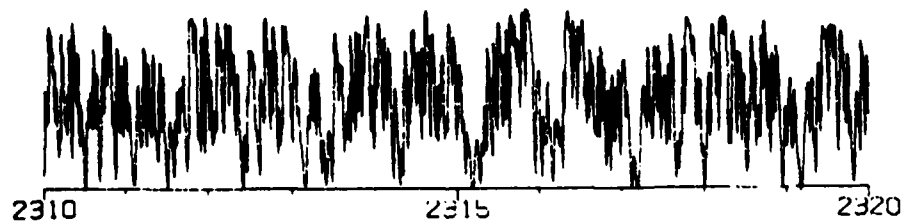
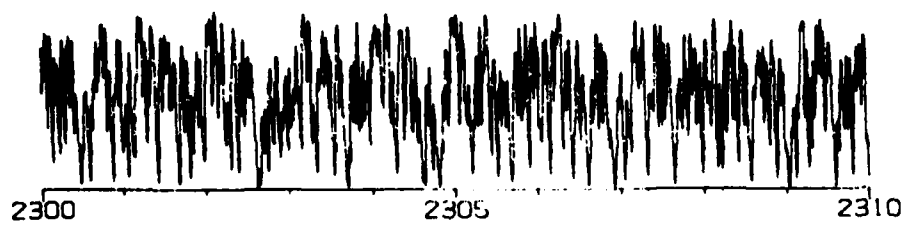
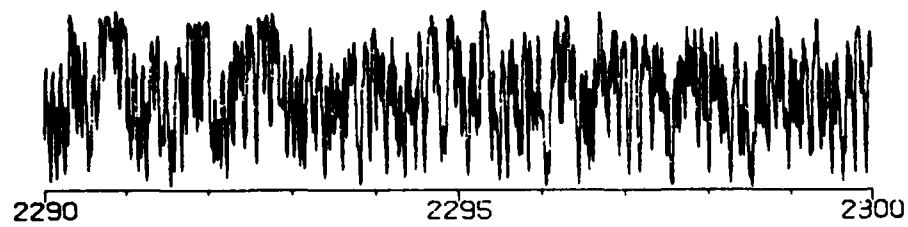
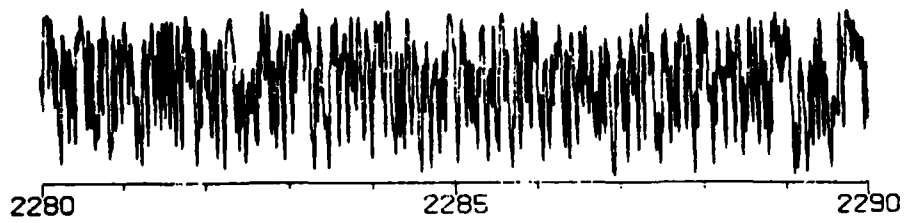
MICROCOPY RESOLUTION TEST CHART  
NATIONAL BUREAU OF STANDARDS 1963-A

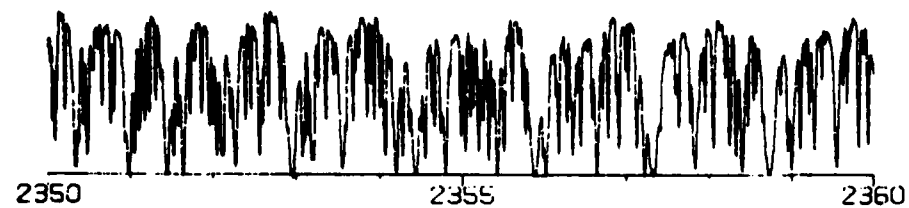
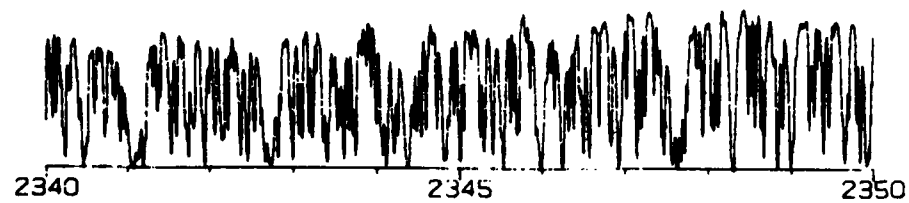
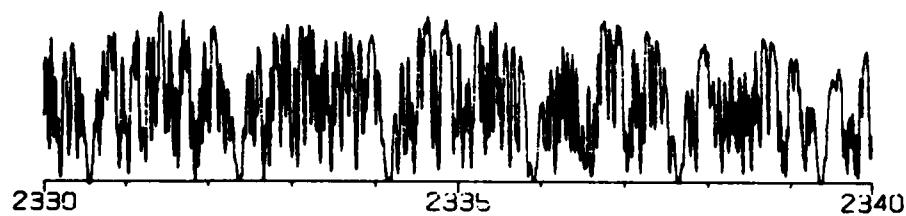
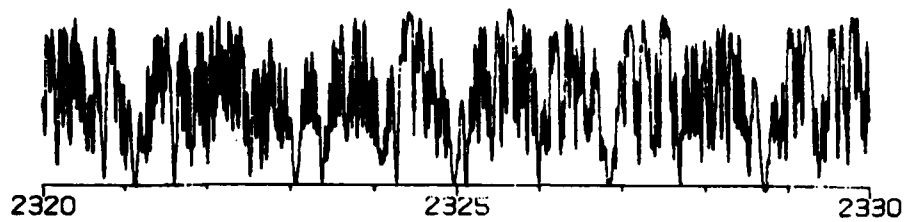


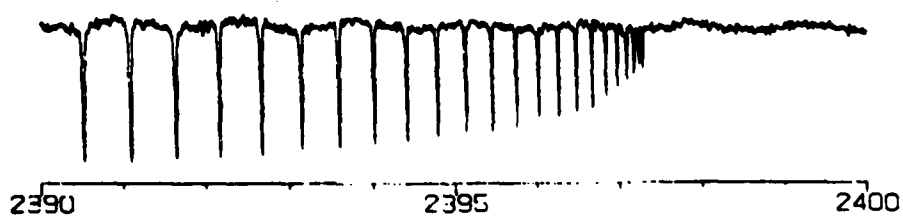
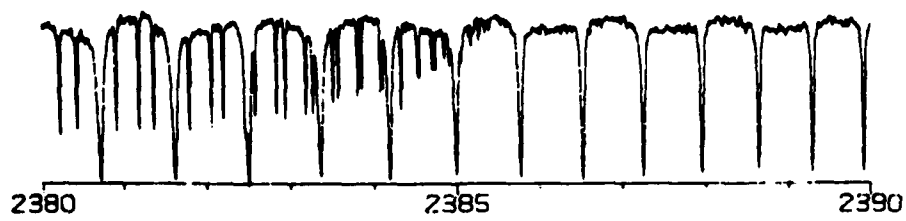
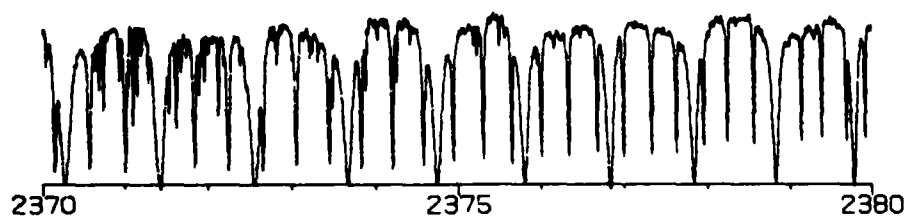
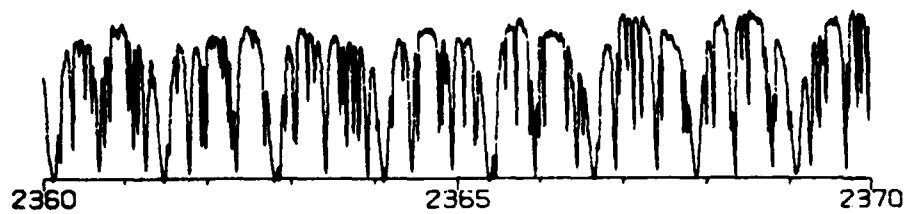














## APPENDIX B

### Lines Used in Least-Squares Fits

Observed line positions (Obs) are in  $\text{cm}^{-1}$ . Observed minus calculated values (O-C) and expected uncertainties (Unc) are in units of  $10^{-4} \text{ cm}^{-1}$ . Isotope codes are:  
626 =  $^{12}\text{C}^{16}\text{O}_2$ , 636 =  $^{13}\text{C}^{16}\text{O}_2$ , 628 =  $^{12}\text{C}^{16}\text{O}^{18}\text{O}$ , etc.

# The 4.3 $\mu\text{m}$ Bands Included in Line Listing

Transition	Isotope	Band Center ( $\text{cm}^{-1}$ )	Range of Measurement	Page
05511 05501	$^{12}\text{C}^{16}\text{O}_2$	2286.753	P( 85)-	221
13311 13301		2288.3903	P( 68)-R( 63)	219
13312 13302		2290.6806	P( 80)-R( 71)	219
04411 04401		2299.2141	P( 89)-R( 75)	221
02221e 02211e		2299.2395	P( 79)-R( 71)	213
02221f 02211f		2299.2395	P( 78)-R( 76)	213
12211e 12201e		2301.0539	P( 88)-R( 60)	215
12211f 12201f		2301.0539	P( 89)-R( 81)	215
10022 10012		2302.3735	P( 77)-R( 73)	207
20011 20001		2302.5227	P( 80)-R( 78)	206
20013 20003		2305.2568	P( 86)-R( 74)	205
20012 20002		2306.6920	P( 62)-R( 56)	205
03311 03301		2311.6681	P( 90)-R( 85)	217
01121e 01111e		2311.7008	P( 86)-R( 60)	208
01121f 01111f		2311.7008	P( 89)-R( 91)	208
11111e 11101e		2313.7726	P( 95)-R( 89)	211
11111f 11101f		2313.7726	P( 92)-R( 88)	211
11112e 11102e		2315.2350	P( 61)-R( 61)	211
11112f 11102f		2315.2350	P( 98)-R( 88)	211
02211e 02201e		2324.1410	P(102)-R(104)	213
02211f 02201f		2324.1410	P(107)-R(103)	213
00021 00011		2324.1820	P( 99)-R( 79)	207
10011 10001		2326.5980	P(108)-R(106)	204
10012 10002		2327.4327	P(106)-R(102)	204
01111e 01101e		2336.6330	P(113)-R(115)	208
01111f 01101f		2336.6330	P(114)-R(110)	208
00011 00001		2349.1446	P(126)-R(118)	203
04411 04401	$^{13}\text{C}^{16}\text{O}_2$	2236.6789	P( 90)-R( 95)	250
02221e 02211e		2236.6790	P( 61)-R( 55)	248
02221f 02211f		2236.6790	P( 72)-R( 60)	248
12211e 12201e		2238.5706	P( 88)-R( 40)	248
12211f 12201f		2238.5706	P( 89)-R( 77)	248
20013 20003		2240.5362	P( 88)-R( 90)	244
20012 20002		2242.3238	P( 82)-R( 62)	244
03311e 03301e		2248.3567	P( 95)-R( 93)	250
03311f 03301f		2248.3567	P( 98)-R( 96)	250
01121e 01111e		2248.3618	P(100)-R( 92)	245
01121f 01111f		2248.3618	P( 87)-R( 71)	245
11111e 11101e		2250.6054	P( 97)-R( 83)	245
11111f 11101f		2250.6054	P(100)-R( 84)	245

Transition	Isotope	Band Center ( $\text{cm}^{-1}$ )	Range of Measurement	Page
11112f 11102f	$^{13}\text{C}^{16}\text{O}_2$	2250.6931	P( 98)-R( 78)	247
02211e 02201e		2260.0500	P(106)-R(104)	231
02211f 02201f		2260.0500	P(103)-R(101)	231
00021 00011		2260.0617	P(105)-R(103)	243
10012 10002		2261.9102	P(104)-R(104)	228
10011 10001		2262.8486	P(102)-R(102)	229
01111e 01101e		2271.7604	P(113)-R(107)	225
01111f 01101f		2271.7604	P(116)-R(112)	225
00011 00001		2283.4874	P(122)-R(122)	224
02211e 02201e	$^{13}\text{C}^{16}\text{O}^{18}\text{O}$	2242.8075	P( 86)-R( 75)	257
02211f 02201f		2242.8075	P( 77)-R( 74)	257
10011 10001		2245.2726	P( 83)-R( 81)	253
10012 10002		2245.4960	P( 84)-R( 80)	253
01111e 01101e		2254.3803	P( 94)-R( 94)	255
01111f 01101f		2254.3803	P( 99)-R(101)	255
00011 00001		2265.9719	P(106)-R(100)	233
02211e 02201e	$^{12}\text{C}^{18}\text{O}_2$	2289.5689	P( 94)-R( 72)	231
02211f 02201f		2289.5689	P(101)-R( 69)	231
10011 10001		2290.9720	P( 98)-R( 54)	229
10012 10002		2294.8795	P( 98)-R( 88)	228
01111e 01101e		2301.7996	P(111)-R(101)	225
01111f 01101f		2301.7996	P(122)-R(102)	225
00011 00001		2314.0489	P(128)-R(106)	224
02211e 02201e	$^{12}\text{C}^{16}\text{O}^{18}\text{O}$	2307.3830	P(100)-R( 92)	240
02211f 02201f		2307.3830	P( 96)-R( 98)	240
10011 10001		2309.2898	P(100)-R( 98)	238
10012 10002		2311.7151	P(103)-R( 92)	238
01111e 01101e		2319.7380	P(113)-R(113)	236
01111f 01101f		2319.7380	P(111)-R(105)	236
00011 00001		2332.1127	P(119)-R(117)	233
00011 00001	$^{13}\text{C}^{16}\text{O}^{17}\text{O}$	2274.0884	P( 73)-R( 80)	259

The 2.8  $\mu\text{m}$  Bands Included in Line Listing

Transition	Isotope	Band Center ( $\text{cm}^{-1}$ )	Range of Measurement	Page
12212e 02201e	$^{12}\text{C}^{16}\text{O}_2$	3552.8568	P( 46)-R( 50)	276
12212f 02201f		3552.8568	P( 41)-R( 43)	276
20013 10002		3568.2165	P( 56)-R( 60)	273
11112e 01101e		3580.3265	P( 57)-R( 65)	274
11112f 01101f		3580.3265	P( 70)-R( 74)	274
20012 10001		3589.6520	P( 56)-R( 52)	274
10012 00001		3612.8416	P( 82)-R( 86)	272
20012 10002		3692.4278	P( 62)-R( 64)	273
20011 10001		3711.4776	P( 56)-R( 58)	274
21111e 11101e		3713.7218	P( 39)-R( 35)	277
21111f 11101f		3713.7218	P( 40)-R( 40)	277
10011 00001		3714.7825	P( 84)-R( 86)	272
11111e 01101e		3723.2501	P( 77)-R( 75)	274
11111f 01101f		3723.2501	P( 70)-R( 70)	274
12211e 02201e		3726.6475	P( 52)-R( 56)	276
12211f 02201f		3726.6475	P( 53)-R( 57)	276
12212 02201	$^{12}\text{C}^{16}\text{O}^{18}\text{O}$	3511.4117	P( 33)-R( 28)	270
20013 10002		3531.8352	P( 56)-R( 59)	263
11112e 01101e		3538.7785	P( 64)-R( 68)	265
11112f 01101f		3538.7785	P( 67)-R( 66)	265
20012 10001		3539.0176	P( 53)-R( 53)	264
10012 00001		3571.1409	P( 82)-R( 82)	261
20012 10002		3645.4356	P( 53)-R( 53)	263
10011 00001		3675.1337	P( 77)-R( 77)	261
20011 10001		3676.7399	P( 48)-R( 50)	264
11111e 01101e		3683.8136	P( 66)-R( 66)	267
11111f 01101f		3683.8136	P( 65)-R( 66)	267
12211e 02201e		3687.4754	P( 51)-R( 52)	268
12211f 02201f		3687.4754	P( 50)-R( 53)	268
10012 00001	$^{12}\text{C}^{18}\text{O}_2$	3525.2048	P( 62)-R( 74)	271
10011 00001		3638.0657	P( 78)-R( 74)	271

00011 - 00001 626				
J	P Obs	O-C Unc	R Obs	O-C Unc
50	2300.4765	-1 30	2380.7163	5 28
52	2298.2768	-20 24	2381.6236	15 28
54	2296.0563	-8 19	2382.5033	1 16
56	2293.8131	16 20	2383.3596	6 16
58	2291.5427	6 12	2384.1895	1 12
60	2289.2485	-5 12	2384.9947	1 13
62	2286.9308	-12 19	2385.7752	-7 17
64	2284.5913	-1 9	2386.5288	7 13
66	2282.2276	6 7	2387.2588	1 10
68	2279.8388	-2 11	2387.9619	-3 9
70	2277.4274	5 10	2388.6398	-3 9
72	2274.9925	-6 10	2389.2927	-1 12
74	2272.5326	9 13	2389.9205	-9 6
76	2270.0517	5 13	2390.5214	0 8
80	2267.5453	0 4	2391.0904	6 6
82	2265.0154	-9 14	2391.6497	7 4
84	2262.4617	-5 7	2392.1745	-6 7
86	2259.8858	21 23	2392.6755	-4 0
88	2254.6658	10 11	2393.1488	5 4
90	2252.0183	0 4	2393.5979	3 5
92	2246.6548	2 4	2394.0214	4 4
94	2241.1996	-11 12	2394.4181	-3 0
96	2238.4358	1 5	2394.7902	-4 1
98	2235.6515	-2 4	2395.1359	0 0
100	2232.8425	0 3	2395.4568	1 0
102	2230.0109	-1 5	2395.7515	-3 4
104	2221.3776	11 18	2396.0202	-1 0
106	2218.4551	2 6	2396.2637	0 0
108	2212.5383	-11 25	2396.4813	2 5
110	2209.5448	-8 27	2396.6730	5 4
112	2203.4924		2396.8392	5 5
114			2396.9794	5 7
116			2397.0936	1 0
118			2397.1819	-12 14
120			2397.2434	
122				
124				
126				

10012 - 10002 626				10011 - 10001 626					
J	P	Obs	O-C	Unc	R	Obs	O-C	Unc	J
0	2325	8638	-10	15	2328	2074	-3	7	0
2	2324	2756	25	30	2329	7383	-15	21	2
4	2322	6597	20	24	2331	2474	-7	11	4
6	2321	0179	-6	11	2332	7327	3	5	6
8	2319	3540	-16	22	2335	6304	11	16	8
10	2317	6691	-1	11	2337	0429	12	12	10
12	2315	9586	-1	9	2338	4302	1	10	12
14	2314	2248	0	9	2339	7945	0	10	14
16	2312	4675	1	9	2342	4525	17	20	16
18	2310	6863	0	9	2343	7415	-13	21	18
20	2308	8822	-17	25	2347	4737	2	14	20
22	2307	0520	-6	13	2348	6685	0	7	22
24	2305	2014	-8	15	2349	8395	3	10	24
26	2303	3265	0	10	2352	1078	3	17	26
28	2299	5068	9	15	2353	2055	5	13	28
30	2297	5625	-6	15	2354	2777	-4	10	30
32	2295	5930	-3	5	2355	3265	-2	11	32
34	2293	6005	-1	9	2356	3510	-2	8	34
36	2291	5862	-8	14	2358	3247	-6	13	36
38	2289	5473	17	17	2359	2747	-9	16	38
40	2287	4857	-4	9	2360	2012	-1	12	40
42	2285	3999	-3	10	2361	1018	-5	10	42
44	2281	1630	-9	16	2361	9782	-4	10	44
46	2279	0064	-2	7	2363	6568	0	7	46
48	2276	8289	-4	8	2365	2350	-8	15	48
50	2274	6276	-2	7	2365	9870	-10	13	50
52	2272	4045	1	9	2368	0946	-1	8	52
54	2270	1580	-4	8	2368	7475	5	5	54
56	2267	8876	-2	7	2369	3740	-2	5	56
58	2265	5950	10	10	2369	9766	-4	4	58
60	2263	2803	13	13	2371	1045	-4	7	60
62	2260	9417	7	8	2371	6306	-9	12	62
64	2256	1946	-2	16	2372	1328	0	4	64
66	2253	7861	-18	19					66
68	2251	3575	-18	22					68
70	2246	4242	-18	22					70
72									72
74									74
76									76
78									78
80									80
82									82
84									84
86									86



56	2340.0816	-5	8	2253.8233	2	10	2340.9881	12	18	56
58	2340.9505	-4	10	2251.5927	20	17				58
60										60
62	2245.9136	-9	9	2342.6165	8	10	2247.0557	-1	7	62
64										64
66	2241.3402	-6	8							66
68	2239.0204	-3	5							68
70	2236.6793	10	10	2345.6540	5	6				70
72	2234.3160	22	18	2346.3500	-20	19				72
74	2231.9264	-7	14	2347.0234	-27	25				74
76	2229.5204	20	13							76
78										78
80	2224.6339	-8	21							80
82	2222.1593	-5	23							82

20011 - 20001 626						
J	P	Obs	O-C	Unc	R	Obs O-C Unc
0						
2						
4						
6	2297.7420	-6	7		2306.3364	11 12
8						
10	2294.4333	14	14		2309.2718	-17 18
12	2292.7400	5	7			
14	2291.0238	15	15		2312.1118	-3 5
16						
18	2287.5125	-13	14			
20	2285.7230	4	16		2317.4887	-10 12
22					2318.7727	11 12
24					2320.0269	-16 17
26						
28	2278.3104	-9	11		2322.4672	0 4
30	2276.3970	0	3		2323.6499	10 12
32	2274.4598	17	17		2324.8033	-22 25
34	2272.4936	-11	13		2325.9383	13 14
36	2270.5066	-2	4		2327.0436	2 3
38	2268.4936	-8	9			
40					2329.1813	5 6
42	2264.3964	2	4			
44	2262.3089	-15	16			
46	2260.2001	-1	4			
48	2258.0645	-11	13		2333.1533	-2 4

50	2253.7237	3	4	2334.0849	12	21
52						
54	2249.2817	-21	23	2336.7223	-3	4
56	2247.0293	17	16	2337.5535	17	24
58						
60						
62	2240.1152	17	16	2339.1350	9	10
64				2339.8866	-8	8
66				2340.6148	-5	6
68	2235.3824	-6	11	2341.3179	1	5
70	2232.9814	-2	5	2341.9959	9	12
72	2230.5583	23	22			
74	2228.1075	12	12	2343.2736	3	6
76	2225.6312	-13	22	2343.8754	11	12
78				2344.4483	-17	17
80	2220.6121	-7	10			

00021 - 00011 626				10022 - 10012 626			
J	P Obs	O-C Unc	R Obs	O-C Unc	P Obs	O-C Unc	J
1	2320.2496	4	8		2298.4380	-12	13
3	2318.6341	10	15				3
5	2316.9932	7	12		2295.1833	-16	14
7	2315.3254	-20	24		2293.5197	-25	25
9	2313.6380	2	9		2291.8331	-28	25
11	2311.9243	4	10				11
13	2310.1854	-1	7				13
15	2308.4205	-22	20		2313.9620	12	15
17							17
19					2316.6178	0	5
21					2317.9114	13	19
23							21
25	2302.9900	15	19		2320.4228	4	9
27	2301.1294	9	17				23
29	2299.2440	-3	6		2322.8368	-11	16
31	2297.3360	2	8				29
33	2295.4047	15	17				31
35	2293.4456	-8	9				33
37	2291.4661	-7	14				35
39	2289.4594	-10	13		2328.4527	10	14
41							39
43	2285.3785	4	14				41
45							43
1	2325.7140	18	21				1
3	2327.2147	-30	28				3
5							5
7	2330.1564	17	22				7
9							9
11	2334.3753	4	19				11
13	2335.7313	-8	12				13
15	2337.0646	0	12				15
17	2338.3712	-10	16				17
19	2339.6552	3	10				19
21	2340.9128	0	12				21
23	2342.1461	3	12				23
25	2343.3539	0	14				25
27	2344.5366	-4	8				27
29	2345.6946	-5	9				29
31							31
33	2347.9370	6	11				33
35	2349.0200	5	24				35
37	2350.0776	1	4				37
39	2351.1105	0	6				39
41							41
43	2353.1000	-10	14				43
45							45



10	2327.7052	6 20	2345.5322	2 16	2301.1294	-20 22	2321.9261	4 9	10
11	2326.0036	12 25	2346.9288	-7 29	2299.4131	-9 7	2323.2867	-12 11	11
12	2324.2756	-4 21	2347.6335	3 22	2298.5719	28 29	2323.9450	-3 16	12
13	2323.3812	15 29	2348.9958	7 21	2297.6729	7 11	2325.2729	35 25	13
14	2321.6131	-3 20			2296.8184	-4 16	2325.9383	1 6	14
15	2320.7501	-5 29			2295.9064	2 7	2326.5698	9 5	15
16	2319.8219	-9 23			2295.0477	34 25	2327.8433	-4 18	16
17	2318.9509	-9 25	2351.6449	2 18	2293.2460	3 6	2328.4899	4 12	17
18	2318.0068	-12 29			2292.3035	21 28	2329.0951	11 9	18
19	2317.1300	12 23			2290.4625	-3 5			19
20	2316.1679	-10 28			2289.5770	6 6			20
21	2315.2807	-11 26			2288.5998	-1 3			21
22	2314.3064	7 19			2287.7067	-9 9			22
23	2313.4100	-8 25			2286.7106	-24 25			23
24	2312.4194	11 26							24
25	2311.5162	5 17							25
26	2310.5064	-3 18							26
27	2309.5961	-6 16							27
28	2308.5716	-15 24							28
29	2307.6522	-8 16							29
30	2306.6105	-19 30							30
31	2304.6256	5 20							31
32	2303.6965	8 17							32
33	2302.6205	-9 17							33
34	2301.6805	13 17							34
35	2300.5891	-1 10							35
36	2299.6428	6 19							36
37	2297.5813	-1 9							37
38	2296.4522	4 15							38
39	2295.4950	2 12							39
40	2294.3488	-12 17							40
41	2293.3837	0 7							41
42	2292.2211	-4 13							42
43	2291.2510	-1 18							43
44	2290.0696	6 10							44
45	2289.0949	1 15							45
46	2287.8946	5 18							46
47	2286.9140	-6 9							47
48	2285.6949	-2 8							48
49	2284.7089	5 9							49
50	2282.4817	-10 12							50
51	2281.2253	4 10							51
52	2280.2301								52
53									53
54									54
55									55
56									56
57									57
58									58
59									59

60	2278.9562	1	6	2372.6576	2	10	2254.5323	-13	14	2347.3552	14	12	60
61	2277.9547	1	8	2373.0518	5	11	2253.2617	-11	11	2347.7511	-15	14	61
62	2276.6607	-15	21	2373.4448	4	11	2252.2586	-5	10				62
63	2275.6567	6	11	2373.8277	-6	13	2250.9704	4	5	2348.5153	-1	4	63
64	2274.3451	4	14	2374.2060	-2	7	2249.9610	-2	8				64
65	2273.3344	2	9	2374.5810	-7	7	2248.6536	0	4	2349.2532	3	4	65
66	2272.0036	0	15	2374.9426	-1	9							66
67	2270.9887	-2	11	2375.3080	9	7	2245.2972	22	15				67
68	2269.6386	-3	6	2375.6532	-7	10				2350.6526	4	7	68
69	2268.6196	-5	14	2376.0090	-1	6	2242.9284	17	9				69
70	2267.2506	0	3	2376.3396	-2	6	2241.5645	16	17	2351.3143	5	7	70
71	2266.2278	-3	8	2376.6853	-2	6							71
72	2264.8388	-9	5	2377.0004	1	5	2239.1510	-13	13				72
73	2263.8118	0	14	2377.3373	4	5	2238.1206	5	5				73
74	2262.4035	0	4	2377.6353	-1	5	2236.7178	-4	6	2352.5614	4	11	74
75				2377.9625	-7	9	2235.6820	2	7				75
76	2259.9448	0	3	2378.2450	-2	5	2234.2616	8	9	2353.1444	-21	19	76
77	2258.9136	15	13	2378.5643	0	3							77
78										2353.7065	-1	6	78
79	2256.4281	11	10	2379.1398	-3	4							79
80	2254.9575	4	5	2379.3888	-3	4	2229.2756	-1	6				80
81	2253.9188	1	5	2379.6905	5	5	2228.2289	16	23				81
82	2252.4285	3	4	2379.9224	0	5							82
83	2251.3885	12	11	2380.2162	-2	3	2225.6953	-7	9				83
84	2249.8760	1	4	2380.4296	-2	27							84
85				2380.7163	-1	4	2223.1399	-16	11				85
86	2247.2997	-7	8	2380.9122	-4	4				2355.6914	-11	17	86
87	2246.2547	-5	8	2381.1909	-4	5							87
88				2381.3692	-1	4	2219.0256	-1	21	2356.1250	-3	26	88
89										2356.5326	1	21	89
90	2242.0797	4	4	2381.8006	-1	4							90
91	2241.0334	24	28	2382.0651	-1	4							91
92	2239.4347	4	6	2382.2066	0	4							92
93	2238.3835	-9	11	2382.4665	23	30							93
94				2382.5866	-3	5							94
95	2235.7142	-7	9	2382.8373	-5	6							95
96	2234.0741	-2	3	2382.9415	-1	5							96
97	2233.0216	-10	10	2383.1855	-6	8							97
98	2231.3593	-3	4	2383.2708	-1	4							98
99	2230.3051	-22	24	2383.5090	1	4							99
100	2228.6198	-21	22	2383.5743	-2	3							100
101	2227.5710	17	17	2383.8065	-2	4							101
102				2383.8517	-3	5							102
103	2224.8084	-1	4	2383.8517	-3	5							103
104	2223.0775	2	4	2384.0790	1	3							104
105	2222.0254	4	6	2384.1041	0	4							105
106	2220.2702	-3	9	2384.3280	24	22							106
107	2219.2185	-3	4										107
108	2217.4411	3	7	2384.5469	-1	10							108
109	2216.3915	16	20	2384.5318	5	10							109
				2384.7431	1	5							

110	2213.5386	2	6	2384.7063	0	7	110
111	2211.7118	-8	14	2384.9147	12	15	111
112	2210.6651	8	14	2385.0587	2	16	112
113	2208.8145	1	9	2385.1805	24	27	113
114							114
115							115

11112 - 11102 626							11111 - 11101 626						
J	P	Obs	O-C	Unc	R	Obs	O-C	Unc	R	Obs	O-C	Unc	J

1	2313.6623	0	12	2316.7806	4	8	1
2	2312.8751	23	15	2318.3027	11	5	2
3							3
4	2311.2693	9	4				4
5	2310.4444	-10	6				5
6	2309.6409	-5	15	2321.2749	16	10	6
7	2308.7989	-23	16				7
8	2307.9899	11	9				8
9	2307.1328	-5	8				9
10	2306.3130	-7	15				10
11	2305.4412	-5	15	2323.4561	-12	21	11
12							12
13	2303.7253	-10	9	2324.8732	-11	13	13
14	2302.8934	7	10	2325.5516	-5	11	14
15				2326.9306	0	10	15
16				2327.6357	-3	6	16
17	2301.1453	-17	25	2328.9812	5	13	17
18	2300.2246	-1	9	2329.6161	2	6	18
19	2299.3779	0	9	2330.3012	0	8	19
20	2298.4380	-4	9	2330.9202	-24	25	20
21				2331.5960	-15	15	21
22	2296.6279	-7	7	2332.2046	-7	16	22
23	2295.7692	-2	6	2332.8691	-5	4	23
24	2294.7945	-7	6				24
25	2293.9311	10	17				25
26	2292.9388	5	12	2334.6984	-3	9	26
27	2292.0675	0	9				27
28	2291.0568	-11	9				28
29	2290.1817	1	11				29
30	2289.1518	-22	29				30
31	2288.2721	-3	8	2337.0977	17	27	31
32	2287.2271	4	8				32
33	2286.3378	-23	24	2338.2595	10	24	33

1	2310.6047	0	6	2317.5925	-5	4	1
2	2309.8066	-11	12	2318.3299	4	13	2
3							3
4							4
5							5
6							6
7	2306.5268	4	10				7
8							8
9							9
10							10
11	2304.8478	-16	17				11
12	2303.9727	4	7	2323.3812	-12	25	12
13	2303.1478	-4	4				13
14	2302.2522	-4	12	2324.7661	-14	12	14
15				2325.4332	-23	26	15
16				2326.1262	-14	11	16
17	2300.5091	9	22	2326.7841	9	22	17
18	2299.6730	-2	9	2327.4629	1	13	18
19	2298.7393	1	22	2328.1066	2	8	19
20							20
21	2296.9447	-10	11				21
22							22
23							23
24	2294.2789	-9	15	2330.6795	5	9	24
25	2293.2849	-1	5	2331.3182	0	9	25
26	2292.4341	3	4	2331.9288	4	7	26
27	2291.4192	13	15	2332.5523	-10	5	27
28	2290.5647	8	18	2333.1533	1	4	28
29							29
30	2288.6697	-3	10	2334.3548	14	18	30
31	2287.6108	4	6	2334.9483	1	10	31
32	2286.7533	12	13	2335.5300	10	12	32
33	2285.6719	18	22	2336.1088	8	16	33
	2284.8127	23	22	2336.6800	2	6	

2285.2752	-8	9	2338.8655	-1	8	2283.7054	1	4	2337.2442	15	26	34
2284.3850	4	11				2282.8441	-6	13				35
2282.4063	2	10	2340.5110	-3	20	2281.7175	-13	21	2338.3532	10	27	36
2281.3036	-8	11				2280.8545	-8	12	2338.9073	-3	14	37
2280.4050	6	13	2341.6016	1	8	2279.7036	7	10				38
			2342.1691	-13	22	2278.8432	12	14				39
2278.3803	5	17				2276.8076	27	28				40
2277.2391	-5	9	2343.2229	-2	8							41
2276.3305	-17	16	2343.7097	0	8	2273.5173	2	4	2342.0645	5	12	42
2275.1737	15	15	2344.2512	0	8	2272.6602	6	3	2342.5374	-12	15	43
2274.2593	-25	27	2344.7270	-7	9	2271.4072	4	6	2343.0664	-3	11	44
			2345.2527	-21	25	2270.5514	-1	7	2343.5226	4	10	45
			2345.7218	2	8	2269.2724	-2	6				46
2270.9682	3	9				2268.4195	-3	8	2344.4818	13	18	47
2270.0517	-8	16	2346.6902	-12	16	2267.1134	-2	4				48
						2266.2667	23	20	2345.9265	1	16	49
2267.9135	-4	9							2346.3215	1	6	50
2266.6702	-6	13	2348.1190	11	17							51
2265.7553	27	26	2348.5601	11	9	2262.7249	8	13				52
2264.4893	17	28				2260.4939	7	12				53
2263.5690	1	5	2349.4553	-16	22							54
2262.2834	20	21										55
												56
2260.0524	4	3	2350.7589	-2	5	2258.2373	-11	8				57
2259.1346	3	4	2351.1808	-1	4	2257.4082	1	3				58
2257.7891	-6	9	2351.5909	9	10	2255.9594	-2	5	2349.6989	-7	9	59
2256.8834	-4	5	2352.0078	7	16	2255.1366	11	11	2350.1973	-1	7	60
2255.5267	23	24	2352.3961	-1	4							61
												62
2253.2270	8	8				2252.8394	-2	4	2351.2369	2	3	63
						2251.3286	-16	11	2351.7320	-3	8	64
2250.9047	-3	5	2353.9345	4	5				2351.9688	16	16	65
									2352.4618	-8	11	66
2248.5598	-12	12	2354.6665	6	7	2246.6025	-28	21	2352.6728	4	5	67
						2245.8102	-21	18				68
2246.1944	3	5	2355.3729	1	6	2244.2070	-2	8	2353.3541	19	19	69
						2243.4231	-4	4	2353.8504	16	17	70
						2241.7855	3	13	2354.0061	-4	5	71
						2241.0117	1	7	2354.5033	-14	18	72
			2356.7122	1	5	2239.3406	10	19	2354.6372	17	18	73
						2238.5764	-3	4	2355.1361	2	7	74
2238.9551	-19	15				2236.8706	-3	13	2355.2399	9	11	75
						2236.1185	-2	5	2355.7425	3	10	76
2236.4994	2	7	2357.9509	-10	8							77
												78
			2358.5343	-1	3	2231.8602	-5	5	2356.8812	7	17	79
						2229.3203	-2	7				80
												81
												82
												83

84	2228.9910	5 12	2359.6237	-10 11	2226.7541	-26 22	2357.9204	7 22	84
85	2226.4410	-15 11			2226.0577	-2 4			85
86	2223.8718	-4 10	2360.6164	11 10	2223.4847	-10 9	2358.3996	-26 22	86
87	2221.2788	-6 6			2221.5596	8 10	2358.3247	-11 8	87
88	2218.6631	-13 15			2220.8912	5 5	2358.8599	1 22	88
89	2216.0278	7 8			2218.9260	14 12			89
90	2213.3682	6 9			2216.2676	5 7			90
91	2210.6873	13 17			2212.9715	12 8			91
92									92
93									93
94									94
95									95
96									96
97									97
98									98

02211 - 02201 626									
02221 - 02211 626									
J	P Obs	O-C Unc	R Obs	O-C Unc	P Obs	O-C Unc	R Obs	O-C Unc	J
2	2321.7742	14 16	2326.4543	-3 4					2
3	2320.9706	-7 10	2327.2147	10 14					3
4			2327.9668	1 4					4
5			2329.4554	10 15	2295.2933	5 3			5
6					2294.4814	-40 27			6
7	2317.7042	-7 10	2330.9202	23 25	2293.6708	-10 17	2305.2420	29 28	7
8	2316.8731	-1 6	2331.6408	4 7			2305.9614	-2 11	8
9	2316.0356	2 6					2306.6775	-7 12	9
10							2307.3685	-1 14	10
11			2333.0675	2 8	2290.3571	-4 10			11
12	2314.3424	5 10	2333.7693	-23 28					12
13	2313.4849	-12 16	2334.4699	1 11					13
14	2312.6240	-3 9	2335.1621	2 8					14
15	2311.7556	-8 12	2335.8485	7 18			2310.8516	22 21	15
16	2310.8826	0 6	2336.5281	4 23					16
17	2310.0025	-2 8	2337.2019	5 8					17
18	2309.1169	0 8	2337.8694	3 12	2285.2049	-4 18	2312.8483	-40 29	18
19	2308.2247	-3 11	2338.5307	2 11					19
20	2307.3270	-3 16	2339.1852	-8 22	2282.5478	-4 12	2314.1578	7 17	20
21	2306.4239	6 8	2339.8335	-16 20			2314.8027	18 18	21
22	2305.5136	0 8	2340.4792	7 25	2280.7465	-3 6	2315.4364	-10 13	22
23	2304.5979	3 10			2279.8388	17 12			23
24			2341.7473	9 15			2316.6902	-31 27	24
25	2302.7481	0 10	2342.3704	-4 14			2317.3129	-1 3	25

26	2301.8161	14 18	2342.9907	9 15	2276.1384	-4 10	2317.9244	-1 17	26
27	2300.8745	-1 6	2343.6008	-9 14	2275.2001	10 15			27
28	2299.9299	-1 9	2344.2077	-9 15			2319.7273	3 5	28
29	2298.9762	-1 15	2344.8082	1 15	2273.3030	8 14			29
30	2298.0203	0 10	2345.4025	-3 12	2272.3447	-4 10	2320.8966	-7 6	30
31	2297.0561	0 10	2346.5731	6 11	2271.3808	-6 5			31
32	2296.0876	2 17	2347.1468	-2 6					32
33	2295.1109	-2 10	2347.7177	2 14					33
34	2294.1299	-9 12							34
35	2293.1426	3 9							35
36	2292.1504	-1 7			2267.4691	6 8	2323.1644	3 12	36
37	2291.1497	-1 6			2266.4785	21 26	2323.7139	20 23	37
38	2290.1461	-4 7	2349.3875	2 9	2265.4753	-12 11			38
39	2289.1193	2 10	2350.4702	-2 9			2325.3310	-17 13	39
40	2288.1133	4 9					2326.3790	-12 9	40
41	2287.0936	-1 7	2351.5286	-1 10					41
42	2286.0682	6 12	2352.0517	4 12	2261.4213	0 4			42
43	2285.0308	6 13	2352.5614	-9 12					43
44	2283.9929	0 6	2353.0733	3 9	2259.3576	-6 8			44
45	2282.9429	-1 7					2328.4016	4 10	45
46	2281.8945	-1 8	2354.0693	-7 15					46
47	2280.8323	1 10	2354.5548	-4 11	2256.2222	-4 7			47
48	2279.7735	7 9	2355.0423	-1 14	2255.1600	-13 16	2329.8429	6 5	48
49	2278.6984	5 10	2355.5140	-4 7					49
50	2277.6274	-2 11	2355.9894	-5 16	2253.0253	-22 25	2330.7766	-7 14	50
51	2276.5393	-8 11	2356.4489	1 9	2251.9560	-5 8	2331.2474	-6 6	51
52	2275.4592	1 5	2356.9126	-2 9	2250.8700	-2 6	2331.6877	2 4	52
53					2249.7877	-7 9			53
54	2273.2670	-1 5			2248.6900	6 5			54
55	2272.1542	3 13	2358.2443	12 21	2247.5968	-1 4	2333.0223	-4 15	55
56	2271.0523	3 12			2246.4853	1 3	2333.4345	11 14	56
57	2269.9249	-8 12	2359.1018	-11 13					57
58	2268.8150	15 21			2244.2576	1 3	2334.2699	9 14	58
59			2359.9380	2 8	2243.1435	-6 8	2334.6984	-3 9	59
60	2266.5538	19 24	2360.3569	4 8					60
61			2360.7478	1 7	2240.8853	24 24	2335.4994	-3 9	61
62	2264.2667	-4 9	2361.1550	-5 6					62
63	2263.1003	-5 9			2238.5998	13 14			63
64	2261.9616	24 23	2361.9284	-12 16			2336.6277	14 25	64
65	2260.7806	13 16	2362.2908	-20 23	2236.2914	4 4			65
66	2259.6280	-3 17	2362.6804	14 18			2337.3630	8 18	66
67	2258.4353	9 11	2363.0282	3 7					67
68			2363.4019	-16 25	2232.7680	-9 22	2338.0741	10 17	68
69	2256.0655	2 8	2363.7384	5 9	2231.6066	-2 7			69
70	2254.8976	1 6			2230.3992	-22 17			70
71	2253.6756	5 5			2229.2320	17 18	2339.1350	3 5	71
72	2252.4975	-3 8	2364.7784	3 6	2228.0121	14 20			72
73	2251.2604	-3 6	2365.0831	1 4	2226.8302	-6 11			73
74	2250.0748	-4 9			2225.5957	-12 13	2340.0553	-4 5	74
75			2365.7179	-1 4	2224.4067	-17 19			75

76	2246.3614	-12	13	2366.0540	7	9	2221.9626	-6	12	2340.6659	-6	19	76
77	2245.1632	14	16	2366.3290	11	14	2220.7004	6	22				77
78	2243.8784	-5	8	2366.9107	-21	23	2219.4960	8	23				78
79	2242.6710	-2	6	2367.2300	7	9							79
80	2241.3720	-3	6	2367.4727	2	5							80
81	2240.1579	0	5	2367.7795	-5	12							81
82	2238.8438	12	14	2368.0067	-4	5							82
83	2237.6222	1	5	2368.5169	2	5							83
84	2236.2914	13	12	2369.0015	5	12							84
85	2235.0639	0	4	2369.4602	-1	3							85
86	2232.4834	2	3	2369.7339	-6	7							86
87	2231.1166	3	6	2369.8946	3	5							87
88	2229.8786	-17	19	2370.6868	-1	4							88
89	2228.4942	-10	9	2370.9396	-3	6							89
90	2227.2546	-5	6	2371.0447	-7	12							90
91	2224.6076	-1	4	2371.2924	3	6							91
92	2221.9400	17	21	2371.6883	15	17							92
93	2220.4958	6	12	2371.9223	1	11							93
94	2219.2469	1	7	2371.9696	0	5							94
95	2217.7834	2	11	2372.2006	5	20							95
96	2215.0481	-5	18										96
97	2213.7989	8	20										97
98	2212.2910	-3	12										98
99													99
100													100
101													101
102													102
103													103
104													104
105													105
106													106
107	2206.7098	5	29										107

12211 - 12201 626					
J	P	Obs	O-C	Unc	O-C Unc
2					
3					
4					
5					
6					
7					
8					
2303.3659 -10 28					
2304.1254 -4 7					
2305.6233 -21 17					
2306.3653 -8 26					
2296.2638 -8 19					
2295.4457 4 8					
2294.6195 -5 14					



59	2244.6326	-3	3	2336.8897	12	24
60	2243.5558	12	11	2337.3304	26	13
61	2242.3618	3	8			
62	2240.0646	-25	20			
63	2238.9803	-16	20			
64				2339.2605	12	11
65	2236.6609	-14	21			
66	2235.4096	4	10			
67						
68	2233.0459	2	9			
69	2231.9565	-4	8			
70	2230.6596	2	10	2341.4083	-10	14
71	2229.5719	6	6			
72	2228.2502	1	7			
73						
74	2225.8187	6	11			
75	2224.7348	-3	10			
76	2223.3625	-7	7			
77	2222.2853	6	8			
78				2343.9327	0	3
79	2219.8153	25	27			
80	2218.3848	-6	12	2344.5044	21	26
81	2217.3168	-28	26			
82	2215.8625	1	9			
83						
84						
85	2212.2705	6	16			
86	2210.7530	42	30			
87	2209.7122	-14	14			
88	2208.1591	8	23			
89						

03311 - 03301 626						
J	P	Obs	O-C	Unc	R	Obs O-C Unc
3	2308.4942	11	13	2314.7467	-4	5
4				2315.5000	-18	18
5				2316.2508	3	10
6	2306.8717	21	25	2316.9932	1	6
7	2306.0476	-13	24	2317.7298	1	22
8				2318.4605	2	4
9	2304.3891	-4	5			
10				2319.9026	-8	9
11	2302.7063	1	11			

12	2301.8559	3	16	8	2321.3214	-10	11
13	2300.9992	-3	5	8			
14	2300.1363	12	16		2323.4055	1	26
15	2299.2683	12	16				
16	2298.3949	6	10		2324.7661	23	25
17	2297.5139	9	12		2325.4332	-7	19
18	2296.6279	1	7		2326.0973	-7	11
19	2295.7349	-3	6		2326.7560	0	10
20	2294.8363	-14	15		2327.4072	-7	8
21	2293.9311	-8	11		2328.0534	-4	6
22	2293.0217	8	11				
23	2292.1073	-1	9		2329.3269	-4	7
24	2291.1845	7	9		2329.9555	6	8
25	2289.3238	-12	19		2331.1926	7	16
26	2288.3838	6	7		2331.8015	2	9
27	2287.4368	14	17		2332.9993	-24	28
28	2286.4872	3	13		2333.5923	-5	7
29	2285.5300	-11	13				
30	2284.5675	17	22		2336.4570	2	8
31	2283.5974	23	27		2337.0127	14	21
32	2282.6210	9	10				
33	2281.6430				2338.1025	6	10
34	2280.6532				2338.6382	1	14
35	2279.6643						
36	2278.6645						
37							
38							
39							
40							
41	2273.5838	1	4		2340.2101	3	25
42	2271.5102	-6	7		2340.7211	-4	10
43	2270.4668	11	13				
44	2269.4135	-12	18				
45	2268.3559	-20	24		2342.2202	4	7
46	2267.2954	1	4				
47	2266.2278	9	11		2343.1882	2	4
48	2265.1506	-21	25		2343.6632	3	6
49	2264.0742	15	29				
50	2262.9865	-4	5		2344.5948	5	7
51					2345.0505	-2	7
52							
53							
54	2259.6941	-7	9				
55					2346.3835	1	4
56							
57	2256.3511	3	4		2347.2414	3	5
58	2255.2245	-1	4				
59	2254.0949	22	24				
60	2252.9541	-9	10		2348.4810	-5	7
61							

62	2251.8116	0	4	2349.2770	-7	9
63	2250.6615	-10	10			
64	2249.5069	-7	8			
65	2248.3476	6	7	2350.0492	-1	4
66				2350.4258	-1	4
67	2246.0086	-1	3	2350.7962	-1	4
68	2244.8309	-1	4	2351.1607	1	6
69						
70	2242.4580	-4	9	2351.8705	-1	3
71	2241.2653	17	18	2352.2166	3	6
72	2240.0646	15	14			
73	2238.8585	15	17			
74	2237.6436	-15	16			
75	2236.4295	19	18			
76	2235.2037	-8	9	2353.8504	-23	22
77	2233.9758	1	3			
78						
79						
80	2230.2553	-1	4			
81						
82	2227.7459	-11	12			
83						
84	2225.2177	15	15	2356.1501	0	7
85				2356.4113	18	23
86	2222.6619	-10	11			
87	2221.3776	-3	5			
88	2220.0894	21	20			
89						
90	2217.4901	8	7			

13312 - 13302 626										13311 - 13301 626									
J	P	Obs	O-C	Unc	R	Obs	O-C	Unc	P	Obs	O-C	Unc	R	Obs	O-C	Unc	J		
3													2291.4661	-24	27		3		
4													2292.2211	-21	23		4		
5	2285.8808	3	6						2283.5974	26	26		2293.7164	16	21		5		
6																	6		
7					2296.7506	-4	6										7		
8					2297.4825	-7	8										8		
9	2283.4024	12	12		2298.2111	16	18		2281.9497	7	9		2295.1833	8	9		9		
10	2282.5620	-11	18						2281.1169	-3	7		2295.9064	-10	11		10		
11	2281.7175	-16	17		2299.6428	-16	19		2280.2795	0	5		2296.6279	16	17		11		
12					2300.3526	-3	6										12		
13	2280.0137	1	4						2277.7295	-15	14						13		

14	2279.1529	8	8	2301.7550	28	29	14
15				2302.4422	-7	8	15
16				2303.1290	13	15	16
17				2303.8053	-12	13	17
18							18
19							19
20	2273.8613	5	6	2305.8087	13	24	20
21							21
22	2271.1339	-28	27	2307.7555	8	9	22
23	2270.2174	-4	6	2308.3921	3	4	23
24	2269.2900	-16	19				24
25							25
26	2267.4235	1	4	2310.2687	12	16	26
27	2266.4785	-21	29	2310.8826	19	19	27
28	2265.5339	18	20				28
29	2264.5772	-5	6	2312.0887	-6	15	29
30	2263.6176	-1	3	2312.6830	-17	18	30
31	2262.6513	-5	6	2313.2735	-5	6	31
32	2261.6787	-15	17	2313.8573	0	4	32
33				2314.4353	6	7	33
34				2315.0032	-28	30	34
35							35
36							36
37	2256.7365	5	18	2316.1311	4	17	37
38	2255.7300	1	4				38
39	2254.7177	-5	5	2317.7737	9	10	39
40	2253.7003	-4	5				40
41	2252.6775	0	3	2318.8388	14	14	41
42							42
43	2250.6138	-1	3	2319.8788	8	10	43
44	2249.5751	15	15	2320.3889	-3	5	44
45	2248.5280	4	6	2320.8966	21	21	45
46	2247.4759	0	4	2321.3933	-4	4	46
47				2321.8876	8	9	47
48	2245.3562	8	10				48
49	2244.2869	3	4				49
50	2243.2138	16	16				50
51							51
52	2239.9570	20	21	2324.7188	-3	5	52
53	2238.8585	6	10				53
54	2237.7549	-3	8	2325.6123	-26	26	54
55	2236.6475	7	15				55
56	2235.5322	-6	18	2326.4865	0	5	56
57	2234.4144	12	12	2327.3344	6	7	57
58	2233.2873	-7	3				58
59	2232.1574	-3	4				59
60	2231.0203	-3	12				60
61	2229.8786	0	5				61
62							62
63							63

14	2276.0015	-11	10	2300.8151	5	5	14
15	2275.1294	-1	5	2301.4918	0	3	15
16				2302.1647	17	18	16
17							17
18							18
19	2272.4731	-21	22				19
20	2271.5780	-8	9	2303.4876	2	5	20
21	2270.6765	-1	4	2304.1401	-5	6	21
22	2269.7675	-8	8				22
23	2268.8531	-11	12				23
24	2267.9345	1	5				24
25	2267.0087	0	4	2306.6930	-7	13	25
26							26
27							27
28	2263.2506	27	27	2309.1517	5	7	28
29				2309.7506	0	4	29
30	2261.3330	3	4				30
31							31
32							32
33							33
34	2257.4338	8	9	2312.0887	2	14	34
35				2312.6592	12	13	35
36							36
37	2255.4509	23	28				37
38	2254.4473	-5	5				38
39	2253.4433	20	21				39
40	2252.4285	-5	6				40
41	2251.4111	1	4				41
42				2316.4772	-2	4	42
43							43
44	2248.3242	12	13	2317.5146	-3	5	44
45							45
46	2246.2367	9	10				46
47	2245.1808	-29	30				47
48	2244.1274	14	14	2319.5159	-26	27	48
49	2243.0640	13	14	2320.0035	-10	12	49
50	2241.9939	2	7				50
51							51
52	2239.8390	2	4	2321.4281	13	12	52
53	2238.7517	-12	13	2321.8876	-15	15	53
54	2237.6603	-12	18	2322.3454	0	3	54
55	2236.5646	-2	6	2322.7945	-13	14	55
56	2235.4615	-3	9				56
57							57
58	2233.2392	-7	10				58
59	2232.1193	-13	19	2324.5409	29	30	59
60	2230.9977	19	22				60
61							61
62	2228.7294	-2	5				62
63				2326.1865	9	10	63



26	2276.8561	9 18	2318.1855	-2 4	2263.4732	-11 15	26
27			2318.8061	16 17	2261.5807	-3 5	27
28	2274.0195	-6 9	2319.4167	-5 10	2260.6265	7 7	28
29							29
30	2272.1019	9 9			2258.6981	-1 5	30
31	2272.1339	12 11					31
32	2272.1580	-6 11	2322.3902	-6 14			32
33	2260.1799	12 13	2322.9686	12 11			33
34	2268.1939	9 7	2323.5390	10 9	2255.7639	-3 4	34
35			2324.1032	6 15			35
36	2266.2065	22 22					36
37	2265.2012	-1 4	2325.2134	-3 21			37
38			2325.7596	-6 10	2251.7727	1 4	38
39	2263.1765	-14 17			2250.7595	-11 11	39
40	2262.1574	-2 9					40
41	2261.1325	10 11					41
42	2260.1001	4 4					42
43	2259.0601	-20 22	2328.4016	-6 10	2246.6548	-11 12	43
44	2258.0205	18 15			2245.6177	20 23	44
45					2244.5698	0 4	45
46	2255.9154	5 8			2243.5189	5 7	46
47	2254.8545	1 3	2330.4062	-8 14			47
48	2253.7861	-21 28			2241.3975	-12 24	48
49	2252.7156	-6 10	2331.8459	-13 24	2240.3308	4 4	49
50					2239.2565	-1 4	50
51	2250.5561	9 8			2238.1776	3 5	51
52	2249.4659	-3 6	2333.2324	-6 10	2237.0915	-8 10	52
53	2248.3715	0 3	2333.6840	12 9	2236.0030	12 14	53
54					2234.9078	20 20	54
55	2246.1651	1 4	2334.5645	2 4	2233.8029	-13 15	55
56	2245.0557	24 26	2334.9943	-17 25			56
57					2230.4675	11 11	57
58	2242.8125	-3 5			2229.3429	1 6	58
59	2241.6842	1 7					59
60	2240.5488	-9 11	2336.2565	18 17			60
61							61
62	2238.2634	-7 9	2337.0646	10 15	2225.9388	-3 5	62
63	2237.1129	1 3	2337.4605	16 16			63
64					2223.6408	-18 25	64
65	2234.7927	-8 9	2338.2323	8 10	2222.4849	-14 15	65
66			2338.6072	-15 15	2221.3240	-4 9	66
67	2232.4516	-1 4			2220.1568	-4 8	67
68	2231.2735	10 12			2218.9845	-1 6	68
69	2230.0870	-6 6			2217.8090	24 25	69
70	2228.8968	-4 4	2340.0553	-17 14	2216.6225	-6 12	70
71	2227.7007	-5 5	2340.7425	-24 22	2215.4365	21 19	71
72					2214.2421	19 17	72
73	2225.2918	-7 8	2341.4083	-2 6	2213.0409	2 14	73
74					2211.8357	-2 9	74
75							75



00011 - 00001 636				00011 - 00001 828					
J	P Obs	O-C Unc	R Obs	O-C Unc	P Obs	O-C Unc	R Obs	O-C Unc	J
0	2281.9200	-6	9	-4	8	-14	17	9	15
2	2278.7139	-19	35	5	7	-4	10	-3	16
4	2277.0792	12	26	-13	20	2	9	-1	4
6	2275.4144	-21	27	-17	32	5	4	6	6
8	2273.7337	22	29	23	26	-2	4	4	8
10	2272.0232	3	15	-20	36	15	22	8	10
12	2270.2927	19	30	20	27	16	20	4	12
14	2268.5342	-9	21	-10	27	1	4	-7	14
16	2266.7547	-13	19	-9	21	18	28	-2	16
18	2264.9543	-21	38	-12	25	-5	10	-4	18
20	2263.1254	12	17	0	18	-2	5	0	20
22	2261.2773	-9	18	6	38	-5	14	-3	22
24	2259.4066	-3	16	-17	24	2	10	3	24
26	2257.5091	-16	20	-9	16	-2	11	-6	26
28	2255.6476	6	23	-8	12	-11	10	0	28
30	2253.6810	2	8	-7	10	-7	8	-8	30
32	2249.6906	2	6	-7	9	-6	7	-9	32
34	2247.6805	-1	6	-4	5	3	3	-19	34
36	2245.6445	1	4	1	3	0	0	0	36
38	2243.5859	1	4	2	3	0	0	0	38
40	2241.5038	1	4	2	3	0	0	0	40
42	2239.4004	1	4	2	3	0	0	0	42
44	2237.2715	1	4	2	3	0	0	0	44
46	2235.1204	1	4	2	3	0	0	0	46
48	2232.9463	1	4	2	3	0	0	0	48
50	2230.7495	1	4	2	3	0	0	0	50
52	2228.5298	1	4	2	3	0	0	0	52
54	2226.2872	1	4	2	3	0	0	0	54
56	2224.0212	1	4	2	3	0	0	0	56
58	2221.7327	1	4	2	3	0	0	0	58
60	2219.4215	1	4	2	3	0	0	0	60
62	2217.0872	1	4	2	3	0	0	0	62
64	2214.7284	1	4	2	3	0	0	0	64
66	2212.3504	1	4	2	3	0	0	0	66
68	2209.9482	1	4	2	3	0	0	0	68
70	2207.5236	1	4	2	3	0	0	0	70
72	2205.0754	1	4	2	3	0	0	0	72
74	2202.6041	1	4	2	3	0	0	0	74
76	2200.1134	1	4	2	3	0	0	0	76
78									78
80									80
82									82

84	2197.5983	2	4	2327.8560	1	3	2237.0344	-1	3	2352.8297	-15	9	84
86	2195.0603	-1	4	2328.3700	2	3	2234.7446	-5	6	2353.2591	13	11	86
88	2192.5004	-2	5	2328.8591	0	3							88
90	2189.9161	-14	11	2329.3240	3	3	2230.1059	23	30	2354.0417	-15	11	90
92	2187.3109	-16	10	2329.7634	-1	3	2227.7515	-1	9				92
94	2184.6861	10	7	2330.1795	8	6	2225.3797	8	6	2354.7406	26	17	94
96	2182.0353	1	3				2222.9850	-4	7				96
98	2179.3646	14	9	2330.9340	-7	7	2220.5690	-22	28				98
100	2176.6694	5	5	2331.2752	-3	3				2355.6111	7	11	100
102	2173.9520	-3	7	2331.5921	5	4	2215.6820	14	11				102
104	2171.2127	-8	3	2331.8831	3	4	2213.2046	2	4				104
106	2168.4526	1	3	2332.1491	-2	3	2210.7070	-5	13	2356.2824	39	17	106
108	2165.6696	2	4	2332.3904	-4	8	2208.1897	-3	12				108
110				2332.6074	-1	3							110
112	2160.0372	3	11	2332.7992	-1	3							112
114	2157.1877	1	4	2332.9662	-1	4	2200.5134	-7	14				114
116	2154.3160	-3	8	2333.1089	6	7	2197.9141	-3	25				116
118	2151.4217	-13	19	2333.2270	17	7	2195.2930	-12	22				118
120	2148.5085	7	10	2333.3186	12	15	2192.6539	3	21				120
122	2145.5735	28	27	2333.3835	-11	15							122
124							2187.3092	-19	18				124
126							2184.6086	-7	42				126
128							2181.8862	-10	29				128

01111 - 01101 636													01111 - 01101 828												
J	P	Obs	O-C	Unc	R	Obs	O-C	Unc	P	Obs	O-C	Unc	R	Obs	O-C	Unc	J								
1	2270.1896	1	3		2273.3068	16	11		2300.4044	11	6		2303.1721	-3	6		1								
2	2269.3996	5	5		2274.0727	3	5		2299.7002	2	5		2304.5229	-5	4		2								
3	2268.5936	-15	22		2274.8258	-8	8		2298.9829	-24	36		2305.1964	10	18		3								
4	2267.7959	2	4		2275.5864	22	27		2298.2740	7	22		2305.8507	-21	28		4								
5	2266.9773	2	5		2276.3246	-23	40						2306.5159	3	5		5								
6	2266.1694	5	8		2277.0700	-2	5						2306.5159	-4	7		6								
7	2265.3362	7	7		2277.7986	1	4						2307.1601	10	4		7								
8	2264.5186	-2	6		2278.5368	1	4						2307.8150	-8	6		8								
9	2263.6699	-6	6		2279.2496	-5	6						2308.4457	-2	3		9								
10	2262.8442	-11	15		2279.9769	4	4						2309.0904	-20	35		10								
11	2261.9817	-3	4		2280.6771	1	5						2309.7079	-20	35		11								
12	2261.1484	-1	5		2281.3944	-4	10						2310.3458	-5	6		12								
13					2282.0799								2310.9524	-9	7		13								

14	2260.2691	-9	9	2282.7868	-7	7	2291.5702	-1	6	2311.5765	-17	21	14
15	2259.4271	-13	22	2283.4597	-6	9	2290.8166	2	10	2312.1736	-5	6	15
16	2258.5349	2	4	2284.1564	-5	7	2290.0226	1	3	2312.7897	-5	4	16
17	2257.6853	-1	3	2284.8173	-4	8		4		2313.3710	-21	23	17
18	2256.7746	-13	38	2285.5020	-4	5	2288.4535	-12	4	2313.9788	-4	21	18
19	2255.9180	-5	4	2286.1494	-9	8	2287.6824	2	9	2314.5504	2	11	19
20	2254.9935	-4	6	2286.8232	-2	5	2286.0847	6	8		-4	3	20
21	2254.1284	-4	5	2287.4585	-5	4	2285.2504	3	9	2315.7052	-14	13	21
22	2253.1880	-4	6	2288.1214	-2	5	2284.4640	-3	5	2316.8377	-14	13	22
23	2252.3155	-4	5	2288.7437	-2	4	2283.6157	-1	8	2317.4121	-12	32	23
24	2251.3596	2	5	2289.3958	0	5	2282.8223	-5	5	2317.9495	-12	13	24
25	2250.4799	1	6	2290.0055	0	6	2281.9607	-2	4	2318.5157	-2	7	25
26	2248.6205	-2	5	2290.6458	0	6	2281.1602	3	7	2319.0401	-3	8	26
27	2247.6314	-6	4		4	6	2280.2833	-3	6	2320.1085	0	3	27
28	2246.7393	-9	9	2291.8716	-3	4	2279.4753	-3	3	2320.6526	5	5	28
29	2245.7332	-2	11	2292.4571	4	6	2278.5856	-2	3				29
30	2244.8335	-2	4	2293.6469	1	4	2277.7718	17	38				30
31	2243.8115	-2	4				2276.8658	1	5	2321.6878	4	3	31
32	2242.9050	-2	3	2294.8129	-2	4	2276.0412	-1	3	2322.1778	-4	9	32
33	2241.8665	-2	5	2295.4055	-6	6	2275.1265	-19	16	2322.7011	-5	5	33
34	2240.9530	-5	7	2295.9546	-10	12	2274.2949	-2	13	2323.1799	-3	4	34
35	2239.8984	-5	7	2296.5363	4	4	2273.3624	-2	6	2323.6939	-21	26	35
36	2238.9788	-5	7	2297.0745	1	4	2272.5267	-9	14	2324.1591	-12	9	36
37	2237.9072	-5	3	2297.6424	3	4	2271.5783	-2	4	2324.6609	-1	3	37
38	2236.9819	-2	5	2298.1689	1	4	2270.7736	11	15	2325.1200	16	21	38
39	2235.8929	-2	3	2298.7238	-2	3	2269.7735	1	4	2325.6077	-1	4	39
40	2234.9609	-11	28	2299.2395	-1	6	2268.9234	0	4	2326.0551	-7	40	40
41	2233.8547	-10	9				2267.9470	0	3	2326.5324	-2	4	41
42	2232.9195	-4	4	2300.2865	1	4	2267.0904	0	4				42
43	2231.7954	1	4	2300.8155	1	4	2266.0995	1	3	2327.4365	12	16	43
44	2230.8533	0	4	2301.3092	-1	5	2265.2363	0	4	2327.8603	-1	6	44
45	2229.7126	7	4	2301.8245	-4	4	2264.2306	1	3	2328.3156	-2	3	45
46	2228.7651	4	7	2302.3091	9	20	2263.3616	-5	5				46
47	2227.6053	-3	4	2302.8105	3	4	2262.3402	-2	3	2329.1742	1	3	47
48	2226.4764	0	4	2302.8830	-1	3	2261.4644	-3	1	2329.5780	-2	5	48
49	2225.5197	1	4	2303.7713	0	3	2260.4290	0	5	2330.0100	-2	9	49
50	2224.4764	4	3	2303.7713	0	4	2259.5476	4	5	2330.4051	12	4	50
51	2223.3236	-5	6	2304.2340	2	4	2258.4965	0	3	2330.8273	32	46	51
52	2222.3631	10	8	2305.1610	0	3	2257.6087	0	3	2331.2083	8	6	52
53	2221.1500	-1	3	2306.6208	0	3	2256.5432	-8	7	2331.6161	4	5	53
54	2220.1829	-4	4	2306.0636	-2	4	2255.6484	13	15	2331.9897	7	7	54
55	2218.9506	1	3	2306.5090	-4	5	2254.5693	0	5				55
56	2217.9810	11	1	2307.3737	-4	5	2253.6691	0	16	2333.1320	-2	3	56
57	2216.7313	0	4	2307.7974	4	5	2252.5721	0	5				57
58	2215.7566	4	3	2308.2138	4	9		-2	3				58
59	2214.4867	0	16	2308.6268	7	7	2250.5549	3	3	2333.8551	-19	29	59
60	2213.5107	-1	3	2309.0286	-7	3	2249.6448	3	5				60
61	2212.2203	-1	1	2309.4340	1	3	2248.5171	-3	4	2334.5595	0	4	61
62	2211.2391						2247.6008						62
63													63

64	2209.9315	2	6	2309.8188	-8	6	2246.4577	-3	4	2335.2391	-5	5	64
65	2208.9468	1	5	2310.2155	-7	5	2245.5370	3	4	2335.5630	-7	10	65
66	2207.6207	12	7	2310.5863	0	2	2243.4515	1	5	2336.2126	5	6	66
67	2205.2848	-3	3	2310.9743	-1	3	2242.2764	-2	9	2336.5298	-30	31	67
68	2204.2942	-4	5	2311.3285	0	3	2241.3456	3	7	2337.1446	-12	14	68
69	2202.9282	15	3	2311.7082	0	3	2240.1542	-8	9	2337.4434	15	18	69
70	2201.9364	1	11	2312.0465	0	3	2239.2175	-1	4	2337.7363	-2	9	70
71	2200.5480	-4	4	2312.7400	0	3	2238.0113	-5	6				71
72	2199.5529	0	3	2313.1034	0	3	2237.0710	-6	4				72
73	2198.1465	0	3	2313.7649	2	3	2235.8468	4	4	2338.5817	-9	16	73
74	2197.1485	0	3	2314.0535	-1	3	2234.9023	-6	11				74
75	2195.7221	-13	6	2314.6736	0	3	2233.6619	-1	3	2339.1182	-13	26	75
76	2194.7205	11	15	2315.0143	-2	4	2232.7124	-1	5	2339.3731	-6	12	76
77	2193.2752	-6	6	2315.6030	0	3	2231.4568	6	7	2339.6343	2	4	77
78	2192.2723	-14	9	2315.8402	-2	4	2230.5030	2	3				78
79	2190.8029	-20	14	2316.1677	0	3	2229.2302	9	10	2340.1267	4	9	79
80	2189.7997	-20	14	2316.3864	1	3	2228.2724	13	12				80
81	2188.3120	21	15	2316.7070	-1	3	2226.9838	-6	4	2340.5964	2	5	81
82	2187.3105	13	8	2316.9085	-1	3	2226.0194	1	7				82
83	2185.7987	-6	3		1	3	2224.7143	-12	18				83
84	2184.7923	-22	16	2317.4058	1	3	2222.4240	-12	18	2341.4681	-7	10	84
85	2183.2602	17	16	2317.7124	-16	11	2221.4546	21	17	2341.6529	2	10	85
86	2182.2550	-18	13	2317.8783	0	3	2220.1174	-5	10	2341.8722	7	10	86
87	2180.7027	-18	13	2318.1809	0	3	2219.1411	-1	6	2342.0424	16	16	87
88	2179.6937	-13	7	2318.3266	3	3	2217.7846	-6	8	2342.2501	-16	9	88
89	2178.1193	-1	2	2318.6237	3	3	2216.8069	-3	10				89
90	2177.1125	5	5	2318.7496	-1	3	2215.4331	-3	4				90
91	2175.5155	-7	4	2318.8842	-3	3	2214.4526	5	11				91
92	2174.5105	-1	2	2319.0413	-3	3	2213.0619	13	18				92
93	2172.8884	-6	4	2319.1489	0	3	2212.0783	24	35				93
94	2171.8842	-4	5	2319.4353	-1	3	2210.6701	9	14	2343.2564	-14	17	94
95	2170.2401	6	5	2319.5222	-8	10	2209.6829	-3	8				95
96	2169.2370	2	7	2319.8039	0	3	2208.2579	12	10	2343.8164	2	21	96
97	2167.5706	-3	3	2319.8716	3	4	2207.2670	-11	20	2343.8963	13	17	97
98	2166.5673	-35	24	2320.1500	-2	4	2205.8213	-12	21				98
99	2164.8779	-2	4	2320.1960	1	4	2204.8307	-6	24				99
100	2163.1621	-2	4	2320.4961	-21	24	2203.3660	-12	21				100
101	2161.1590	-2	4	2320.7689	-21	24	2200.8909	-6	24				101
102	2159.4277	-1	4	2321.0377	-2	7	2199.8945	2	18				102
103	2158.4277	-14	14	2321.0200	-13	7	2198.3967	4	25				103
104	2156.6662	9	10		0	5		-13	27				104
105	2155.6694	6	5	2321.2467	0	5	2194.8795	19	19				105
106	2153.8861	-3	10	2321.4477	3	10	2193.3424	-1	16				106
107	2152.8929	17	12				2192.3426						107
108	2151.0818	20	22				2190.7866						108
109	2150.0940												109
110	2148.2574												110
111	2147.2726												111
112													112
113													113

114	2145.4082	-20	21	2188.2111	20	36	114
115							115
116	2142.5435	21	26	2185.6105	-7	28	116
117							117
118							118
119				2180.3533	-9	45	119
120				2177.6958	6	36	120
121							121
122							122

10012 - 10002 636							10012 - 10002 828						
J	P Obs	O-C Unc	R Obs	O-C Unc	P Obs	O-C Unc	R Obs	O-C Unc	P Obs	O-C Unc	R Obs	O-C Unc	J
0	2260.3406	-2	5	1	3		2293.4877	-4	3		2295.5680	8	13
2	2258.7483	-1	9	15	10		2292.0737	-17	17				0
4	2257.1333	3	4	-6	6		2290.6437	23	11				2
6	2255.4950	3	4	-2	4		2289.1880	19	30		2300.8743	-22	22
8	2253.8330	-5	4	-2	4						2303.4033	6	4
10	2252.1493	-1	3	1	3		2284.6925	-5	8				10
12	2250.4428	4	4	-11	10		2283.1517	-12	9				12
14	2248.7124	-3	4	3	4		2281.5911	-6	5		2307.0313	5	8
16	2246.9599	-2	4	3	4		2280.0104	11	8		2308.1966	-5	5
18				-8	7		2278.4063	5	6		2309.3417	-1	25
20	2243.3854	-13	10	-9	9		2276.7804	-8	7		2310.4658	9	4
22	2241.5660	1	3	14	19								26
24	2239.7217	-8	7	1	3		2273.4683	-5	6				28
26	2237.8566	1	3	1	3								30
28	2235.9683	5	5	2	4		2270.0726	5	14		2314.7396	-12	7
30	2234.0561	-5	5	-3	4		2268.3421	-2	5		2315.7537	-18	17
32				-4	5		2266.5908	-7	8				34
34	2230.1689	22	15	0	3		2264.8201	4	4				36
36	2228.1881	1	3	1	3		2263.0263	-6	8		2318.6664	-25	36
38	2226.1866	-3	4	-6	7		2261.2135	3	5		2319.5949	-14	8
40	2224.1631	-2	3	-1	3		2259.3804	19	17				42
42	2222.1174	0	3	-1	3						2321.3871	15	25
44	2220.0493	1	3	-1	4		2255.6472	7	4		2322.2475	2	7
46	2217.9588	1	5	6	5		2253.7492	0	5				48
48	2215.8464	5	7	-2	3		2251.8313	3	4		2323.9052	3	8
50	2213.7109	0	7	-2	3						2324.7002	-4	10
52	2211.5537	0	7	-6	5		2247.9295	-26	33				54
54	2209.3740	-3	7	-5	5		2245.9513	-1	5		2326.2254	-5	8
56	2207.1730	2	4										58

60	2204.9493	1	3	2298.5773	-3	5	2243.9492	-6	13	2327.6634	7	20	60
62	2202.7036	0	2	2299.4075	-6	5	2241.9274	-1	6	2328.3472	-6	12	62
64	2200.4358	-1	3	2300.2154	7	4	2239.8846	2	5	2329.0114	6	8	64
66	2198.1464	2	3	2300.9984	9	7	2237.8227	22	35				66
68	2195.8351	5	5				2235.7354	-5	3				68
70	2193.4985	-25	25	2302.4902	-10	9	2233.6313	8	14	2330.2698	0	5	70
72	2191.1446	-10	7	2303.2013	-8	8	2231.5043	0	7				72
74	2188.7695	12	9	2303.8909	18	12	2229.3576	1	10	2331.4391	-5	8	74
76	2186.3688	-4	3	2304.5523	2	4				2331.9899	-10	17	76
78	2183.9487	4	3	2305.1918	8	9	2225.0012	-4	14				78
80	2181.5057	0	3	2305.8075	16	9	2222.7910	-16	13	2333.0257	-6	13	80
82	2179.0413	0	3	2306.3977	9	5				2333.5111	8	4	82
84	2176.5553	0	3							2333.9728	10	13	84
86													86
88	2171.5185	2	5	2308.0244	-3	3	2213.7499	0	16	2334.8248	-22	8	88
90	2168.9662	-13	10	2308.5189	-2	3	2211.4377	1	8				90
92	2166.3939	-12	8	2308.9892	-1	3	2209.1049	2	6				92
94	2163.8014	3	4	2309.4342	-11	7	2206.7518	7	11				94
96	2161.1858	1	3	2309.8573	2	4							96
98	2158.5497	8	8	2310.2557	10	9	2201.9820	0	26				98
100	2155.8904	-2	4	2310.6290	10	11							100
102	2153.2112	-2	4	2310.9747	-24	23							102
104	2150.5098	-2	5	2311.3032	13	21							104

10011 - 10001 636													10011 - 10001 828												
J	P	Obs	O-C	Unc	R	Obs	O-C	Unc	P	Obs	O-C	Unc	J	P	Obs	O-C	Unc	R	Obs	O-C	Unc	J			
0													0												
2	2259.6951	1	3		2265.1508	-1	4		2289.5767	-2	7		2	2259.6951	2293.0236	2	3								
4	2258.0825	2	3		2266.6552	-7	9		2288.1600	2	3		4	2258.0825	2296.9770	-3	13								
6	2256.4457	0	3						2286.7203	-4	14		6	2256.4457	2295.6817	3	7								
8	2254.7851	-2	5		2269.5934	-3	4		2283.7774	7	7		8	2254.7851	2298.5061	-10	32								
10	2253.1018	7	3		2271.0243	-22	16		2282.2721	3	5		10	2253.1018	2299.7500	32	13								
12	2251.3935	5	5		2272.4351	-1	4						12	2251.3935	2300.7318	-6	6								
14	2249.6617	5	5		2273.8199	0	3						14	2249.6617	2301.9396	-2	11								
16	2247.9049	-7	4		2275.1805	1	5		2279.1961	-2	2		16	2247.9049	2303.1248	-3	5								
18	2246.1266	5	6		2276.5171	3	4						18	2246.1266	2304.2868	-14	20								
20	2244.3249	17	4		2277.8300	9	8						20	2244.3249	2305.4324	33	33								
22	2242.4963	-1	4		2279.1165	-6	7						22	2242.4963	2306.5477	-1	4								
24		3	4		2280.3808	-2	4						24												
26	2240.6463		4		2281.6195	-11	9						26	2240.6463		6	8								

28	2238.7718	-1	2	2282.8368	8	10	2269.4458	0	3	2308.7177	-8	10	28
30				2284.0276	5	5	2267.7445	0	5	2309.7706	1	6	30
32				2285.1940	11	9	2266.0211	-4	4	2310.8006	3	5	32
34				2286.3375			2264.2755	-12	10	2311.8079	2	4	34
36							2262.5102	-1	4	2312.7909	-20	19	36
38							2260.7214	-8	9	2313.7556	-1	10	38
40							2258.9129	-4	4	2314.6964	2	4	40
42							2257.0796	-16	21	2315.6143	-1	5	42
44							2255.2273	-10	9	2316.5103	1	5	44
46							2253.3542	3	3				46
48							2251.4581	3	6				48
50							2249.5409	6	8				50
52							2247.6018	5	3				52
54							2245.6445	38	29	2319.8725	28	24	54
56							2243.6595	7	5	2320.6522	-14	10	56
58							2241.6549	-5	5				58
60							2239.6331	-25	30				60
62							2237.5842	-2	5				62
64							2235.5171	3	5				64
66							2233.4301	21	21				66
68							2231.3174	-4	3				68
70													70
72							2227.0334	-2	3				72
74							2224.8595	-2	6				74
76							2222.6640	-5	6				76
78							2220.4479	-3	19				78
80							2218.2103	-4	8				80
82							2215.9521	0	27				82
84							2213.6704	-19	21				84
86							2211.3724	9	10				86
88							2209.0497	0	10				88
90							2206.7089	21	20				90
92													92
94							2201.9611	29	28				94
96							2199.5521	-3	12				96
98							2197.1277	20	15				98
100													100
102													102

02211 - 02201 636				02211 - 02201 828					
J	P Obs	O-C Unc	R Obs	O-C Unc	P Obs	O-C Unc	R Obs	O-C Unc	J
2	2257.6851	22	2262.3641	-5			2291.6285	32	2
3	2256.8811	-11	2263.1250	5					3
4	2256.0753	-4	2263.8785	0			2292.9696	3	4
5	2255.2647	13	2264.6266	-1	2286.0335	-4	2293.6348	15	5
6	2254.4440	-13	2265.3690	-3	2285.3106	-1			6
7			2266.1052	-3			2294.9450	1	7
8			2266.8363	1			2295.5931	5	8
9	2252.7913	-3	2267.5626	17	2283.1090	-2	2296.2321	-28	9
10	2251.9560	-1	2268.2810	11	2283.3648	2	2296.8738	20	10
11	2251.1147	-1	2268.9937	8	2281.6149	2			11
12	2250.2675	-1	2269.7001	0					12
13	2249.4146	-1	2270.4027	14	2280.0998	10	2298.7493	-8	13
14	2248.5560	0	2271.0971	2	2279.3318	-11	2299.3666	13	14
15	2247.6910	-5	2271.7869	6	2278.5617	2	2299.9747	-5	15
16	2246.8218	15	2272.4702	1					16
17	2245.9467	15	2273.1476	-1			2301.1789	3	17
18	2245.0632	-1	2273.8199	0	2276.2162	5			18
19	2244.1764	-5	2274.4849	-7			2302.3603	1	19
20	2243.2823	-1	2275.1460	-1	2274.6276	25			20
21	2242.3835	1	2275.8000	1	2273.8214	-1			21
22			2276.4487	0					22
23	2240.5660	-19	2277.7279	1	2272.1990	1	2304.6582	-2	23
24	2239.6536	22	2278.3577	-1	2271.3802	0	2305.2190	-3	24
25			2278.9833	-1	2270.5549	-1	2305.7742	-6	25
26	2237.8018	4	2279.6003	1	2269.7259	1	2306.3247	-2	26
27	2236.8685	5	2280.2153	-10	2268.8894	-4	2306.8675	-20	27
28	2235.9286	2		3	2268.0501	-2	2307.4086	-1	28
29	2234.9828	-8		3	2267.2038	4	2307.9424	1	29
30	2234.0325	0	2281.4228	-5	2266.3535	0	2308.4727	20	30
31	2233.0764	1	2282.0175	3	2265.4958	0	2308.9926	-7	31
32			2282.6081	3	2264.6353	-4	2309.5102	-7	32
33	2231.1463	1	2283.1898	2	2263.7675	5	2310.0226	1	33
34	2230.1691	-30	2283.7690	3	2262.8969	2			34
35	2229.1935	29	2284.3381	3	2262.0170	18	2311.0314	16	35
36	2228.2070	-4	2284.9040	-2	2261.1384	0			36
37	2227.2174	7		22	2260.2470	10	2312.0147	-5	37
38	2226.2207	2	2286.0187	-6	2259.3555	7	2312.5004	0	38
39	2225.2181	-5			2258.4539	4	2312.9773	-14	39
40	2224.2125	20				5	2313.4535	3	40
41	2223.1968	-4	2287.6414	-3	2256.6403	-1	2313.9207	4	41
42	2222.1773	-5	2288.1754	4	2255.7300	-2	2314.3851	10	42
43			2288.6950	-3	2254.8056	-5	2314.8412	13	43
44	2220.1223	-1	2289.2174	-2	2253.8857	-4			44
45	2219.0862	-1	2289.7247	-3	2252.9508	1	2315.7356	-20	45

46	218.0446	3	3	2290.2365	8	33	2252.0196	-15	20	2316.6128	-6	8	46
47	2216.9967	-1	0	2290.7307	-2	3	2251.0746	-3	6	2317.0457	-3	8	47
48	2215.9437	0	2				2250.1349	5	5	2317.4661	-10	10	48
49	2214.8845	-2	3	2291.7105	-23	22	2249.1773	-5	3	2317.8900	-13	11	49
50	2213.8198	-7	5	2292.2010	-1	3	2248.2279	-5	5	2318.2981	-7	7	50
51	2212.7498	-2	1				2247.2589	-8	7	2318.7120	-20	20	51
52	2211.6747	-1	0	2293.1485	4	6	2246.2999	7	10	2319.1108	23	18	52
53	2210.5928	0	9	2293.6049	-2	3	2245.3197	3	8				53
54	2209.5075	9	7	2294.0692	-21	18	2244.3526	14	7				54
55	2208.4137	7	8				2243.3602	-11	10	2319.9017	55	17	55
56	2207.3170	11	10	2294.9712	6	5	2242.3821	-6	10				56
57	2206.2101	-10	7				2241.3931	-2	17	2321.0435	12	8	57
58	2205.1019	-6	3	2295.8478	18	27	2240.3752	-3	19				58
59	2203.9862	-2	6	2296.2639	-1	3	2239.3825	-2	6	2321.7754	-4	4	59
60	2202.8669	-6	3	2296.6978	2	4	2238.3531	-5	8	2322.1261	-7	11	60
61	2201.7388	0	7	2297.1017	-6	7	2237.3508	-6	6	2322.4898	24	29	61
62	2200.6112	14	3	2297.5254	1	3	2236.3087	-2	15	2322.8279	18	23	62
63	2199.4689	-4	3	2297.9166	-1	2	2235.2994	-2	6	2323.1791	22	25	63
64	2198.3305	6	4	2298.3292	2	3	2234.2430	-14	23	2323.5040	7	17	64
65							2233.2271	0	19	2323.8445	0	15	65
66	2196.0262	-15	15	2299.1096	7	6	2232.1340	-1	4	2324.1575	-8	17	66
67	2194.8641	-9	3	2299.4732	-2	4	2229.0521	-10	15	2324.4894	-6	11	67
68	2193.7033	-1	3	2299.8646	-1	3	2228.0184	-22	27	2324.7912	0	11	68
69	2192.5265	-2	4	2300.2154			2226.9257	-6	18				69
70	2191.3583	13	4							2325.7149	-2	4	70
71	2190.1684	-7	4	2300.9339	2	4							71
72	2188.9878	-7	11				2224.7798	9	7				72
73	2187.7878	-1	3	2301.6279	1	3	2223.7335	12	20				73
74	2186.5979	-1	3	2301.9876	-14	42	2222.6116	8	7				74
75	2185.3839	-1	16	2302.2974	-4	42							75
76	2184.1839	-17	16	2302.6508	17	14	2220.4238	18	33				76
77	2182.9587	-1	3	2302.9440	-3	3	2219.3622	-2	6				77
78				2303.2829	-24	13	2218.2116	-10	21				78
79	2180.5120	5	3				2217.1473	4	5				79
80	2179.2949	-2	15				2215.9855	29	29				80
81	2178.0421	-1	3				2214.9110	-2	11				81
82	2176.8177	6	3										82
83	2175.5511	2	3				2212.6559	6	9				83
84	2173.0375	-1	3	2305.0501	0	4	2211.4611	1	5				84
85	2171.7955	-7	4	2305.2834	-25	18	2210.3776	-16	29				85
86				2305.5916	12	12	2209.1694	0	5				86
87							2208.0828	-1	14				87
88	2169.2540	7	14	2306.1062	-5	4							88
89	2167.9444	-9	6	2306.3127	7	4							89
90	2166.6878	-10	5				2204.5244	-5	8				90
91	2165.3641	-23	20	2306.7898	10	8	2203.4329	28	21				91
92	2164.1023	-6	9										92
93	2162.7647	-10	2	2307.2412	-2	3	2201.0751	14	13				93
94	2161.4938	-19	22	2307.5116	-1	4	2199.7978	-8	15				94
95	2160.1438	6	6										95

96	2158.8670	-1	4			2197.4023	-25	26	96
97	2157.4978	-13	10						97
98	2156.2173	1	3	0	4				98
99	2154.8337	5	8	4	7				99
100	2153.5456	-6	7	13	10				100
101	2152.1478	20	23	-14	7				101
102	2150.8546	5	6			2192.5543	-21	16	102
103	2149.4375	6	20						103
104	2148.1406	-4	11						104
105				6	12				105
106	2145.4082	12	9						106

00011 - 00001 628										00011 - 00001 638									
J	P	Obs	O-C	Unc	R	Obs	O-C	Unc	J	P	Obs	O-C	Unc	R	Obs	O-C	Unc	J	
0	2330.6339	-2	3		2333.5680	0	4		0	2265.2334	-22	22		2266.7032	5	11	0		
1	2329.8865	3	7		2334.2863	-7	17		1	2264.4944	8	7		2267.4285	6	4	1		
2	2329.8865	-2	3		2334.9997	-4	16		2	2263.7465	4	5					2		
3	2328.1323	-2	3		2335.7095	20	45		3	2262.9907	-24	24					3		
4	2328.3731	1	5		2336.4088	-8	12		4	2262.2349	5	5					4		
5	2327.6080	3	9		2337.1040	-8	12		5	2261.4677	-25	20					5		
6					2337.7954	7	12		6	2260.7004	0	3					6		
7					2338.4794	6	14		7	2260.9699	15	12					7		
8	2326.0592	-5	12						8	2271.6615	0	3					8		
9	2325.2762	-9	13		2339.8314	19	29		9	2272.3484	15	12					9		
10	2324.4891	-4	13		2340.4960	-2	8		10	2273.0280	0	4					10		
11	2323.6939	-7	13		2341.1564	-6	10		11	2273.7031	-3	5					11		
12	2322.8949	3	11		2341.8126	-7	13		12	2274.3718	0	4					12		
13	2322.0881	-9	14		2342.4603	-8	24		13	2275.0356	-1	3					13		
14	2321.2774	-1	6		2343.1041	-3	6		14	2275.6935	-2	4					14		
15	2320.4601	-2	4						15	2276.3450	11	16					15		
16	2319.6381	-7	16						16	2276.9926	-6	5					16		
17	2318.8078	-9	10		2344.3713	-22	37		17	2277.6341	3	4					17		
18	2317.9742	0	6		2345.0001	9	37		18	2278.2700	-1	3					18		
19	2317.1321	-19	25		2345.6193	1	4		19	2278.8995	-2	3					19		
20	2316.2880	-1	5						20	2279.5241	-3	4					20		
21	2315.4364	0	6		2346.8405	-9	13		21	2280.1410	-2	3					21		
22	2314.5788	-2	10		2347.4444	6	10		22	2280.7551	-3	7					22		
23	2313.8471	-4	10		2348.0403	0	4		23	2281.3622	-10	12					23		
24	2312.8471	0	7		2348.6308	-2	5		24	2281.9640	-9	12					24		
25	2311.9724	-1	4		2349.2159	2	7		25	2282.5598	-16	12					25		
26	2311.0940	18	44		2349.7951	5	10		26	2283.1509	-2	6					26		
27	2310.2059	-2	7		2350.3681	4	10		27	2283.7356	-1	4					27		

28	2309.3145	1	7	2350.9349	0	18	2243.2558	6	6	2284.8885	7	7	28
29	2308.4176	6	14	2351.4963	1	7	2242.3643	5	5	2286.0186	10	9	29
30	2307.5136	-2	28	2352.0517	-7	14	2240.5653	8	9	2287.1242	-6	20	30
31	2306.6051	-11	14	2353.1452	1	25	2239.6595	-2	4	2288.2093	0	3	31
32	2305.6892	-6	17	2354.2131	-13	2	2237.8242	-1	12	2289.7935	6	3	32
33	2304.7695	6	17	2355.2608	3	4	2235.9688	0	3	2290.8214	0	9	33
34	2303.8447	2	9	2356.7853	2	1	2234.0942	0	3	2291.8267	2	3	34
35	2302.9126	5	12	2357.7726	-1	12	2233.1480	0	3	2292.3202	0	3	35
36	2301.9756	3	8	2358.2569	7	9	2232.1963	-3	3	2293.7677	1	4	36
37	2300.0825	-8	9	2359.7365	-3	4	2231.2388	-1	3	2294.7041	1	3	37
38	2298.1689	1	7	2360.1351	-5	4	2230.2766	-8	5	2295.1644	2	6	38
39	2297.2025	-5	11	2361.0412	-2	2	2229.3077	-4	3	2296.0642	0	4	39
40	2296.2316	0	6	2362.3523	-17	28	2228.3354	-1	3	2297.3775	2	3	40
41	2295.2544	13	26	2363.1983	-2	1	2227.3716	0	3	2298.8032	-2	7	41
42	2294.2730	-4	10	2364.0194	1	4	2226.3868	3	12	2299.8473	-4	6	42
43	2293.2828	-6	10	2365.2066	0	5	2225.3876	19	12	2300.2342	8	3	43
44	2292.2897	-2	3	2366.3407	2	3	2221.3689	9	6	2301.3737	1	2	44
45	2291.2891	-3	1	2367.0666	1	7	2220.3502	-8	5	2302.1042	-2	3	45
46	2290.2840	-27	38	2368.4468	0	2	2219.3286	0	3	2303.4985	8	4	46
47	2289.2702	-2	4	2369.4195	0	3	2218.3007	-1	3	2304.8105	1	2	47
48	2288.2560	-2	4	2370.0380	-1	2	2217.2678	3	5	2305.1064	1	3	48
49	2287.2342	-3	1	2371.4790	-7	7	2216.2289	-1	3	2306.0034	-2	4	49
50	2286.2055	0	2	2372.7687	23	35	2215.1849	-13	14	2307.7974	1	2	50
51	2285.1723	-1	8	2373.4175	0	3	2214.1340	-1	3	2308.8105	1	3	51
52	2284.1329	-21	21	2374.7687	0	3	2213.0805	-1	3	2309.8473	1	3	52
53	2283.0882	-13	11	2375.5905	2	4	2212.0200	-1	3	2310.9984	-9	6	53
54	2282.0377	-1	3	2376.7068	5	5	2210.9545	7	1	2312.1042	0	3	54
55	2280.9814	8	3	2377.7687	-29	45	2209.8840	-13	14	2313.4985	-16	1	55
56	2278.8520	-21	21	2378.7793	2	3	2208.8055	-10	11	2314.8105	17	21	56
57	2277.7770	-3	1	2379.4195	0	3	2207.7259	-5	0	2316.1545	-1	3	57
58	2276.7002	-13	11	2380.0380	0	3	2206.6367	-10	11	2317.4608	-1	3	58
59	2275.6149	-1	0	2381.4790	23	35	2205.5446	-5	0	2318.7974	-12	3	59
60	2274.5265	0	2	2382.7687	0	3	2204.4471	8	7	2319.8105	-23	4	60
61	2273.4309	-2	4	2383.7793	0	3	2203.3446	7	1	2320.8300	3	3	61
62	2272.3297	1	1	2384.7793	0	3	2202.2357	2	3	2321.8473	19	12	62
63	2271.2235	9	15	2385.4195	-1	2	2201.1211	-24	5	2322.8105	19	12	63
64	2270.1114	-3	1	2386.0380	-2	1	2199.9991	5	6	2323.4985	16	1	64
65	2269.9933	-1	0	2387.4790	-1	0	2198.8771	2	3	2324.8105	1	3	65
66	2268.8693	0	2	2388.7687	-7	7	2195.4702	13	10	2325.1064	-1	3	66
67	2267.7417	-3	1	2389.7793	0	3	2193.1735	13	10	2326.0034	-2	4	67
68	2266.6059	-1	0	2390.0380	-1	0				2327.7974	1	3	68
69	2265.4664	0	3	2391.4790	-1	0				2328.8105	1	3	69
70	2264.3203	0	3	2392.7687	-1	0				2329.8473	1	3	70
71	2263.1691	0	3	2393.7793	-1	0				2330.9984	1	3	71
72	2262.0125	0	3	2394.7687	-1	0				2332.1042	1	3	72
73	2260.8499	0	3	2395.4195	-1	0				2333.4985	1	3	73
74	2259.6823	0	3	2396.0380	-1	0				2334.8105	1	3	74
75		0	3	2397.4790	-1	0				2335.1064	1	3	75
76		0	3	2398.7687	-1	0				2336.0034	1	3	76
77		0	3	2399.7793	-1	0				2337.7974	1	3	77

78	2257.5099	16	15	2371.7499	-2	3	2192.0143	-10	8	2306.2907	1	3	78
79	2256.3284	-9	9	2372.0143	-1	3	2190.8527	-4	3	2306.5722	0	3	79
80				2372.2728	0	4	2189.6851	-4	6	2306.8482	1	3	80
81	2253.9548	3	4	2372.5266	15	24				2307.1166	-15	13	81
82	2252.7583	-4	4	2372.7712	-3	3	2187.3344	0	3				82
83	2251.5548	-27	28	2373.0116	-2	3	2186.1506	-2	3				83
84	2250.3500	-7	11	2373.2461	0	3	2184.9612	-7	7	2307.8938	2	3	84
85	2249.1380	-4	6	2373.4745	0	6							85
86	2247.9228	23	42				2182.5681	-2	3	2308.3810	-6	4	86
87	2246.6972	0	3	2373.9129	-2	3	2181.3633	-2	3				87
88	2245.4679	-4	10	2374.1233	0	3	2180.1532	-1	5	2308.8464	0	4	88
89	2244.2337	-1	3	2374.3275	-1	3	2178.9379	0	3	2309.0701	0	2	89
90	2242.9941	2	3	2374.5258	0	3	2177.7192	20	18				90
91	2241.7503	18	16				2176.4915	3	3	2309.4997	-3	4	91
92				2374.9041	-1	2	2175.2601	2	3	2309.7048	-15	9	92
93	2239.2412	1	10	2375.0842	-2	3	2174.0232	-1	3	2309.9068	0	2	93
94	2237.9798	7	8	2375.2583	-2	4	2172.7827	12	8				94
95	2236.7115	-2	6	2375.4264	-2	3	2171.5341	-2	27	2310.2901	-2	14	95
96	2235.4390	3	6	2375.5886	0	3	2170.2826	7	5	2310.4744	11	7	96
97	2234.1617	14	14	2375.7457	10	13	2169.0247	5	7	2310.6504	-1	6	97
98				2375.8945	-1	3	2167.7594	-18	14	2310.8224	6	7	98
99	2231.5853	-17	22	2376.0385	-1	4				2311.1476	5	12	99
100	2230.2925	-4	25	2376.1764	-1	4	2163.9395	-13	8				100
101	2228.9914	-4	26	2376.3074	-9	9	2162.6580	12	14				101
102	2227.6832	-27	37	2376.4337	-4	4							102
103	2226.3730	-16	16	2376.5539	0	4							103
104	2225.0573	-6	7										104
105	2223.7346	-11	11	2376.7757	5	10							105
106	2222.4079	-1	17				2157.4674	-9	10				106
107	2221.0747	-2	8	2376.9728	5	6							107
108	2219.7362	-1	10	2377.0619	1	4							108
109				2377.1458	6	8							109
110				2377.2230	5	4							110
111				2377.2942	4	4							111
112	2214.3266	-9	26										112
113				2377.4181	0	13							113
114				2377.4721	9	11							114
115	2210.2144	5	17	2377.5184	2	10							115
116	2208.8312	-6	27	2377.5601	10	12							116
117	2207.4476	33	42	2377.5947	8	14							117
118	2206.0544	30	28										118
119	2204.6533	2	26										119

01111e - 01101e 628					01111f - 01101f 628				
J	P Obs	O-C Unc	R Obs	O-C Unc	P Obs	O-C Unc	R Obs	O-C Unc	J
1			2321.1969	17 8			2321.1969	-3 8	1
2	2318.2574	-4 14	2321.9179	27 15			2321.9179	-3 15	2
3	2317.5078	-13 19	2322.6319	24 18			2322.6319	-14 18	3
4	2316.7525	-21 36	2323.3413	33 22			2323.3413	-14 22	4
5	2315.9928	-17 16	2324.0448	41 39			2324.0448	-15 39	5
6	2315.2258	-28 36					2324.7418	-23 27	6
7							2325.4336	-26 36	7
8							2326.1208	-16 31	8
9							2326.8025	-3 29	9
10									10
11							2328.1455	-8 17	11
12							2328.8076	-17 45	12
13	2309.7077	4 15	2329.4575	23 49					13
14			2330.1091	30 46					14
15	2308.0785	1 9							15
16	2307.2554	0 9							16
17	2306.4260	-7 11	2332.0246	8 16					17
18	2305.5927	3 5							18
19			2333.2747	13 17			2332.0363	-9 25	19
20	2303.9068	2 6	2333.8895	0 21			2332.6632	-21 35	20
21	2303.0555	3 3	2334.5016	18 17			2333.2876	0 16	21
22	2302.1980	-1 3	2335.1048	5 14			2333.9050	9 15	22
23	2301.3353	0 4							23
24			2336.2963	5 11			2335.1189	-7 11	24
25	2299.5930	2 6	2336.8830	1 9					25
26	2298.7133	3 6	2337.4639	-2 4			2336.8993	3 9	26
27	2297.8274	-2 5	2338.0389	-6 7			2337.4807	3 10	27
28	2296.9379	14 14	2338.6077	-15 18			2338.0565	11 16	28
29							2339.1877	-20 32	29
30			2339.7305	-4 5			2339.7490	12 18	30
31	2294.2287	-6 10	2340.2825	-5 7			2340.3003	3 9	31
32	2293.3157	-1 4	2340.8295	-2 5			2340.8462	-1 3	32
33	2292.3961	-1 4	2341.3696	-2 5					33
34	2291.4711	-2 4	2341.9041	-4 8			2341.3870	-2 3	34
35	2290.5404	-2 4	2342.4332	-1 4					35
36	2289.6044	0 3							36
37	2288.6628	3 10	2343.4728	-5 7			2343.4902	2 7	37
38	2287.7144	-3 9	2343.9846	0 4			2344.0013	-2 4	38
39	2286.7613	-6 7	2344.4914	14 24			2344.5061	-2 25	39
40	2285.8020	-11 14							40
41	2284.8394	7 16	2345.4833	0 3			2345.5006	14 18	41
42	2283.8703	16 32					2345.9859	-9 35	42
43	2282.8930	-1 3	2346.4529	-2 3			2346.4691	-6 9	43
44	2281.9117	-2 7	2346.9300	7 10					44

45	2279.9309	-18	31	2347.3983	-12	14	2280.8473	9	14	2347.4155	13	18	45
46	2278.9345	-2	3	2347.8636	-4	7	2278.8524	14	21	2347.8784	2	15	46
47	2277.9315	5	9	2348.7754	2	7	2277.8451	3	4	2348.3362	-2	7	47
48	2276.9227	9	4				2276.8327	-3	8	2348.7888	-2	8	48
49	2275.9074	4	6				2275.8160	11	13	2349.2339	-10	13	49
50	2274.8865	-2	3	2350.0977	-2	4	2274.7937	4	3	2349.6738	-15	18	50
51	2273.8604	-3	4	2350.5292	21	16	2273.7637	-2	3	2350.1087	-2	14	51
52	2272.8296	-1	5	2350.9523	20	46				2350.5384	0	8	52
53	2271.7901	-19	29				2271.6896	-2	3	2351.3768	-11	20	53
54	2270.7476	-18	34	2351.7833	41	31	2270.6441	-2	3	2351.7833	-54	31	54
55	2269.7017	-6	7				2269.5927	-6	3	2352.1906	-31	42	55
56	2268.6471	-2	4	2352.5853	8	28	2268.5359	-7	0				56
57	2267.5886	-7	9				2267.4743	0	4				57
58	2266.5226	-4	4	2353.3694	31	32	2266.4064	-1	4	2353.3694	-35	32	58
59	2265.4524	-1	5	2353.7513	30	26	2265.3337	7	6	2353.7513	-28	26	59
60	2264.3761	-3	4	2354.1279	35	16	2264.2542	2	12	2354.1279	-15	16	60
61	2263.2949	-1	4	2354.4970	23	12	2263.1695	1	4	2354.4970	-18	12	61
62	2262.2076	-1	7	2354.8604	14	11	2262.0796	4	4	2354.8604	-18	11	62
63	2261.1156	16	17				2260.9827	-7	1				63
64	2260.0184	16	17	2355.5709	10	6	2259.8833	12	4	2355.5709	-3	6	64
65	2258.9130	0	3				2258.7756	12	4				65
66	2257.8037	0	5	2356.2581	10	21	2257.6631	3	7	2356.2581	17	21	66
67				2356.5911	-8	14	2256.5438	-3	6	2356.5911	10	14	67
68				2356.9170	-37	38	2255.4213	1	5	2356.9170	-8	38	68
69	2255.5694	8	9	2357.5580	-27	32	2254.2921	-1	3				69
70	2254.4429	-1	16				2253.1550	-23	39				70
71	2253.3103	-11	16				2252.0179	-8	7				71
72	2252.1740	-5	16				2250.8733	20	15				72
73	2251.0311	-10	18				2249.7191	-9	18				73
74	2249.8835	-8	16				2248.5618	-14	15				74
75	2248.7310	1	1				2247.4010	-2	4				75
76	2247.5721	1	1										76
77	2246.4087	11	10										77
78	2245.2381	3	7	2359.8827	-6	21	2245.0608	13	16	2359.8689	17	26	78
79	2244.0623	-1	6				2243.8797	-2	13				79
80	2242.8824	15	15	2360.4036	-10	12	2242.6962	-9	14	2360.3862	8	11	80
81	2241.6968	-24	29				2241.5051	-15	19	2360.6361	6	8	81
82	2240.5011	-9	6	2360.9017	-4	5	2240.3090	-8	8	2360.8804	8	8	82
83	2239.3054	7	9				2239.1087	25	36				83
84	2238.1043	24	29	2361.3760	1	5	2237.9055	13	19	2361.3499	0	6	84
85	2236.8978	4	12	2361.6038	-1	4	2236.6923	-11	16	2361.5764	3	7	85
86	2235.6822	7	25	2361.8262	-2	4	2234.2494	-4	8	2362.0106	2	5	86
87	2234.4635	23	26	2362.0418	-2	4	2233.0216	-7	10	2362.2188	2	6	87
88	2233.2405	-16	19	2362.2515	-7	21	2231.7887	-15	17	2362.4206	-2	3	88
89	2232.0067	-9	9	2362.4563	-1	3	2230.5470	-25	35	2362.6168	-1	4	89
90	2230.7738	-8	27	2362.6558	12	13		-21	23	2362.9914	2	4	90
91	2229.5313	-8	27				2228.0506	10	13	2363.1709	15	25	91
92	2227.0334	-8	5				2226.7951	-21	23				92
93	2225.7764	-7	6				2225.5369	10	13				93



20	2295.9253	0	10	2325.8695	-15	10	2293.4362	-1	6	2323.4039	-19	24	20
21				2326.4829	3	4	2291.7223	-2	3	2324.6142	-1	5	21
22	2293.3643	0	5	2327.0889	4	4	2290.8572	4	13	2325.2098	4	6	22
23	2292.4989	-5	6				2289.9854	1	3	2325.7994	4	7	23
24	2291.6286	-5	4	2328.2844	11	13				2326.3821	-4	3	24
25	2290.7536	-4	5	2328.8720	-1	3	2288.2233	-16	16				25
26	2289.8717	0	4				2287.3360	0	5	2327.5316	0	4	26
27	2288.9851	0	4	2330.0332	7	8	2286.4410	-3	3	2328.0990	17	26	27
28	2288.0921	0	5	2331.1704	-4	7	2285.5401	-7	5	2328.6569	-1	5	28
29				2331.7291	-10	14	2284.6346	1	4	2329.2103	-5	3	29
30				2332.2842	-3	4	2283.7219	-5	18	2329.7580	-7	6	30
31	2286.2905	2	3							2330.3012			31
32	2285.3808	-3	3	2333.3764	3	5	2281.8809	1	18				32
33	2284.4641	-23	17				2280.9512	-1	4	2331.8880	-26	23	33
34	2283.5459	-3	3	2334.4436	-11	10							34
35	2282.6204	0	3	2334.9722	19	18				2332.9206	-3	5	35
36	2281.6891	0	3	2335.4911	9	10	2277.1750	-6	4	2333.4274	3	8	36
37	2280.7524	2	8	2336.0037	-6	4	2276.2167	-5	3				37
38	2279.8107	8	7				2275.2529	-2	5	2334.4230	14	13	38
39							2273.3072	-3	4	2335.3894	-29	37	39
40	2277.9088	2	4	2337.0149	-3	15				2336.3390	-2	4	40
41	2276.9491	-6	4	2338.9680	4	3	2271.3388	-2	5				41
42	2275.9855	-3	4	2339.4396	-16	16	2270.3461	1	7				42
43	2275.0143	-10	11	2339.9087	-3	5	2269.3477	3	5	2337.2618	-4	5	43
44	2274.0402	4	4	2340.3717	7	8	2268.3425	-5	7	2337.7142	-5	11	44
45	2273.0593	4	5	2340.8286	14	13	2267.3327	-1	3				45
46	2272.0730	2	4	2341.2786	10	10	2266.3168	-1	6				46
47	2271.0806	3	6	2341.7243	21	21	2265.2954	1	9	2339.0363	-2	4	47
48				2342.1619	10	15				2339.4646	-6	6	48
49	2269.0803	2	5	2342.5940	1	7	2263.2353	5	5	2339.8859	-20	16	49
50	2268.0717	9	11	2343.0208	-1	5				2340.7190	37	13	50
51	2267.0585	-18	23	2343.4418	-4	10	2260.1004	-9	12				51
52	2266.0363	-3	9	2343.8581	5	8	2259.0454	1	5				52
53	2265.0135	-2	5	2344.2667	-5	10	2257.9854	18	10				53
54	2263.9825	-2	5	2344.6708	-1	4	2256.9170	7	7	2342.2996	11	15	54
55				2345.0685	-3	4	2255.8447	15	23				55
56	2261.9049	-5	14	2345.4615	7	20	2254.7651	7	10	2343.0555	14	41	56
57	2260.8571	-14	11	2345.8469	0	20							57
58	2259.8064	-1	6	2346.6017	1	7				2343.7850	-9	17	58
59	2258.7477	3	6	2346.9715	13	26	2251.4957	18	21				59
60	2257.6848	-6	4				2250.3933	9	10	2344.4934	-2	23	60
61	2256.6160	-2	5				2249.2847	-5	11	2344.8367	-19	28	61
62	2255.5413	-6	7	2348.0403	-2	6	2248.1714	-9	18	2345.1774	-1	5	62
63	2254.4620	-1	4	2348.3852	-3	4							63
64	2253.3765	-4	3	2348.7229	-18	18	2245.9286	-9	11	2346.1577	-5	18	64
65	2252.2862	-3	7	2349.0577	-2	12	2244.7999	3	6				65
66	2251.1897	-6	7										66
67	2250.0878	-3	6										67
68	2248.9808	-5	6										68
69	2247.8672	-16	22										69

70	2244.4986	3	7	2349.3875	23 26	2242.5237	9 13	2346.7827	6 6	70
71				2349.7039	-27 27	2241.3764	5 7	2347.0857	7 10	71
72				2350.0215	-6 4	2240.2240	5 12			72
73				2350.3329	13 16	2239.0655	3 4			73
74				2350.6363	10 6					74
75				2350.9335	5 33					75
76				2351.2277	29 35					76
77										77
78										78
79										79
80										80
81										81
82										82
83										83
84										84
85										85
86										86
87										87
88										88
89										89
90										90
91										91
92										92
93										93
94										94
95										95
96										96
97										97
98										98
99										99
100										100
101										101
102										102
103										103

02211e - 02201e 628										02211f - 02201f 628									
J	P	Obs	O-C	Unc	R	Obs	O-C	Unc	J	P	Obs	O-C	Unc	R	Obs	O-C	Unc	J	
2	2305.1488	3	7	2309.5666	5	8	2305.1488	3	7	2309.5666	5	8	2309.5666	5	8	2309.5666	5	8	
3	2304.3923	1	6	2310.9930	1	7	2304.3923	1	6	2310.9930	1	7	2310.9930	1	7	2310.9930	1	7	
4	2303.6305	2	4	2311.6983	2	9	2303.6305	2	4	2311.6983	2	9	2311.6983	2	9	2311.6983	2	9	
5	2302.8628	2	7	2312.3993	6	14	2302.8628	2	7	2312.3993	6	14	2312.3993	6	14	2312.3993	6	14	
6					26	43					26	43			26	43			

7	2302.0896	2313.0901	0	6	2302.0896	2313.0901	0	6	7
8	2300.5255	2313.7776	-1	6	2300.5255	2313.7776	-1	6	8
9	2299.7353				2299.7353				9
10	2298.1356	2315.8056	-4	9	2298.1356	2315.8056	-4	9	10
11	2297.3298	2316.4706	-1	5	2297.3298	2316.4706	-1	5	11
12	2296.5166	2317.7829	2	6	2296.5166	2317.7829	2	6	12
13	2295.6975	2318.4318	17	16	2295.6975	2318.4318	17	16	13
14	2294.8736	2319.0715	-2	26	2294.8736	2319.0715	-2	26	14
15	2294.0432	2319.7087	12	4	2294.0432	2319.7087	12	4	15
16	2293.2073	2320.3376	0	5	2293.2073	2320.3376	0	5	16
17	2291.5197	2321.5807	20	29	2291.5197	2321.5807	20	29	17
18	2289.8072	2322.1923	-2	38	2289.8072	2322.1923	-2	38	18
19	2288.9439	2323.4019	4	17	2288.9439	2323.4019	4	17	19
20	2288.0747	2324.5863	-3	4	2288.0747	2324.5863	-3	4	20
21	2287.1974	2325.1702	-3	6	2287.1974	2325.1702	-3	6	21
22	2286.3181	2325.7492	6	4	2286.3181	2325.7492	6	4	22
23	2285.4314	2326.3209	0	18	2285.4314	2326.3209	0	18	23
24	2284.5391				2284.5391				24
25	2283.6412				2283.6412				25
26	2282.7382				2282.7382				26
27	2279.9948	2327.4457	-25	32	2279.9948	2327.4457	-25	32	27
28	2278.1337	2328.0027	-5	6	2278.1337	2328.0027	-5	6	28
29	2277.1999	2328.5493	-30	34	2277.1999	2328.5493	-30	34	29
30	2276.2569	2329.0952	-5	9	2276.2569	2329.0952	-5	9	30
31	2275.3091	2330.1643	-7	6	2275.3091	2330.1643	-7	6	31
32	2274.3531	2331.2086	-24	37	2274.3531	2331.2086	-24	37	32
33	2273.3952	2331.7273	19	32	2273.3952	2331.7273	19	32	33
34	2272.4301	2332.2334	-5	8	2272.4301	2332.2334	-5	8	34
35	2271.4601	2332.7353	-13	11	2271.4601	2332.7353	-13	11	35
36	2270.4853	2333.2329	-6	16	2270.4853	2333.2329	-6	16	36
37	2269.5022	2333.7236	-10	12	2269.5022	2333.7236	-10	12	37
38	2268.5154	2334.6904	11	21	2268.5154	2334.6904	11	21	38
39	2267.5238	2335.1617	-12	7	2267.5238	2335.1617	-12	7	39
40	2266.5224	2335.6300	-8	9	2266.5224	2335.6300	-8	9	40
41	2265.5182	2336.0919	-8	8	2265.5182	2336.0919	-8	8	41
42	2264.5110	2336.5486	-3	36	2264.5110	2336.5486	-3	36	42
43	2263.4948	2336.9989	-3	14	2263.4948	2336.9989	-3	14	43
44	2262.4735	2337.4436	-1	26	2262.4735	2337.4436	-1	26	44
45	2260.4215	2338.3134	-18	15	2260.4215	2338.3134	-18	15	45
46		2338.7397	-26	9		2338.7397	-26	9	46
47		2339.5790	2	20		2339.5790	2	20	47
48		2339.9872	-11	17		2339.9872	-11	17	48
49									49
50									50
51									51
52									52
53									53
54									54
55									55
56									56



00021 - 00011 636					
J	P Obs	O-C Unc	R Obs	O-C Unc	
1	2259.2886	15 12	2261.5929	-1 6	
3					
5	2256.1297	-1 9			
7			2266.0456	11 9	
9	2252.8782	3 3	2267.4808	0 4	
11	2251.2161	-5 7	2268.8949	16 19	
13					
15	2247.8247	13 10			
17	2246.0915	0 8	2272.9875	0 5	
19					
21	2242.5565	-8 7			
23	2240.7543	-8 6	2276.8661	-3 4	
25	2238.9292	-2 5	2278.1113	-2 3	
27	2237.0811	6 9			
29	2235.2083	2 3	2280.5301	6 5	
31	2233.3126	1 3	2281.7022	-2 3	
33	2231.3949	13 11			
35	2229.4511	-3 3	2283.9764	4 7	
37	2227.4870	10 11	2285.0763	-3 3	
39	2225.4952	-22 24			
41	2223.4854	-2 4			
43	2221.4504	-2 4	2288.2320	-14 14	
45	2219.3929	3 4	2289.2380	8 15	
47	2217.3136	21 12			
49	2215.2069	-4 5	2291.1718	-4 4	
51	2213.0805	5 4			
53	2210.9280	-18 15			
55					
57	2206.5600	-5 4	2293.0104	4 4	
59	2204.3428	14 13	2293.8926	2 3	
61	2202.0975	-19 20	2294.7505	1 3	
63	2199.8347	1 3	2295.5850	9 8	
65	2197.5472	2 4	2296.3946	12 9	
67	2195.2361	-5 4	2297.9383	-3 5	
69	2192.9014	-20 12	2298.6744	-2 3	
71	2190.5494	20 12	2299.3850	-11 10	
73	2188.1688	0 3	2300.0747	17 18	
75	2185.7677	2 3	2300.7356	1 4	
77	2183.3443	8 7	2301.3734	0 7	
79	2180.8971	2 4	2301.9875	8 7	
81			2302.5752	-3 3	
83	2175.9357	-3 6	2303.6780	-11 9	
85	2173.4209	-9 6	2304.1948	8 7	
87			2304.6816	-26 21	
89	2168.3255	-3 5			

91	2165.7441	-1	4	2305.5920	15	9
93	2163.1427	25	21	2306.0037	-29	19
95	2160.5145	7	9	2306.3977	-3	5
97				2306.7649	3	8
99	2155.1941	1	7			
101	2152.5027	21	19	2307.4249	15	28
103				2307.7149	-6	18
105	2147.0462	-11	18			

20013 - 20003					20012 - 20002					636				
J	P Obs	O-C Unc	R Obs	O-C Unc	P Obs	O-C Unc	R Obs	O-C Unc	J					
0			2242.8513	-9	12		2240.7572	-21	22	2244.6258	-19	11	0	
2			2244.3693	14	8								2	
4			2245.8617	8	5		2237.5615	-5	4				4	
6	2235.7532	13	8	2247.3328	15	8	2235.9289	-3	5				6	
8			2248.7791	2	4								8	
10													10	
12			2251.6082	24	19		2230.8946	0	3	2251.9363	7	13	12	
14							2229.1730	18	19	2253.3295	12	12	14	
16	2227.3295	4	4	2254.3416	2	4	2227.4249	-2	7	2254.6994	14	8	16	
18	2225.5766	-9	5	2255.6757	8	5	2225.6572	-8	6	2256.0449	1	4	18	
20	2223.8028	-9	5	2256.9850	-5	5	2223.8649	-3	3				20	
22	2222.0073	-3	3				2222.0530	14	11	2258.6692	1	5	22	
24							2220.2156	2	3				24	
26	2218.3477	-13	24	2259.5373	-4	8				2261.1991	-20	18	26	
28													28	
30	2214.6023	4	8				2214.5713	-10	8				30	
32				23	24		2212.6470	4	4				32	
34	2210.7672	4	8	2263.1957	1	3	2210.7000	15	11				34	
36				2264.3659	6	5				2267.1282	18	14	36	
38	2206.8427	-11	4	2265.5157	-23	15				2268.2425	6	9	38	
40	2204.8480	-15	6	2266.6390	6	6							40	
42	2202.8345	11	12	2267.7448	6	6							42	
44							2204.7201	-7	5	2270.4027	-5	7	44	
46				2269.8799	-6	4	2202.6838	-1	5				46	
48	2196.6536	-9	8	2270.9130	-7	4	2198.5440	4	4	2272.4702	-14	11	48	
50				2271.9235	-1	4	2196.4417	13	11	2273.4721	12	11	50	
52	2192.4254	-15	15										52	
54	2190.2831	24	17				2192.1679	0	4				54	
56	2188.1111	-19	12	2275.7277	-23	13	2189.9987	0	4	2277.2339	-13	7	56	
58	2185.9261	23	13										58	
60	2183.7136	4	4										60	
62	2181.4819	8	3							2279.8150	15	9	62	

64	2179.2285	7	6	2181.1028	-7	6	64
66	2176.9525	-6	6	2178.8265	13	7	66
68	2174.6574	3	3				68
70	2172.3412	12	3	2281.4894	7	7	70
72	2167.6411	-11	9	2282.9222	0	4	72
74	2162.8602	1	7	2284.2611	0	8	74
76	2160.4369	-7	5				76
78	2157.9937	-4	5				78
80	2155.5310	13	17				80
82	2153.0425	-20	16				82
84	2150.5374	-12	13				84
86							86
88							88
90							90

2287.7121 27 23

11111 - 11101 636										01121 - 01111 636										
J	P Obs	O-C	Unc	R Obs	O-C	Unc	P Obs	O-C	Unc	R Obs	O-C	Unc	J	P Obs	O-C	Unc	R Obs	O-C	Unc	J
1	2249.0357	-1	4	2252.1492	11	9							1							1
2				2252.9156	5	9							2							2
3													3							3
4	2247.4424	-1	4	2254.4237	-15	12							4	2246.0136	-7	12	2252.1495	-12	9	4
5	2246.6485	21	19										5	2245.2249	-2	9	2252.8993	19	18	5
6	2245.8258	4	6										6	2244.4200	2	6	2253.6241	-11	17	6
7	2245.0218	-2	5										7							7
8				2256.6354	-4	4							8							8
9				2257.3731	-5	4							9	2241.9950	1	4	2255.0750	-12	9	9
10	2242.5186	-14	10	2258.0828	-20	11							10	2241.1617	13	8	2255.8019	-10	7	10
11	2241.7022	-12	7	2258.8096	-24	17							11							11
12	2240.8328	10	9	2259.5121	18	18							12	2239.4957	2	3	2257.9058	-16	15	12
13	2240.0079	-14	9	2260.2269	4	7							13	2238.6697	-18	11	2258.6137	1	3	13
14	2239.1196	-4	3	2261.6166	-5	3							14							14
15	2238.2929	-4	3	2262.2896	-12	11							15	2236.0955	1	4	2259.2890	14	12	15
16	2237.3841	-4	10										16							16
17	2236.5531	17	11	2263.6450	-8	10							17							17
18	2235.6251	-3	2	2264.3268	6	5							18	2233.5121	3	4				18
19	2234.7877	-1	4										19							19
20				2265.6444	-4	3							20	2231.7456	1	3	2262.6513	1	4	20
21				2266.2848	-2	3							21	2230.8207	9	11	2263.2861	-3	2	21
22				2266.9399	6	5							22	2229.9560	0	3	2263.9488	-6	7	22
23	2232.0362	-3	3										23	2229.0138	-8	7				23
24	2230.2067	0	3	2268.2108	10	6							24	2228.1433	-1	4				24
25	2229.3588	5	4	2268.8296	-2	6							25	2227.1844	-18	13	2266.4768	26	28	25
26													26				2267.0698	-19	19	26

27	2227.5019	-5	7	2270.0684	17	10	2225.3333	-12	13	2267.7019	12	7	27
28	2226.4770	2	3	2270.6807	21	20	2224.4490	2	4				28
29	2225.6236	1	3	2271.2810	10	10							29
30	2224.5787	21	21	2271.8777	8	5	2222.5659	-11	8				30
31	2223.7203	-14	13	2272.4702	5	5							31
32	2222.6517	-13	9	2273.0511	1	6	2220.6617	-3	3	2270.6432	2	4	32
33	2221.7979	3	6	2273.6353	-13	3	2219.6395	-7	10	2271.2380	14	6	33
34	2220.7063	-6	3	2274.1996	5	9	2218.7360	19	12	2271.7870	12	7	34
35	2219.8488	3	6	2274.7784	-13	3	2217.6959	2	3				35
36	2218.7361	-4	3	2275.3286	19	18	2216.7820	-13	14	2272.9062	15	9	36
37	2217.8798	9	5	2275.8963	-2	4	2215.702	20	12	2273.4721	-16	13	37
38				2276.4297	14	15				2273.9983	-13	8	38
39	2215.8859	2	7	2276.9930	17	12				2274.5556	-6	5	39
40				2277.5054	-3	4							40
41				2278.0620	-4	10							41
42	2211.8314	5	8				2209.6879	7	6	2276.1179	1	3	42
43	2210.6212	0	5							2276.6477	-12	7	43
44	2209.7706	12	4										44
45	2208.5353	9	8										45
46				2280.5930	4	4	2206.6851	0	4	2278.1400	-1	3	46
47	2206.4244	-1	4	2281.1341	8	5	2205.5446	-1	3	2278.6452	2	10	47
48				2281.5733	3	4	2204.5989	19	11	2279.1162	10	6	48
49				2282.1075	-19	19							49
50	2204.2937	24	11				2202.4853	-7	25	2280.0664	0	2	50
51				2283.0615	-2	4							51
52	2202.1350	-1	5	2283.4604	-5	9	2200.3544	21	18	2280.9914	-21	20	52
53	2201.3002	27	26				2199.1591	0	3				53
54	2199.9546	-11	9										54
55	2199.1241	10	5	2284.3679	-5	5	2196.9825	-22	16				55
56				2285.2516	0	3							56
57	2196.9267	3	5				2194.7862	-14	16	2283.2144	29	15	57
58	2195.5288	10	5	2286.1089	-15	18	2193.8140	-10	7	2283.6300	-4	3	58
59	2194.7065	-7	10				2192.5692	16	10				59
60							2191.5922	16	17				60
61	2192.4656	0	4				2190.3244	-4	4				61
62	2191.0071	-7	6	2287.7548	-1	3	2189.3420	-16	10				62
63	2190.2011	-6	4	2288.2753	-5	4	2188.0592	-1	3	2285.6597	-1	5	63
64	2188.7146	12	8				2187.0744	4	4				64
65	2187.9168	12	8	2289.0613	-1	3							65
66	2186.3965	5	5										66
67	2185.6067	-5	6	2289.8232	-1	4	2183.4599	-3	6	2286.4271	0	3	67
68	2184.0558	0	3	2290.5638	25	21	2182.4662	-10	12	2287.5445	13	9	68
69													69
70	2181.6925	-3	3										70
71	2180.9235	-3	3	2291.2761	7	6	2180.1311	10	11	2288.2534	0	4	71
72							2178.7711	8	11	2288.5826	0	4	72
73	2178.5472	-18	10	2291.9670	12	7	2176.3925	11	7	2288.9404	9	9	73
74	2176.8960	-20	19				2175.3867	-20	16				74
75	2176.1517	-4	3	2292.6344	21	11	2173.9903	4	5				75
76	2174.4653	-13	5	2292.7409	-2	5	2172.9858	14	10				76

77	2173.7331	-2	3	2293.3557	2	4	2171.5659	0	17	2290.8517	-11	8	77
78	2172.0123	0	3	2293.8922	-15	6	2170.5594	17	12				78
79	2171.2919	-5	5	2293.9447	-7	8	2169.1185	-8	9	2291.4443	20	16	79
80	2169.5356	2	4	2294.4906	19	22	2168.1083	-5	7				80
81	2168.8302	5	6	2294.5128	21	25	2166.6493	-9	12	2292.0064	-12	10	81
82													82
83	2166.3455	4	6				2164.1606	19	16				83
84	2164.5134	-3	4				2163.1429	-14	11	2292.5491	2	5	84
85	2163.8391	3	13				2161.6457	11	12				85
86	2161.9688	-1	4				2160.6286	-1	6				86
87	2161.3097	-9	10				2159.1072	-9	9				87
88	2159.4016	1	6				2158.0935	25	23				88
89	2158.7635	27	26										89
90	2156.8114	-2	5				2155.5310	-3	7	2294.0279	-1	7	90
91	2156.1914	20	10										91
92							2152.9506	11	13	2294.4743	14	29	92
93	2153.5970	7	12										93
94	2151.5648	4	4				2150.3453	-4	22				94
95	2150.9839	22	13										95
96													96
97	2148.3490	34	19										97
98													98
99	2143.5274	18	14				2142.4033	3	19				99
100													100

11112f - 11102f 636					
J	P	Obs	O-C	Unc	R
2					Obs
4					O-C
6					Unc
8					
10	2244.2599	0	3		2256.0214
12	2242.5948	5	4		2258.9379
14	2240.9062	4	5		2260.3597
16	2239.1943	-2	3		2261.7618
18	2237.4603	-2	3		
20	2235.7042	-2	5		2264.4942
22	2233.9238	-2	3		2265.8246
24					2267.1293
26	2230.2955	-13	14		2268.4124
28	2228.4490	-2	3		2269.6757
30	2226.5787	-3	3		2270.9126
32	2224.6860	-2	3		2272.1249
	2222.7710	1	3		

34	2218.8728	1	2	2274.4845	3	8
36	2216.8902	2	3			
38	2214.8847	-1	4	2276.7456	-18	12
40						
42	2210.8074	0	26			
44	2208.7351	-2	12	2280.9911	2	3
46				2281.9924	-3	4
48	2204.5238	-4	4	2282.9713	4	4
50	2202.3866	12	10	2283.9253	0	3
52	2200.2244	0	3			
54	2198.0416	3	8			
56	2195.8358	-4	4	2286.6454	-13	12
58	2193.6094	3	3	2287.5065	2	5
60	2191.3591	-9	8	2288.3431	8	6
62	2189.0904	13	13	2289.1536	-10	6
64	2186.7964	2	3			
66	2184.4818	2	3	2290.7086	7	11
68	2182.1449	-3	4			
70	2179.7877	6	5	2292.1663	-1	3
72	2177.4074	0	3	2292.8604	3	3
74	2175.0061	0	2			
76				2294.1764	-1	3
78						
80	2167.6717	-19	11			
82	2165.1854	-14	9			
84	2162.6782	-6	5			
86						
88						
90	2157.6009	15	17			
92	2155.0292	9	9			
94						
96	2149.8240	3	6			
98	2147.1902	-2	25			

12211 - 12201 636				02221 - 02211 636			
J	P Obs	O-C Unc	R Obs	O-C Unc	P Obs	O-C Unc	J
2	2236.2077	14 15	2240.8819	-9 7			2
3	2235.4054	-12 24	2241.6419	0 7			3
4	2234.6010	-1 6					4
5	2233.7920	22 12	2243.8841	-2 4	2232.7356	16 12	5
6					2231.9240	-36 8	6
7					2231.1178	25 6	7
8	2232.1482	-17 18			2230.2955	-18 8	8
					2240.4764	-22 3	
					2241.2225	15 7	
					2242.6916	32 7	

9	2231.3198	-16	7	2246.7941	12	21	2229.4771	37	5	9
10	2230.4865	-4	6	2247.5039	-13	23				10
11	2229.6478	9	11	2248.2117	-6	4	2245.5549	21	5	11
12	2228.8011	2	9	2248.9147	19	8				12
13				2249.6078	-6	7	2248.3246	11	5	13
14				2250.2973	3	10	2249.0023	11	8	14
15	2225.3609	13	9	2250.9806	-6	2				15
16	2224.4845	-6	3				2250.3397	3	10	16
17							2251.0001	-1	4	17
18	2222.7176	-10	4							18
19							2221.7979	-10	6	19
20							2220.0277	-23	8	20
21	2220.0277	21	9	2254.9575	-26	19	2219.1398	35	12	21
22	2219.1161	-6	3				2218.2371	-9	4	22
23	2218.2014	-4	8	2256.2403	5	7	2216.4236	6	9	23
24										24
25	2216.3552	0	7	2258.1130	18	4				25
26	2214.4869	10	3	2258.7291	-5	10	2211.7832	-5	6	26
27	2213.5419	-7	3	2259.3309	-7	7				27
28	2212.5947	-8	3	2260.5303	18	5				28
29				2261.1241	-24	27				29
30	2210.6806	14	4	2261.7042	23	5	2207.9699	4	5	30
31	2209.7123	-3	3	2262.2897	-5	10	2207.0032	-1	5	31
32							2206.0281	0	3	32
33	2207.7651	15	17				2205.0495	-11	9	33
34							2204.0645	7	9	34
35	2205.7897	-23	13							35
36	2204.8012	12	3	2265.0794	-20	10				36
37	2203.7974	-3	3	2265.6440	17	4				37
38	2202.7943	-10	13				2263.4958	-14	17	38
39	2201.7807	-2	3				2264.0294	-15	9	39
40	2200.7707	24	9							40
41	2199.7413	-3	3				2199.0562	10	9	41
42										42
43	2197.6775	-23	15							43
44	2195.5957	1	3							44
45							2195.9769	-19	22	45
46							2194.9457	15	17	46
47										47
48							2192.8548	2	5	48
49							2191.7979	-24	11	49
50										50
51	2191.3588	-13	8	2271.2053	-6	4				51
52	2190.3011	4	8				2188.6078	3	3	52
53							2187.5319	1	6	53
54	2188.1433	21	10				2186.4500	0	3	54
55	2187.0368	14	12				2185.3649	9	10	55
56							2184.2707	7	9	56
57	2184.8396	-1	4	2273.9505	-2	9	2183.1731	-8	7	57
58							2182.0652	-24	13	58



12	2238.5631	9	10	2258.0301	3	8	2226.8732	-3	3	2246.3769	0	3	12
13							2226.0196	0	3	2247.0823	-6	5	13
14							2225.1602	1	3	2247.7829	-2	4	14
15													15
16							2223.4226	-15	11	2249.1669	5	6	16
17	2234.2373	0	4	2260.1235	6	4	2222.5471	-5	6	2249.8485	-9	10	17
18	2233.3556	-5	5	2260.8082	-7	6	2221.6653	-2	10	2250.5259	-8	11	18
19	2232.4669	-2	6	2261.4882	-10	13	2220.7778	4	2	2251.1995	12	10	19
20	2231.5736	-2	4	2262.1628	-8	6	2219.8868	23	26	2251.8653	12	14	20
21	2230.6748	2	3	2263.4949	0	5	2218.9856	0	3	2252.5251	10	11	21
22	2229.7689	-8	4	2264.8015	-14	17	2217.1718	8	3				22
23	2228.8592	1	2				2216.2553	1	3	2254.4707	10	10	23
24	2227.9432	4	4				2215.3341	2	3				24
25	2226.0934	2	3	2267.3465	-24	26	2214.4069	-1	3	2255.7376	-4	25	25
26	2225.1600	2	4	2267.9713	6	15	2213.4749	-4	5	2256.3639	4	3	26
27							2212.5363	-1	3	2256.9849	17	11	27
28	2223.2762	0	4	2269.1972	2	5	2211.5944	17	10	2257.5966	-6	9	28
29	2222.3267	9	7	2269.8031	18	13	2210.6437	2	3				29
30	2221.3689	-10	7	2270.4018	21	18	2209.6887	0	4	2258.8087	9	11	30
31	2220.4066	-16	13				2207.7649	25	27	2259.4066	22	22	31
32													32
33	2218.4664	-16	8	2271.5793	2	5				2260.5803	-1	4	33
34	2217.4896	2	4	2272.1591	-9	8	2205.8138	0	4				34
35	2216.5052	0	3	2272.7351	1	3	2204.8320	7	5				35
36	2215.5143	-11	10	2273.3068	26	17	2203.8443	12	7				36
37	2214.5199	0	6	2273.8677	13	8							37
38				2274.4262	3	3							38
39				2274.9767	3	3	2200.8454	-2	3	2263.4201	10	8	39
40	2212.5118	-3	4	2275.5228	7	6	2199.8348	-6	5				40
41	2211.5007	9	6	2276.0618	0	4	2198.8191	-5	5	2265.0525	-4	6	41
42	2210.4814	-5	3	2276.5950	-8	8	2197.7982	-2	4	2265.5853	-6	5	42
43	2209.4583	-1	4				2196.7719	3	3				43
44													44
45	2207.3947	1	4	2278.1621	0	4							45
46	2206.3544	2	3	2278.6733	8	10	2193.6578	-6	5	2267.6597	-3	5	46
47	2205.3081	-3	3	2279.1768	-1	3							47
48	2204.2582	14	9	2279.6754	-2	5							48
49	2203.1998	-1	4	2280.1673	-9	8	2191.5554	-1	4	2268.6641	19	13	49
50	2202.1372	1	11	2280.6536	-15	24	2190.4952	-6	3	2269.1562	16	10	50
51	2201.0692	1	6	2281.1344	-15	8	2189.4310	-3	6				51
52	2199.9974	22	15				2188.3595	-6	4				52
53	2198.9159	-2	3	2282.0803	3	8	2187.2837	-4	4	2270.5963	-7	6	53
54	2197.8298	-13	9				2186.2027	1	3				54
55	2196.7413	4	4	2283.0007	3	4	2185.1172	15	10				55
56	2195.6451	3	3				2184.0224	-9	8				56
57				2283.8970	-3	2	2182.9258	3	7	2272.4367	-22	27	57
58	2193.4366	3	3	2284.3383	12	9	2181.8244	21	12	2272.8852	3	4	58
59	2192.3226	-16	12	2284.7696	-9	12							59
60	2191.2059	1	1										60
61	2190.0829	2	4	2285.6196	-5	4	2179.6007	12	7				61

62	2188.9531	-2	3	2286.4467	6	7	2176.2243	-6	4	2274.6106	0	4	62
63	2187.8177	-16	17				2175.0898	5	6				63
64	2186.6790	3	3	2287.2490	7	8				2275.8429	-9	8	64
65	2185.5337	-1	4	2287.6410	-1	3	2172.8016	-2	5	2276.2427	-6	5	65
66	2184.3819	-4	4	2288.0247	-23	19							66
67	2183.2271	6	7										67
68	2182.0649	10	6	2288.7822	3	22	2169.3301	-2	6				68
69	2180.8971	-2	3	2289.1535	24	20	2168.1621	-4	4				69
70	2179.7238	2	4	2289.5134	3	3	2166.9902	9	6				70
71	2178.5470	7	5	2289.8706	1	4	2165.8104	-3	6				71
72	2177.3589	-27	19				2164.6284	16	11				72
73	2176.1743	-8	5	2290.5642	-21	8	2163.4365	-11	10				73
74	2174.9777	-1	3	2290.9047	2	2	2162.2459	28	23	2279.5760	-5	8	74
75	2173.7788	-2	6	2291.2397	12	13	2161.0435	3	7				75
76				2291.5649	2	4							76
77	2171.3625	-4	4				2158.6262	-14	12				77
78	2170.1422	-30	21	2292.2013	1	3							78
79	2168.9252	0	5	2292.5105	-11	10	2156.1918	9	5	2281.2245	-1	4	79
80	2167.6963	-2	5										80
81	2166.4652	-8	5				2153.7335	5	13	2281.8423	-8	15	81
82	2165.2247	-16	8							2282.1439	2	3	82
83	2163.9853	1	3	2293.6884	-15	25				2282.4392	8	6	83
84	2162.7361	15	12	2294.2458	23	26				2282.7270	-3	4	84
85							2148.7520	-20	14				85
86	2160.2218	4	5										86
87	2158.9598	2	4	2294.7744	9	9	2146.2326	-5	11	2283.5593	2	5	87
88	2157.6871	2	3										88
89	2156.4153	6	3				2143.6890	-23	20	2284.0845	0	4	89
90	2155.1308	-3	6	2295.5218	-1	3				2284.3384	-1	4	90
91	2153.8490	3	6										91
92	2152.5546	5	6	2295.9931	7	16							92
93	2151.2599	-16	11										93
94	2149.9556	-3	4										94
95	2148.6533	-1	10	2296.6564	2	20				2285.2957	-7	19	95
96	2147.3354	-12	17										96
97													97
98	2144.6971	9	13										98

10012 - 10002 638				10011 - 10001 638					
J	P Obs	O-C Unc	R Obs	O-C Unc	P Obs	O-C Unc	R Obs	O-C Unc	J
0	2244.7594	4 5	2247.6747	-1 27					0
1			2248.3910	8 6			2248.8678	1 4	1
2			2249.1006	4 4			2249.5699	3 3	2
3			2249.8062	15 7			2250.2669	10 8	3
4	2241.7569	2 12							4
5	2240.9928	1 4							5
6	2240.2236	3 3	2251.1995	19 12					6
7									7
8	2238.6688	5 7			2238.4429	-21 18	2251.6396	-19 20	8
9	2237.8822	-5 17					2252.9922	-21 29	9
10			2253.9162	-19 14					10
11					2236.0674	0 4			11
12									12
13	2235.4929	-9 6			2234.4539	-3 4	2255.6300	-17 17	13
14	2234.6872	5 5			2233.6390	-2 6	2256.2771	3 3	14
15					2232.8178	-7 6	2256.9161	-1 3	15
16	2232.2334	-1 3	2257.1950	-12 9	2231.9918	-4 4			16
17			2257.8334	-20 21			2258.1787	8 5	17
18			2258.4678	-14 10					18
19	2230.5699	-13 8	2259.0976	1 4	2230.3244	17 10			19
20					2229.4790	-5 5			20
21	2228.8876	1 4	2260.3396	19 14	2228.6302	-6 8	2260.0298	22 24	21
22	2228.0376	-1 3	2260.9500	4 3	2227.7765	1 4			22
23	2227.1836	11 9	2261.5556	-3 4	2226.9157	-7 6	2261.2342	20 22	23
24					2226.0501	-7 6			24
25	2225.4542	-20 19	2262.7521	-2 4			2262.4119	-20 14	25
26			2263.3421	-1 3	2224.3026	-2 9	2263.5729	2 3	26
27			2263.9285	19 11	2223.4214	10 10			27
28	2222.8268	0 3					2264.7095	8 5	28
29	2221.9392	-5 3	2265.0794	5 4					29
30	2221.0468	-5 4	2265.6448	-20 21					30
31	2220.1497	1 5	2266.2082	-10 8					31
32	2219.2457	-8 5			2219.8358	10 19	2266.3693	-3 3	32
33					2218.9246	-2 7	2266.9115	-2 3	33
34	2217.4248	2 4	2267.3167	-8 13	2218.0061	-24 24	2267.4484	3 7	34
35	2216.5052	-4 3	2267.8634	1 6	2217.0871	1 3			35
36	2215.5813	-1 3			2216.1622	23 23			36
37	2214.6531	12 9	2268.9383	-1 4	2215.2290	18 15			37
38							2269.0232	3 6	38
39			2269.9937	23 16	2213.3469	17 12	2269.5372	8 5	39
40	2211.8314	-2 8	2270.5091	-5 4	2211.4392	-16 11	2270.0467	26 20	40
41			2271.0247	25 17	2210.4815	12 7	2270.5455	-5 3	41
42									42
43			2272.5281	12 8					43

44	2207.9967	-7	6	2273.5018	-4	3	2207.5652	-3	3	2272.9685	-10	18	44
45	2207.0279	22	22	2273.9814	-1	3	2206.5818	-10	23	2273.4363	-6	3	45
46	2206.0486	-1	3	2274.4552	0	3	2205.5924	-18	11				46
47							2204.5989	2	5				47
48	2204.0793	3	4				2203.6016						48
49	2203.0856	-7	8										49
50				2275.8432	2	3	2201.5848	-13	8	2275.2499	11	6	50
51							2200.5695	-6	7				51
52	2200.0744	-21	21							2276.1204	2	7	52
53				2277.1801	-5	6	2198.5219	3	4				53
54	2198.0422	-16	16				2197.4894	3	4				54
55	2197.0202	6	7										55
56	2195.9886	-16	16				2195.4085	10	7	2277.7957	21	25	56
57	2194.9553	-2	5				2194.3577	-7	13				57
58	2193.9158	1	7				2193.3043	5	5	2278.5950	-6	8	58
59	2192.8707	2	3										59
60				2279.7045	-2	4	2191.1783	2	5	2279.3743	-2	5	60
61	2190.7662	15	9	2280.1058	1	4	2190.1082	12	8	2279.7551	-2	3	61
62	2189.7035	-4	7	2280.5002	-10	7	2189.0284	-20	25				62
63	2188.6383	3	3	2280.8901	-9	8	2187.9504	21	16	2280.5000	6	5	63
64	2187.5688	20	12	2281.2764	12	9	2186.8610	3	4				64
65	2186.4908	4	4	2281.6518	-19	16	2185.7676	-1	4				65
66	2185.4107	19	9	2282.3950	10	6				2281.5734	12	8	66
67							2183.5678	28	24	2281.9200	18	17	67
68	2183.2280	-21	16	2283.1131	15	8							68
69				2283.4608	-12	13	2181.3412	7	6				69
70	2181.0312	6	10				2180.2183	-17	9	2282.9211	-2	8	70
71	2179.9243	12	7				2179.0928	-13	7				71
72							2177.9646	19	13	2283.5597	-14	8	72
73	2177.6931	6	6							2283.8716	-7	6	73
74				2285.1300	10	6							74
75							2174.5356	0	6				75
76							2173.3843	19	17	2284.7693	-16	15	76
77	2173.1680	-11	14				2172.2218	-19	11				77
78							2171.0597	2	8	2285.3417	8	6	78
79	2169.7216	-8	7				2169.8883	-16	9	2285.6196	24	12	79
80	2168.5623	-9	12							2285.8862	-14	27	80
81				2286.9396	-28	14	2167.5354	10	12				81
82	2166.2266	-26	8				2166.3468	-16	19				82
83	2165.0548	2	27				2165.1591	20	30				83
84													84

01111e - 01101e 638										01111f - 01101f 638									
J	P	Obs	O-C	Unc	R	Obs	O-C	Unc	P	Obs	O-C	Unc	R	Obs	O-C	Unc	J		
1	2252.9003	-3	14		2256.5577	-8	10		2252.9003	20	14			2257.2767	-9	18	1		
2					2257.2767	32	18		2252.1491	1	6			2257.9873	-8	3	2		
3									2251.3937	-4	3			2258.6916	-13	6	3		
4	2250.6384	-12	11														4		
5	2249.8731	-18	14											2260.0834	-25	12	5		
6																	6		
7																	7		
8																	8		
9																	9		
10																	10		
11	2245.9684	-6	13		2263.4615	24	16						2262.8023	-26	20		11		
12																	12		
13	2244.3693	11	8						2244.3499	-11	12						13		
14									2243.5403	-5	7						14		
15	2242.7456	2	4						2242.7259	8	9						15		
16	2241.9241	-17	13		2266.0646	8	25		2241.9052	13	21						16		
17	2241.0990	-17	16		2266.7032	21	23		2241.0778	6	10						17		
18	2240.2695	-7	7											2267.3465	-13	8	18		
19	2239.4345	4	6											2267.9734	-9	10	19		
20	2238.5932	5	5											2268.5936	-17	18	20		
21	2237.7473	16	8		2269.1967	23	23		2238.5630	-10	5						21		
22					2269.8031	-7	6							2269.8215	11	11	22		
23	2236.0357	3	4						2236.0006	-7	6			2270.4241	-4	4	23		
24	2235.1725	10	5		2271.0071	13	17							2271.0247	-17	17	24		
25	2234.3043	5	3		2271.5997	13	24		2234.2672	18	14			2271.6141	-17	16	25		
26	2233.4296	1	3		2272.1860	6	5		2233.3889	-3	4			2272.2036	-6	6	26		
27	2232.5495	1	3		2272.7680	12	9		2232.5081	-2	5			2272.7842	-4	3	27		
28	2231.6644	1	5		2273.3424	-2	4		2231.6202	16	19			2273.3608	2	3	28		
29	2230.7742	4	7		2273.9127	-1	4		2230.7294	16	19			2273.9312	3	4	29		
30	2229.8782	4	3						2229.8305	7	5						30		
31	2228.9771	7	5		2275.0355	-9	7		2228.9265	3	5			2275.0560	14	13	31		
32	2228.0701	6	3						2228.0171	-1	3						32		
33	2227.1587	15	12		2276.1376	0	4		2227.1013	-15	11			2276.1563	5	7	33		
34	2226.2381	-14	9		2276.6799	-2	3		2226.1853	25	27			2276.6984	5	6	34		
35	2225.3179	15	9		2277.2159	-4	4		2225.2587	12	10			2277.2345	2	4	35		
36	2224.3869	-10	7		2277.7463	-9	10		2224.3264	-3	4			2277.7668	17	15	36		
37	2223.4557	18	11		2278.2703	-22	16		2223.3889	-15	19						37		
38	2222.5142	-4	11		2278.7933	11	8		2222.4485	-2	3			2278.8085	-12	9	38		
39	2221.5678	-20	15		2279.3046	-16	11		2221.5016	1	5						39		
40	2220.6204	-7	6		2279.8145	-1	4		2220.5494	3	4			2279.8326	10	11	40		
41	2219.6633	-8	5						2219.5912	0	3						41		
42	2218.7043	12	2						2218.6274	-8	6						42		
43	2217.7370				2281.3065	5	5		2217.6577					2281.3228	8	4	43		

44	2216.7640	-10	7	2281.7932	13	8	2216.6844	2	4	2281.8066	-9	7	44
45	2215.7875	-4	3	2282.2724	3	6	2215.7042	-2	4	2282.2865	-7	11	45
46	2214.8047	-6	6							2282.7628	15	19	46
47	2213.8193	19	12	2283.2149	-7	8	2213.7298	11	18	2283.2291	-6	13	47
48	2212.8217	-25	20	2283.6807	18	23	2212.7320	-7	9				48
49													49
50	2209.8138	17	17	2285.0375	27	17	2210.7229	-16	10				50
51							2209.7123	0	2				51
52							2208.6948	1	4				52
53	2206.7508	-9	7	2286.3376	-22	15							53
54	2205.7205	-4	3										54
55	2204.6847	0	4										55
56	2203.6427	-5	3										56
57							2204.5700	-3	5				57
58	2201.5448	7	8	2288.0038	34	22	2203.5240	-17	11	2288.4040	-24	22	58
59	2200.4865	0	4	2288.4040	26	14	2201.4208	4	4				59
60	2199.4225	-11	7										60
61	2198.3553	-1	3	2289.1882	20	6	2199.2936	0	4	2289.1882	-8	6	61
62	2197.2822	3	7	2289.5714	12	8	2198.2209	-13	12	2289.5714	-5	8	62
63	2196.2029	-1	3	2289.9481	-3	10	2197.1483	29	24	2289.9481	-9	10	63
64							2196.0639	7	7				64
65	2194.0294	1	4	2290.6857	-21	18	2194.9754	-3	4	2290.6857	-3	18	65
66	2192.9343	-2	4	2291.0487	-3	17	2193.8841	13	10	2291.0487	28	17	66
67	2191.8326	-17	12	2291.4020	-25	19	2192.7849	-13	12	2291.4020	19	19	67
68	2190.7291	2	8	2292.0980	-3	4	2191.6797	-13	12	2291.7508	23	14	68
69	2189.6173	-9	8				2190.5730	9	15				69
70							2189.4557	-21	18				70
71	2187.3788	-20	12				2188.3379	-3	4				71
72	2186.2542	0	3				2187.2137	-3	4				72
73							2186.0838	8	12	2293.4067	21	17	73
74							2184.9469	-5	6				74
75	2182.8429	3	6	2294.0427	-2	6	2183.8075	10	6	2294.0278	10	8	75
76	2181.6925	-23	13	2294.3481	11	6	2182.6596	-6	4	2294.3300	8	7	76
77	2180.5412	-6	14	2294.6444	-10	7				2294.6250	-9	7	77
78	2179.3857	22	21	2294.9380	-1	3				2294.9166	-3	3	78
79	2178.2202	3	3	2295.2247	-4	4	2180.3520	2	3	2295.2017	-4	3	79
80	2177.0501	-9	6				2179.1894	-2	3				80
81	2175.8783	14	8	2295.7805	-13	21	2178.0208	-13	9				81
82							2176.8475	-18	16	2296.0230	0	6	82
83	2173.5135	5	4	2296.3153	-4	4	2174.4882	4	6				83
84	2172.3233	2	4	2296.5752	12	9	2173.2985	-6	4				84
85	2171.1307	27	22				2172.1057	-6	7	2296.7923	4	3	85
86	2169.9302	25	17	2297.0745	11	9	2170.9062	4	11				86
87	2168.7222	1	4				2169.6995	-17	11				87
88	2167.5104	-9	9				2168.4924	10	8				88
89	2166.2952	0	8	2298.0020	-14	13	2167.2762	-1	2				89
90	2165.0728	-12	14	2298.2217	2	5	2166.0555	-4	4				90
91													91
92							2163.5998	5	7				92
93							2162.3634	3	19				93



32	2216.4517	9	8	2264.0947	6	9	2216.4517	10	8	2264.0947	11	9	32
33	2215.5374	-2	4	2265.1907	11	11	2215.5374	-1	4	2265.1907	16	11	33
34	2214.6185	-5	8	2266.7310	20	27	2214.6185	-4	8	2266.7310	25	27	34
35				2266.2613	-15	11				2266.2613	-9	11	35
36	2211.8311	2	13				2211.8311	4	13				36
37													37
38	2208.0369	-12	14	2267.8293	-14	11	2208.0369	-11	14	2267.8293	-7	11	38
39	2207.0752	-13	16	2268.3421	0	5	2207.0752	-12	16	2268.3421	7	5	39
40	2206.1100	4	15	2269.3473	-8	5	2206.1100	-6	15	2269.3473	-2	5	40
41	2205.1371	-1	4	2269.8420	-6	7	2205.1371	-1	4	2269.8420	-1	7	41
42	2204.1603	7	8				2204.1603	-8	8				42
43	2203.1763	-2	6				2203.1763	-2	6				43
44	2202.1883	1	5				2202.1883	1	5				44
45	2201.1947	3	5				2201.1947	1	5				45
46	2200.1959	3	6				2200.1959	3	6				46
47	2199.1909	-1	9				2199.1909	-4	9				47
48				2272.6919	-2	6				2272.6919	-2	6	48
49				2273.1476	3	6				2273.1476	1	6	49
50				2273.5973	4	4				2273.5973	0	4	50
51				2274.0422	13	9				2274.0422	7	9	51
52	2196.1438	-20	16										52
53	2194.0899	9	7				2195.1235	24	16				53
54	2193.0544	18	16				2194.0899	-4	7				54
55	2192.0139	29	15				2193.0544	2	16				55
56	2190.9654	14	7				2192.0139	10	15				56
57	2189.9154	37	16				2190.9654	-8	7				57
58	2188.8510	-31	23				2189.9154	11	16				58
59	2187.7892	-20	12							2276.9930	-10	13	59
60	2186.7255	25	13										60
61							2186.7255	-16	13				61
62							2185.6546	4	7				62
63							2184.5760	-1	10				63
64													64
65	2182.3947	-25	13							2279.3045	-21	12	65
66	2181.2991	-34	24							2279.6752	27	23	66
67	2180.2022	-4	13										67
68													68
69													69
70	2177.9845	-23	10							2281.0813	9	5	70
71	2176.8715	5	16										71
72	2175.7476	-24	10							2281.7505	-6	12	72
73	2174.6231	-6	15										73
74	2173.4929	8	6							2282.3950	-45	19	74
75													75
76	2171.2127	-4	6										76
77	2170.0643	-14	9										77
78													78
79	2167.7592	40	26										79
80	2166.5895	-25	24										80
81	2165.4260	24	13										81

82  
83  
84  
85  
86

2164.2484 -16 17  
2163.0724 13 30  
2161.8868 -1 15  
2159.5043 14 11

00011 - 00001 637					
J	P Obs	O-C Unc	R Obs	O-C Unc	
0					
1	2272.5665	-17 22	2275.5864	8 9	
2			2276.3248	-8 9	
3	2271.0247	-3 4			
4					
5	2269.4595	6 5			
6	2268.6660	-13 28	2279.9393	1 6	
7					
8	2267.0682	14 8			
9					
10			2282.7265	3 5	
11			2283.4087	1 4	
12			2284.0848	-3 4	
13					
14	2262.9685	28 26			
15	2262.1286	3 5	2285.4212	4 4	
16			2286.0816	16 21	
17	2260.4354	-11 9	2286.7337	4 5	
18	2259.5853	32 28	2287.3809	0 4	
19			2288.0227	0 5	
20	2257.8553	-9 8	2288.6587	1 4	
21	2256.9850	3 3			
22	2256.1086	11 5	2289.9128	-4 4	
23	2255.2244	-2 3	2290.5330	13 8	
24			2291.1457	13 11	
25	2253.4420	1 3	2291.7511	-2 4	
26			2292.3512	-12 7	
27	2251.6377	12 16	2292.9467	-10 7	
28	2250.7247	-6 4	2293.5356	-15 16	
29	2249.8061	-23 19	2294.1226	18 15	
30	2248.8854	-5 3			
31	2247.9563	-14 10	2295.2707	2 4	
32	2247.0250	11 6	2296.3949	-20 12	
33					
34	2245.1399	6 9			

35	2243.2318	-4	4	2297.5005	6	8
36	2242.2696	-6	5	2298.0423	-3	5
37	2241.3005	-20	15	2298.5773	-22	19
38	2240.3312	20	13	2299.1096	-9	7
39	2239.3507	4	6	2300.1552	2	3
40				2300.6685	0	3
41				2301.1758	-3	3
42				2301.6801	23	24
43	2235.3778	-7	26	2302.1726	-10	6
44	2234.3733	17	11			
45				2303.6256	-3	4
46	2232.3403	-5	3	2304.0982	-1	4
47	2231.3187	17	8			
48				2305.0255	2	3
49	2229.2534	7	9	2305.4801	1	3
50				2306.3719	2	3
51	2226.1171	28	20	2306.8087	-1	4
52	2225.0593	23	11	2307.2404	5	5
53				2308.0845	1	4
54				2308.4979	1	3
55	2219.6885	15	10	2308.9033	-20	16
56	2218.5962	-1	6	2309.7048	23	12
57	2216.3978	-5	9	2310.4749	-12	11
58				2310.8541	1	4
59				2311.2258	-2	4
60	2211.9361	4	9	2311.9523	1	4
61	2210.8074	12	27	2312.3068	4	7
62				2312.6544	-2	6
63				2312.9974	5	7
64				2313.3342	9	10
65				2313.6664	26	20
66				2313.9896	13	19
67	2205.0756	-2	4	2314.3058	-10	8
68	2203.9142	10	18	2314.6192	-2	12
69				2314.9254	-7	12
70				2315.2258	-10	11
71				2315.5209	-6	24
72				2315.8092	-11	11
73				2316.0942	11	18
74						
75						
76						
77						
78						
79						
80						

10012 - 00001 628					10011 - 00001 628				
J	P	Obs	O-C	Unc	R	Obs	O-C	Unc	J
0	3570.4046	3571.8717	2	5	3674.3971	3675.8648	-1	4	0
1	3569.6621	3572.5966	3	4	3673.6561	3676.5908	0	3	1
2	3568.9133				3672.9090	3677.3113	-2	5	2
3	3568.1611	3574.0290	3	5	3672.1572	3678.0269	0	4	3
4	3567.4017	3575.4383	2	4	3671.3974		-3	8	4
5	3566.6369	3576.1342	1	4	3670.6371	3679.4419	-2	10	5
6	3565.8660	3577.8244	1	4	3669.8697	3680.1417	-2	4	6
7	3565.0889	3577.5087	0	4	3669.0968	3681.5257	0	5	7
8	3564.3072	3578.1871	-2	4	3668.3187	3682.2097	-1	4	8
9	3563.5187	3578.8602	-1	5	3667.5354	3683.8883	-2	4	9
10	3562.7245	3579.5270	-1	4	3666.7471	3685.5621	-2	4	10
11	3561.9268	3580.1882	-1	3	3665.9535	3686.2304	-2	4	11
12	3561.1194	3580.8435	-1	4	3665.1548	3687.8935	-3	4	12
13	3560.3090	3581.4930	-1	4	3664.3510	3688.5514	-1	4	13
14	3559.4921	3582.1365	-1	4	3663.5420	3689.2044	-1	4	14
15	3558.6694	3582.7744	-2	4	3662.7280	3689.8519	-1	4	15
16	3557.8419	3583.4058	-1	9	3661.9088	3687.4942	-1	3	16
17	3557.0070	3584.0324	-1	3	3661.0847	3688.1311	-3	6	17
18	3556.1669	3584.6527	0	3	3660.2547	3688.7635	-1	4	18
19	3555.3214	3585.2672	3	4	3659.4198	3689.3899	-2	3	19
20	3554.4694	3585.8752	0	4	3658.5801	3690.0120	-4	5	20
21	3553.6125	3586.4778	2	4	3657.7362	3690.6283	-4	4	21
22	3552.7497				3656.8862	3691.2394	2	4	22
23	3551.8810	3587.6645	-1	4	3656.0312	3691.8456	1	4	23
24	3551.0069	3588.2490	-1	3		3692.4470	9	16	24
25	3550.1254	3588.8284	7	4	3654.3067	3693.0419	4	4	25
26	3549.2393	3589.4000	-2	4	3653.4367	3693.6325	4	4	26
27	3548.3473	3589.9668	-2	5	3652.5617	3694.2183	3	4	27
28	3547.4493	3590.5272	0	4	3651.6819	3694.7986	3	5	28
29	3546.5455	3591.0815	-2	3	3650.7961	3695.3739	3	4	29
30	3545.6353	3591.6300	-1	5	3649.9071	3695.9440	3	4	30
31	3544.7210	3592.1723	-1	4	3649.0125	3696.5091	3	4	31
32	3543.7987	3592.7088	2	4	3648.1121	3697.0687	3	4	32
33	3542.8714	3593.2384	-3	3	3647.2082	3697.6239	-1	5	33
34	3541.9383	3593.7626	-1	6	3646.2984	3698.1740	4	4	34
35	3541.0091	3594.2804	-2	4	3645.3844	3698.7184	2	4	35
36	3540.0540	3594.7922	0	3	3644.4654	3699.2588	0	5	36
37	3540.0540	3595.2977	0	5	3643.5412				37
38	3539.1030	3595.7969	0	5	3642.6121	3700.3232	3	4	38
39	3538.1461	3596.2900	-1	5	3641.6791	3700.8478	1	4	39
40	3537.1832	3596.7770	0	4	3640.7403	3701.3678	2	6	40
41	3536.2143	3597.2575	1	4	3639.7970	3701.8825	0	4	41
42	3535.2394						-1	5	42

43	3534.2596	11	13	3597.7317	0	3	3638.8493	4	3702.3945	20	16	44
44	3533.2717	1	3	3598.2006	10	16	3637.8970	5	3703.3973	-4	5	45
45	3532.2786	0	3	3598.6614	1	5	3636.9397	4	3704.3931	1	4	46
46	3531.2797	1	4	3599.1169	2	5	3635.9777	4	3705.3855	21	17	47
47	3530.2745	0	4	3599.5656	-6	3	3635.0106	5	3706.3795	5	4	48
48	3529.2637	0	4	3600.0074	-3	6	3634.0398	4	3707.3705	-2	4	49
49	3528.2460	0	5	3600.4438	-5	4	3632.0840	3	3708.3625	1	3	50
50	3527.2233	7	3	3600.8742	0	4	3631.0990	3	3709.3548	-3	4	51
51	3526.1934	-1	4	3601.2970	1	4	3630.1092	4	3710.3467	0	4	52
52	3525.1573	-4	5	3601.7138	1	4	3629.1155	4	3711.3382	-3	4	53
53	3524.1152	-2	4	3602.1244	-1	4	3628.1165	6	3712.3296	0	5	54
54	3523.0674	-1	5	3602.5275	1	4	3627.1139	4	3713.3210	-5	4	55
55	3522.0135	4	5	3602.9248	-1	5	3626.1067	4	3714.3124	0	5	56
56	3520.9533	-1	5	3603.3155	2	4	3625.0950	8	3715.3038	-10	9	57
57	3519.8862	2	6	3603.6992	0	5	3624.0796	4	3716.2952	-2	5	58
58	3518.8135	-1	5	3604.0764	-4	7	3623.0581	9	3717.2866	-9	9	59
59	3517.7362	21	11	3604.4468	-2	7	3622.0339	4	3718.2780	-1	3	60
60	3516.6481	-6	5	3605.1687	2	6	3621.0150	10	3719.2694	0	3	61
61	3515.5569	0	5	3605.5188	-3	4	3619.9729	8	3720.2608	-2	3	62
62	3514.4586	-1	4	3605.8627	-2	4	3618.9343	6	3721.2522	7	11	63
63	3513.3542	-1	4	3606.1998	-1	3	3617.8930	4	3722.2436	-2	8	64
64	3512.2428	-6	3	3606.5301	-1	4	3616.8470	6	3723.2350	23	5	65
65	3511.1259	-3	5	3606.8540	0	6	3615.7977	7	3724.2264	-2	5	66
66	3510.0028	-2	4	3607.1701	0	3	3614.7432	9	3725.2178	-1	8	67
67	3508.8722	-4	8	3607.4800	3	6	3613.6861	9	3726.2092	-3	7	68
68	3507.7364	3	14	3607.7818	-7	8	3612.6231	9	3727.2006	-12	15	69
69	3506.5937	6	9	3608.0776	-7	6	3611.5577	11	3728.1920	16	16	70
70	3505.4437	-3	6	3608.3671	0	5	3610.4876	8	3729.1834	10	10	71
71	3504.2874	-5	14	3608.6492	2	6	3609.4133	13	3730.1748	13	13	72
72	3503.1247	-12	13	3609.915	-1	9	3608.3350	19	3731.1662	-6	16	73
73	3501.9550	-3	13	3609.4526	3	13	3607.2578	12	3732.1576	10	10	74
74	3500.7803	0	13				3606.1678	16	3733.1490	13	13	75
75	3499.5984	-3	13				3605.0793	15	3734.1404	-6	13	76
76	3498.4096	0	14				3603.9857	11	3735.1318	22	11	77
77	3497.2139	-3	14						3736.1232			78
78	3496.0124	-4	16						3737.1146			79
79	3494.8029											80
80												81
81												82
82	3491.1387	18	15									

20013 - 10002 628					20012 - 10002 628				
J	P Obs	O-C Unc	R Obs	O-C Unc	P Obs	O-C Unc	R Obs	O-C Unc	J
0	3531.0980	-10 24					3646.8876	-8 20	0
1	3530.3580	-1 7					3647.6065	15 21	1
2	3529.6108	-16 15	3534.7342	13 21			3648.3129	-21 27	2
3	3528.8616	-4 16	3535.4448	-7 13					3
4									4
5									5
6									6
7	3526.5810	-16 16	3536.8552	-11 15	3642.4516	-2 13	3651.0887	-6 10	7
8	3525.8136	2 10	3537.5535	-12 13	3641.6874	-9 12	3651.7674	9 9	8
9	3525.0399	4 8	3538.2488	-6 10	3640.1446	1 15	3652.4378	6 10	9
10	3524.2609	1 8	3538.9368	-2 17	3639.3626	1 16	3653.1011	-1 7	10
11	3523.4768	-7 7	3539.6232	23 25	3637.7788	-2 14	3653.7591	3 9	11
12	3522.6896	-2 7	3540.3001	0 8	3636.9777	-1 9	3654.4107	-12 12	12
13	3521.8956	-10 10	3540.9760	15 20	3636.1694	-1 9	3655.0530	0 5	13
14			3541.6451	10 13	3635.5340	-3 11	3655.6921		14
15			3542.3095	6 6	3634.7068	1 19			15
16	3520.2968	0 10	3542.9694	-4 4	3633.8734	-5 8	3657.5667	-1 6	16
17	3519.4903	5 7		11 13	3632.0319	-5 7	3658.1792	5 8	17
18	3517.8608	-8 23	3544.2737	-3 5	3631.1855	-8 11	3658.7837	-4 5	18
19	3517.0405	1 6	3544.9205	-12 15	3630.3322	3 8			19
20	3516.2146	2 4	3545.5596	-1 5			3659.9754	0 5	20
21	3515.3836	-1 9	3546.1959	-12 15	3628.6081	3 8	3660.5615	-9 13	21
22	3514.5471	-11 4	3546.8260	5 5	3627.7357	2 7	3661.7140	-4 6	22
23	3513.7083	-4 7	3547.4506	1 8	3626.8574	1 5	3661.7144	6 7	23
24	3512.8623	-5 6	3548.0730	1 5	3625.9726	2 6	3662.2813	-2 4	24
25	3512.0136	-8 9	3548.6889	-18 21			3663.8411	-2 7	25
26	3511.1587	4 8	3549.2994	5 10	3624.1843	2 16	3663.9423	-2 7	26
27	3510.2996	-9 9	3549.9054	-5 10	3623.2803	15 16	3664.4840	-4 6	27
28	3509.4336		3550.5042	9 11	3622.3722	3 6	3665.0188	-3 4	28
29			3551.1023	-5 6	3621.4550	4 8	3665.5466	-3 6	29
30	3507.6920	6 23	3552.2792	-5 6			3666.0689	-15 17	30
31	3506.8133	8 3	3552.8584	2 5	3618.6701	-3 2	3666.5851	-9 7	31
32	3505.9289	1 3		0 9	3617.7288	3 14	3667.5991	-1 10	32
33	3505.0400	-2 5	3554.0050	8 13	3616.7826	6 16	3668.5864	0 9	33
34			3554.5700	-13 16	3615.6299	-1 9	3669.5500	-6 13	34
35	3503.2498	15 13	3555.1309	1 7	3614.8709	-4 5	3670.0219	15 23	35
36	3502.3447	-2 18	3555.6837	-5 12	3613.9066	-5 13			36
37	3501.4371	-5 9	3556.2350	9 12	3612.9351	-5 13			37
38	3500.5220	-13 12	3556.7792	-9 12	3611.9581	-9 12			38
39	3499.6041	-14 12	3557.3177	-9 12					39
40	3498.6804	-14 12		-9 12	3608.9923	-5 13			40
41	3497.7540	4 4	3558.3798	-5 13	3607.9930	-5 13			41
42	3496.8206	-3 5	3558.9040	-11 13					42
43			3559.4212						43
44			3559.9331						44

45	3493.0371	8 12	3560.4417	5 8	3605.9738	-9 12	3672.2935	-8 9	45
46			3560.9433	5 9	3604.9570	-1 9	3672.7297	-9 20	46
47	3491.1144	8 12	3561.4380	-10 17	3603.9336	-2 12			47
48	3490.1451	6 12	3561.9295	-1 14					48
49			3562.4138	-9 12	3601.8687	-16 22	3674.0047	7 8	49
50			3562.8958	16 26			3674.4158	-10 14	50
51	3487.2064	4 15	3563.8364	-1 9	3599.7850	6 16			51
52					3598.7339	7 10			52
53	3485.2186	-20 18	3564.7547	-14 17	3597.6754	-11 27	3675.6205	3 9	53
54	3484.2200	0 13	3565.2077	4 16					54
55	3483.2140	0 16							55
56			3566.0931	5 15					56
57			3566.5270	6 17					57
58			3566.9563	18 22					58
59									59

20012 - 10001 628										20011 - 10001 628									
J	P Obs	O-C Unc	R Obs	O-C Unc	P Obs	O-C Unc	R Obs	O-C Unc	J	P Obs	O-C Unc	R Obs	O-C Unc	J	P Obs	O-C Unc	R Obs	O-C Unc	J
0									0					0					0
1	3538.2807	2 10							1					1					1
2	3537.5369	7 11							2					2					2
3									3					3					3
4									4					4					4
5									5					5					5
6									6					6					6
7	3534.4872	19 23	3543.2867	12 20	3673.7635	2 14	3682.4647	2 10	7					7					7
8			3543.9705	-6 19	3672.2467	13 27	3671.4822	-15 19	8					8					8
9			3544.6493	0 11	3670.7108	-1 10	3669.9342	-14 13	9					9					9
10			3545.3192	-10 14	3668.3716	0 6	3668.5570	-5 9	10					10					10
11			3545.9819	-18 23			3687.8851	-2 12	11					11					11
12			3546.6416	18 22			3688.5401	-4 10	12					12					12
13									13					13					13
14									14					14					14
15									15					15					15
16									16					16					16
17									17					17					17
18									18					18					18
19									19					19					19
20									20					20					20
21									21					21					21
22									22					22					22
23									23					23					23
24									24					24					24



12	3529.5539	21	15	3547.8352	-1	4	3529.5665	-22	14	3547.8911	-3	4	3547.8911	12
13	3528.7454	20	5	3549.1414	-1	4	3528.7661	-6	5	3548.5548	-1	3	3548.5548	13
14	3527.9332	19	3	3549.7859	-1	4	3527.9593	-1	3	3549.2129	0	3	3549.2129	14
15	3527.1160	18	3	3550.4241	-2	4	3527.1468	-1	4	3549.8658	2	4	3549.8658	15
16	3526.4625	17	4	3551.0573	-4	4	3526.5055	-2	3	3550.5130	1	5	3550.5130	16
17	3525.6274	16	4	3551.6840	4	4	3524.6771	-2	4	3551.1547	0	3	3551.1547	17
18	3524.7868	15	3	3552.3051	4	6	3523.8436	-1	4	3551.7910	-1	3	3551.7910	18
19	3523.9403	14	3	3552.9197	3	3	3523.0041	-2	4	3552.4219	-2	4	3552.4219	19
20	3522.0877	13	3	3553.5287	3	3	3522.1596	-1	4	3553.0477	1	3	3553.0477	20
21	3521.2300	12	3	3554.1319	2	3	3521.3097	-2	4	3553.6678	1	3	3553.6678	21
22	3520.3652	11	6	3554.7293	2	3	3520.5949	-3	4	3554.2824	1	3	3554.2824	22
23	3518.6205	10	3	3555.3214	10	4	3518.7285	3	4	3554.8946	2	4	3554.8946	23
24	3517.7373	9	4	3555.9062	4	2	3517.8582	0	4	3555.4931	-3	4	3555.4931	24
25	3516.8522	8	20	3556.4855	2	0	3516.9804	9	4	3555.0931	-1	3	3555.0931	25
26	3515.9598	7	4	3557.0589	2	0	3515.2112	9	4	3556.6852	-4	9	3556.6852	26
27	3515.0608	6	5	3557.6271	0	6	3514.4185	3	4	3557.2720	-6	9	3557.2720	27
28	3514.1561	5	4	3558.1884	0	3	3513.5173	-2	4	3558.4314	14	16	3558.4314	28
29	3513.2468	4	6	3558.7439	3	5	3512.5173	-2	4	3559.0005	2	5	3559.0005	29
30	3512.3301	3	3	3559.2932	1	3	3511.6081	-2	5	3559.5653	3	5	3559.5653	30
31	3511.4082	2	3	3559.8375	-4	8	3510.6932	-7	4	3560.1246	3	5	3560.1246	31
32	3510.4811	1	3	3560.3759	11	8	3509.7741	-7	4	3560.6777	-1	5	3560.6777	32
33	3509.5481	0	8	3561.4323	2	8	3508.8494	-7	5	3561.2254	1	5	3561.2254	33
34	3508.6088	0	8	3562.4650	2	8	3507.9178	-8	5	3561.7676	-1	5	3561.7676	34
35	3507.6634	0	8	3563.4726	-5	8	3506.9829	-4	5	3562.3045	3	5	3562.3045	35
36	3506.7127	0	8	3564.4583	-14	12	3506.0407	2	5	3563.3605	4	7	3563.3605	36
37	3505.7560	0	8	3565.4181	-7	8	3505.0935	1	5	3563.8790	-5	6	3563.8790	37
38	3504.7933	0	8	3566.4650	-2	13	3504.1426	18	4	3564.3931	0	4	3564.3931	38
39	3503.8242	0	8	3567.4583	-2	4	3503.1827	0	4	3564.9012	2	4	3564.9012	39
40	3502.8496	0	8	3568.4181	-4	13	3502.2192	1	4	3565.4052	21	26	3565.4052	40
41	3501.8693	0	8	3569.4181	-4	13	3501.2497	-3	4	3566.3892	-7	9	3566.3892	41
42	3500.8836	0	8	3570.4181	-8	7	3500.2753	-3	6	3566.8737	-8	9	3566.8737	42
43	3499.8930	0	8	3571.4181	-3	9	3499.2952	0	4	3567.3548	16	13	3567.3548	43
44	3498.8930	0	8	3572.4181	-6	9	3497.3177	0	4	3567.8255	-9	10	3567.8255	44
45	3497.8930	0	8	3573.4181	-6	9	3496.3208	2	4	3568.2922	-1	3	3568.2922	45
46	3496.8930	0	8	3574.4181	-6	9	3495.3190	10	11	3569.7540	-7	9	3569.7540	46
47	3495.8930	0	8	3575.4181	-6	9	3494.3102	10	11	3570.6594	-8	13	3570.6594	47
48	3494.8930	0	8	3576.4181	-6	9	3493.2956	10	11	3571.1011	11	9	3571.1011	48
49	3493.8930	0	8	3577.4181	-6	9	3492.2763	11	12	3572.5379	-6	9	3572.5379	49
50	3492.8930	0	8	3578.4181	-6	9	3491.2518	11	13	3573.9691	-4	9	3573.9691	50
51	3491.8930	0	8	3579.4181	-6	9	3490.2188	11	13	3574.3944	-4	9	3574.3944	51
52	3490.8930	0	8	3580.4181	-6	9	3489.1810	11	13	3575.8152	-4	9	3575.8152	52
53	3489.8930	0	8	3581.4181	-6	9	3488.1402	11	13	3576.2265	-4	9	3576.2265	53
54	3488.8930	0	8	3582.4181	-6	9	3487.0905	11	13	3577.6339	-4	9	3577.6339	54
55	3487.8930	0	8	3583.4181	-6	9	3486.0378	11	13	3578.0338	-4	9	3578.0338	55
56	3486.8930	0	8	3584.4181	-6	9	3485.9775	11	13	3579.4275	-4	9	3579.4275	56
57	3485.8930	0	8	3585.4181	-6	9	3484.9120	11	13	3580.8160	-4	9	3580.8160	57
58	3484.8930	0	8	3586.4181	-6	9	3483.8483	11	13	3582.2038	-4	9	3582.2038	58
59	3483.8930	0	8	3587.4181	-6	9	3482.7833	11	13	3583.5904	-4	9	3583.5904	59
60	3482.8930	0	8	3588.4181	-6	9	3481.7177	11	13	3584.9775	-4	9	3584.9775	60
61	3481.8930	0	8	3589.4181	-6	9	3480.6522	11	13	3586.3605	-4	9	3586.3605	61

62	3482.1195	-12 16		3482.8400	-8 16	3574.1974	0 14	62
63	3481.0238	26 24	14 17	3481.7628	-6 7			63
64	3479.9171	14 16	7 15	3480.6815	14 23	3574.9425	3 15	64
65			15 14	3574.3305		3575.3063	12 18	65
66			1 18	3574.6607	6 13	3575.6609	-7 23	66
67					-1 15			67
68			21 10	3575.3063				68

11111e - 01101e 628									
J	P	Obs	O-C	Unc	R	Obs	O-C	Unc	J
1	3682.3311	-24 27		3685.2732	3682.3311	-8 27		3685.2732	1
2	3681.5835	-14 15			3681.5835	2 15		3685.9951	2
3	3680.8298	-9 14	1 16	3687.4143	3680.8298	1 14		3686.7135	3
4	3680.0707	0 6			3680.0707	-2 3		3687.4281	4
5	3679.3061	10 6			3679.3061	-10 6			5
6	3678.5355	16 13			3678.5355	-26 13			6
7	3677.7599	30 17			3676.9828	-21 19			7
8									8
9									9
10	3675.3930	8 6			3675.4110	-3 4			10
11	3674.5948	21 20			3674.6171	-2 5			11
12	3673.7877	2 3			3673.8173	-2 3			12
13	3672.9771	4 3			3673.0129	-1 3			13
14	3672.1591	-11 17			3672.2031	-3 3			14
15	3671.3383	1 5							15
16	3670.5112	7 3			3670.5691	-1 3			16
17	3669.6775	3 3			3669.7443	-2 3			17
18	3668.8384	1 4			3668.9146	-2 3			18
19	3667.9940	2 5			3668.0799	-2 4			19
20	3667.1435	2 5			3667.2404	0 3			20
21	3666.2885	-3 3			3666.3955	-2 4			21
22	3665.4276	7 3			3665.5459	-1 4			22
23	3664.5607	5 6			3664.6913	0 3			23
24	3663.6885	6 5			3663.8310	-1 3			24
25	3662.8099	-1 3			3662.9672	-1 3			25
26					3662.0975	-1 5			26
27					3661.2240	9 4			27
28	3661.0377	0 3			3661.2240	1 3			28
29	3660.1432	0 3			3660.3439	1 3			29
30	3659.2432	-1 4			3659.4596	-1 3			30
31	3658.3380	1 4			3657.6760	-4 6			31
32					3656.7778	9 7			32
33	3656.5106	1 4			3655.8746				33
34	3655.5883	-4 5							34

35	3654.6611	-2	4	3706.5603	13	8	3654.9653	2	5	3706.9830	3	5	35
36	3653.7286	0	5	3707.0863	5	8	3654.0518	2	5	3707.5325	2	7	36
37	3652.7913	9	9	3707.6068	-1	8	3653.1335	1	4	3708.0777	8	8	37
38	3651.8461	-7	5	3708.1229	4	15	3652.2108	4	6				38
39	3650.8977	0	4				3651.2827	2	6	3709.1513	1	11	39
40	3649.9419	-14	12	3709.1388	21	16	3650.3507	7	9				40
41	3648.9835	0	4	3709.6366	11	14	3649.4145	19	19				41
42	3648.0182	-1	4	3710.1283	-3	8				3710.7237	-17	12	42
43	3647.0479	1	6							3711.2383	-20	14	43
44	3646.0731	12	10	3711.1043	62	19				3711.7520	18	22	44
45	3645.0912	5	13							3712.2539	-13	12	45
46										3712.7547	-6	11	46
47										3713.2494	-12	11	47
48	3642.1129	-23	16	3712.0439	-14	11	3646.5718	-5	11	3713.7409	0	15	48
49	3641.1122	-6	14	3712.5094	-12	8	3645.6156	-4	15	3714.2258	-8	13	49
50	3640.1037	-15	20	3712.9695	-8	7	3644.6549	-7	11	3715.1832	3	11	50
51	3639.0920	-3	8	3713.4237	-8	6	3643.6891	-3	4	3715.6536	-3	15	51
52	3638.0749	0	6	3713.8735	3	9	3642.7194	-3	6	3716.1198	8	10	52
53	3637.0508	8	14				3641.7446	9	11	3716.5824	8	10	53
54	3636.0215	-7	6				3640.7665			3717.0389	-2	10	54
55										3717.4898	-2	10	55
56	3633.9494	-2	8	3714.7535	-5	16				3717.9371	0	10	56
57	3632.9053	-2	13	3715.1839	-22	19				3718.3809	14	16	57
58				3715.6129	-15	20							58
59	3630.8003	-17	20	3716.4505	-3	13							59
60				3717.2651	3	10							60
61										3719.2493	-9	10	61
62	3627.6079	-6	17	3718.0581	0	15							62
63	3626.5342	3	13	3718.8299	1	9				3720.5210	-2	7	63
64	3625.4532	-10	25							3720.9366	10	13	64
65	3624.3691	-4	15	3719.5818	18	22				3721.3470	16	26	65
66	3623.2803	4	4	3720.3114	27	22				3721.7529	23	25	66

12211e - 02201e 628													
J	P	Obs	O-C	Unc	R	Obs	O-C	Unc	P	Obs	O-C	Unc	J
2													2
3													3
4	3684.	4838	-21	20	3690.	3787	17	18	3684.	4838	-21	22	4
5	3683.	7251	-3	10	3691.	0883	-3	18	3683.	7251	3	9	5
6	3682.	9581	-1	10	3691.	7952	-6	11	3682.	9581	-1	10	6
7					3692.	4947	-6	9					7
8					3693.	1898	-6	13					8
9	3681.	4082	-4	11	3693.	8788	-12	12	3681.	4082	-4	11	9
10	3680.	6262	6	12	3693.	8788	-12	12	3680.	6262	5	13	10
	3679.	8375	3	14	3694.	5642	2	8	3679.	8375	3	15	

12211f - 02201f 628													
J	P	Obs	O-C	Unc	R	Obs	O-C	Unc	P	Obs	O-C	Unc	J
2													2
3													3
4													4
5													5
6													6
7													7
8													8
9													9
10													10

11	3679.0435	3	7	3695.9157	1	5	3679.0435	2	10	3695.9157	-1	6	11
12	3678.2432	-7	9	3696.5836	-6	5	3678.2432	-7	9	3696.5836	-3	8	12
13	3677.4394	4	5	3697.2431	-19	28	3677.4394	3	9	3697.2431	-22	25	13
14	3676.6299	12	11	3697.9010	-4	12	3676.6299	10	18	3697.9010	-9	12	14
15	3675.8126	-4	9	3698.5527	-4	15	3675.8126	-6	4	3698.5527	-2	16	15
16	3674.9922	4	3	3699.1963	-13	19	3674.9922	1	9	3699.1963	-21	19	16
17	3673.3327	-4	9	3699.8375	-1	8	3673.3327	-23	16	3699.8375	-8	5	17
18				3700.4725	9	4		-9	9	3700.4725	-3	7	18
19				3701.1004	1	8		-7	5	3701.1004	-14	13	19
20	3671.6528	2	7	3701.7256	21	14	3671.6528	-12	16	3701.7256	3	13	20
21				3702.3433	22	17		2	29	3702.3433	1	13	21
22	3669.9506	1	16	3702.9543	12	5	3669.9506	-12	16	3702.9543	-14	6	22
23	3669.0931	18	28				3669.0931	2	29				23
24				3704.1599	-5	14							24
25	3667.3575	10	4	3704.7579	21	16	3667.3575	-15	8	3704.7579	-22	16	25
26	3666.4814	3	17	3705.3486	31	17	3666.4814	-26	17	3705.3486	-20	17	26
27	3665.5989	-13	16	3705.9320	23	15	3665.5989	-23	20	3705.9320	-36	15	27
28	3664.7158	20	20				3664.7158	17	27				28
29							3663.8289	-35	30				29
30	3662.9274	25	30	3707.6508	22	26	3662.9274	-25	25	3707.6508	-7	10	30
31	3662.0269	45	25	3708.2097	-7	8	3662.0269	-30	27	3708.2097	19	28	31
32				3708.7655	-10	22				3708.7655	0	20	32
33	3660.2004	-5	12				3660.2004						33
34	3659.2831	10	18	3709.8636	17	29	3659.2831			3709.8636	11	21	34
35				3710.3985	-26	27				3710.3985	3	9	35
36													36
37	3655.5524	0	9	3711.4616	-9	10	3655.5524	7	8	3711.4616	14	23	37
38	3654.6043	-21	15				3654.6043	23	25				38
39													39
40	3652.6982	2	13	3713.0119	-1	21	3652.6982	2	9	3713.0119	8	10	40
41	3651.7369	13	25	3713.5152	-18	14	3651.7369	2	7	3713.5152	21	30	41
42				3714.0141	-22	14				3714.0141	-2	14	42
43				3714.5103	4	26				3714.5103	17	17	43
44	3649.7937	-6	9	3714.9978	2	13	3649.7937	4	16	3714.9978	20	20	44
45	3648.8134	-21	16				3648.8134	0	21				45
46	3647.8294	-16	15				3647.8294						46
47	3646.8411	0	25				3646.8411	8	18				47
48	3645.8464	8	19				3645.8464	8	18				48
49				3716.8893	-9	21				3716.8893	8	20	49
50	3643.8391	12	18	3717.3519	33	28	3643.8391	-3	8	3717.3519	11	18	50
51	3642.8286	30	23	3717.8027	16	17	3642.8286			3717.8027			51
52													52
53										3719.2492	-4	7	53

12212 - 02201 628								
J	P	Obs	O-C	Unc	R	Obs	O-C	Unc
2								
3								
4								
5								
6								
7								
8								
9								
10								
11								
12								
13								
14								
15								
16								
17								
18								
19								
20								
21								
22								
23								
24								
25								
26								
27								
28								
29								
30								
31								
32								
33								

10012 - 00001				10011 - 00001				828						
J	P Obs	O-C Unc	R Obs	O-C Unc	P Obs	O-C Unc	R Obs	O-C Unc	J	P Obs	O-C Unc	R Obs	O-C Unc	J
0	3523.8116	-1	3525.8925	0	3636.6743	2	3638.7551	2	0	3636.6743	4	3638.7551	3	0
2	3522.9946	-2	3527.2501	-1	3635.2649	-3	3640.1208	3	2	3640.1208	4	3640.1208	6	2
4	3520.9539	-4	3528.5837	-4	3633.2649	15	3641.4687	-1	4	3641.4687	11	3641.4687	4	4
6	3519.4903	1	3529.8939	-2	3632.3957	1	3642.7996	-2	4	3642.7996	4	3642.7996	4	6
8	3518.0023	-2	3531.1805	0	3630.4579	-1	3644.1130	-1	4	3644.1130	4	3644.1130	5	8
10	3516.4910	-1	3533.4818	-2	3629.9646	7	3645.4093	-4	4	3645.4093	14	3645.4093	4	10
12	3514.9560	-1	3534.8969	1	3627.9646	24	3646.6878	-1	4	3646.6878	16	3646.6878	5	12
14	3513.8151	0	3536.0876	0	3626.4500	-3	3647.9496	-1	4	3647.9496	4	3647.9496	5	14
16	3511.8151	0	3537.2547	3	3624.9214	0	3649.1937	-2	4	3649.1937	4	3649.1937	4	16
18	3510.2091	-3	3538.3972	2	3623.8127	0	3650.4205	0	4	3650.4205	5	3650.4205	5	18
20	3508.5792	-1	3539.5159	2	3621.8127	1	3651.6303	1	4	3651.6303	4	3651.6303	4	20
22	3506.9260	-1	3540.6104	-2	3620.2336	0	3652.8228	-3	4	3652.8228	4	3652.8228	7	22
24	3505.2490	2	3541.6799	6	3618.2336	-2	3653.9976	12	19	3653.9976	5	3653.9976	7	24
26	3503.5482	4	3542.7264	5	3617.0237	-2	3656.2982	12	19	3656.2982	4	3656.2982	26	26
28	3501.8236	4	3543.7475	1	3615.3943	-1	3657.4221	11	9	3657.4221	5	3657.4221	28	28
30	3500.0749	4	3544.7159	3	3613.7487	1	3658.5282	-1	4	3658.5282	4	3658.5282	30	30
32	3498.3024	4	3545.7159	3	3612.0865	1	3659.6181	5	4	3659.6181	5	3659.6181	32	32
34	3496.5058	4	3546.6631	4	3610.4079	-1	3660.6920	0	4	3660.6920	4	3660.6920	34	34
36	3494.6848	0	3547.5856	4	3608.7136	-1	3661.7480	1	4	3661.7480	4	3661.7480	36	36
38	3492.8407	6	3548.4841	14	3607.0013	-17	3662.7880	3	4	3662.7880	17	3662.7880	38	38
40	3490.9716	4	3549.3548	-2	3605.2766	2	3663.8116	-3	4	3663.8116	4	3663.8116	40	40
42	3489.0781	0	3550.2020	-2	3603.5348	2	3664.8179	0	4	3664.8179	3	3664.8179	42	42
44	3487.1610	4	3551.8204	0	3601.7770	25	3665.8087	14	48	3665.8087	5	3665.8087	44	44
46	3485.2186	-2	3552.5906	-6	3600.0063	17	3666.7830	0	4	3666.7830	17	3666.7830	46	46
48	3483.2517	-4	3553.3360	-4	3596.4117	-1	3667.7425	-3	9	3667.7425	3	3667.7425	48	48
50	3481.2611	4	3554.0550	-6	3594.5925	-8	3668.6829	14	50	3668.6829	8	3668.6829	50	50
52	3479.2463	-1	3554.7477	-12	3592.7593	0	3669.6085	-3	9	3669.6085	6	3669.6085	52	52
54	3477.2054	-6	3555.4157	-14	3590.9118	0	3672.2935	-4	6	3672.2935	6	3672.2935	54	54
56	3475.1397	-8	3556.0568	-1	3589.0493	6	3673.1579	1	3	3673.1579	3	3673.1579	56	56
58	3473.0492	4	3556.6738	25	3587.1731	6	3674.0061	-5	12	3674.0061	12	3674.0061	58	58
60	3470.9351	-4		25			3675.6601	11	13	3675.6601	13	3675.6601	60	60
62							3676.4656	25	19	3676.4656	19	3676.4656	62	62
64							3677.2528	-2	10	3677.2528	10	3677.2528	64	64
66							3678.0267	-1	14	3678.0267	14	3678.0267	66	66
68														68
70														70
72														72
74														74
76														76
78														78

10012 - 00001 626				10011 - 00001 626			
J	P Obs	O-C Unc	R Obs	O-C Unc	P Obs	O-C Unc	J
0	3611.2754	1	3613.6172	6	3713.2152	-1	0
2	3609.6876	3	3615.1506	3	3711.6233	4	2
4	3608.0777	1	3616.6623	1	3710.0056	3	4
6	3606.4465	2	3618.1524	10	3708.3626	0	6
8	3604.7933	1	3619.6215	15	3706.6948	0	8
10	3603.1182	-2	3621.0669	3	3705.0019	0	10
12	3601.4218	-1	3622.8933	3	3703.2840	-1	12
14	3599.7036	-1	3625.2731	2	3701.5414	0	14
16	3597.9636	0	3626.6305	4	3699.7750	11	16
18	3596.2019	2	3627.9646	10	3697.9824	8	18
20	3594.4179	0	3629.2785	-14	3696.1647	0	20
22	3592.6118	-2	3630.5687	2	3694.3232	-1	22
24	3590.7841	-2	3631.8360	3	3690.5672	-1	24
26	3588.9343	0	3633.0797	9	3688.6529	-1	26
28	3587.0622	1	3634.3016	4	3686.7133	-13	28
30	3585.1675	-1	3635.4995	4	3684.7323	0	30
32	3583.2505	-1	3636.6743	4	3682.7662	-1	32
34	3581.3109	-1	3637.8252	4	3680.7229	-2	34
36	3579.3487	-1	3638.9527	4	3678.6672	-7	36
38	3577.3637	0	3640.0556	4	3676.6882	-1	38
40	3575.3558	-26	3641.1347	4	3674.5860	2	40
42	3573.3220	18	3642.1897	4	3672.4860	3	42
44	3571.2707	5	3643.2200	5	3670.3607	-1	44
46	3569.1928	5	3644.2245	4	3668.2140	5	46
48	3567.0913	4	3645.2052	4	3666.0440	1	48
50	3564.9656	-1	3646.1602	2	3663.8522	-2	50
52	3562.8169	-4	3647.0894	0	3661.6389	-1	52
54	3560.6431	-1	3647.9935	4	3659.4062	20	54
56	3556.2242	9	3648.8703	-4	3657.1483	-2	56
58	3553.9760	-3	3649.7210	-11	3654.8710	-1	58
60	3551.7039	-4	3650.5467	-1	3650.2551	-1	60
62	3549.4068	-3	3651.3452	6	3647.9176	5	62
64	3547.0844	-2	3652.8593	1	3645.5582	-9	64
66	3542.3618	-5	3653.5757	2	3643.1812	-5	66
68	3539.9618	-4	3654.2621	7	3640.7851	-1	68
70	3537.5369	12	3655.5537	13	3638.3712	12	70
72	3535.0826	0	3656.1553	-6	3635.9362	-1	72
74	3532.6027	10	3657.2737	-9	3633.4862	-3	74
76	3530.0976	19	3657.7871	1	3631.0143	27	76
78		18	3658.2711	5		25	78
80		13		-2		22	80
82		12		13		17	82
84		17		15		12	84
86		17		-15		6	86

20013 - 10002 626				20012 - 10002 626					
J	P Obs	O-C Unc	R Obs	O-C Unc	P Obs	O-C Unc	R Obs	O-C Unc	J
0			3570.5324	5 15	3690.8565	-15 22	3694.7244	10 14	0
2			3572.0533	7 15	3689.2569	3 14	3696.2125	-17 28	2
4			3573.5552	3 6			3697.6736	-2 6	4
6	3563.4615	-9 15	3575.0395	8 16			3699.1000	-10 17	6
8	3561.8400	-12 24	3576.5040	0 6	3685.9596	2 5	3700.4970	1 4	8
10	3560.2016	-1 11	3577.9509	2 13	3684.2636	-1 5			10
12	3558.5437	-4 7	3579.3786	-1 4	3682.5366	0 4			12
14	3556.8675	-6 7	3580.7878	-2 12			3703.1935	-4 7	14
16	3555.1737	-2 5	3582.1783	-2 12	3678.9885	-1 4	3704.4952	1 9	16
18			3583.5503	0 6	3677.1682	3 5	3705.7641	-6 8	18
20	3551.7304	-1 5	3584.9018	6 6	3675.3162	-1 5	3707.0026	-2 9	20
22	3549.9812	0 4	3586.2356	-1 16	3673.4340	3 5	3708.2097	-3 5	22
24	3548.2135	1 5	3587.5483	7 6	3671.5199	-4 4	3709.3835	-12 16	24
26	3546.4283	12 11		-3 5	3669.5763	1 4	3710.5280	-7 9	26
28	3544.6225	4 5			3667.5993	-24 23			28
30	3542.7980	-5 7	3590.1182	11 12	3665.5979	12 15			30
32	3540.9570	10 10	3591.3713	-3 7			3712.7232	0 3	32
34					3661.4967	4 7	3713.7740	2 7	34
36	3537.2141	0 6	3593.8203	-1 4			3714.7944	8 9	36
38	3535.3156	11 17	3595.0139	-4 6	3657.2756	-8 8	3715.7824	-2 7	38
40	3533.3953	-3 11			3655.1219	-2 6	3716.7410	0 6	40
42	3531.4571	-2 10	3597.3410	10 30	3652.9388	2 4	3717.6690	0 10	42
44	3529.4976	-18 16	3598.4708	-7 8	3650.7267	6 10			44
46	3527.5222	4 12					3719.4344	1 9	46
48			3600.6707	4 11	3646.2152	1 13	3720.2724	3 6	48
50	3523.5078	13 16			3643.9168	-4 10	3721.0802	0 11	50
52	3521.4695	9 15	3602.7837	16 13	3641.5918	4 17	3721.8581	-9 19	52
54			3603.8046	-1 10	3639.2400	20 20	3723.3289	-5 8	54
56					3636.8567	-8 11	3724.0217	0 14	56
58	3517.3301	-10 12			3634.4494	-7 11			58
60			3606.7365	2 29	3629.5575	10 15	3725.3234	13 29	60
62							3726.5128	1 12	62
64									64

20012 - 10001 626				20011 - 10001 626			
J	P Obs	O-C Unc	R Obs	O-C Unc	P Obs	O-C Unc	J
0					3712.2535	9 9	0
2							2
4					3715.2984	-2 10	4
6	3584.8596	-4 15	3593.4440	-2 13	3716.7888	-5 12	6
8	3583.2046	3 9	3594.9092	-6 17	3718.2580	-5 12	8
10	3581.5188	-5 9	3596.3466	6 10	3719.7060	-1 4	10
12	3579.8046	-5 7			3721.1323	0 4	12
14	3578.0616	0 9	3600.4792	16 15	3722.5373	4 3	14
16	3576.2890	1 7	3601.7943	-14 18	3723.9200	-1 10	16
18	3574.4863	-1 9	3603.0841	1 6	3725.2827	-6 11	18
20	3572.6554	-1 9	3604.3425	0 4	3726.6216	-2 11	20
22	3570.7951	3 7	3605.5712	2 6	3727.9411	7 9	22
24	3568.9060	13 17			3729.2398	2 4	24
26	3566.9856	6 7			3730.5159	1 4	26
28	3565.0357	-1 6	3609.0756	-5 6	3731.7713	1 4	28
30	3563.0567	-3 9	3610.1855	17 17	3733.0056	-1 3	30
32	3561.0488	-4 7			3734.2199	0 4	32
34	3559.0082	-18 23	3612.3074	-2 9	3735.4120	0 4	34
36	3556.9429	12 17	3613.3231	-3 11	3736.5838	-2 5	36
38	3554.8429	-6 7	3614.3073	-9 15	3737.7354	1 4	38
40	3552.7153	2 12	3615.2621	3 7	3738.8663	-4 9	40
42	3550.5567	3 12	3616.1841	-1 6	3739.9763	12 11	42
44			3617.0732	-8 25	3741.0681	-1 6	44
46	3546.1472	-7 22	3617.9346	4 10	3742.1369	-1 7	46
48	3543.8984	7 16	3618.7617	2 11	3743.1872	-6 13	48
50	3541.6170	3 14			3744.2171	2 10	50
52	3539.3058	10 18			3745.2287	2 10	52
54					3746.2200		54
56	3534.5843	-32 28					56
58					3748.1460	12 25	58

11112 - 01101 626				11111 - 01101 626			
J	P Obs	O-C Unc	R Obs	O-C Unc	P Obs	O-C Unc	J
1					3724.7932	2 8	1
2	3578.7568	4 7	3581.8721	2 18	3725.5614	0 6	2
3	3577.9653	-2 10	3582.6435	1 4	3726.3096	-1 4	3
4	3577.1658	-1 6	3583.3935	-10 19	3727.0701	-19 18	4
5	3576.3628	-2 6	3584.1627	3 5	3727.8002	-1 3	5
6	3575.5549	-1 4	3584.8943	2 6	3728.5583	-1 3	6
			3585.6611	1 3			
					3729.7932	2 8	
					3730.5614	0 6	
					3731.3096	-1 4	
					3732.0701	-19 18	
					3732.8002	-1 3	
					3733.5583	-1 3	



57	3526.6531	-2	8	3615.6210	2	8	3668.4829	1	10	3757.3882	-5	12	57
58	3526.4011	2	7	3616.4741	2	11	3668.1635	-4	6	3758.8181	-1	5	58
59				3618.0111	6	9	3666.1955	-2	9	3758.1805	2	9	59
60	3524.2203	12	19	3617.2999	-19	30	3665.9314	19	24	3759.6699	7	12	60
61				3618.8868	-5	10	3663.8847	-4	7	3758.9461	-8	13	61
62	3522.0138	-6	7	3618.1066	22	21				3760.4997	15	21	62
63				3619.7388	-3	11				3759.6905	19	16	63
64	3519.7869	4	10	3620.5667	10	19	3661.5507	-4	10	3761.3059	5	7	64
65							3661.3992	1	9	3760.4069	12	11	65
66	3517.5362	8	15	3621.3661	-8	25	3659.1027	-8	11	3762.0911	2	14	66
67										3761.0983	5	21	67
68	3515.2616	9	17				3654.4107	1	9	3762.8554	5	21	68
69							3654.4540	13	14	3761.7666	3	14	69
70	3512.9614	-9	24				3651.9858	10	24	3763.5982	6	30	70
71										3762.4114	13	16	71
72													72
73													73
74													74
75													75

12212 - 02201 626													12211 - 02201 626												
J	P Obs	O-C	Unc	R Obs	O-C	Unc	P Obs	O-C	Unc	R Obs	O-C	Unc	J	P Obs	O-C	Unc	R Obs	O-C	Unc	J	P Obs	O-C	Unc		
2				3555.1737	-3	5							2				3730.4698	-1	15	2					
3				3555.9345	-9	29							3				3731.2156	-1	11	3					
4													4				3731.9534	-13	13	4					
5													5				3732.6885	-7	10	5					
6													6				3733.4139	-5	7	6					
7													7				3734.1352	-4	7	7					
8													8							8					
9													9				3735.5574	7	5	9					
10													10				3736.2573	-5	6	10					
11													11							11					
12													12							12					
13													13							13					
14													14							14					
15													15							15					
16													16							16					
17													17							17					
18													18							18					
19													19							19					
20													20							20					
21													21							21					
22													22							22					
23													23							23					

24	3532.5593	0 13	3570.6578	-8 7	3706.1212	3 4	3744.1809	8 10	24
25	3531.6418	17 15	3571.9356	3 7	3705.1924	3 3	3745.4109	-6 8	25
26	3530.7293	5 13			3704.2485	1 5	3746.0250	-5 7	26
27	3529.7978	8 12					3746.6179	5 5	27
28			3573.1917	13 16	3702.3509	-2 12	3747.2213	3 1	28
29	3527.9334	9 14	3573.7975	-2 15	3701.4006	0 7	3747.7979	3 1	29
30	3527.0045	-2 11	3574.4240	3 10	3700.4290	0 6	3748.3917	1 1	30
31	3526.0460	-5 6			3699.4691	0 8	3748.9513	-13 18	31
32	3525.1126	15 24			3698.4821	-1 8	3749.5366	-7 5	32
33							3750.0824	-1 5	33
34	3523.1954	-11 11	3576.8248	-4 6	3696.5101	-6 12	3750.6582	2 8	34
35	3522.2094	-9 28	3577.3888	-1 13	3695.5323	-4 7			35
36	3521.2609	1 7	3577.9942	9 12	3694.5149	4 7			36
37	3520.2598	-3 8	3578.5416	1 8			3751.7524	-15 13	37
38	3519.3050	9 11	3579.1395	0 18	3692.4946	9 8	3752.2635	-1 8	38
39	3518.2884	1 10	3579.6711	-5 19	3691.5002	-2 5	3752.8251	1 8	39
40			3580.2638	2 10	3690.4490	8 10	3753.3161	1 8	40
41	3516.2963	12 19			3689.4494	9 17	3753.8707	-6 9	41
42	3515.3268	1 9	3581.3659	3 25	3688.3794	13 14	3754.3433	6 13	42
43					3687.3720	-9 11	3754.8936	0 11	43
44	3513.3068	10 21			3686.2832	-2 9	3755.3437	0 11	44
45					3685.2733	-5 7	3755.8896	-5 11	45
46	3511.2625	-5 12	3583.5015	-7 15			3756.3193	-3 9	46
47			3584.5363	1 12	3683.1526	13 13	3756.8623	-4 9	47
48					3682.0187	-16 13	3757.2687	2 10	48
49			3585.5469	1 12	3681.0063	8 11	3757.8119	10 14	49
50									50
51					3677.6581	-11 20	3758.7363	16 17	51
52					3676.6460	13 17	3759.0887	-14 16	52
53							3759.6344	1 12	53
54							3759.9622	0 17	54
55									55
56							3760.8077	-7 13	56

-----				
21111 - 11101 626				
-----				
J	P Obs	O-C Unc	R Obs	O-C Unc
-----				
1				
2				
3	3711.3599	-13 26	3716.0369	-2 13
4	3710.5589	2 23		
5	3709.7585	10 15	3717.5534	-1 24
6	3708.9437	-10 18		
7	3708.1296	-2 11	3719.0481	-1 23
8			3719.7539	19 20
			3720.5210	-1 7

9	3703.1057	22 27	3724.0217	0 14	3721.1999	5 12
10	3702.2730	1 18	3725.8094	0 11		
11			3725.3961	-6 21		
12			3726.1942	-11 20		
13	3700.5512	0 18	3726.7498	-21 26		
14	3699.6325	-12 14	3727.5611	16 19		
15	3698.8096	14 21	3728.0740	-5 11		
16			3728.9016	-5 11		
17			3729.3775	-2 10		
18			3730.2228	-2 14		
19	3697.0434	-5 29	3730.6567	-6 16		
20	3696.0694	2 26				
21			3731.9118	9 17		
22	3694.2521	4 9	3732.7998	-1 11		
23	3693.4521	5 20	3733.1404	-13 18		
24	3692.4121	13 25	3734.0561	1 24		
25	3691.6245	8 20	3734.3486	0 19		
26						
27	3689.7740	-9 15				
28			3735.5314	-2 18		
29	3687.9039	-12 21	3736.5041	3 11		
30	3686.7476	-7 17	3736.6922	14 30		
31			3737.6946	-10 28		
32						
33						
34	3684.1020	-12 28				
35						
36			3738.8663	3 6		
37	3680.8776	-6 16				
38	3680.2194	6 12				
39	3678.8765	6 17				
40	3678.2458	-1 12	3741.1419	-13 16		

APPENDIX C  
Computer Program Listings

## Software Listings

CONTST - Performs control and data acquisition for the AFGL High Resolution Interferometer . . .	281
FILFIX - Performs phase correction and numerical filtering on a single sided interferogram . .	293
BIGFFT - A Fast Fourier Transform (FFT) program which can be used to transform a data set larger than will fit into the central memory of a computer . . . . .	307
REGFIT - An interactive rotation-vibration line assignment program . . . . .	317

/CONTST

PAL8-V7

```

/CONTST
/PROGRAM FOR DIGITAL CONTROL OF INTERFEROMETER.
/ 9/18/80
/EXTERNAL SUBROUTINES NEEDED: LAB8C,PLOT,PLTRTE,
/MTHLE,MAXCKB,LAB8E,WERI,PRISUB.
6007 CAF=6007
6732 MCAF=6732
7443 DAD=7443
7445 DST=7445
7621 CAM=7621
7763 DLD=7763
7765 DDZ=7765
7431 SWAB=7431
7415 ASR=7415
0010 *10
00010 0000 ERRPOI,0
0200 *200
00200 7000 NOP
00201 4777' JMS START
00202 4776' CONT1,JMS INITL
00203 4775' CONT2,JMS SETCR
00204 7000 NOP
00205 4774' JMS STEP
00206 4773' BUFWR,JMS AREAD
00207 4772' JMS BUFWRT
00210 2771' ISZ WCC
00211 5203 JMP CONT2

00212 7300 DUMP,CLL CLA
00213 4632 JMS I POUT
00214 2000 2000
00215 7777 7777
00216 4631 JMS I MTWRT
00217 5400 5400
00220 4633 JMS I PLOTB
00221 2770' ISZ RCNTR
00222 5224 JMP R1
00223 5227 JMP R2
00224 7300 R1,CLA CLL
00225 4767' JMS CHKB
00226 5202 JMP CONT1
00227 4766' R2,JMS FINISH
00230 7402 HLT

00231 4431 MTWRT,4431
00232 5021 POUT,5021
00233 1600 PLOTB,1600
```

```

/SUBROUTINE WRERR
/WRITES INFORMATION TO FIELD TWO WHEN AN
/ERROR OCCURES.
/NOTE ERRPOI IS AUTO INCREMENT
/STORED IN THIS ORDER
/RECORD, STEP, STEP MAX, STEP MIN,
/HOLD MAX, LENGTH OF STEP, HOLD MIN.

```

```

00234 0000 WRERR,0
00235 7300 CLA CLL
00236 2273 ISZ ECOUNT
00237 5245 JMP WRE2
00240 1365 TAD (2777
00241 3010 DCA ERRPOI
00242 2274 ISZ EPAGE
00243 1364 TAD (-555
00244 3273 DCA ECOUNT
00245 1763' WRE2,TAD RCNR
00246 7041 CIA
00247 7001 IAC
00250 1770' TAD RCNTR
00251 6221 6221
00252 3410 DCA I ERRPOI
00253 1275 TAD NUMSTP
00254 3410 DCA I ERRPOI
00255 1276 TAD STPMAX
00256 3410 DCA I ERRPOI
00257 1277 TAD STPMIN
00260 3410 DCA I ERRPOI
00261 1300 TAD STPLEN
00262 3410 DCA I ERRPOI
00263 1301 TAD HLDMAX
00264 3410 DCA I ERRFOI
00265 1302 TAD HLDMIN
00266 3410 DCA I ERRPOI
00267 6201 6201
00270 3301 DCA HLDMAX
00271 3302 DCA HLDMIN
00272 5634 JMP I WRERR

```

```

00273 0000 ECOUNT,0
00274 0000 EPAGE,0
00275 0000 NUMSTP,0
00276 0000 STPMAX,0
00277 0000 STPMIN,0
00300 0000 STPLEN,0
00301 0000 HLDMAX,0
00302 0000 HLDMIN,0

```

/ROUTINE HOLER

00303	7300	HOLER,CLA CLL
00304	1334	TAD TWOTH
00305	3311	DCA RBUF
00306	4736	JMS I ADBUF1
00307	0000	0
00310	6000	6000
00311	0000	RBUF,0
00312	7300	CLA CLL
00313	1334	TAD TWOTH
00314	3320	DCA MBU1
00315	1334	TAD TWOTH
00316	3321	DCA MBU2
00317	4735	JMS I MAXMIN
00320	0000	MBU1,0
00321	0000	MBU2,0
00322	7300	CLA CLL
00323	1320	TAD MBU1
00324	3301	DCA HLDMAX
00325	1321	TAD MBU2
00326	3302	DCA HLDMIN
00327	4234	JMS WRERR
00330	7300	CLA CLL
00331	3301	DCA HLDMAX
00332	3302	DCA HLDMIN
00333	5762	JMP AREAD2

00334	2000	TWOTH,2000
00335	5400	MAXMIN,5400
00336	5102	ADBUF1,5102

00362	0436
00363	0647
00364	7223
00365	2777
00366	1000
00367	1007
00370	0645
00371	0663
00372	1063
00373	0435
00374	0676
00375	0664
00376	0652
00377	0617

0400 \*400

/ROUTINE STERR

```
00400 7300 STERR,CLA CLL
00401 1377 TAD (-240
00402 1776' TAD STPLEN
00403 7700 SMA CLA
00404 5227 JMP TOOLG
00405 1376 TAD (300
00406 1775' TAD STPMIN
00407 7700 SMA CLA
00410 5225 JMP NONRE
00411 1374 TAD (-300
00412 1773' TAD STPMAX
00413 7500 SMA
00414 5225 JMP NONRE
00415 7300 RECOV,CLA CLL /RECOVERABLE STEP ERROR
00416 1372 TAD (777
00417 3771' DCA HLDMAX /TO SHOW RECOVERED
00420 4770' JMS WRERR
00421 7040 CMA
00422 1767' TAD NUMSTP
00423 3767' DCA NUMSTP
00424 5766' JMP STEP2
00425 4770' NONRE,JMS WRERR /NON RECOVERABLE
00426 5765' JMP BUFWR

00427 7300 TOOLG,CLA CLL /TOOK TOO LONG TO STEP
00430 1776' TAD STPLEN /CHECK TO SEE IF IT WAS 2777
00431 1364 TAD (-2777
00432 7440 SZA
00433 5225 JMP NONRE
00434 5215 JMP RECOV

00435 0000 AREAD,0
00436 4763' AREAD2,JMS CLRSUM
00437 1311 TAD CHPCNT
00440 3312 DCA WWC
00441 4714 JMS I RADCK
00442 0000 0
00443 7500 7500
00444 0350 350
00445 5762' JMP HOLER
00446 7300 C1,CLA CLL
00447 6007 CAF
00450 4716 JMS I CLIO2
00451 4713 JMS I PINAD
00452 0000 0
00453 4000 4000
00454 5762' JMP HOLER
00455 4717 JMS I MICRO
00456 7770 7770
```

00457	4715	JMS I POUT2
00460	1000	1000
00461	7776	7776
00462	4761	JMS ADSUM
00463	0001	1
00464	7750	7750
00465	4715	JMS I POUT2
00466	1000	1000
00467	7776	7776
00470	4714	JMS I RADCK
00471	0000	0
00472	7756	7756
00473	0150	150
00474	5762	JMP HOLER
00475	4715	JMS I POUT2
00476	1000	1000
00477	7777	7777
00500	4761	JMS ADSUM
00501	0002	2
00502	7750	7750
00503	4715	JMS I POUT2
00504	1000	1000
00505	7776	7776
00506	2312	ISZ WWC
00507	5246	JMP C1
00510	5635	JMP I AREAD
00511	7764	CHPCNT,7764
00512	0000	WWC,0
00513	5132	PINAD,5132
00514	5301	RADCK,5301
00515	5021	POUT2,5021
00516	5056	CLIO2,5056
00517	5045	MICRO,5045
00520	5065	ADREA,5065
00561	1025	
00562	0303	
00563	1056	
00564	5001	
00565	0206	
00566	0677	
00567	0275	
00570	0234	
00571	0301	
00572	0777	
00573	0276	
00574	7500	
00575	0277	
00576	0300	
00577	7540	

	0600	*600
00600	0000	INITS,0
00601	7300	CLA CLL
00602	3215	DCA PNTR
00603	1214	TAD WC2
00604	3216	DCA CNTR
00605	6221	6221
00606	3615	DCA I PNTR
00607	6201	6201
00610	2215	ISZ PNTR
00611	2216	ISZ CNTR
00612	5205	JMP .-5
00613	5600	JMP I INITS
00614	5400	WC2,5400
00615	0000	PNTR,0
00616	0000	CNTR,0
00617	0000	START,0
00620	7300	CLA CLL
00621	6032	KCC
00622	6031	KSF
00623	5222	JMP .-1
00624	6036	KRB
00625	6046	TLS
00626	6041	TSF
00627	5226	JMP .-1
00630	7300	CLA CLL
00631	6732	MCAF
00632	4646	JMS I REWIND
00633	7300	CLA CLL
00634	1377	TAD (2777
00635	3010	DCA ERRPOI
00636	1376	TAD (-555
00637	3775'	DCA ECOUNT
00640	1247	TAD RCNR
00641	3245	DCA RCNTR
00642	3250	DCA CKK
00643	3651	DCA I ERCOUN
00644	5617	JMP I START
00645	0000	RCNTR,0
00646	4506	REWIND,4506
00647	4000	RCNR,4000
00650	0000	CKK,0
00651	4453	ERCOUN,4453
00652	0000	INITL,0
00653	7300	CLA CLL
00654	3774'	DCA B2PNTR
00655	3773'	DCA NUMSTP
00656	1372	TAD (6600
00657	3263	DCA WCC

AD-A173 808

CARBON DIOXIDE LINE POSITIONS IN THE 28 AND 43 MICRON  
REGIONS AT 800 KELV. (U) UTAH STATE UNIV BEDFORD WA  
STEMART RADIANCE LAB M P ESPLIN ET AL. 19 FEB 86

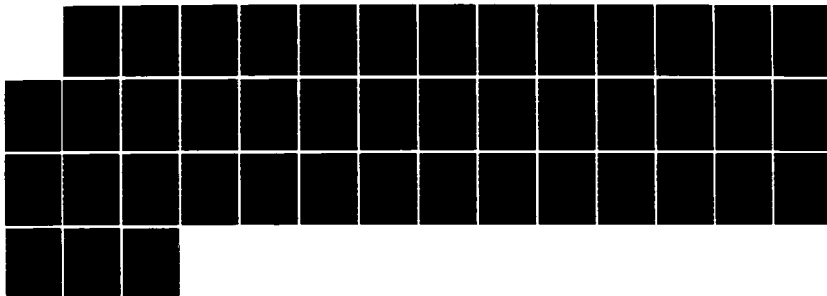
4/4

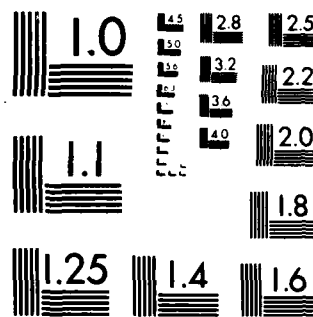
UNCLASSIFIED

SCIENTIFIC-16 AFGL-TR-86-0046

F/G 7/4

NL





MICROCOPY RESOLUTION TEST CHART  
NATIONAL BUREAU OF STANDARDS 1963 A

00660	4200	JMS INITS
00661	4267	JMS CLIO
00662	5652	JMP I INITL
00663	0000	WCC,0
00664	0000	SETCR,0
00665	7200	CLA
00666	5664	JMP I SETCR
00667	0000	CLIO,0
00670	7300	CLA CLL
00671	7040	CMA
00672	6503	6503
00673	6505	6505
00674	6500	6500
00675	5667	JMP I CLIO
00676	0000	STEP,0
00677	7300	STEP2,CLA CLL
00700	2773	ISZ NUMSTP
00701	4744	JMS I POUT3
00702	4000	4000
00703	7740	7740
00704	4267	JMS CLIO
00705	4745	JMS I PNADM
00706	0000	0
00707	2000	2000
00710	0000	A1,0
00711	0000	A2,0
00712	0000	NUM,0
00713	7300	CLA CLL
00714	1312	TAD NUM
00715	3771	DCA STPLEN
00716	1310	TAD A1
00717	3770	DCA STPMAX
00720	1311	TAD A2
00721	3767	DCA STPMIN
00722	1310	TAD A1
00723	7041	CIA
00724	1346	TAD MAXA
00725	7700	SMA CLA
00726	5342	JMP STPERR /NO MAX
00727	1347	TAD MINA
00730	7041	CIA
00731	1311	TAD A2
00732	7700	SMA CLA
00733	5342	JMP STPERR /NO MIN
00734	1350	TAD MAXNUM
00735	7041	CIA
00736	1312	TAD NUM
00737	7700	SMA CLA
00740	5342	JMP STPERR /TOOK TOO LONG

00741 5676 JMP I STEP  
 00742 5766' STPERR,JMP STERR  
 00743 5676 JMP I STEP

00744 5021 POUT3,5021  
 00745 5200 PNADM,5200  
 00746 0200 MAXA,200  
 00747 7550 MINA,7550  
 00750 1000 MAXNUM,1000

00766 0400  
 00767 0277  
 00770 0276  
 00771 0300  
 00772 6600  
 00773 0275  
 00774 1076  
 00775 0273  
 00776 7223  
 00777 2777

1000 \*1000  
 01000 0000 FINISH,0  
 01001 7300 CLA CLL  
 01002 4606 JMS I WRTEOF  
 01003 7300 CLA CLL  
 01004 1777' TAD RCNTR  
 01005 5600 JMP I FINISH  
 01006 4517 WRTEOF,4517

01007 0000 CHKB,0  
 01010 6036 KRB  
 01011 1215 TAD NEGS  
 01012 7440 SZA  
 01013 5216 JMP RR  
 01014 5776' JMP R2

01015 7455 NEGS,7455

01016 7300 RR,CLA CLL  
 01017 4624 JMS I ADREDD  
 01020 0004 0004  
 01021 0000 IIC,0  
 01022 7300 CLA CLL  
 01023 5607 JMP I CHKB

01024 5065 ADREDD,5065

/SUBROUTINE ADSUM  
 /READS DATA FROM A/D CHANAL ARG1 AND SUMS  
 /DOUBLE PRECISION TO AAM.  
 /ARG2 IS WORD COUNT (TWO'S COMPLEMENT)

01025 0000 ADSUM,0  
 01026 1625 TAD I ADSUM

01027	6531	6531
01030	6532	6532
01031	2225	ISZ ADSUM
01032	1625	TAD I ADSUM
01033	3253	DCA WBC
01034	2225	ISZ ADSUM
01035	7431	SWAB
01036	6534	CKAD,6534
01037	5236	JMP CKAD
01040	6533	6533
01041	6532	6532
01042	7415	ASR
01043	0014	14
01044	7443	DAD
01045	1054	AAM
01046	7445	DST
01047	1054	AAM
01050	2253	ISZ WBC
01051	5236	JMP CKAD
01052	5625	JMP I ADSUM

01053	0000	WBC,0
01054	0000	AAM,0
01055	0000	AAM2,0

/SUBROUTINE CLRSUM  
/CLEARS DOUBLE PRECISION AAM.

01056	0000	CLRSUM,0
01057	7431	SWAB
01060	7765	DDZ
01061	1054	AAM
01062	5656	JMP I CLRSUM

/SUBROUTINE BUFVRT  
/WRITES AAM TO BUFFER

01063	0000	BUFVRT,0
01064	7300	CLA CLL
01065	1255	TAD AAM2
01066	6221	6221
01067	3676	DCA I B2PNTR
01070	2276	ISZ B2PNTR
01071	1254	TAD AAM
01072	3676	DCA I B2PNTR
01073	2276	ISZ B2PNTR
01074	6201	6201
01075	5663	JMP I BUFVRT

01076	0000	B2PNTR,0
01176	0227	
01177	0645	

\$

/LAB8C

PAL8-V7

/LAB8C

/SUBROUTINE PNADM (READ A/D AND FIND MAX

/AND MIN WHILE WAITING FOR A FLAG)

/ARG1 IS A/D CHANAL, ARG2 IS WHICH FLAG

/ARG3 IS MAX, ARG4 IS MIN, ARG5 IS LENGTH

	5200	*5200	
05200	0000	PNADM,0	
05201	7300	CLA CLL	
05202	1600	TAD I PNADM	
05203	6531	6531	
05204	6532	6532	
05205	2200	ISZ PNADM	
05206	1600	TAD I PNADM	
05207	3277	DCA PIN	
05210	2200	ISZ PNADM	
05211	1377	TAD (2000	
05212	3275	DCA MIN	
05213	1376	TAD (-2000	
05214	3274	DCA MAX	
05215	3276	DCA LENGTH	
05216	6502	PINCK,6502	
05217	5240	JMP ADCK	
05220	6504	6504	
05221	6503	6503	
05222	0277	AND PIN	
05223	7450	SNA	
05224	5240	JMP ADCK	
05225	7300	RET,CLA CLL /RETURN	
05226	1274	TAD MAX	
05227	3600	DCA I PNADM	
05230	2200	ISZ PNADM	
05231	1275	TAD MIN	
05232	3600	DCA I PNADM	
05233	2200	ISZ PNADM	
05234	1276	TAD LENGTH	
05235	3600	DCA I PNADM	
05236	2200	ISZ PNADM	
05237	5600	JMP I PNADM	
05240	6534	ADCK,6534	
05241	5216	JMP PINCK	
05242	6533	6533	
05243	3300	DCA POINT	
05244	6532	6532	/START A/D AGAIN
05245	2276	ISZ LENGTH	
05246	5253	JMP .+5	
05247	7300	CLA CLL	

05250	1375	TAD (2777
05251	3276	DCA LENGTH
05252	5225	JMP RET
05253	1274	TAD MAX
05254	7041	CIA
05255	1300	TAD POINT
05256	7700	SMA CLA
05257	5266	JMP LAR
05260	1275	TS,TAD MIN
05261	7041	CIA
05262	1300	TAD POINT
05263	7710	SPA CLA
05264	5271	JMP SML
05265	5216	JMP PINCK
05266	1300	LAR,TAD POINT
05267	3274	DCA MAX
05270	5260	JMP TS
05271	1300	SML,TAD POINT
05272	3275	DCA MIN
05273	5216	JMP PINCK
05274	0000	MAX,0
05275	0000	MIN,0
05276	0000	LENGTH,0
05277	0000	PIN,0
05300	0000	POINT,0

```

/SUBROUTINE RADCK (READ A/D AND CHECK
/FOR ERRORS)
/ARG1 IS A/D CHANAL
/ARG2 IS WORD COUNT (TWO'S COMPLEMENT)
/ARG3 IS MAX ALLOWED DIFFERENCE
/RETURN AT ARG3+1 IF A/D VALUE OUTSIDE
/OF RANGE.
/RETURN AT ARG3+2  NORMAL RETURN

```

05301	0000	RADCK,0
05302	7300	CLA CLL
05303	1701	TAD I RADCK
05304	6531	6531
05305	6532	6532
05306	2301	ISZ RADCK
05307	1701	TAD I RADCK
05310	3340	DCA COUNT
05311	2301	ISZ RADCK
05312	1701	TAD I RADCK
05313	3341	DCA MAXR
05314	2301	ISZ RADCK
05315	1341	TAD MAXR
05316	7041	CIA
05317	3342	DCA NMAX

05320	6534	CKAD,6534
05321	5320	JMP CKAD
05322	6533	6533
05323	6532	6532
05324	1342	TAD NMAX
05325	7500	SMA
05326	5337	JMP ERR /TOO LARGE
05327	1341	TAD MAXR
05330	1341	TAD MAXR
05331	7510	SPA
05332	5337	JMP ERR /TOO SMALL
05333	2340	ISZ COUNT
05334	5320	JMP CKAD

05335	2301	ISZ RADCK
05336	5701	JMP I RADCK

05337	5701	ERR, JMP I RADCK
-------	------	------------------

05340	0000	COUNT,0
05341	0000	MAXR,0
05342	0000	NMAX,0
05375	2777	
05376	6000	
05377	2000	

\$

# PROGRAM FILFIX

This program is used for phase correction and numerical filtering.

```

PROGRAM FILFIX(INPUT,OUTPUT,TAPE5=INPUT,TAPE6=OUTPUT,
1 TAPE1,TAPE2,TAPE9)
  DIMENSION A(4096),B(512),OUT(512),S(512)
  DIMENSION IB(512),DBUF(256)
  COMMON BUF(640),INV(512)
  EQUIVALENCE (BUF(1),S(1)),(INV(1),DBUF(1))
  EQUIVALENCE (IA,A),(IB,B)
C   THIS PROGRAM CAN BE USED WITH EITHER A NORMAL OR AN
C   INVERTED INTERFEROGRAM.
  DATA DOL/'$'/
  L=4096
  NE=8
  NEC=0
200 WRITE(6,104)
104 FORMAT(* ENTER M, N, LASER*,/)
      '5,*) M,N,LASER
      *M
      M=-2*M
      M34=M4-M
      M21=M2+1
      WAVMAX=7899.000598/LASER
C   M=NUMBER OF REAL POINTS IN CORRECTION FUNCTION (ONE SIDE)
C   N=NUMBER OF POINTS IN EVEN INTERFEROGRAM
C   L=NUMBER OF INTERFEROGRAM POINTS HELD IN MEMORY.
  WRITE(6,105)
105 FORMAT(* ENTER NUMBER OF PIECES, WHICH PIECE *,/)
  READ(5,*) NF,NP
C   THE FREE SPECTRAL RANGE IS DIVIDED INTO "NF" EQUAL PIECES.
C   ONLY THE "NP" PIECE IS PROCESSED.
C   ALL SPECTRAL FREQUENCIES WHICH ARE NOT IN THE "NP" PIECE MUST BE
C   FILTERED OUT OR ALIASING WILL OCCUR.
      (see reference 32 page 85)
40  WRITE(6,106)
106 FORMAT(* ENTER FILTER ON, OFF*,/)
  READ(5,*) ON,OFF
  IONM=2*IFIX(M*ON/WAVMAX+.5)
  MWID=2*IFIX(M*OFF/WAVMAX+.5)-IONM+2
  WFI=WAVMAX/M2
  FON=WFI*IONM
  FOFF=WFI*(IONM+MWID-2)
  WRITE(6,120) FON,FOFF
120 FORMAT(* FILTER FROM*,F8.2,* TO*,F8.2,* ENTER 1 TO CONTINUE*,/)
  READ(5,*) ICON
  IF(ICON.NE.1) GO TO 40
  WRITE(6,100) M,N,L
100 FORMAT(* M=*,I5,* N=*,I7,* L=*,I5)
  TM=FLOAT(L)/FLOAT(M)
  IF((TM-FLOAT(L/M)).NE.0) GO TO 50
  IF(M.LT.16) GO TO 53
  IF(L.LE.M2) GO TO 54
  WRITE(6,501)
501 FORMAT(* ENTER TITLE*,/)
  READ(5,502) TITLE
502 FORMAT(A7)
  AE=0.
  NUM=N/NF
  IREV=1+(-1)**NP
  STEP=WAVMAX/N
  STARTO=0
  IF(NP.NE.1) STARTO=WAVMAX*(NP-1)/FLOAT(NF)+STEP
  WRITE(2,500) DOL,TITLE,NUM,IREV,AE,STEP,STARTO
500 FORMAT(A1,A7,2I8,3E18.11)
  CALL RTADEC(A,BUF,DBUF,1,1,1,L,IUNIT)
  IF(IUNIT.NE.-1) GO TO 115

```

```

SUM=0.
AMAX=-1.0E+30
DO 30 I=1,L
X=A(I)
SUM=SUM+X
IF(X.LT.AMAX) GO TO 30
AMAX=X
IMAX=I
30 CONTINUE
NME=M2
AV=SUM/L
NE2=NE*2
IF((NME*NE2).GT.L) NME=L/NE2
C MOVE MAX TO MIDDLE OF NME
J=IMAX-NME/2
DO 32 I=1,NME
A(I)=A(J)-AV
32 J=J+1
CALL EXPAND(A,S,INV,NME,NE)
NNE=NME*NE
CALL XMXMN(A,XMAX,IMX,XMIN,IMN,NNE)
IF(XMAX.GT.(ABS(XMIN))) GO TO 34
NEG=1
IMX=IMN
34 PM=IMAX-NME/2+FLOAT(IMX-1)/NE
IMAX=PM+.5
AMAX=A(IMX)
WRITE(6,102) AMAX,PM,AV
102 FORMAT(/, * MAX IS * F10.3, * AT * F10.3, * AV=*, F10.3,/)
CALL RTADEC(A,BUF,DBUF,1,1,1,L,IUNIT)
IF(IUNIT.NE.-1) GO TO 115
J=IMAX-M
DO 1 I=1,M2
A(I)=A(J)-AV
1 J=J+1
IF(NEG.LE.0) GO TO 18
DO 13 I=1,M2
A(I)=-A(I)
13 C PREPARE FOR TRANSFORM
18 CALL APTD(A,M)
CALL PREHAR(A,M2)
MH=LOG2(M2)
CALL HARM1D(A,MH,INV,S,1,IER)
IF(IER.NE.0) WRITE(6,110) IER
WRITE(9,103) (A(I),I=1,M2)
110 C FORMAT(/, * ERROR CONDITION*,I3,/)
C GET CORRECTION AND FILTER IT
ISA=1
ISO=IONM
CALL ZERO(A,ISA,ISO)
ISA=ISO+1
ISO=ISO+MWID
CALL MHER(A,ISA,ISO)
ISA=ISO+1
ISO=M2+2
CALL ZERO(A,ISA,ISO)
C NEGATIVE PART
J=M4-1
DO 4 I=3,M2,2
A(J)=A(I)
A(J+1)=-A(I+1)
4 J=J-2
C TRANSFORM BACK TO INTERFEROGRAM DOMAIN
WRITE(9,103) (A(I),I=1,M2)
DO 15 I=1,M2,2
I2=I+1
IB(I)=0
IF(ABS(A(I)).LT.1.E-3) GO TO 15

```

```

15      IB(I)=572.958*ATAN(A(I2)/A(I))+.5
      CONTINUE
C      WRITE OUT PHASE FUNCTION
      WRITE(9,101) (IB(I),I=1,M2,2)
101     FORMAT(16I5)
      CALL HARMID(A,MH,INV,S,-2,IER)
      IF(IER.NE.0) WRITE(6,110) IER
C      PULL OUT AND REVERSE REAL PART
      J=M2+1
      MT=M+1
      DO 5 I=1,MT
        B(I)=A(J)
5       J=J-2
        J=M4-1
        MT=MT+1
        DO 6 IJ=MT,M2
          B(IJ)=A(J)
6       J=J-2
      CALL APTD(B,M)
C      SCALE B SO THAT THE MAX IS ABOUT 100,000
      BSCAL=100000./ABS(AMAX)
      CALL BNORM(B,M2,BAV,BSCAL)
C      READ IN INTERFEROGRAM
      CALL RTADEC(A,BUF,DBUF,1,1,1,L,IUNIT)
      IF(IUNIT.NE.-1) GO TO 115
      DO 7 I=1,L
        A(I)=A(I)-AV
        IF(NEG.LE.0) GO TO 78
7       DO 73 I=1,L
        A(I)=-A(I)
73      C      NS=POINT AT WHICH TO START CONVOLUTING
      NS=IMAX
C      NCOUN=NUMBER OF POINTS CONVOLUTED
      NCOUN=0
C      NM=NUMBER OF POINTS OUTPUTED
      NM=N/NF
C      IOUTBU TELLS HOW MANY POINTS IN OUT BUFF-1
      IOUTBU=1
8       CALL CONVOL(A,B,OUT,IOUTBU,M,L,NS,NF,NCOUN)
      IF(NCOUN.GE.NM) GO TO 9
      CALL REFILL(A,IA,M,NM,L,NF,AV,NEG,NCOUN)
      GO TO 8
9       IF(IOUTBU.EQ.1) STOP
      IOUTBU=IOUTBU-1
      WRITE(2,103) (OUT(I),I=1,IOUTBU)
103     FORMAT(8F10.3)
      STOP
50      WRITE(6,111)
111     FORMAT(/,*, INCOMPATIBLE L, M:  M SHOULD BE A FACTOR OF L*)
      GO TO 200
115     WRITE(6,116)
116     FORMAT(* BAD TAPE1 *)
      STOP
53      WRITE(6,113)
113     FORMAT(* M MUST BE GREATER THAN OR EQUAL TO 16*)
      GO TO 200
54      WRITE(6,114)
114     FORMAT(* L MUST BE LARGER THAN 2 TIMES M *)
      GO TO 200
      END
C      SUBROUTINE BNORM(A,N,AV,BSCAL)
      DIMENSION A(1)
      SUM=0.
      DO 1 I=1,N
        SUM=SUM+A(I)
1       R=N
      AV=SUM/R

```

```

2      DO 2 I=1,N
      A(I)=BSCAL*(A(I)-AV)
      RETURN
      END
C
      SUBROUTINE ZERO(A,ISA,ISO)
      DIMENSION A(1)
      IF(ISA.GE.ISO) RETURN
      DO 1 I=ISA,ISO
      1  A(I)=0.
      RETURN
      END
C
      SUBROUTINE MHER(A,ISA,ISO)
      DIMENSION A(1)
      IF(ISA.GE.ISO) RETURN
      DO 1 I=ISA,ISO,2
      I1=I+1
      AMOD=SQRT(A(I)**2+A(I1)**2)
      IF(AMOD.LE.1.E-6) GO TO 1
      A(I)=A(I)/AMOD
      A(I1)=-A(I1)/AMOD
      1  CONTINUE
      RETURN
      END
C
      SUBROUTINE REFILL(A,IA,M,NM,L,NF,AV,NEG,NCOUN)
      C THIS ROUTINE REFILLS THE INPUT BUFFER.
      DIMENSION A(1),IA(1)
      COMMON BUF(640),DBUF(512)
      M2=2*M
      C NCOUN=NUMBER OF POINTS CONVOLUTED
      C IF AT END FILLS WITH ZEROS
      C NREAD=NUMBER OF POINTS LEFT TO READ + M2
      C NOTE THERE IS ALREADY M POINTS LOADED WHEN REFILL IS CALLED
      NREAD=(NM-NCOUN+1)*NF+M
      C COULD READ NF-1 POINTS MORE THAN N PAST ZERO
      C PATH DIFFERENCE.
      C LEREAD IS LAST POINT TO BE READ
      LEREAD=L
      IF(LEREAD.GT.NREAD) LEREAD=NREAD
      C SHIFT UNCONVOLUTED PART TO LEFT
      J=L-M2
      DO 1 I=1,M2
      J=J+1
      1  A(I)=A(J)
      C FILL A(I)
      MS=M2+1
      IF(LEREAD.LT.MS) GO TO 3
      IF(IOF.NE.1) GO TO 12
      LEREAD=MS
      GO TO 3
      12 CALL RTADEC(A,BUF,DBUF,1,0,MS,LEREAD,IUNIT)
      IF(IUNIT) 15,16,17
      16 IOF=1
      LEREAD=I
      15 IF(NEG.GT.0) GO TO 10
      DO 2 I=MS,LEREAD
      2  A(I)=A(I)-AV
      GO TO 30
      C INVERTED INTERFEROGRAM
      10 DO 20 I=MS,LEREAD
      20 A(I)=-A(I)+AV
      30 IF(LEREAD.GE.L) RETURN
      C FILL REST OF WAY WITH ZERO'S
      3  NI=LEREAD
      4  DO 4 I=NI,L
      A(I)=0.

```

```

17      RETURN
110     WRITE(6,110) NCOUN
      FORMAT(* PARITY ERROR AT*,I10)
      STOP
      END

C
      SUBROUTINE CONVOL(A,B,OUT,IOUTBU,M,L,NS,NF,NCOUN)
      DIMENSION A(1),B(1),OUT(1)
C      NS=NUMBER TO START CONVOLUTION
C      NF=REDUCTION IN SIZE FROM INPUT TO OUTPUT
C      NM=NUMBER OF POINTS ON OUTPUT OF CONVOLUTION
C      NCOUN=NUMBER OF POINTS CONVOLUTED
C      NCON=NUMBER OF POINTS TO CONVOLUTE
      NCON=(L-NS-M)/NF+1
      ICON=NS-M-NF
      DO 3 IC=1,NCON
C      IS=FIRST ADDRESS IN A(I) WHEN EACH POINT IS CONVOLUTED
      IS=ICON+IC*NF
C      CONVOLUTE POINT
      SUM=0
      M2=2*M
      J=IS
      DO 1 I=1,M2
      SUM=A(J)*B(I)+SUM
1      J=J+1
      OUT(IOUTBU)=SUM
C      OUTPUT 512 POINTS AT A TIME
      IF(IOUTBU.LT.512) GO TO 2
      WRITE(2,103) (OUT(IO),IO=1,512)
103     FORMAT(8F10.3)
      IOUTBU=0
2      IOUTBU=IOUTBU+1
3      CONTINUE
      NCOUN=NCOUN+NCON
      NS=IS+NF+3*M-L
      RETURN
      END

C
      SUBROUTINE APTD(B,M)
      DIMENSION B(1)
C      DOUBLE SIDED TRIANGULAR APODIZATION
C      ZERO PATH DIFFERENCE IS AT M+1
      M2=2*M
      DEL=1./FLOAT(M)
      WH=0.
      DO 15 I=1,M
      B(I)=WH*B(I)
15     WH=WH+DEL
      MT=M+1
      DO 16 I=MT,M2
      B(I)=WH*B(I)
16     WH=WH-DEL
      RETURN
      END

C
      SUBROUTINE EXPAND(A,S,INV,N,NE)
      DIMENSION A(1),S(1),INV(1)
C      THIS ROUTINE INTERPOLATES "A" BY "NE" TIMES
C      N IS THE NUMBER OF POINTS TO START WITH
C      SPACE NEEDED MUST BE TWICE THE SIZE OF NEW N
C      THE SIZE OF S AND INV IS A/8
      N2=2*N
      NNEW=N*NE
      NNH=NNEW/2
      CALL PREHAR(A,N)
      MH=LOG2(N)
      CALL HARM1D(A,MH,INV,S,1,IER)

```

```

MS=N+1
MZ=2*NNEW-N
J=MZ
DO 10 I=MS,N2
J=J+1
10 A(J)=A(I)
DO 20 I=MS,MZ
20 A(I)=0.
MB=MH+LOG2(NE)
CALL HARM1D(A,MB,INV,S,-1,IER)
I=NNEW
J=NNEW-1
DO 30 ID=1,NNH
A(I)=A(J)*NE
I=I-1
30 J=J-2
J=NNEW+1
DO 40 I=1,NNH
A(I)=A(J)*NE
40 J=J+2
RETURN
END

C
FUNCTION LOG2(N)
LOG2=ALOG(FLOAT(N))/.693147+.5
RETURN
END

C
SUBROUTINE PREHAR(A,M2)
DIMENSION A(1)
C THIS ROUTINE GETS A REAL DOUBLE SIDED INPUT READY
C FOR HARM1D.
C M2 IS THE NUMBER OF REAL POINTS
M=M2/2
J=M2+1
DO 2 I=1,M
A(J)=A(I)
A(J+1)=0
2 J=J+2
MT=M+1
J=1
DO 3 IJ=MT,M2
A(J)=A(IJ)
A(J+1)=0
3 J=J+2
RETURN
END

C
SUBROUTINE XMXMN(A,XMAX,IMAX,XMIN,IMIN,N)
DIMENSION A(1)
XMAX=-1.0E+30
XMIN=1.0E+30
DO 20 I=1,N
IF(A(I).LT.XMAX) GO TO 10
XMAX=A(I)
IMAX=I
GO TO 20
10 IF(A(I).GT.XMIN) GO TO 20
XMIN=A(I)
IMIN=I
20 CONTINUE
RETURN
END

C
SUBROUTINE RTADEC(A,B,D,ITAP,IFUN,ISTR,IEND,IUNIT)
DIMENSION A(1),B(640),D(256)
C THIS ROUTINE READS DATA FROM TAPE UNIT "ITAP"
C AND PUTS IT IN ARRAY "A" BEGINING AT "ISTR" AND GOING TO

```

```

C      "IEND."
C      IF "IFUN" = 0 NO REWIND WILL OCCUR, IF "IFUN" IS NOT EQUAL
C      TO ZERO A REWIND WILL OCCUR BEFORE THE READ.
C      IUNIT=UNIT(ITAP)
C      FULL BUFFERS OF INFORMATION WILL BE PASSED DIRECTLY TO "A"
C      PARTIAL BUFFERS WILL BE TEMPORARILY STORED IN B
      COMMON /RTABUF/ IBUFP
      DATA IBUFP,NBD,NAD/0,256,640/
      IRD=ISTR
      IF(IFUN.EQ.0) GO TO 10
      REWIND ITAP
      IBUFP=0
10     IF(IBUFP.EQ.0) GO TO 40
C      BUFFER HAS AT LEAST PART OF NEEDED DATA
15     IQUIT=IEND
      IF((IQUIT-IRD).GT.(NAD-IBUFP)) IQUIT=IRD+NAD-IBUFP
20     IF(IRD.GT.IQUIT) GO TO 30
      A(IRD)=B(IBUFP)
      IBUFP=IBUFP+1
      IRD=IRD+1
      GO TO 20
30     IF(IBUFP.GT.NAD) IBUFP=0
      IF(IRD.GT.IEND) RETURN
C      NEED MORE POINTS
40     BUFFER IN (ITAP,1) (D(1),D(NBD))
      IUNIT=UNIT(ITAP)
      IF(IUNIT.NE.-1) RETURN
      IF((IEND-IRD+1).GE.NAD) GO TO 50
C      REFILL BUFFER
      CALL TPDCCODE(D,B)
      IBUFP=1
      GO TO 15
C      READ DIRECTLY INTO A
50     CALL TPDCCODE(D,A(IRD))
      IRD=IRD+NAD
      GO TO 40
      END

C
C      SUBROUTINE TPDCCODE(D,F)
C      INPUT IS 256 WORDS EACH 60 BITS LONG IN D
C      OUTPUT IS 640 WORDS EACH 24 BITS IN F
      DIMENSION D(2),F(2),IA(6),IB(5)
      DATA (IA(I),I=1,6)/7777777770000000000000B,0000000077777777700000B,
10000000000000000000007777B,77770000000000000000B,00007777777700000000
20B,0000000000007777777B/
      IXX=40000000B
      L=1
      J=1
      DO 11 I=1,128
      IX=D(L).AND. IA(1)
      IB(1)=SHIFT(IX,-36)
      IX=D(L).AND. IA(2)
      IB(2)=SHIFT(IX,-12)
      IX=D(L).AND. IA(3)
      IY=D(L+1).AND. IA(4)
      IZZ=SHIFT(IY,-48)
      IZ=SHIFT(IX,+12)
      IZZ=IZZ.AND. IA(3)
      IZX=IZ.OR. IZZ
      IB(3)=IZ+IZZ
      IX=D(L+1).AND. IA(5)
      IB(4)=SHIFT(IX,-24)
      IB(5)=D(L+1).AND. IA(6)
      L=L+2
      DO 12 II=1,5
      IF(IB(II).GE. IXX) IB(II)=IB(II)-(2*IXX)
      F(J)=IB(II)
      J=J+1

```

```

12 CONTINUE
11 CONTINUE
  RETURN
  END

```

```

SUBROUTINE HARM1D(A,M,INV,S,IFSET, IFERR)

```

```

.....
SUBROUTINE HARM1D

```

```

PURPOSE

```

```

  PERFORMS DISCRETE COMPLEX FOURIER TRANSFORMS ON A COMPLEX
  THREE DIMENSIONAL ARRAY

```

```

USAGE

```

```

  CALL HARM1D(A,M,INV,S,IFSET,IFERR)

```

```

DESCRIPTION OF PARAMETERS

```

```

A  - AS INPUT, A CONTAINS THE COMPLEX, 1-DIMENSIONAL
    - ARRAY TO BE TRANSFORMED. THE REAL PART OF
    - A(I1) IS STORED IN VECTOR FASHION IN A CELL
    - WITH INDEX 2*(I1) + 1 WHERE
    - NI = 2**MI AND I1 = 0,1,...,NI-1 ETC.
    - THE IMAGINARY PART IS IN THE CELL IMMEDIATELY
    - FOLLOWING.
    - THE NUMBER OF CORE LOCATIONS OF
    - ARRAY A IS 2*(NI)
M  - A ONE CELL VECTOR WHICH DETERMINES THE SIZES
    - OF THE DIMENSIONS OF THE ARRAY A. THE SIZE,
    - NI, OF THE DIMENSION OF A IS 2**MI
INV - A VECTOR WORK AREA FOR BIT AND INDEX MANIPULATION
    - OF DIMENSION ONE EIGHTH THE NUMBER OF CORE
    - LOCATIONS OF A, VIZ., (1/8)*2*NI
S  - A VECTOR WORK AREA FOR SINE TABLES WITH DIMENSION
    - THE SAME AS INV
IFSET - AN OPTION PARAMETER WITH THE FOLLOWING SETTINGS
      0  SET UP SINE AND INV TABLES ONLY
      1  SET UP SINE AND INV TABLES ONLY AND
          CALCULATE FOURIER TRANSFORM
     -1  SET UP SINE AND INV TABLES ONLY AND
          CALCULATE INVERSE FOURIER TRANSFORM (FOR
          THE MEANING OF INVERSE SEE THE EQUATIONS
          UNDER METHOD BELOW)
      2  CALCULATE FOURIER TRANSFORM ONLY (ASSUME
          SINE AND INV TABLES EXIST)
     -2  CALCULATE INVERSE FOURIER TRANSFORM ONLY
          (ASSUME SINE AND INV TABLES EXIST)
IFERR - ERROR INDICATOR. WHEN IFSET IS 0,+1,-1,
      IFERR = 1 MEANS THE MAXIMUM M(I) IS LESS THAN 3
      OR GREATER THAN 20, I=1,2,3 WHEN IFSET IS
      +2,-2, IFERR = 1 MEANS THAT THE SINE AND INV
      TABLES ARE NOT LARGE ENOUGH OR HAVE NOT BEEN
      COMPUTED. IF ON RETURN IFERR = 0 THEN NONE OF
      THE ABOVE CONDITIONS ARE PRESENT

```

```

REMARKS

```

```

  THIS SUBROUTINE IS TO BE USED FOR COMPLEX, 1-DIMENSIONAL
  ARRAYS IN WHICH EACH DIMENSION IS A POWER OF 2. THE
  MAXIMUM MI MUST NOT BE LESS THAN 3 OR GREATER THAN 20.

```

```

SUBROUTINES AND FUNCTION SUBPROGRAMS REQUIRED
  NONE

```

```

THIS IS A 1-DIMENSIONAL MODIFICATION BY MARK ESPLIN OF THE
ORIGINAL 3-DIMENSIONAL HARM.

```

```

C      SEE J.W. COOLEY AND J.W. TUKEY, "AN ALGORITHM FOR THE
C      MACHINE CALCULATION OF COMPLEX FOURIER SERIES",
C      MATHEMATICS OF COMPUTATIONS, VOL. 19 (APR. 1965), P. 297.
C
10  DIMENSION A(1),INV(1),S(1),W(2),W2(2),W3(2)
12  IF( IABS(IFSET) - 1) 900,900,12
    MTT=M-2
    ROOT2 = SQRT(2.)
    IF (MTT-MT ) 14,14,13
13  IFERR=1
    RETURN
14  IFERR=0
    M1=M
    N1=2**M1
16  IF(IFSET) 18,18,20
18  NX= N1
    FN = NX
    DO 19 I = 1,NX
      A(2*I-1) = A(2*I-1)/FN
19  A(2*I) = -A(2*I)/FN
20  NP=N1*2
    IL=0
    IL1=1
    MI=M1
30  IDIF=NP
    KBIT=NP
    MEV = 2*(MI/2)
    IF (MI - MEV )60,60,40
C
C      M IS ODD. DO L=1 CASE
40  KBIT=KBIT/2
    KLAST=KBIT-1
    DO 50 K=1,KLAST,2
      KD=K+KBIT
C
C      DO ONE STEP WITH L=1,J=0
      A(K)=A(K)+A(KD)
      A(KD)=A(K)-A(KD)
      T=A(KD)
      A(KD)=A(K)-T
      A(K)=A(K)+T
      T=A(KD+1)
      A(KD+1)=A(K+1)-T
50  A(K+1)=A(K+1)+T
52  LFIRST =3
C
C      DEF - JLAST = 2** (L-2) -1
      JLAST=1
      GO TO 70
C
C      M IS EVEN
60  LFIRST = 2
      JLAST=0
70  DO 240 L=LFIRST,MI,2
      JJDIF=KBIT
      KBIT=KBIT/4
      KL=KBIT-2
C
C      DO FOR J=0
      DO 80 I=1,IL1,IDIF
      KLAST=I+KL
      DO 80 K=I,KLAST,2
      K1=K+KBIT
      K2=K1+KBIT
      K3=K2+KBIT

```

```

C
CCCCC
DO TWO STEPS WITH J=0
A(K)=A(K)+A(K2)
A(K2)=A(K)-A(K2)
A(K1)=A(K1)+A(K3)
A(K3)=A(K1)-A(K3)

A(K)=A(K)+A(K1)
A(K1)=A(K)-A(K1)
A(K2)=A(K2)+A(K3)*I
A(K3)=A(K2)-A(K3)*I

T=A(K2)
A(K2)=A(K)-T
A(K)=A(K)+T
T=A(K2+1)
A(K2+1)=A(K+1)-T
A(K+1)=A(K+1)+T

C
T=A(K3)
A(K3)=A(K1)-T
A(K1)=A(K1)+T
T=A(K3+1)
A(K3+1)=A(K1+1)-T
A(K1+1)=A(K1+1)+T

C
T=A(K1)
A(K1)=A(K)-T
A(K)=A(K)+T
T=A(K1+1)
A(K1+1)=A(K+1)-T
A(K+1)=A(K+1)+T

C
R=-A(K3+1)
T = A(K3)
A(K3)=A(K2)-R
A(K2)=A(K2)+R
A(K3+1)=A(K2+1)-T
80 A(K2+1)=A(K2+1)+T
IF (JLAST) 235,235,82
82 JJ=JJDIF +1

C
DO FOR J=1
ILAST= IL +JJ
DO 85 I = JJ, ILAST, IDIF
KLAST = KL+I
DO 85 K=I, KLAST, 2
K1 = K+KBIT
K2 = K1+KBIT
K3 = K2+KBIT

CCCCC
LETTING W=(1+I)/ROOT2, W3=(-1+I)/ROOT2, W2=I,
A(K)=A(K)+A(K2)*I
A(K2)=A(K)-A(K2)*I
A(K1)=A(K1)*W+A(K3)*W3
A(K3)=A(K1)*W-A(K3)*W3

A(K)=A(K)+A(K1)
A(K1)=A(K)-A(K1)
A(K2)=A(K2)+A(K3)*I
A(K3)=A(K2)-A(K3)*I

R = -A(K2+1)
T = A(K2)
A(K2) = A(K)-R
A(K) = A(K)+R
A(K2+1)=A(K+1)-T
A(K+1)=A(K+1)+T

```

```

C
AWR=A(K1)-A(K1+1)
AWI = A(K1+1)+A(K1)
R=-A(K3)-A(K3+1)
T=A(K3)-A(K3+1)
A(K3)=(AWR-R)/ROOT2
A(K3+1)=(AWI-T)/ROOT2
A(K1)=(AWR+R)/ROOT2
A(K1+1)=(AWI+T)/ROOT2
T= A(K1)
A(K1)=A(K)-T
A(K)=A(K)+T
T=A(K1+1)
A(K1+1)=A(K+1)-T
A(K+1)=A(K+1)+T
R=-A(K3+1)
T=A(K3)
A(K3)=A(K2)-R
A(K2)=A(K2)+R
A(K3+1)=A(K2+1)-T
85 A(K2+1)=A(K2+1)+T
IF(JLAST-1) 235,235,90
90 JJ= JJ + JJDIF

C
C
NOW DO THE REMAINING J'S
DO 230 J=2,JLAST

C
C
FETCH W'S
DEF- W=W**INV(J), W2=W**2, W3=W**3
96 I=INV(J+1)
98 IC=NT-I
W(1)=S(IC)
W(2)=S(I)
I2=2*I
I2C=NT-I2
IF(I2C)120,110,100

C
C
2*I IS IN FIRST QUADRANT
100 W2(1)=S(I2C)
W2(2)=S(I2)
GO TO 130
110 W2(1)=0.
W2(2)=1.
GO TO 130

C
C
2*I IS IN SECOND QUADRANT
120 I2CC = I2C+NT
I2C=-I2C
W2(1)=-S(I2C)
W2(2)=S(I2CC)
130 I3=I+I2
I3C=NT-I3
IF(I3C)160,150,140

C
C
I3 IN FIRST QUADRANT
140 W3(1)=S(I3C)
W3(2)=S(I3)
GO TO 200
150 W3(1)=0.
W3(2)=1.
GO TO 200

C
160 I3CC=I3C+NT
IF(I3CC)190,180,170

C
C
I3 IN SECOND QUADRANT
170 I3C=-I3C
W3(1)=-S(I3C)

```

```

      W3(2)=-S(I3CC)
      GO TO 200
180  W3(1)=-1.
      W3(2)=0.
      GO TO 200
C
C      3*I IN THIRD QUADRANT
190  I3CCC=NT+I3CC
      I3CC = -I3CC
      W3(1)=-S(I3CCC)
      W3(2)=-S(I3CC)
200  ILAST=IL+JJ
      DO 220 I=JJ, ILAST, IDIF
      KLAST=KL+I
      DO 220 K=I, KLAST, 2
      K1=K+KBIT
      K2=K1+KBIT
      K3=K2+KBIT

C
C      DO TWO STEPS WITH J NOT 0
C      A(K)=A(K)+A(K2)*W2
C      A(K2)=A(K)-A(K2)*W2
C      A(K1)=A(K1)*W+A(K3)*W3
C      A(K3)=A(K1)*W-A(K3)*W3
C
C      A(K)=A(K)+A(K1)
C      A(K1)=A(K)-A(K1)
C      A(K2)=A(K2)+A(K3)*I
C      A(K3)=A(K2)-A(K3)*I
C
      R=A(K2)*W2(1)-A(K2+1)*W2(2)
      T=A(K2)*W2(2)+A(K2+1)*W2(1)
      A(K2)=A(K)-R
      A(K)=A(K)+R
      A(K2+1)=A(K+1)-T
      A(K+1)=A(K+1)+T
C
      R=A(K3)*W3(1)-A(K3+1)*W3(2)
      T=A(K3)*W3(2)+A(K3+1)*W3(1)
      AWR=A(K1)*W(1)-A(K1+1)*W(2)
      AWI=A(K1)*W(2)+A(K1+1)*W(1)
      A(K3)=AWR-R
      A(K3+1)=AWI-T
      A(K1)=AWR+R
      A(K1+1)=AWI+T
      T=A(K1)
      A(K1)=A(K)-T
      A(K)=A(K)+T
      T=A(K1+1)
      A(K1+1)=A(K+1)-T
      A(K+1)=A(K+1)+T
      R=-A(K3+1)
      T=A(K3)
      A(K3)=A(K2)-R
      A(K2)=A(K2)+R
      A(K3+1)=A(K2+1)-T
220  A(K2+1)=A(K2+1)+T
      END OF I AND K LOOPS
C
C      230  JJ=JJDIF+JJ
      END OF J-LOOP
C
C      235  JLAST=4*JLAST+3
240  CONTINUE
      END OF L LOOP
C
C      WE NOW HAVE THE COMPLEX FOURIER SUMS BUT THEIR ADDRESSES A
      BIT-REVERSED. THE FOLLOWING ROUTINE PUTS THEM IN ORDER

```

```

      N1VNT=N1/NT
      JJD1=N1/(N1VNT*N1VNT)
      J=1
800  JJ1=1
      DO 860 JPP1=1,N1VNT
      IPP1=INV(JJ1)
      DO 850 JP1=1,NT
810  IP1=INV(JP1)*N1VNT
830  I=2*(IPP1+IP1)+1
      IF (J-I) 840,845,845
840  T=A(I)
      A(I)=A(J)
      A(J)=T
      T=A(I+1)
      A(I+1)=A(J+1)
      A(J+1)=T
845  CONTINUE
850  J=J+2
860  JJ1=JJ1+JJD1
      END OF JPP1 AND JP2
C
C
C
890  IF(IFSET)891,895,895
891  DO 892 I = 1,NX
892  A(2*I) = -A(2*I)
895  RETURN
C
C
C      THE FOLLOWING PROGRAM COMPUTES THE SIN AND INV TABLES.
C
900  MT=M-2
      MT = MAXO(2,MT)
904  IF (MT-20)906,906,905
905  IFERR = 1
      GO TO 895
906  IFERR=0
      NT=2**MT
      NTV2=NT/2
C
C      SET UP SIN TABLE
C      THETA=PIE/2** (L+1) FOR L=1
910  THETA=.7853981634
C
C      JSTEP=2** (MT-L+1) FOR L=1
      JSTEP=NT
C
C      JDIF=2** (MT-L) FOR L=1
C      JDIF=2** (MT-L) FOR L=1
      JDIF=NTV2
      S(JDIF)=SIN(THETA)
      DO 950 L=2,MT
      THETA=THETA/2.
      JSTEP2=JSTEP
      JSTEP=JDIF
      JDIF=JSTEP/2
      S(JDIF)=SIN(THETA)
      JC1=NT-JDIF
      S(JC1)=COS(THETA)
      JLAST=NT-JSTEP2
      IF(JLAST - JSTEP) 950,920,920
920  DO 940 J=JSTEP,JLAST,JSTEP
      JC=NT-J
      JD=J+JDIF
940  S(JD)=S(J)*S(JC1)+S(JDIF)*S(JC)
950  CONTINUE
C
C      SET UP INV(J) TABLE
C
960  MTLEXP=NTV2

```

```

C      MTLEXP=2**(MT-L). FOR L=1
C      LM1EXP=1
C
C      LM1EXP=2**(L-1). FOR L=1
C      INV(1)=0
C      DO 980 L=1,MT
C      INV(LM1EXP+1) = MTLEXP
C      DO 970 J=2,LM1EXP
C      JJ=J+LM1EXP
970    INV(JJ)=INV(J)+MTLEXP
C      MTLEXP=MTLEXP/2
980    LM1EXP=LM1EXP*2
982    IF(IFSET)12,895,12
C      END

```

# Program for performing large FFT

The large FFT program was broken up into four separate programs to conserve memory space. They are EVEFT, SORTFT, RECFFT, ERECOV. The large FFT is performed by running the four programs in sequence.

Part of the programming was performed by Steve Walker.

```

PROGRAM EVEFT(OUTPUT=104B,TAPE3=104B,TAPE4,TAPE6=OUTPUT
2,TAPE2)
C THIS PROGRAM CONVERTS A REAL EVEN FUNCTION INTO A NEW
C COMPLEX FUNCTION WITH NO REDUNDANCY.
  DIMENSION A(4096),B(4096),S(4096),C(2048),SINE(16)
  DIMENSION COSINE(16),SC(4098),MASTIX(300)
  EQUIVALENCE (SC(3),S(1)),(S(2049),C(1))
  IBLKSZ=4096
  IBLKS2=IBLKSZ/2
  REWIND 2
  REWIND 3
  READ(2,500) TYPE,TITLE,NUM,IREV,AE,STEP,STARTO
  WRITE(3,500) TYPE,TITLE,NUM,IREV,AE,STEP,STARTO
500  FORMAT(A1,A7,2I8,3E18.11)
  NBLK=NUM/IBLKSZ
  NBLK1=NBLK+1
  IFORM=FLOAT(NBLK)/8.+0.9999
  NBLK3=NBLK+IFORM+2
  CALL OPENMS(4,MASTIX,150,0)
C
C PREPARE 180 DEGREE SINE-COSINE TABLE
  S(IBLKSZ)=0.
  S(IBLKSZ-1)=-1.
  CALL SCTABL(SC,DELT,IBLKSZ)
  CALL WRITMS(4,S,IBLKSZ,NBLK3)
  CALL WRITMS(4,SC,IBLKSZ,NBLK1)
  WRITE(6,520) NUM
520  FORMAT(* N=*,I8)
C
C TRIANGULAR APODIZATION
  AP=1.
  APT=1./FLOAT(NUM)
  DO 30 IBLK=1,NBLK
    READ(2,540) (B(I),I=1,IBLKSZ)
540    FORMAT(8F10.3)
    DO 10 I=1,IBLKSZ
      A(I)=B(I)*AP
      AP=AP-APT
10    CONTINUE
    CALL WRITMS(4,A,IBLKSZ,IBLK)
30    CONTINUE
C
C PREPARE TAPE4 FOR REAL TRANSFORM
  CALL HERMFC(IBLKSZ,A,B,NBLK)
  NPASS=LOG2(NBLK)
  THETA=3.14159265359/FLOAT(IBLKSZ)
  CALL SINGEN(THETA,NPASS,SINE,COSINE)
  CALL TRPREP(IBLKSZ,NBLK,NPASS,A,B,S,C,SINE,COSINE)
  STOP
  END
C
C SUBROUTINE HERMFC(IBLKSZ,A,B,NBLK)
C
C CREATES ONE HALF OF A HERMITION FUNCTION.
C READS AND WRITES USING TAPE4
C   A,B= WORK SPACE
C   NBLK= NO. BLOCKS OF INPUT
C   IBLKSZ= BLOCK SIZE

```



```

C      A(2)=T-A(2)
      WORK FROM BOTH ENDS
      DO 200 K1=1,NBLK2
        K2=NBLK+1-K1
        CALL READMS(4,B,IBLKSZ,K2)
        IEND=IBLKSZ-1
        DO 170 IL=3,IEND,2
          IF(IC.LT.IBLKS2) GO TO 160
          CALL EXPSCT(S,C,MK,IBLKS2,NPASS,SINE,COSINE)
          IC=1
160         CONTINUE
          J=IBLKSZ-IL+2
          IP=IL+1
          JP=J+1
          CALL EVESET(A(IL),A(IP),B(J),B(JP),C(IC),C(IC+1))
          IC=IC+2
170         CONTINUE
          CALL WRITMS(4,A,IBLKSZ,K1,1)
          IF(K1.EQ.NBLK2) GO TO 180
          IBLK=K1+1
          CALL READMS(4,A,IBLKSZ,IBLK)
          GO TO 190
180         CONTINUE
          A(1)=B(1)
          A(2)=B(2)
190         CONTINUE
          CALL EVESET(A(1),A(2),B(1),B(2),C(IC),C(IC+1))
          IC=IC+2
          CALL WRITMS(4,B,IBLKSZ,K2,1)
200         CONTINUE
      RETURN
      END

C
C
C      SUBROUTINE EXPSCT(S,C,MK,IBLKSZ,NPASS,SINE,COSINE)
C
C      THIS ROUTINE EXPANDS A SINE-COSINE TABLE, STARTING
C      AT THE SUBSCRIPT MK, 2**(NPASS) TIMES
C      IBLKSZ= NO. OF POINTS IN C AFTER EXPANSION
C
      DIMENSION S(1),C(1),SINE(1),COSINE(1)
      IEND=IBLKSZ-1
      ISTEP=2**(NPASS+1)
      ISTART=ISTEP-1

C
C      SPACE APPROPRIATE VALUES FROM S INTO C.
      DO 40 J=ISTART,IEND,ISTEP
        C(J)=S(MK+1)
        C(J+1)=S(MK)
        MK=MK+2
40      CONTINUE
      PREPARE FOR EXPANSION
      KLEAP=ISTEP
      KSTART=IBLKSZ-KLEAP-1
      KEND=KLEAP-1
      KSTEP=2*KLEAP
      DO 90 IK=1,NPASS
        KLEAP=KLEAP/2
        KSTEP=KSTEP/2
        KEND=KEND-KLEAP
        KSTART=KSTART+KLEAP
        IMT=IBLKSZ/KSTEP

C
      DO 80 ICOUNT=KEND,KSTART,KSTEP
        MTO=IBLKSZ-ICOUNT-2
        C(MTO)=COSINE(IK)*C(KSTEP*IMT-1)-SINE(IK)*C(KSTEP*IMT)
        C(MTO+1)=COSINE(IK)*C(KSTEP*IMT)+SINE(IK)*C(KSTEP*IMT-1)
        IMT=IMT-1

```

```

80      CONTINUE
90      CONTINUE
      RETURN
      END

C
C
      SUBROUTINE EVESET(A1,A2,B1,B2,SN,CS)
C
C      TO BE USED ONLY WITH ROUTINE TRPREP
C      PERFORMS A SPECIAL OPERATION ON THE PARAMETERS
C
      SN=0-SN
      CS=0-CS
      AP=A1+B1
      AM=A1-B1
      APP=A2+B2
      APM=A2-B2
      SAC=SN*AM+CS*APP
      CAS=SN*APP-CS*AM
      A1=AP+SAC
      A2=APM+CAS
      B1=AP-SAC
      B2=CAS-APM
      RETURN
      END

C
C
      SUBROUTINE SCTABL(S,DELT,IBLKSZ)
C      DIMENSION S(2)
C      THIS ROUTINE GENERATES A SIN-COS TABLE
C      FROM THETA EQUAL ZERO TO 180 DEGREES
      IBLKS2=IBLKSZ/2
      IBLKS4=IBLKSZ/4
      DELT=3.14159265359/FLOAT(IBLKS2)
      ROOT2=1./SQRT(2.)
      THA=DELT
      IAD2=IBLKS2+3
      IAD3=IBLKSZ+3
      S(1)=1.
      S(2)=0.
      S(IBLKS2+1)=0.
      S(IBLKS2+2)=1.
      DO 10 I=3,IBLKS4,2
      I2=I+1
      COST=COS(THA)
      SINT=SIN(THA)
      S(I)=COST
      S(I2)=SINT
      S(IAD2-I2)=SINT
      S(IAD2-I)=COST
      S(I+IBLKS2)=-SINT
      S(I2+IBLKS2)=COST
      S(IAD3-I2)=-COST
      S(IAD3-I)=SINT
10    THA=THA+DELT
      S(IBLKS4+1)=ROOT2
      S(IBLKS4+2)=ROOT2
      IBLKS34=IBLKS2+IBLKS4
      S(IBLKS34+1)=-ROOT2
      S(IBLKS34+2)=ROOT2
      RETURN
      END

      PROGRAM SORTFT(TAPE4,TAPE3=104B)
      DIMENSION A(4096),B(4096),MASTIX(300),S(512),INV(512)
      EQUIVALENCE(B(1),S(1)),(B(2048),INV(1))

```

```

C   THIS PROGRAM SORTS THE BLOCKS THEN TRANSFORMS THEM
C   THE PROGRAM ALSO GENERATES THE SIN-COS TABLE
      IBLKSZ=4096
      CALL OPENMS(4,MASTIX,150,0)
      REWIND 3
500  READ(3,500) TYPE,TITLE,N,IREV,AE,STEP,STARTO
      FORMAT(A1,A7,2I8,3E18.11)
      NBLK=N/IBLKSZ
      CALL SORTFF(A,B,NBLK,IBLKSZ)
      CALL FFTBLK(A,S,INV,NBLK,IBLKSZ)
      STOP
      END

C   SUBROUTINE SORTFF(A,B,NBLK,IBLKSZ)
      COMPLEX A(1),B(1),H
C   THIS SUBROUTINE SORTS DATA TO GET READY FOR A FFT.
C   EVERY NBLK'TH POINT IS SORTED OUT INTO A SEPARATE BLOCK
C   THEN THE BLOCKS ARE PUT IN BIT INVERTED ORDER.
C   NOTE MEMORY REQUIRED FOR A COMPLEX ARRAY IS TWICE THAT OF
C   A REAL ARRAY.
C   THE INPUT DATA IS IN THE FIRST NBLK BLOCKS OF TAPE4, WHICH
C   IS A RANDOM ACCESS DISK FILE.
C   THE TOTAL NUMBER OF DISK BLOCKS IS = NBLK+NBLK/8+1
C   THE DATA IS ALWAYS REWRITTEN IN PLACE
C   IBLKSZ = NUMBER OF STORAGE LOCATIONS IN A BLOCK
C   ICOMSZ = IBLKSZ/2 = NUMBER OF COMPLEX POINTS
C   NBLK = NUMBER OF BLOCKS OF DATA
C   ICSUBZ = SIZE OF SUBBLOCKS (COMPLEX) WHICH IS ICOMSZ/NBLK
C   AT THE BEGINNING.
C   NPASS = NUMBER OF PASSES OVER THE DATA

C   THIS SECTION OF CODE SORTS OUT EVERY NBLK'TH POINT IN A
C   BLOCK AND PUTS THE SUBBLOCKS IN BIT INVERTED ORDER.
      ICOMSZ=IBLKSZ/2
      ICSUBZ=ICOMSZ/NBLK
      NPASS=LOG2(NBLK)
      DO 20 IBLK=1,NBLK
      CALL READMS(4,A,IBLKSZ,IBLK)
      DO 10 ISUB=1,NBLK
      IP=ISUB-NBLK
      IB=INVER((ISUB-1),NPASS)*ICSUBZ
      DO 10 I=1,ICSUBZ
      IP=NBLK+IP
10    B(IB+I)=A(IP)
20    CALL WRITMS(4,B,IBLKSZ,IBLK,1)

C   THIS SECTION OF CODE SORTS THE BLOCKS
C   NSUB = NUMBER OF SUBBLOCKS
C   NBB = NUMBER OF BLOCKS IN EACH BUTTERFLY
C   NBUTTE = NUMBER OF BUTTERFLYS
C   IBU = WHICH BLOCK IN BUTTERFLY
C   IBUTT = WHICH BUTTERFLY
C   IBA = BLOCK A
C   IBB = BLOCK B
C   NSUB=NBLK
      NBB=1
      DO 50 IPAS=1,NPASS
      NBUTTE=NSUB/2
      NBB2=NBB*2
      ICSUB2=ICSUBZ*2
      DO 40 IBU=1,NBB
      IBA=IBU-NBB2
      DO 40 IBUTT=1,NBUTTE
      IBA=IBA+NBB2
      IBB=IP+NBB
C   OPERATE ON BLOCK A AND BLOCK B
      CALL READMS(4,A,IBLKSZ,IBA)
      CALL READMS(4,B,IBLKSZ,IBB)

```

```

J=-ICSUB2
DO 30 ISUB=1, NSUB, 2
J=J+ICSUB2
JI=J
DO 30 I=1, ICSUBZ
JI=JI+1
JI2=JI+ICSUBZ
H=A(JI2)
30 A(JI2)=B(JI)
B(JI)=H
40 CALL WRITMS(4, A, IBLKSZ, IBA, 1)
CALL WRITMS(4, B, IBLKSZ, IBB, 1)
NBB=NBB2
ICSUBZ=ICSUB2
50 NSUB=NSUB/2
RETURN
END

C
C
FUNCTION INVER(IVER, N)
THIS FUNCTION TAKES "IVER" AND INVERTS THE BITS
N IS THE NUMBER OF BITS IN THE WORD
THE VALUES OF IVER AND N ARE UNCHANGED
THIS FUNCTION WILL NOT WORK FOR NEGATIVE NUMBERS
C THIS FUNCTION WORKS ONLY ON A CDC COMPUTER.
IVE=IVER
INV=0
DO 10 I=1, N
INV=OR(SHIFT(INV, 1), AND(IVE, 1))
10 IVE=SHIFT(IVE, -1)
INVER=INV
RETURN
END

C
SUBROUTINE FFTBLK(A, S, INV, NBLK, IBLKSZ)
THIS ROUTINE DOES AN FFT OF EACH BLOCK WITH THE USE
C OF HARM1D.
C DIMENSION A(1), S(1), INV(1)
M=LOG2(IBLKSZ)-1
C SET UP SIN AND INV TABLES
CALL HARM1D(A, M, INV, S, 0, IFERR)
C TRANSFORM BLOCKS
DO 10 I=1, NBLK
CALL READMS(4, A, IBLKSZ, I)
CALL HARM1D(A, M, INV, S, 2, IERR)
10 CALL WRITMS(4, A, IBLKSZ, 1, 1)
CONTINUE
RETURN
END

PROGRAM RECFFT(TAPE4, TAPE3=104B)
DIMENSION A(4096), B(4096), S(4096), MASTIX(300)
C THIS PROGRAM RECONSTRUCTS THE BLOCKS THAT HAVE BEEN TRANSFORMED
IBLKSZ=4096
REWIND 3
500 READ(3, 500) TYPE, TITLE, N, IREV, AE, STEP, STARTO
FORMAT(A1, A7, 2I8, 3E18.11)
NBLK=N/IBLKSZ
DELTHA=3.14159265359/FLOAT(IBLKSZ)
CALL OPENMS(4, MASTIX, 150, 0)
DELTHA=DELTHA*2.
CALL RECONS(A, B, S, NBLK, IBLKSZ, DELTHA)
STOP
END

C

```

```

SUBROUTINE RECONS(A,B,S,NBLK,IBLKSZ,DELTHA)
COMPLEX A(2),B(2),S(2)
THIS ROUTINE RECONSTRUCTS THE BLOCKS THAT HAVE ALREADY BEEN
TRANSFORMED.
SEE SUBROUTINE SORTFF FOR DEFINITIONS OF TERMS.
INPUT IS IN THE FIRST "NBLK" BLOCKS ON TAPE4
BLOCK NBLK+1 MUST CONTAIN A COS-SIN TABLE
NSIN= NUMBER OF TIMES THE COS-SIN TABLE NEEDS TO BE READ.
NBSIN= NUMBER OF BLOCKS IN THE COS-SIN TABLE WHEN IT IS
FULLY FILLED OUT.
ISIN= WHICH COS-SIN BLOCK TO READ.
ISRE= ISIN-NBLK
ICOMSZ=IBLKSZ/2
NPASS=LOG2(NBLK)
DELT=DELTHA
NBB=1
NBUTTE=NBLK/2
NBSIN=NBLK/8
IF(NBSIN.LE.0) NBSIN=1
DO 50 IPASS=1,NPASS
C TAKE CARE OF COS-SIN TABLE
NB4B=NBB/4
NSIN=NB4B
IF(NB4B.LE.0) NB4B=1
NOFSIN=NBSIN/NB4B
NOFSI2=NOFSIN/2
ISIN=NBLK+1-NOFSIN
DO 40 ISRE=1,NSIN
ISIN=ISIN+NOFSIN
CALL READMS(4,S,IBLKSZ,ISIN)
IF(IPASS.EQ.NPASS) GO TO 10
C GET TABLE FOR NEXT PASS
DELT=DELTHA/2
CALL EXPAN(A,B,S,DELTHA,IBLKSZ)
CALL WRITMS(4,A,IBLKSZ,ISIN,1)
C FOR THE FIRST TWO PASSES YOU CAN PUT ALL THE INFORMATION IN
C THE COS-SIN TABLE IN ONE BLOCK.
IF(NSIN.NE.NB4B) GO TO 10
ISIN2=ISIN+NOFSI2
CALL WRITMS(4,B,IBLKSZ,ISIN2)
C DETERMINE WHICH BLOCKS TO WORK ON.
C THE FOLLOWING SHUFFLE MAKES IT SO ONLY ONE COS-SIN TABLE BLOCK
C IS NEEDED TO WORK ON 8 DATA BLOCKS.
10 NBB2=NBB/2
IBU=ISRE
20 CALL HERFFT(A,B,S,IBLKSZ,ICOMSZ,IBU,NBB,NBUTTE)
IF(IPASS.LE.1) GO TO 40
CALL ADDNIN(S,IBLKSZ)
IBU=IBU+NBB2
CALL HERFFT(A,B,S,IBLKSZ,ICOMSZ,IBU,NBB,NBUTTE)
IF(IPASS.LE.2) GO TO 40
CALL COMPIN(S,IBLKSZ,DELT)
IBU=NBB2-ISRE+1
CALL HERFFT(A,B,S,IBLKSZ,ICOMSZ,IBU,NBB,NBUTTE)
CALL ADDNIN(S,IBLKSZ)
IBU=NBB-ISRE+1
CALL HERFFT(A,B,S,IBLKSZ,ICOMSZ,IBU,NBB,NBUTTE)
40 CONTINUE
NBB=NBB*2
DELT=DELT/2
50 NBUTTE=NBUTTE/2
RETURN
END

C SUBROUTINE HERFFT(A,B,S,IBLKSZ,ICOMSZ,IBU,NBB,NBUTTE)
C THIS IS THE HEART OF THE EXTENDED FFT.
C SEE SORTFF FOR DEFINITION OF TERMS.
COMPLEX A(1),B(1),S(1),H,T

```

```

NBB2=NBB*2
IBA=IBU-NBB2
DO 40 IBUTT=1,NBUTTE
IBA=IBA+NBB2
IBB=IBA+NBB
C   THIS SECTION OF CODE OPERATES ON TWO BLOCKS.
CALL READMS(4,A,IBLSZ,IBA)
CALL READMS(4,B,IBLSZ,IBB)
DO 30 I=1,ICOMSZ
H=A(I)
T=B(I)*S(I)
A(I)=H+T
30 B(I)=H-T
40 CALL WRITMS(4,A,IBLSZ,IBA,1)
CALL WRITMS(4,B,IBLSZ,IBB,1)
RETURN
END

C   SUBROUTINE EXPAN(A,B,S,DELTHA,IBLSZ)
DIMENSION A(1),B(1),S(1)
C   THIS ROUTINE EXPANDES THE SIN-COS TABLE BY A FACTOR OF
C   TWO BY DOUBLING THE RESOLUTION.
C   THE EXPANDED TABLE GOES INTO A AND B FROM THE ORIGINAL IN S.
COSD=COS(DELTHA)
SIND=SIN(DELTHA)
C   DO FIRST HALF
J=-1
DO 10 I=1,IBLSZ,4
J=J+2
J2=J+1
COSJ=S(J)
SINJ=S(J2)
A(I)=COSJ
A(I+1)=SINJ
A(I+2)=COSJ*COSD-SINJ*SIND
A(I+3)=COSJ*SIND+SINJ*COSD
10 CONTINUE
C   DO SECOND HALF
DO 20 I=1,IBLSZ,4
J=J+2
J2=J+1
COSJ=S(J)
SINJ=S(J2)
B(I)=COSJ
B(I+1)=SINJ
B(I+2)=COSJ*COSD-SINJ*SIND
20 B(I+3)=COSJ*SIND+SINJ*COSD
RETURN
END

C   SUBROUTINE ADDNIN(S,IBLSZ)
DIMENSION S(2)
C   THIS ROUTINE ADDS 90 DEGREES TO THE ANGLE IN THE COS-SIN BLOCK.
DO 10 I=1,IBLSZ,2
I2=I+1
T=S(I)
S(I)=-S(I2)
10 S(I2)=T
RETURN
END

C   SUBROUTINE COMPNIN(S,IBLSZ,DELTHA)
DIMENSION S(4)
C   THIS ROUTINE SUBTRACTS 90 FROM THE ANGLE THEN TRANSFORMS THE
C   COS-SIN TABLE FROM THETA TO 90 MINUS THETA.
IBLSZ2=IBLSZ/2
IEND=IBLSZ2+1
J2=IBLSZ

```

```

DO 10 I=3,IBLSZ2,2
I2=I+1
J=J2-1
T=S(I)
S(I)=-S(J)
S(J)=-T
T=S(I2)
S(I2)=S(J2)
S(J2)=T
J2=J2-2
S(IEND)=-S(IEND)
C FIND COS-SIN FOR THE FIRST POINT (THE ONE NOT IN OLD BLOCK).
COSD=COS(DELTHA)
SIND=SIN(DELTHA)
S(1)=S(3)*COSD+S(4)*SIND
S(2)=S(4)*COSD-S(3)*SIND
RETURN
END

PROGRAM ERECOV(OUTPUT=104B,TAPE3,TAPE4,TAPE6=OUTPUT)
C
C THIS PROGRAM RECOVERS THE SPECTRUM AFTER THE EVEN TRANSFORM
C IT SHOULD ONLY BE USED WITH EVEFFT
C
DIMENSION A(4096),B(4096),S(4096),C(2048),SINE(16)
DIMENSION COSINE(16),IB(4096),MASTIX(300)
EQUIVALENCE (S(2049),C(1)),(B(1),IB(1))
IBLSZ=4096
REWIND 3
500 READ(3,500) TYPE,TITLE,NUM,IREV,AE,STEP,STARTO
FORMAT(A1,A7,2I8,3E18.11)
NBLK=NUM/IBLSZ
NBLK1=NBLK+1
IFORM=FLOAT(NBLK)/8.+0.9999
NBLK3=NBLK+IFORM+2
CALL OPENMS(4,MASTIX,150,0)
CALL READMS(4,S,IBLSZ,NBLK3)
NPASS=LOG2(NBLK*2)
THETA=3.14159265359/FLOAT(IBLSZ)
CALL SINGEN(THETA,NPASS,SINE,COSINE)
CALL RCSPEC(A,B,C,S,NPASS,NBLK,IBLSZ,SINE,COSINE)
C
C NORMALIZE SPECTRUM AND WRITE IT OUT.
XMAX=-1.0E30
DO 20 IBLK=1,NBLK
CALL READMS(4,A,IBLSZ,IBLK)
DO 20 I=1,IBLSZ
IF(A(I).LT.XMAX) GO TO 10
XMAX=A(I)
10 CONTINUE
20 CONTINUE
XNORM=1000./XMAX
IF(IREV.NE.0) GO TO 50
DO 40 IBLK=1,NBLK
CALL READMS(4,A,IBLSZ,IBLK)
DO 30 I=1,IBLSZ
IB(I)=XNORM*A(I)+.5
30 CONTINUE
IBLK1=IBLK+1
WRITE(3,590) (IB(J),J=1,IBLSZ)
40 CONTINUE
GO TO 999
C
50 CONTINUE
DO 70 ICOUNT=1,NBLK
IBLK=NBLK-ICOUNT+1

```

```

        CALL READMS(4,A,IBLKSZ,IBLK)
        IK=IBLKSZ
        DO 60 I=1,IBLKSZ
            IB(I)=XNORM*A(IK)+.5
            IK=IK-1
60      CONTINUE
        WRITE(3,590) (IB(J),J=1,IBLKSZ)
70      CONTINUE
999    CONTINUE
590    FORMAT(16I5)
        STOP
        END

C
C
C      SUBROUTINE RCSPEC(A,B,C,S,NPASS,NBLK,IBLKSZ,SINE,COSINE)
C
C      A,B= WORK SPACE
C      C= SPACE FOR EXPANDED SIN-COS TABLE
C      SINE,COSINE= ARRAYS OF HALF ANGLE SINES AND COSINES
C                  USED IN THE ANGLE ADDITION EQNS IN EXPSCT
C      NBLK,IBLKSZ= NO. BLOCKS AND BLOCK SIZE
C      NPASS= NUMBER OF TIMES S-C TABLE MUST BE EXPANDED BY 2
C
        DIMENSION A(1),B(1),C(1),S(1),SINE(1),COSINE(1)
        NBLK2=NBLK/2
        IBLKS2=IBLKSZ/2
        MK=1
        IC=IBLKS2+1
        CALL READMS(4,A,IBLKSZ,1)
        A(1)=2*A(1)
C      WORK FROM BOTH ENDS
        DO 200 K1=1,NBLK2
            K2=NBLK+1-K1
            CALL READMS(4,B,IBLKSZ,K2)
            DO 170 IP=2,IBLKSZ
                IF(IC.LT.IBLKS2) GO TO 160
                CALL EXPSCT(S,C,MK,IBLKS2,NPASS,SINE,COSINE)
                IC=1
160          CONTINUE
                JP=IBLKSZ-IP+2
                SP=(A(IP)+B(JP))/2.
                SM=(A(IP)-B(JP))/(2.*C(IC))
                A(IP)=SP+SM
                B(JP)=SP-SM
                IC=IC+2
170          CONTINUE
            CALL WRITMS(4,A,IBLKSZ,K1,1)
            IF(K1.EQ.NBLK2) GO TO 180
            IBLK=K1+1
            CALL READMS(4,A,IBLKSZ,IBLK)
            GO TO 190
180          CONTINUE
            A(1)=B(1)
190          CONTINUE
            SP=(A(1)+B(1))/2.
            SM=(A(1)-B(1))/(2.*C(IC))
            A(1)=SP+SM
            B(1)=SP-SM
            IC=IC+2
            CALL WRITMS(4,B,IBLKSZ,K2,1)
200          CONTINUE
        RETURN
        END

```

This is the program that was used to make the spectral line assignments

```

PROGRAM REGFIT(INPUT,OUTPUT,TAPE5=INPUT,TAPE4
2,TAPE6=OUTPUT,TAPE2,TAPE7)
C SPECTRAL LINE ASSIGNMENT PROGRAM
C MARK P. ESPLIN FTN4
COMMON /PAR/ TYP,LIN,MTAB,NUMT,ID,NBLK,IKIND,JP,JR
COMMON /BAND/ G,B1,D1,H1,B2,D2,H2
COMMON /DIREC/ SWAV(30)
COMMON /DTATAB/ IBLK,ILINE,DATAL(16,300)
COMMON /BANDAT/ M(300),WAV(300),IUSE(300),NLBAN
COMMON /FITD/ X(300),Y(300),A(7),SIGMAA(7),R(7),JCON(7),JFIT(7)
2,SCAL(7)
COMMON /OUTST/ NWP,NBST,ILIST,RANG,FRAML,FRAMR
DIMENSION MASTIX(60),BAN(7),BOUT(7),COMKEY(13)
EQUIVALENCE (BAN(1),G)
DATA MTAB,NUMT,ID,NWP,NCOM/300,4800,30,6,13/
DATA NWP,NBST,ILIST,RANG,FRAML,FRAMR/6,3,1,0025,.2,.2/
DATA COMKEY/3HSTP,3HFIT,3HBAN,3HCUS,3HCOF,3HCBT,3HCBC
2,3HWBC,3HNEX,3HBNT,3HGRA,3HNAM,3HHLP/
DATA SCAL /1.,1.,1.E-7,1.E-13,1.,1.E-7,1.E-13/
CALL OPENMS(4,MASTIX,30,0)
CALL READMS(4,SWAV,ID,1)
NBLK=SWAV(1)
IBLK=2
ILINE=1
CALL READMS(4,DATAL,NUMT,IBLK)
20 WRITE(6,110)
110 FORMAT(* ENTER BAND,C OR D*,/)
READ(5,120) BAND,CORD
120 FORMAT(A1,A2)
CALL FNDBAN(BAND,CORD)
IF(G.EQ.0) CALL CHGBAN
10 WRITE(6,100)
100 FORMAT(* ENTER IKIND,L,JP,JR*,/)
READ(5,*) IKIND,L,JP,JR
CALL SETM(M,IKIND,L,JP,JR,NLBAN)
CALL SETWAV(WAV,M,NLBAN,G)
DO 30 I=1,NLBAN
30 IUSE(I)=0
40 WRITE(6,200)
200 FORMAT(/,*,*)
READ(5,201) COMD,COMA
201 FORMAT(A3,A1)
C COMMAND PROCESSOR
DO 50 I=1,NCOM
IF(COMD.EQ.COMKEY(I)) GO TO 60
50 CONTINUE
I=NCOM+1
60 GO TO (210,220,230,240,250,260,270,280,20,300,350,400,900
2,1000), I
210 STOP
220 CALL FIT
GO TO 40
230 CALL WRTBAN
GO TO 40
240 CALL CHGUSE
GO TO 40
250 CALL CHOUPR
GO TO 40
260 GO TO 10
270 CALL CHGBAN
GO TO 40
280 CALL WBANPR(NWP,BAND,CORD)
GO TO 40
300 CALL WRTOTL
GO TO 40
350 CALL GR LIN4

```

```

      GO TO 40
400  CALL NAMLIN(BAND,COMA)
      GO TO 40
900  WRITE(6,910) (COMKEY(I),I=1,NCOM)
910  FORMAT(10(7X,A3))
      GO TO 40
1000 WRITE(6,1005)
1005 FORMAT(* ????)
      GO TO 40
      END

C
      SUBROUTINE CHOUPT
C      CHANGE PROGRAM PARAMETERS
      COMMON /OUTST/ NWP,NBST,ILIST,RANG,FRAML,FRAMR
      DIMENSION IPAR(6),PAR(6)
      EQUIVALENCE(IPAR(1),NWP)
      EQUIVALENCE(IPAR,PAR)
      WRITE(6,*) (IPAR(I),I=1,3),(PAR(I),I=4,6)
      WRITE(6,100)
100  FORMAT(* NWP,NBST,ILIST,RANG,FRAML,FRAMR*,/)
10  READ(5,*) I,CORR
      IF(I.EQ.0) GO TO 30
      IF(I.GE.4) GO TO 20
      IPAR(I)=CORR
      GO TO 10
20  PAR(I)=CORR
      GO TO 10
30  WRITE(6,*) (IPAR(I),I=1,3),(PAR(I),I=4,6)
      RETURN
      END

C
      SUBROUTINE FIT
C      PERFORM A TRIAL LEAST-SQUARES-FIT
      COMMON /BAND/ BAN(7)
      COMMON /DTAB/ IBLK,ILINE,DATAL(16,300)
      COMMON /FITD/ X(300),Y(300),A(7),SIGMAA(7),R(7),JCON(7),JFIT(7)
2  SCAL(7)
      COMMON /BANDAT/ MX(300),WAV(300),IUSE(300),NLBAN
      DIMENSION BOUT(7),YFIT(300)
      DATA IM,MASK/15B,77B/
C      CONSTANT TERM NOT INCULDED SINCE IT IS ALWAYS FIT.
C      MOLECULAR CONSTANTS TO BE FIT MUST BE IN ORDER.
      SIGLAS=0
30  WRITE(6,200)
200  FORMAT(* ENTER M, NUM*,/)
      READ(5,*) M,NUM
      WRITE(6,210)
210  FORMAT(* ENTER PARS OF FIT*,/)
      READ(5,*) (JFIT(I),I=1,M)
C      FIND WHICH MOLECULAR CONSTANTS AREN'T TO BE FIT
      JJ=1
      J=1
      DO 40 I=2,7
      IF(JFIT(J).EQ.1) GO TO 37
      JCON(JJ)=I
      JJ=JJ+1
      GO TO 40
37  J=J+1
40  CONTINUE
      NCON=6-M
      IF(NUM.EQ.-1) CALL CHGBAN
      SET UP FOR FIT
C
45  J=0
      DO 50 I=1,NLBAN
      CALL FINUSE(I,IUSF,WN)
      IF(IUSF.EQ.0) GO TO 50
      J=J+1
      X(J)=MX(I)

```

```

50   Y(J)=WN-WAVN(X,J,NCON,JCON)
      CONTINUE
      NPTS=J
      CALL REGRES(X,Y,SIGMAY,NPTS,M,JFIT,O,YFIT,AO,A,SIGMAO
2,SIGMAA,R,RMUL,CHISQR,FTEST)
      BAN(1)=AO
      DO 60 IF=1,M
      I=M-IF+1
      J=JFIT(I)
      BAN(J)=A(I)
      SIGMAA(J)=SIGMAA(I)/SCAL(J)
60   R(J)=R(I)
      DO 65 I=1,7
65   BOUT(I)=BAN(I)/SCAL(I)
      IF(NCON.EQ.0) GO TO 75
      DO 70 I=1,NCON
      J=JCON(I)
      SIGMAA(J)=0.
70   R(J)=0.
75   SIG=SQRT(CHISQR)
      WRITE(6,215) SIG,RMUL,NPTS
215  FORMAT(2F12.8,I10)
220  FORMAT(3F12.6)
      WRITE(6,220) BAN(1),SIGMAO
230  FORMAT(6F12.8)
      WRITE(6,230) (BOUT(I),I=2,7)
      WRITE(6,230) (SIGMAA(I),I=2,7)
      WRITE(6,230) (R(I),I=2,7)
      CALL SETWAV(WAV,MX,NLBAN,BAN)
      DO 80 I=1,NLBAN
      IF(IUSE(I).GT.0) IUSE(I)=0
80   CONTINUE
      IF(SIG.EQ.SIGLAS) RETURN
      NUM=NUM-1
      IF(NUM.LE.0) RETURN
      SIGLAS=SIG
      GO TO 45
      END

C
C   SUBROUTINE CHGBAN
C   CHANGE MOLECULAR CONSTANTS BY HAND.
      COMMON /BAND/ BAN(7)
      COMMON /FITD/ X(635),SCAL(7)
      DIMENSION BOUT(7),JFIT(7)
      DO 10 I=1,7
10   BOUT(I)=BAN(I)/SCAL(I)
      WRITE(6,100) (BOUT(I),I=1,7)
100  FORMAT(F10.4,/,6F12.8)
      WRITE(6,110)
110  FORMAT(* CHANGE BAND CONSTANTS*,/)
20   READ(5,*) I,CON
      IF(I.LE.0) GO TO 30
      IF(I.GT.7) GO TO 30
      BOUT(I)=CON
      BAN(I)=SCAL(I)*CON
      GO TO 20

C
30   WRITE(6,100) (BOUT(I),I=1,7)
      RETURN
      END

C
C
C
C
C   SUBROUTINE WBANPR(NWP,BAND,CORD)
C   THIS ROUTINE WRITES MOLECULAR CONSTANTS ABOUT A BAND.
      COMMON /BAND/ BAN(7)

```

```

COMMON /FITD/ X(621),JCON(7),JFIT(7),SCAL(7)
COMMON /PAR/ TYP,LIN,MTAB,NUMT,ID,NBLK,IKIND,JP,JR
DIMENSION BOUT(7)
EQUIVALENCE (BOUT,JCON)
REWIND 2
10 READ(2,900) UP,TYP,XLOW,TYP,ISOTOP,GV1,GV2,STR,ZETA,BKEY
   IF(EOF(2).NE.0) GO TO 20
   READ(2,910) (BOUT(I),I=2,7)
   IF(BKEY.NE.BAND) GO TO 10
   IF(CORD.NE.TYP) GO TO 10
   GO TO 25
20 WRITE(6,100)
100 FORMAT(* ENTER UP XLOW TYP*,/)
   READ(5,110) UP,XLOW,TYP
110 FORMAT(2A10,A2)
   WRITE(6,120)
120 FORMAT(* ENTER GV1,ISOTOP,STR,ZETA*,/)
   READ(5,*) GV1,ISOTOP,STR,ZETA
25 DO 30 I=2,7
30 BOUT(I)=BAN(I)/SCAL(I)
   GV2=GV1+BAN(1)
   WRITE(NWP,900) UP,TYP,XLOW,TYP,ISOTOP,GV1,GV2,STR,ZETA,BAND
2,IKIND,JP,JR
   WRITE(NWP,910) (BOUT(I),I=2,7)
900 FORMAT(2(A10,A2),I4,2F10.4,F14.5,F6.3,1X,A1,3I5)
910 FORMAT(6F12.8)
   RETURN
   END

C
C SUBROUTINE WRTBAN
C WRITE A TABLE OF EXPERIMENTAL LINE PROPERTIES
COMMON /BANDAT/ M(300),WAV(300),IUSE(300),NLBAN
COMMON /DATALIN/POS(50),BANID(50),STR(50),YO(50),YHIGHT(50)
2,XL(50),XR(50),HW(50),OFF(50),OMCA(50),IBES(20)
COMMON /DTATAB/ IBLK,ILINE,DATAL(16,300)
COMMON /OUTST/ NWP,NBST,ILIST,RANG,FRAML,FRAMR
DATA IAST/ 47B/
5 WRITE(6,130)
130 FORMAT(* ENTER RANGE*,/)
   READ(5,140) BST,JST,BSP,JSP
140 FORMAT(A1,I3,1X,A1,I3)
   CALL MFIND(MST,IFST,BST,JST)
   CALL MFIND(MSTP,IFSP,BSP,JSP)
   IF((IFST+IFSP).NE.0) GO TO 5
   SUM=0
   SUMSQ=0
   IU=0
   DO 40 I=1,NLBAN
   IUSL=55B
   CALL FINUSE(I,IUSF,WN)
   IF((IUSF.EQ.0).AND.(ILIST.EQ.0)) GO TO 40
   IF(M(I).GT.0) GO TO 10
   J=-M(I)
   TYP="P"
   GO TO 20
10 J=M(I)-1
   TYP="R"
20 IF(WN.GT.0) GO TO 30
   WRITE(NWP,100) WAV(I),TYP,J
   GO TO 40
100 FORMAT(F10.4,1X,A1,I3,* NOT FOUND*)
30 OMC=WN-WAV(I)
   IF(IUSF.EQ.0) GO TO 35
   IUSL=IAST
   IU=IU+1
   SUM=SUM+OMC
   SUMSQ=SUMSQ+OMC*OMC
35 HIGT=AMAX1(DATAL(7,ILINE),DATAL(10,ILINE))-DATAL(8,ILINE)

```

```

IF(M(I).LT.MST) GO TO 40
IF(M(I).GT.MSTP) GO TO 40
IF(IUSE(I).GE.1) GO TO 37
WRITE(NWP,110) WN,TYP,J,IUSL,DATAL(2,ILINE),OMC,DATAL(5,ILINE)
2,DATAL(8,ILINE),HIGT,DATAL(11,ILINE),DATAL(12,ILINE)
GO TO 40
37 II=IBES(IUSE(I))
WRITE(NWP,110) POS(II),TYP,J,IAST,BANID(II),OMCA(II),STR(II)
2,YO(II),YHIGHT(II),HW(II),OFF(II)
110 FORMAT(F10.4,1X,A1,I3,1X,R1,A10,6F10.4)
40 CONTINUE
AV=SUM/IU
SIG=SQRT((SUMSQ-IU*AV*AV)/(IU-1))
WRITE(NWP,120) IU,AV,SIG
120 FORMAT(/,*,N=*,I5,*,AV=*,F8.4,*,SIG=*,F8.4,/)
RETURN
END

C
C SUBROUTINE MFIND(M,IFOUND,BRANCH,J)
C THIS ROUTINE CALCULATES AN M VALUES FROM A BRANCH AND J NUMBER.
C IF IFOUND = 1 BRANCH NAME NOT VALID
DATA RB,PB/1HR,1HP/
IFOUND=0
IF(BRANCH.NE.PB) GO TO 20
P BRANCH
M=-J
RETURN
20 IF(BRANCH.NE.RB) GO TO 30
R BRANCH
M=J+1
RETURN
30 IFOUND=1
RETURN
END

C
C SUBROUTINE BESTLN(ILIN,NBSTL)
C THIS ROUTINE FINDS AND SORTS INTO ORDER THE "NBST" LINES CLOSEST
C TO THE CALCULATED LINE POSITION IN EACH FRAME.
COMMON /BANDAT/ M(300),WAV(300),IUSE(300),NLBAN
COMMON /DATALIN/ POS(50),X(400),OMC(50),IBES(20)
COMMON /OUTST/ NWP,NBST,ILIST,RANG,FRAML,FRAMR
CALL LINFRM4(WAV(ILIN)-FRAML,WAV(ILIN)+FRAMR,NLIN)
NBSTL=MINO(NBST,NLIN)
IF(NBSTL.EQ.0) RETURN
DO 10 I=1,NLIN
OMC(I)=POS(I)-WAV(ILIN)
10 THIS STRANGE SORTING ALGORITHM IS USED SINCE THE ANTICIPATED
C NUMBER OF PASSES IS VERY LOW.
DO 30 IPAS=1,NBSTL
OMCB=10000.
DO 20 I=1,NLIN
IF(ABS(OMC(I)).GE.OMCB) GO TO 20
OMCB=ABS(OMC(I))
IBES(IPAS)=I
20 CONTINUE
SO IT WON'T FIND THE SAME ONE AGAIN
30 OMC(IBES(IPAS))=20000.
C RESTORE RIGHT OMC VALUE
DO 40 I=1,NBSTL
40 OMC(IBES(I))=POS(IBES(I))-WAV(ILIN)
RETURN
END

C
C SUBROUTINE LINFRM4(START,STOP,NLIN)
C THIS ROUTINE FINDS ALL THE LINES IN A FRAME.
C "NLIN" IS THE NUMBER OF LINES FOUND.
C BLOCK "IBLK" MUST HAVE BEEN READ IN PREVIOUSLY.
COMMON /DATALIN/ POS(50),BANID(50),STR(50),YO(50),YHIGT(50)

```

```

2,XL(50),XR(50),HW(50),OFF(50),OMC(50),IBES(20)
COMMON /DIREC/ SWAV(30)
COMMON /DTAB/ IBLK,ILINE,DATAL(16,300)
COMMON /PAR/ TYP,LIN,MTAB,NUMT,ID,NBLK
C DETERMINE WHICH BLOCK "START" IS IN
IBLKL=IBLK
NLIN=0
10 IF(IBLK.GE.NBLK) GO TO 20
IF(SWAV(IBLK+1).GT.START) GO TO 20
IBLK=IBLK+1
GO TO 10
20 IF(SWAV(IBLK).LE.START) GO TO 25
IBLK=IBLK-1
IF(IBLK.GE.2) GO TO 20
C NOT IN FILE
RETURN
C FIND "START" IN BLOCK
25 IF(IBLK.EQ.IBLKL) GO TO 30
CALL READMS(4,DATAL,NUMT,IBLK)
ILINE=1
30 IF(START.LT.DATAL(6,ILINE)) ILINE=1
40 IF(START.LE.DATAL(9,ILINE)) GO TO 60
ILINE=ILINE+1
IF(ILINE.LE.MTAB) GO TO 40
ILINE=1
IF(IBLK.EQ.NBLK) RETURN
IBLK=IBLK+1
CALL READMS(4,DATAL,NUMT,IBLK)
60 IF(STOP.LT.DATAL(6,ILINE)) RETURN
IF(DATAL(1,ILINE).NE.0) GO TO 70
ILINE=1
RETURN
C LINE FOUND
70 NLIN=NLIN+1
IF(NLIN.GT.50) GO TO 90
POS(NLIN)=DATAL(1,ILINE)
XL(NLIN)=DATAL(6,ILINE)
XR(NLIN)=DATAL(9,ILINE)
HW(NLIN)=DATAL(11,ILINE)
OFF(NLIN)=DATAL(12,ILINE)
BANID(NLIN)=DATAL(2,ILINE)
STR(NLIN)=DATAL(5,ILINE)
YO(NLIN)=DATAL(8,ILINE)
YHGT(NLIN)=AMAX1(DATAL(7,ILINE),DATAL(10,ILINE))-YO(NLIN)
ILINE=ILINE+1
IF(ILINE.LE.MTAB) GO TO 60
ILINE=1
IF(IBLK.EQ.NBLK) RETURN
IBLK=IBLK+1
CALL READMS(4,DATAL,NUMT,IBLK)
GO TO 60
90 WRITE(6,900)
900 FORMAT(* MORE THAN 50 LINES IN ONE FRAME*)
STOP
END
C
C SUBROUTINE FINUSE(ILIN,IUSF,WN)
C THIS ROUTINE IS USED TO FIND THE LINES WHICH ARE
C TO BE USED IN THE FIT.
COMMON/BANDAT/ M(300),WAV(300),IUSE(300),NLBAN
COMMON /OUTST/ NWP,NBST,ILIST,RANG,FRAML,FRAMR
COMMON /DATALIN/ POS(50),X(450),IBES(20)
IF(IUSE(ILIN).GT.0) GO TO 20
IUSF=0
WN=POSL(WAV(ILIN),0)
C DON'T USE NO MATTER WHAT
IF(IUSE(ILIN).LT.0) RETURN
C USE IF IN RANGE

```

```

IF(ABS(WN-WAV(ILIN)).GT.RANG) RETURN
IUSF=1
RETURN
C   USE ONE OF THE OTHER CHOICES
20  CALL BESTLN(ILIN)
    WN=POS(IBES(IUSE(ILIN)))
    IUSF=1
    RETURN
    END

C   SUBROUTINE CHGUSE
C   THIS ROUTINE ALLOWS THE OPERATOR TO CHANGE WHICH LINES WILL
C   BE USED IN THE FIT.
COMMON /BANDAT/ M(300),WAV(300),IUSE(300),NLBAN
DATA IR,IP/22B,20B/
WRITE(6,100)
100  FORMAT(* CHANGE USAGE*,/)
10   READ(5,110) ITYP,J,IWHT
110  FORMAT(I3,I3,I2)
    IF(ITYP.NE.IP) GO TO 20
C   P BRANCH
    MR=-J
    GO TO 30
20   IF(ITYP.NE.IR) RETURN
C   R BRANCH
    MR=J+1
30   II=IBINSC(M,NLBAN,MR)
    IF(II.NE.0) GO TO 40
    WRITE(6,120) MR
120  FORMAT(* M=*,I6,* NOT FOUND*,/)
    GO TO 10
40   IUSE(II)=IWHT
    GO TO 10
    END

C   SUBROUTINE WRTOTL
C   THIS ROUTINE WRITES INFORMATION FOR THE "NBSTL" CLOSEST LINES TO
C   EACH CALCULATED LINE POSITION.
COMMON /OUTST/ NWP,NBST,ILIST,RANG,FRAML,FRAMR
COMMON /BANDAT/ M(300),WAV(300),IUSE(300),NLBAN
COMMON /DATALIN/ POS(50),BANID(50),STR(50),YO(50),YHIGT(50)
2   XL(50),XR(50),HW(50),OFF(50),OMC(50),IBES(20)
DATA ASTR,BLANK /1H*,1H /
5   WRITE(6,900)
900  FORMAT(* ENTER RANGE*,/)
    READ(5,910) BST,JST,BSP,JSP
910  FORMAT(A1,I3,1X,A1,I3)
    CALL MFIND(MST,IFST,BST,JST)
    CALL MFIND(MSTP,IFSP,BSP,JSP)
    IF((IFST+IFSP).NE.0) GO TO 5
    IST=IBINSC(M,NLBAN,MST)
    ISP=IBINSC(M,NLBAN,MSTP)
    IF((IST.EQ.0).OR.(ISP.EQ.0)) GO TO 5
    DO 70 I=IST,ISP
    IF(M(I).GT.0) GO TO 10
    J=-M(I)
    TYP="P"
    GO TO 20
10   J=M(I)-1
    TYP="R"
20   WRITE(NWP,920) TYP,J
920  FORMAT(1X,A1,I3)
    CALL BESTLN(I,NBSTL)
    IF(NBSTL.EQ.0) GO TO 70
    IPICK=0
    IF(IUSE(I)) 50,30,40
C   IUSE(I)=0 USE FIRST CHOICE IF IN RANGE
30   IF(ABS(OMC(IBES(1))).LE.RANG) IPICK=1

```

```

C      GO TO 50
40     IUSE(I)= 1, 2, . . . SET "IPICK" TO THAT ONE
50     IPICK=IUSE(I)
      DO 60 IP=1,NBSTL
      PICK=BLANK
      IF(IP.EQ.IPICK) PICK=ASTR
60     WRITE(NWP,930) PICK,POS(IBES(IP)),BANID(IBES(IP)),OMC(IBES(IP))
      2,STR(IBES(IP)),YO(IBES(IP)),YHGT(IBES(IP)),HW(IBES(IP))
      3,OFF(IBES(IP))
930    FORMAT(5X,A1,1X,F10.4,A10,6F10.4)
70     CONTINUE
      RETURN
      END

C
      SUBROUTINE GRLIN4
C      THIS ROUTINE MAKES AN EXTENDED INFORMATION LOOMIS-WOOD DIAGRAM.
      COMMON /OUTST/ NWP,NBST,ILIST,RANG,FRAML,FRAMR
      COMMON /BANDAT/ M(300),WAV(300),IUSE(300),NLBAN
      COMMON /DATALIN/ POS(50),BANID(50),STR(50),YO(50),YHGT(50)
      2,XL(50),XR(50),HW(50),OFF(50),OMC(50),IBES(20)
      DIMENSION GRA(100)
      DATA BLANK,IBLAN,ASTR,XMERG,L/55B,55B,47B,15B,100/
      SCAL=(L-1)/(FRAMR+FRAML)
5     WRITE(6,900)
900    FORMAT(* ENTER RANGE*,/)
      READ(5,910) BST,JST,BSP,JSP
910    FORMAT(A1,13,1X,A1,13)
      CALL MFIND(MST,IFST,BST,JST)
      CALL MFIND(MSTP,IFSP,BSP,JSP)
      IF((IFST+IFSP).NE.0) RETURN
      IST=IBINSC(M,NLBAN,MST)
      ISP=IBINSC(M,NLBAN,MSTP)
      IF((IST.EQ.0).OR.(ISP.EQ.0)) GO TO 5
      DO 100 ILIN=IST,ISP
      J=1
      IF(M(ILIN).GT.0) GO TO 10
      LIN=-M(ILIN)
      TYP="P"
      GO TO 20
10     LIN=M(ILIN)-1
      TYP="R"
20     START=WAV(ILIN)-FRAML
      CALL LINFRM4(START,WAV(ILIN)+FRAMR,NLIN)
      IF(NLIN.LE.0) GO TO 80
C      DECIDE WHICH SYMBOL TO USE
      DO 40 IL=1,NLIN
      ITMP=AND(77B,BANID(IL))
      IF(ITMP.NE.IBLAN) GO TO 30
C      LINE NOT IDENTIFIED
      BANID(IL)=ASTR
      GO TO 40
30     ITST=AND(77B,SHIFT(BANID(IL),-6))
      IF(ITST.NE.IBLAN) BANID(IL)=XMERG
40     CONTINUE
C      SET "GRA" ARRAY
      DO 70 IL=1,NLIN
      TPOS=POS(IL)
      SL=TPOS-HW(IL)
      IF(SL.LT.XL(IL)) SL=XL(IL)
      ISL=(SL-START)*SCAL+1.5
      STL=TPOS+HW(IL)
      IF(STL.GT.XR(IL)) STL=XR(IL)
      ISTL=(STL-START)*SCAL+1.5
C      BLANK BEFORE
50     IF(ISL.LE.J) GO TO 60
      GRA(J)=BLANK
      J=J+1
      GO TO 50

```

```

60  IF(ISTL.LT.J) GO TO 70
    IF(J.GT.L) GO TO 90
    GRA(J)=BANID(IL)
    J=J+1
    GO TO 60
70  CONTINUE
80  IF(J.GT.L) GO TO 90
    GRA(J)=BLANK
    J=J+1
    GO TO 80
90  WRITE(NWP,920) WAV(ILIN),TYP,LIN,(GRA(I),I-1,L)
920  FORMAT(F10.4,1X,A1,I3,100R1)
100 CONTINUE
    RETURN
    END

C
FUNCTION WAVNUM(M)
C  CALCULATE A LINE POSITION GIVEN THE MOLECULAR CONSTANTS.
COMMON /BAND/ G,B1,D1,H1,B2,D2,H2
MP=M*(M+1)
MM=M*(M-1)
WAVNUM=G+MP*(B1-MP*(D1-MP*H1))-MM*(B2-MM*(D2-MM*H2))
RETURN
END

C
FUNCTION POSL(WN,IW)
C  THIS ROUTINE FINDS LINE "WN" ON RANDOM ACCESS DISK FILE TAPE4.
C  IF IW = 1 IT WILL WRITE OLD BLOCK OF DATA BACK OUT BEFORE
C  IT READS A NEW ONE.
C  IF "POSL" =0 LINE WAS NOT FOUND
C  NOTE THIS FUNCTION ALSO SETS "ILINE" AND "IBLK"
COMMON/DIREC/ SWAV(30)
COMMON /DTATAB/ IBLK,ILINE,DATAL(16,300)
COMMON /PAR/ TYP,LIN,MTAB,NUMT,ID,NBLK
C  DETERMINE WHICH BLOCK "WN" IS IN
IBLKL=IBLK
10  IF(IBLK.GE.NBLK) GO TO 20
    IF(SWAV(IBLK+1).GT.WN) GO TO 20
    IBLK=IBLK+1
    GO TO 10
20  IF(SWAV(IBLK).LE.WN) GO TO 25
    IBLK=IBLK-1
    IF(IBLK.GE.2) GO TO 20
    IBLK=IBLKL
    GO TO 50
C  FIND WHICH POINT
25  IF(IBLK.EQ.IBLKL) GO TO 27
    IF(IW.EQ.1) CALL WRITMS(4,DATAL,NUMT,IBLKL,1)
    CALL READMS(4,DATAL,NUMT,IBLK)
    ILINE=1
27  IF(WN.LT.DATAL(6,ILINE)) ILINE=1
30  IF(WN.LE.DATAL(9,ILINE)) GO TO 40
    ILINE=ILINE+1
    IF(ILINE.LE.MTAB) GO TO 30
    ILINE=1
    GO TO 50
40  IF(WN.GE.DATAL(6,ILINE)) GO TO 60
C  LINE NOT FOUND
50  POSL=0
    RETURN
C  LINE FOUND
60  POSL=DATAL(1,ILINE)
    RETURN
    END

C
FUNCTION FCTN(X,I,J,JVAR)
C  DIMENSION X(1),JVAR(1)
C  THIS FUNCTION DETERMINES COEFFICIENTS OF FITTING PARAMETERS.

```

```

C      THIS ISN'T A VERY EFFICIENT WAY TO DO THINGS SINCE X*(X+1)
C      AND X*(X-1) ARE CALCULATED EACH TIME, BUT IT FITS IN WITH
C      REGRES EASIER.
C      ORDER OF TERMS 1 G, 2 BU, 3 DU, 4 HU, 5BL, 6 DL, 7 HU
C      GO TO (1,2,3,4,5,6,7), JVAR(J)
C      NOTE, REGRES NEVER USES CONSTANT TERM.
1      FCTN=1
      RETURN
2      FCTN=X(I)*(X(I)+1)
      RETURN
3      FCTN=-(X(I)*(X(I)+1))**2
      RETURN
4      FCTN=(X(I)*(X(I)+1))**3
      RETURN
5      FCTN=-X(I)*(X(I)-1)
      RETURN
6      FCTN=(X(I)*(X(I)-1))**2
      RETURN
7      FCTN=-(X(I)*(X(I)-1))**3
      RETURN
      END

C      FUNCTION WAVN(X,I,M,JCON)
      COMMON /BAND/ BAN(7)
      DIMENSION JCON(1),X(1)
C      THIS ROUTINE CALCULATES THE WAVENUMBER POSITIONS OF A SPECTRAL
C      LINE WITH THE CONSTANTS GIVEN BY ARRAY "JCON."
C      THERE ARE "M" CONSTANTS
      TERM=0
      IF(M.EQ.0) GO TO 20
      DO 10 J=1,M
10      TERM=FCTN(X,I,J,JCON)*BAN(JCON(J))+TERM
20      WAVN=TERM
      RETURN
      END

C      SUBROUTINE SETM(M,IKIND,L,JP,JR,N)
C      THIS ROUTINE SETS ALL THE M VALUES IN A BAND.
C      M=-J FOR THE P BRANCH, AND M=J+1 FOR THE R BRANCH.
C      IKIND=1 EVEN LINES ONLY, IKIND=2 ODD ONLY, IKIND=3 ALL LINES.
C      THE TOTAL NUMBER OF LINES IS RETURNED IN N.
      DIMENSION M(1)
      NL=-L
      MAX=JR+1
      IF(IKIND-2) 10,20,30
10      MSTEP=2
      MIN=-(JP/2)*2
      MR=((L+1)/2)*2+1
      GO TO 40
20      MSTEP=2
      MIN=-((JP-1)/2)*2-1
      MR=(L/2)*2+2
      GO TO 40
30      MSTEP=1
      MIN=-JP
      MR=L+1
40      MT=MIN
      I=0
C      P BRANCH
      I=I+1
50      M(I)=MT
      MT=MT+MSTEP
      IF(MT.LT.NL) GO TO 50
C      R BRANCH
      MT=MR
60      I=I+1
      M(I)=MT
      MT=MT+MSTEP

```



```

      GO TO 80
C     NAME
30    DO 70 IL=1,NLBAN
      WN=POSL(WAV(IL),1)
      IF(WN.EQ.0) GO TO 40
      DATAL(2,ILINE)=OR(AND(SHIFT(DATAL(2,ILINE),6),MASK(60-6)),IBNR)
      GO TO 70
C     LIST OUT UNFOUND LINES
C     DECIDE P OR R BRANCH
40    IF(M(IL).GT.0) GO TO 50
      J=-M(IL)
      TYP="P"
      GO TO 60
50    J=M(IL)-1
      TYP="R"
60    WRITE(NWP,900) WAV(IL),TYP,J
900   FORMAT(F10.4,1X,A1,I3,*,NOT FOUND*)
70    CONTINUE
80    CALL WRITMS(4,DATAL,NUMT,IBLK,1)
      RETURN
      END

```

```

C     SUBROUTINE REGRES(X,Y,SIGMAY,NPTS,NTERMS,M,MODE,YFIT,
+   AO,A,SIGMAO,SIGMAA,R,RMUL,CHISQR,FTEST)
C     THIS SUBROUTINE IS FROM BEVINGTON.

```

(see reference 46)

```

C     FUNCTION IBINSC(IA,N,ITAR)
C     THIS ROUTINE DOES A BINARY TREE SEARCH.
C     THE NUMBER OF COMPARISONS NEEDED IS LOG2(N) PLUS A COUPLE
C     FOR ROUND OFF.
C     THE ARRAY TO BE SEARCHED IS "IA". THE TARGET OF THE SEARCH
C     IS "ITAR".
C     THE POSITION OF THE TARGET IS RETURNED AS THE FUNCTION VALUES.
C     "IBINSC" = 0 MEANS NOT FOUND.
C     DIMENSION IA(1)
      DATA MAXZER/5/
      NZ=0
      STEP=N/2.0
      RJ=STEP
C     SET NEXT STEP
10    STEP=STEP/2
      IF(STEP.GT.1.) GO TO 20
      STEP=1.
      NZ=NZ+1
      IF(NZ.LE.MAXZER) GO TO 20
C     NOT FOUND
      IBINSC=0
      RETURN
20    J=RJ+.5
      IF(ITAR-IA(J)) 30,50,40
30    RJ=RJ-STEP
      GO TO 10
40    RJ=RJ+STEP
      GO TO 10
50    IBINSC=J
      RETURN
      END

```

END

12-86

DTIC